OPTIMIZATION OF SHADING EFFECT BY USING SHADING DEVICE INTEGRATED PHOTOVOLTAIC SYSTEM

YUTTANA TONGTUAM

A Thesis Submitted to the Graduate School of Naresuan University
in Partial Fulfillment of the Requirements
for the Doctor of Philosophy Degree in Renewable Energy
July 2014

This thesis entitled "Optimization of Shading Effect by Using Shading Device Integrated Photovoltaic System" submitted by Yuttana Tongtuam in partial fulfillment of the requirements for the Doctor of Philosophy Degree in Renewable Energy is hereby approved.

.... Chair
(Chatchai Sirisamphanwong, Ph.D.)

.... Committee
(Assistant Professor Nipon Ketjoy, Dr.-Ing.)

.... Committee
(Assistant Professor Sarayooth Vaivudh, Ph.D.)

.... Committee
(Assistant Professor Prapita Thanarak, Ph.D.)

.... Committee
(Assistant Professor Patamaporn Sripadungtham, Ph.D.)

.... Committee
(Assistant Professor Pisit Liutanakul, Dr.-Ing.)

Approved

....
(Professor Rattana Buosonte, Ph.D.)
Dean of the Graduate School

18 July 2014

ACKNOWLEDGEMENT

I would like to express my sincere thanks to my advisor, Assistant Professor Dr. Nipon Ketjoy, Assistant Professor Dr. Sarayouth Vaivudh and Assistant Professor Dr. Prapita Thanarak for his invaluable help and constant encouragement throughout the course of this research. I am most grateful for their teaching and advice, not only the research methodologies but also many other methodologies in life. I would not have achieved this far and this thesis would not have been completed without all the support that I have always received from them.

In addition, I am grateful for the staff of SERT, and others person for suggestions and all their help. I most gratefully acknowledge my parents and my friends for all their support throughout the period of this research.

Finally, this thesis supported by Energy Conservation Promotion Fund by Energy Policy and Planning Office Ministry of Energy, Thailand (EPPO).

Yuttana Tongtuam

Title	OPTIMIZATION OF SHADING EFFECT BY USING SHADING DEVICE INTEGRATED PHOTOVOLTAIC SYSTEM
Author	Yuttana Tongtuam
Advisor	Assistant Professor Nipon Ketjoy, Dr.-Ing.
Co - Advisor	Assistant Professor Sarayouth Vaivudh, Ph.D.
	Assistant Professor Prapita Thanarak, Ph.D.
Academic Paper	Thesis Ph.D. in Renewable Energy, Naresuan University, 2013
Keywords	Shading effect, Shading device integrated Photovoltaic system, Optimization

ABSTRACT

Shading device integrated photovoltaic system is one strategy in designing green buildings considering energy and environment conservation. It is the pattern of installation which generates electric power less than rooftop installation as a result from shading provided by buildings. Therefore, the purpose is the optimization of solar heat gain reduction and increase in daylight usability of shading device integrated photovoltaic system as well as the optimization of economic price and benefit

In this study, data collection was through the use of models in order to improve variables in coefficient of diffuse solar radiation and solar radiation reflecting from building envelope. Equation of total solar radiation on inclined plane presented by ASHRAE was used. The adjustment of Daylight Factor (DF) of daylight usability and the study of diffuse solar heat gain reduction in the pattern of Shading Coefficient (SC_d) used in calculating energy value of energy generating system, air conditioning system and lighting system

The variables used in design for calculation were such as directions of installation, incline angle of solar module, room sizes and lighting control technique with condition of minimum lighting level need at 300 lux and the use of air conditioning system containing Coefficient of Performance: COP of 3.22 according to the suggestion declared by law for energy conservation. 3 patterns of utilization

strategy were also considered as follows: the utilization from energy generation only, the utilization from energy generation and heat load reduction, and the utilization from energy generation, heat load reduction and lighting energy saving.

From analyzing and evaluating to create optimization in design according to specific purposes, it is found that installation in the south side with the incline angle of 30 degrees will be able to produce maximum amount of energy for the whole year. The depth of the rooms which is not too much will be suitable for heat reduction and appropriate use of daylight. To do the economic analysis during 30 years of project at system cost of 70 THB/W_p and 86 THB/W_p, cost of electricity at 4 Baht per unit and MRR loan rate at 8% as well as the decrease in efficiency of energy generation down to 20% in 25 years, there were conclusions as follows: the installation should be in the south side with the incline angle of 30 degrees in rooms with less distance from the windows suitable for the use of lighting control system and in rooms with long distance from the windows suitable for dimming technique in order to gain most benefit towards investment up to 2.57 times and receive faster payback within 5.48 years

LIST OF CONTENTS

LIST OF CONTENTS (CONT.)

LIST OF TABLES

LIST OF TABLES (CONT.)

Table **Page**

LIST OF FIGURES

LIST OF FIGURES (CONT.)

Figure **Page**

LIST OF FIGURES (CONT.)

Figure **Page**

LIST OF FIGURES (CONT.)

LIST OF FIGURES (CONT.)

Figure **Page**

LIST OF FIGURES (CONT.)

LIST OF FIGURES (CONT.)

Figure **Page**

LIST OF FIGURES (CONT.)

LIST OF FIGURES (CONT.)

Figure **Page**

LIST OF SYMBOLS

Solar radiation		Units
t_S	Solar time	decimal hours
t_{SL}	Local solar time	decimal hours
EOT	Equation of time	decimal minutes
L_{SM}	local standard time meridian	degrees
L_{ON}	local longitude	degrees
ω	Hour angle	degrees
δ	Declination angle	degrees
θ_Z	Zenith angle	degrees
θ_i	Incident angle	degrees
θ_E	Elevation angle	degrees
ϕ	Latitude angle	degrees
α	Solar altitude	degrees
γ	Azimuth	degrees
γ_S	Surface azimuth	degrees
β	Slope from horizontal plane	degrees
E_0	Extraterrestrial solar irradiance	W/m^2
E_b	Beam solar irradiance	W/m^2
E_d	Diffuse solar irradiance	W/m^2
E_t	Total solar irradiance	W/m^2
E_{DN}	Direct normal of solar irradiance	W/m^2
E_G	Global solar irradiance	W/m^2
E_V	Vertical solar irradiance	W/m^2
E_{tS}	Total solar irradiance on slope surface	W/m^2
$E_{tS\text{-}ISO}$	Total solar irradiance of isotropic sky model	W/m^2

LIST OF SYMBOLS (CONT.)

		Units
E_{tS-ANI}	Total solar irradiance of anisotropic sky model	W/m^2
$E_{tS-HDKR}$	Total solar irradiance of HDKR sky model	W/m^2
E_{t-SIPV}	Total solar irradiance of SIPV	W/m^2
K	Clearness index	decimal %
R_b	Relative of beam irradiance	decimal %
R_d	Relative of diffuse irradiance	decimal %
R_{sd}	Relative of stack effect	decimal %
R_{rG}	Relative of ground reflected irradiance	decimal %
R_{rB}	Relative of building reflected irradiance	decimal %
ρ_g	Ground reflectivity	decimal %
A_i	Anisotropic index	-
AM	Air mass	-
N	Day Number	-

PV technology

P	Power	W
P_i	Power input	W
P_o	Power output	W
P_{SIPV}	Power of SIPV	W
P_{MP}	Maximum power	W
PR	Performance	decimal %
FF	Fill factor or Squareness of the IV curve	decimal %
η	Efficiency	decimal %
η_{PV}	Efficiency of PV	decimal %
η_{SIPV}	Efficiency of SIPV	decimal %

LIST OF SYMBOLS (CONT.)

		Units
η_{inv}	Efficiency of inverter	decimal %
η_D	Efficiency of long term PV degradation	decimal %
I	Current	A
I_{SC}	Short-circuit current	A
I_{MP}	Maximum current	A
I_0	Input current	A
I_L	Light generated current	A
V	Voltage	V
V_{OC}	Open-circuit voltage	V
V_{MP}	Maximum voltage	V
q	Constants	-
k	Constants	-
n	Ideality factor	-
T	Temperature	K or °C
T_m	Module temperature	°C
T_{amb}	Ambient temperature	°C
A_{PV}	Surface call area	m^2
W	Shading extension	m
H	Height of clear window	m

Special subscript

a-Si	Amorphus Silicon
p-Si	Polycrystalline Silicon
SIPV	Shading device Integrated Photovoltaic

Cooling load

q	Heat flux	W

LIST OF SYMBOLS (CONT.)

		Units
q_{cond}	Conduction heat flux	W
q_{rad}	Radiation heat flux	W
q_{cl}	Cooling load from lighting	W
HG_{cl}	Heat gain from lighting	W
W_l	Total lamp power	W
A	Surface area	m^2
U	Concuction heat transfer coefficient	W/ m^2-°C
h	Convection heat transfer coefficient	W/m^2 °C
R_T	Total resistance value	m^2-°C/W
R_G	Resistance value of air gap	m^2-°C/W
R_o	Resistance value of air film out side	m^2-°C/W
R_i	Resistance value of air film in side	m^2-°C/W
V	Room air supply rate	l/s-m^2
dx	Dept of material layer	m
CLTD	Cooling Load Temperature Differences	°C
E_{twS}	Total solar irradiance on window with shading	W/m^2
E_{tw}	Total solar irradiance on window	W/m^2
SHGF	Solar Heat Gain Factor	W/m^2
SC	Shading Coefficient	decimal %
SC_b	Shading Coefficient only diffuse radiation	decimal %
SC_d	Shading Coefficient only beam radiation	decimal %
SHGC	Solar Heat Gain Coefficient	decimal %
VT	Visual transmittance	decimal %
F_{ul}	Lighting use factor	decimal %
F_{sa}	Lighting special allowance factor	decimal %

LIST OF SYMBOLS (CONT.)

		Units
CLF	Cooling Load Factor	-
CLF_{el}	Cooling Load Factor of light	-
COP	Coefficient of performance	-

Daylight Factor

E	Illumination level	fc or lux
E_h	Horizontal illuminance	fc or lux
E_v	Vertical illuminance	fc or lux
E_i	Inside illuminance	fc or lux
E_o	Outside illuminance	fc or lux
E_{sky}	Illuminance from sky	fc or lux
L	luminance	cd/ft^2 or lm/m^2
L_θ	luminance	cd/ft^2 or lm/m^2
L_h	Horizontal luminous	cd/ft^2 or lm/m^2
L_Z	Zenith luminous	cd/ft^2 or lm/m^2
DF	Daylight Factor	decimal %
DF_{av}	Average Daylight Factor	decimal %
IRC	Internal reflected component	decimal %
ERC	External reflected component	decimal %
SC	Sky component	decimal %
SC_W	Sky component of window opening	decimal %
SC_O	Obstructed sky component	decimal %
ρ	Reflectance	decimal %
ρ_{av}	Average reflectance of room surface	decimal %
ρ_{FW}	Average reflectance of wall	decimal %
ρ_{CW}	Average reflectance of ceiling	decimal %
τ	Transmittance	decimal %
C	Obstruction coefficient	decimal %

LIST OF SYMBOLS (CONT.)

		Units
A_W	Area of window less frame	ft^2 or m^2
A_t	Total internal surface area of room	ft^2 or m^2
A_U	Upper surface area of room	ft^2 or m^2
A_L	Lower surface area of room	ft^2 or m^2
MF	Maintenance Factor	decimal %
ρ_{av}	Average reflectance of room surfaces	decimal %
ρ_U	Upper reflectance of room surfaces	decimal %
ρ_L	Lower reflectance of room surfaces	decimal %
GBC	Glazing bar correction	-

Daylight Glare Index

dG	Day lighting glare constant	-
dGI	Day lighting glare Index	-
DGI	Modified Day lighting glare Index	-
GI	Glare Index	-
L_s	Source luminance	cd/ft^2 or lm/m^2
L_b	Background luminance	cd/ft^2 or lm/m^2
E_a	Diffuse illuminance at the plane of aperture	fc or lux
E_{sp}	Illuminance at the station point	fc or lux
E_H	Horizontal illuminance	fc or lux
E_{dGI}	Exterior illuminance on the horizontal	fc or lux
E_{co}	Cut off illuminance	fc or lux
IRE	Interior reflected illuminance	fc or lux
ERE	Exterior reflected illuminance	fc or lux
v	Direction of view factor	-

LIST OF SYMBOLS (CONT.)

		Units
F_{dGI}	Fraction	-
ρ_r	Average room reflectivity	decimal %
T_g	Glazing normal transmittance	decimal %

Lighting

F	Rate of flow visible radiation	lm
E	Illumination level	fc or lux
CP	Luminous intensity	cd
CU	Coefficient of utilization	decimal %
LLD	Lamp lumen depreciation	decimal %
LDD	Luminaire dirt depreciation	decimal %
L	Length of cavity	ft or m
W	Width of cavity	ft or m
A	Using area	ft^2 or m^2
h_C	Height of cavity	ft or m
h_{CC}	Height of ceiling cavity	ft or m
h_{RC}	Height of room cavity	ft or m
h_{FC}	Height of floor cavity	ft or m
CR	Cavity ratio	-
CCR	Ceiling cavity ratio	-
RCR	Room cavity ratio	-
FCR	Floor cavity ratio	-

Economic

PVB	Present value of benefits	THB

LIST OF SYMBOLS (CONT.)

		Units
PVC	Present value of cost	THB
B	Benefits value	THB
C	Costs value	THB
i	Interest	THB
K	Fix cost	THB
B/C	Benefits-Costs ratio	-
t	Time index	-

CHAPTER I

INTRODUCTION

Background and motivation

1. The idea of green building design

The idea of green building design is a current trend for the design of newly constructed buildings. It is a consequence of the energy crisis and environmental problems such as the green house effect, climate change and Global Warming. This results in the idea of sustainable development, which takes into account social, environmental and economic factors. The basis of design integrated with scientific knowledge has been used. Therefore, building science is based on passive design ideas depending on energy gained from the surrounding environment of buildings. This is to create suitable, human comfortable that will also lead to energy conservation. The technology used to build green buildings which are designed for the effective and eco-friendly use of energy, should be suitable and clean to provide building with the better operation of active design using amount of energy, especially, electricity such as air conditioning, lighting and other facility systems. Design based mostly on natural systems should be considered first before involving the use of synthesized energy.

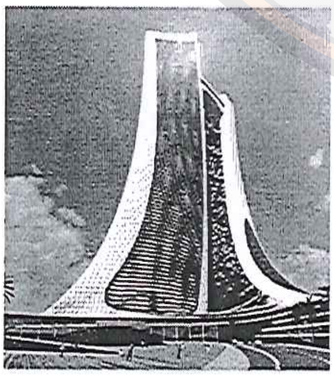

The one of skyscrapers with integrated energy generators will be a live machine with bio-climatic walls for supporting vegetation purifying air. It has photovoltaic arrays for solar energy harnessing, rainwater and atmospheric water collection unit and will also be utilizing air flow between towers with aero generators. Self-powered Eco-Cybernetic City interacts with the surrounding environment.

Figure 1 The one of green building integrated with PV

Source: Volumatrix Group [93]

2. Energy consumption of typical buildings in Thailand

Thailand is located in a hot and humid-tropical climate, passive design techniques are necessary for the design of building envelope to prevent solar radiation, heat, humidity, thermal radiation from nearby buildings and polluted airflow circulation caused from external environment to eventually ventilate into the inside of the buildings where humans live, As the comfort zone cannot be fully controlled at all times of activities by passive techniques. Then active system has to be used to control all the previously mentioned concerns.

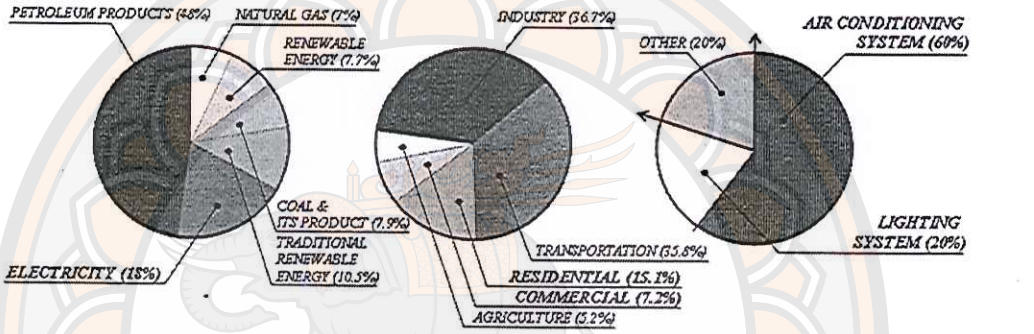

FINAL ENERGY CONSUMPTION BY FUEL TYPE : RESOURCESE *FINAL ENERGY CONSUMPTION BY FUEL TYPE : SECTOR* *ENERGY CONSUMPTION IN THE BUILDING*

Figure 2 The ratio of energy consumption

Source: Ministry of Energy [78]

Figure 1 and Figure 2 Shows that energy consumption of typical buildings in Thailand is divided into 3 parts as follows: about 60% for air conditioning system, 20% for lighting system and 20% for other systems from the information on verification for building design according to Thai Energy Conservation Law. How ever, Thailand was used electricity about 17.5% came form Natural gas and traditional renewable energy and about 7.7% came from renewable energy. Some of the final energy consumption about 22.3% was used in residential and commercial sector. In 2012 Thailand's maximum peak load of electricity was about 26,430 MW [59] which was more than a year before by about 9.2%. This will trend to increase in the future.

3. Passive design integrated with clean energy

Active systems such as air conditioning system and lighting system contain ratios of energy consumption equivalent to 80% of the final energy consumption in the building. Building envelope plays an important role in solar heat gain reduction, effective prevention of heat and humidity transmission. However, all these mentioned problems need the most energy for manipulation.

Passive design is a choice for design in basic control capable of decreasing the severity of the environment surrounding the buildings. It includes designs such as shading devices, insulation and fenestration. Once all these techniques are used in combining with high quality electrical appliances and control equipment like dimmers, energy can be increasingly saved.

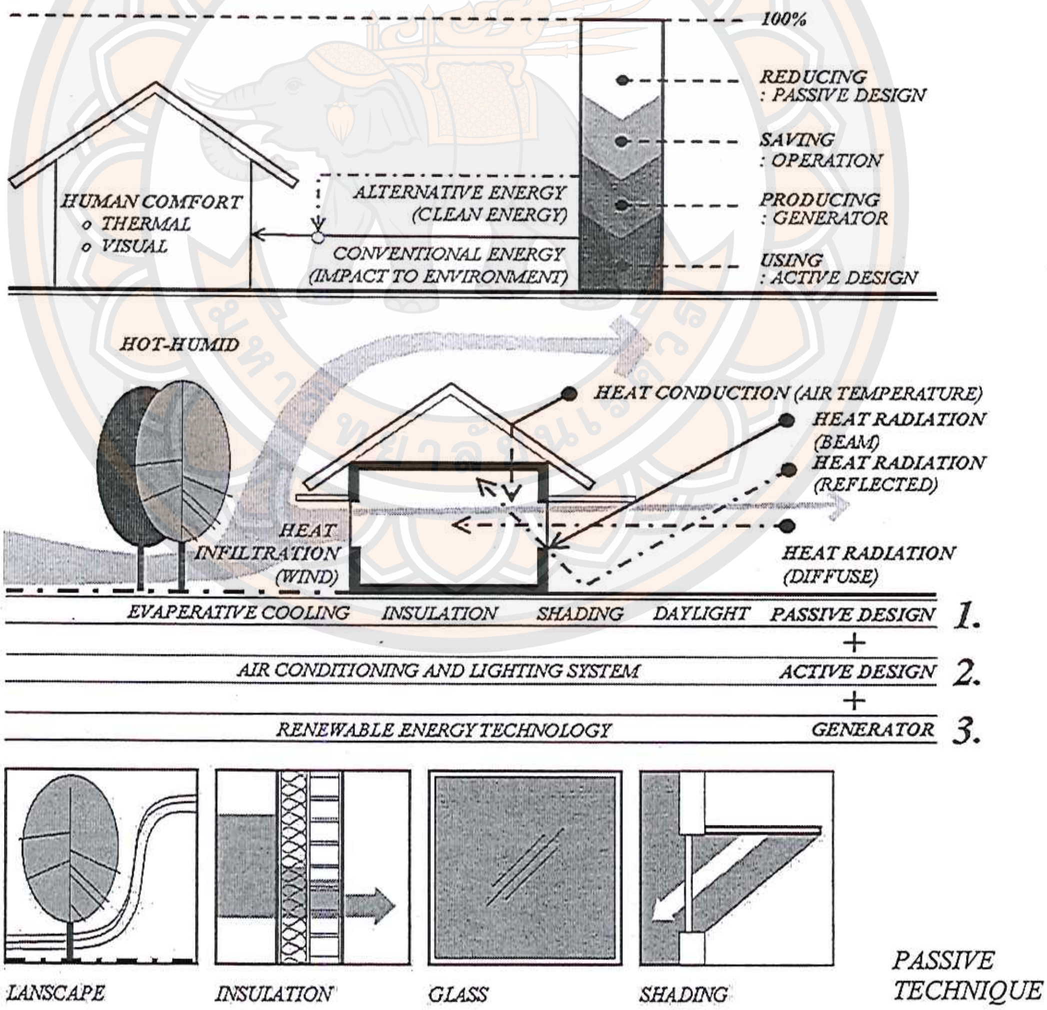

Figure 3 Integration of passive design with clean energy

Energy consumption can be decreased by using passive design techniques and then choosing appropriate, effective, well-managed technology in energy usage. Moreover, when the technology is integrated with expensive renewable energy systems using large amounts of green energy in a form of synthesizing into electrical energy processing like national grid, it will save energy and decrease the cost. However, the aforementioned integration depends on the area for installation on building envelope and the efficiency of the technology.

4. The interesting of the shading element

Concerning the energy consumption ratio of buildings in Thailand, it is seen that shading devices are one of the passive design techniques affecting heat load reduction of air conditioning system and controlling sunlight levels to save lighting system. This is to reduce the ratio of energy used.

Of course, shading devices are designed to be used with windows. It is also important to see good view clearly and exterior aesthetics. Figure 4 Shows the relation between angles and spaces affecting shape, the stand-off part of shading devices to prevent solar radiation in the period needed.

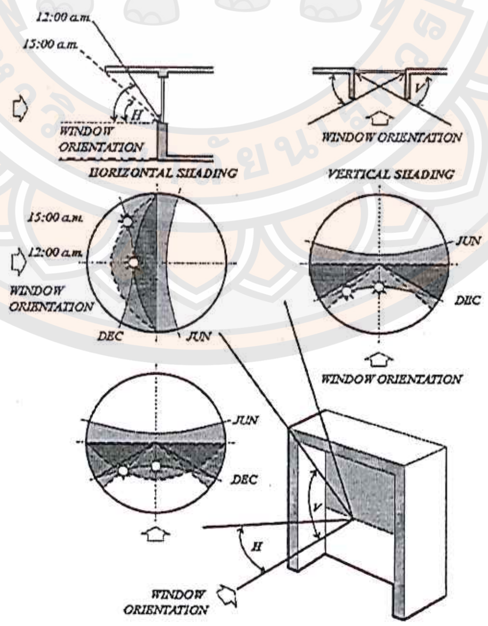

Figure 4 Angular of horizontal and vertical shading devices

Source: Moor, Fuller [25]

5. Advantages of view and daylight

The view surrounding the buildings is connected to the feeling and activities inside the buildings of residence. Atmosphere is being changed at all times of the day through each season for the whole year because of motion of the sun and clouds causing Karsten Harries's light phenomenon [24] stating that "…architecture, beyond providing physical frames for human activities, also interprets to human beings their place in nature and society" which means that humans need to have interaction with surrounding environment.

Revicki, Heerwagen and Turkish study of Alimoglu and Donmez [6, 14] concluded that "daylight significantly impacts the working hour and burnout, which be cause of stress on the job, the study is proved with nurses of Turkish. Furthermore, the color of daylight changes all time of day and seasons then it effects the human cycle time that is the reason from chemical reactions with the UV levels contained in daylights". Therefore, design must create connections with everything outside the building through the use of windows for quality of life besides receiving enough light.

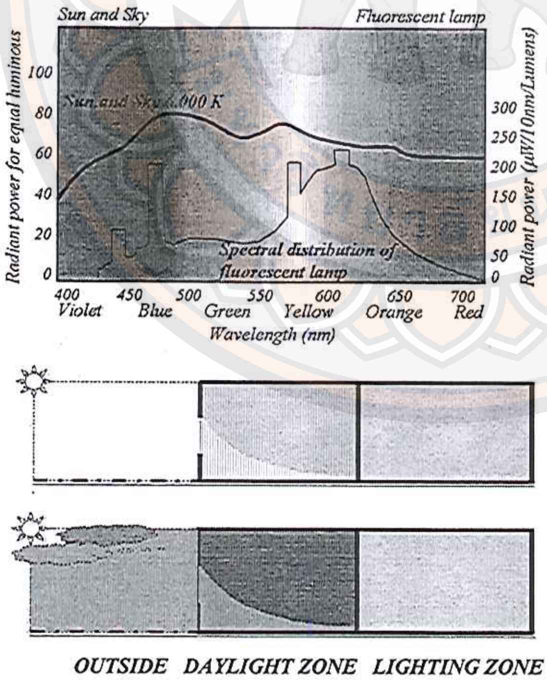

The spectrum curve of electric light sources not same the sunlight spectrum, which effect biological effect not for physiological effect, because the eye can not separate the color of light spectrum only white color [14]. Furthermore, the room that using artificial light has continuously luminance all time but another room that using daylight varies the outside environment condition, which effects to human perception about the circumstance.

THE CLEAR SKY PERIOD

THE CLOUD SKY PERIOD

Figure 5 The comparison between electrical light and daylight

Source: Boubekri, Mohamed Daylighting [6]

6. The effect of shading devices on angles through windows

The form of the shading device affects reduction of solar heat gain including beam radiation and sky radiation. It lowers the angles of view at the same time. It can also be said that a shape of shading device is a factor determining the heat on the glass and clarity of view from the inside to the outside of the building. Figure 6 shows conditions of shapes of shading devices and angles of eyesight. In case (b), the shading device slightly outstretched is easy for a structure system, cheap and able to create clear angles. However, it cannot prevent solar radiation for the period of time when the sun goes down. In cases (a) and (c), the outstretched part of the shading device is longer than case (d), (e) and (f). Normally, shading devices are designed short due to structure, cost, law and aesthetics.

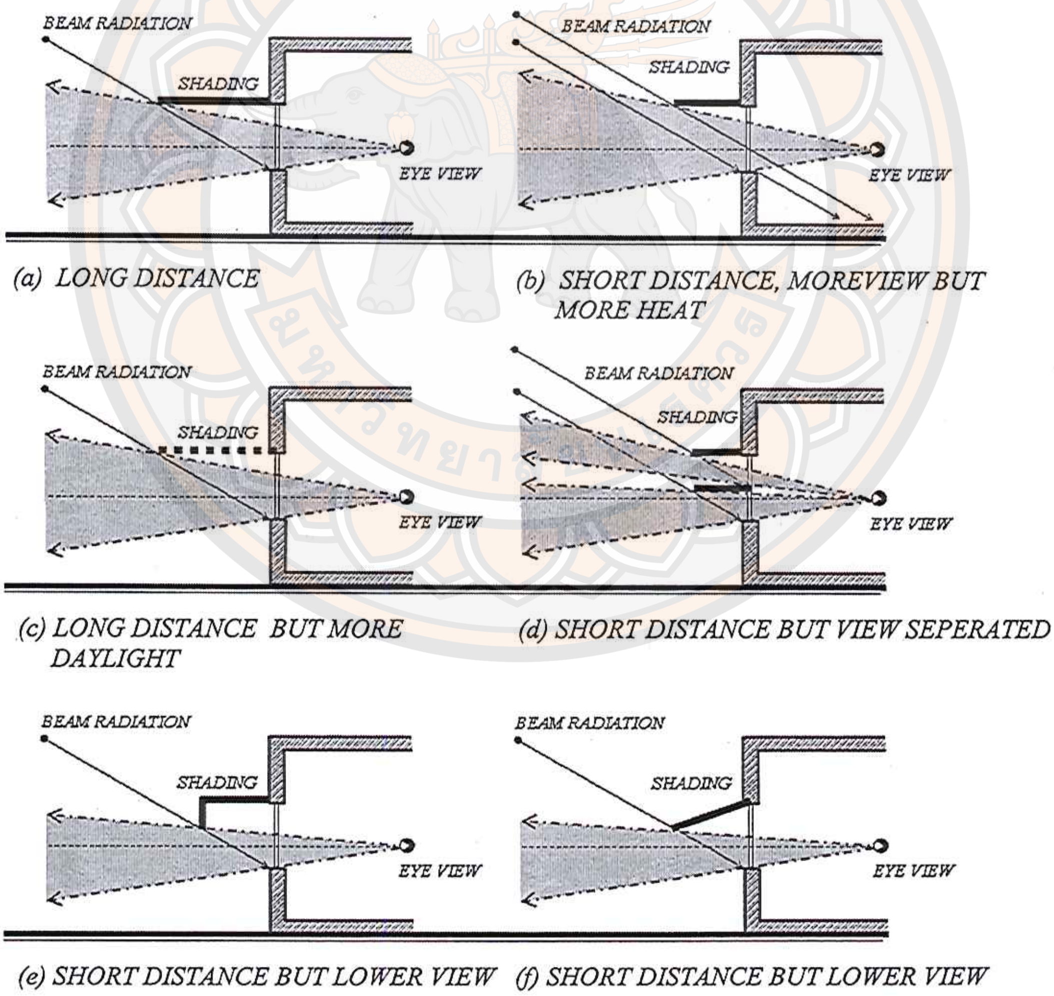

Figure 6 The relation of angle view and shading device form

7. Uncomfortable glare from sky

Daylight used to replace electrical light will shine through the windows on a plane perpendicular to eyesight looking outside. Glass is a material that lets light through it is like a light source shining directly in people's eyesight. The brighter of the sky is more uncomfortable of a glare occurs. Furthermore, windows cannot keep out direct solar radiation or sun light coming through the windows, so visibility is decreased by the disabling glare. This phenomenon, however, depends on luminance around the field of vision, apparent size of the source, direction of eye viewing and level of eye adaptation [8].

In case of a disabling glare occurs when a window receives too much luminance directly shining on the field of vision causing disability in differentiating or sight, which is the same case when perceiving the actual sun in the sky. This is one of the reasons for designing a shading device for direct solar radiation prevention. Additionally, uncomfortable glare will cause eye fatigue.

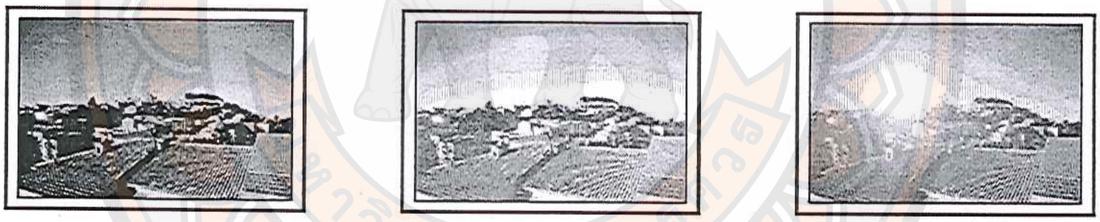

COMFORTABLE *UNCOMFORTABLE GLARE* *DISABLE GLAR*

Figure 7 The glare effect from the window

8. Distance of receiving daylight from side windows

Normally, light outside the building is at 10,000-20,000 lux and about 100,000 lux when including direct solar radiation measured on the working plane in the case of a clear sky or overcast sky. However, it will decrease 30% and get lower when using a more outstretched shading device. In this case, the daylight factor can be used in estimation as the shading device causes daylight reduction in distance far from the window. This causes insufficient light for some activities in the area considered far from the window. However, at the distance very far from the window, there is no change of light in any of shading device case with different outstretched parts.

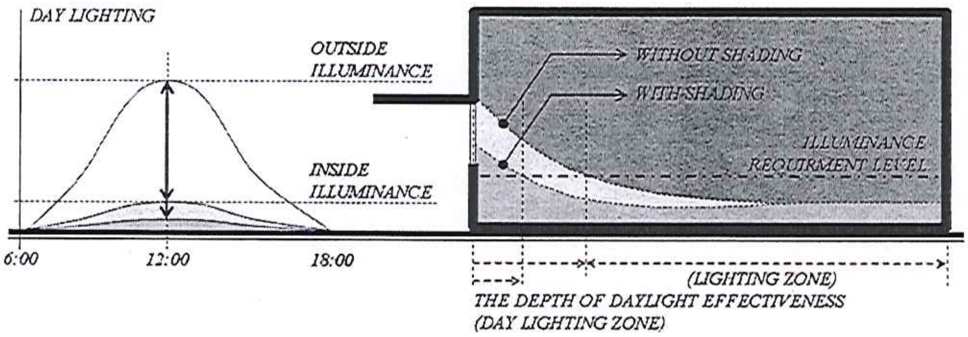

Figure 8 Effectiveness of daylight in working space

9. **Building Integrated Photovoltaic system (BIPV)**

Renewable energy is free, clean, eco-friendly energy generated endlessly by natural sources such as solar, wind, biomass, geothermal, hydro, wave and tidal. Photovoltaic technology is an alternative, turning energy gained from the sun into electrical energy. This technology is uncomplicated and easy to apply and manage. In case of installation on building envelope, PV module should be used instead of other exterior building materials as shown in the Figure 9.

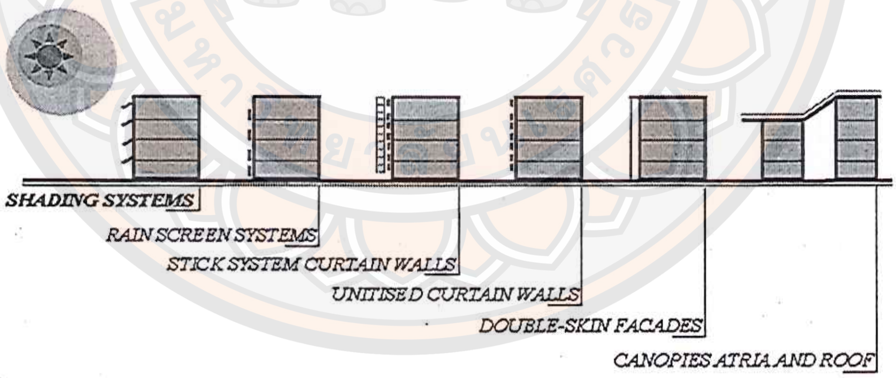

Figure 9 The building integrated PV options

Source: Simon Roberts and Nicolo Guariento [27]

In the past 10 years of studying BIPV systems, 5 aspects that need to be focused on are as follows:

Analysis of Thermal effects affecting capacity of electricity generation.

9.1 Analysis of annual energy generation compared to heat gained in case of designing semi-transparent solar cells

9.2 Analysis of energy and expenses for BIPV systems produced by using semi-transparent solar cells

9.3 Benefits, cost and increasing value for BIPV systems

9.4 Design techniques affecting electrical energy generation

Every aspect is summarized in Table 1 and the aspect of searching for installation ideas for the module on the building mostly focused on aspects of expenses and usability of semi-transparent solar cells.

Table 1 The aspects from international paper since 1999 (10 years)

Problem of studies	Sample of papers
The effect of PV working	
1. Thermal effect of PV efficiency	[43]
2. PV ventilated of PV module	[40], [45]
3. Heat and power output of PV system	[39], [42], [51]
4. Cost and benefit of PV system	[38], [39], [41], [46], [47], [49]
The effect of PV design	
1. Semi-transparent PV module	[43]
(window, wall, skylight, roof)	[38], [39], [42], [46], [49], [51]
2. PV facades Ventilated	[40], [45]
3. Concentrating of PV module	[50]
4. Shading integrated PV module	[44]

10. Advantages and disadvantages of BIPV options.

BIPV options were presented in the form of building envelope such as wall panel, roof, side/top light and shading. In the case of a tropical building, solar heat gain shining through window or glass, which is also called transparent material letting heat in through both conduction and radiation, should be avoided. It is better to use insulating material and prevent solar radiation by using a shading device.

However, as PV module is not considered insulation, it should not be installed instead of vertical plane glass despite that there is a usable type because of its transparency. This is also because it is the worst angle for receiving solar radiation. As for installing it as a roofing material, it still needs to add more layers of heat insulators the same way wallpaper being used. Unlike shading devices, there is no need for insulation because its angle can be adjusted according to appropriateness, and it provides benefits in terms of heat prevention module and light control for both air conditioning systems and lighting systems consuming most of the energy in the building.

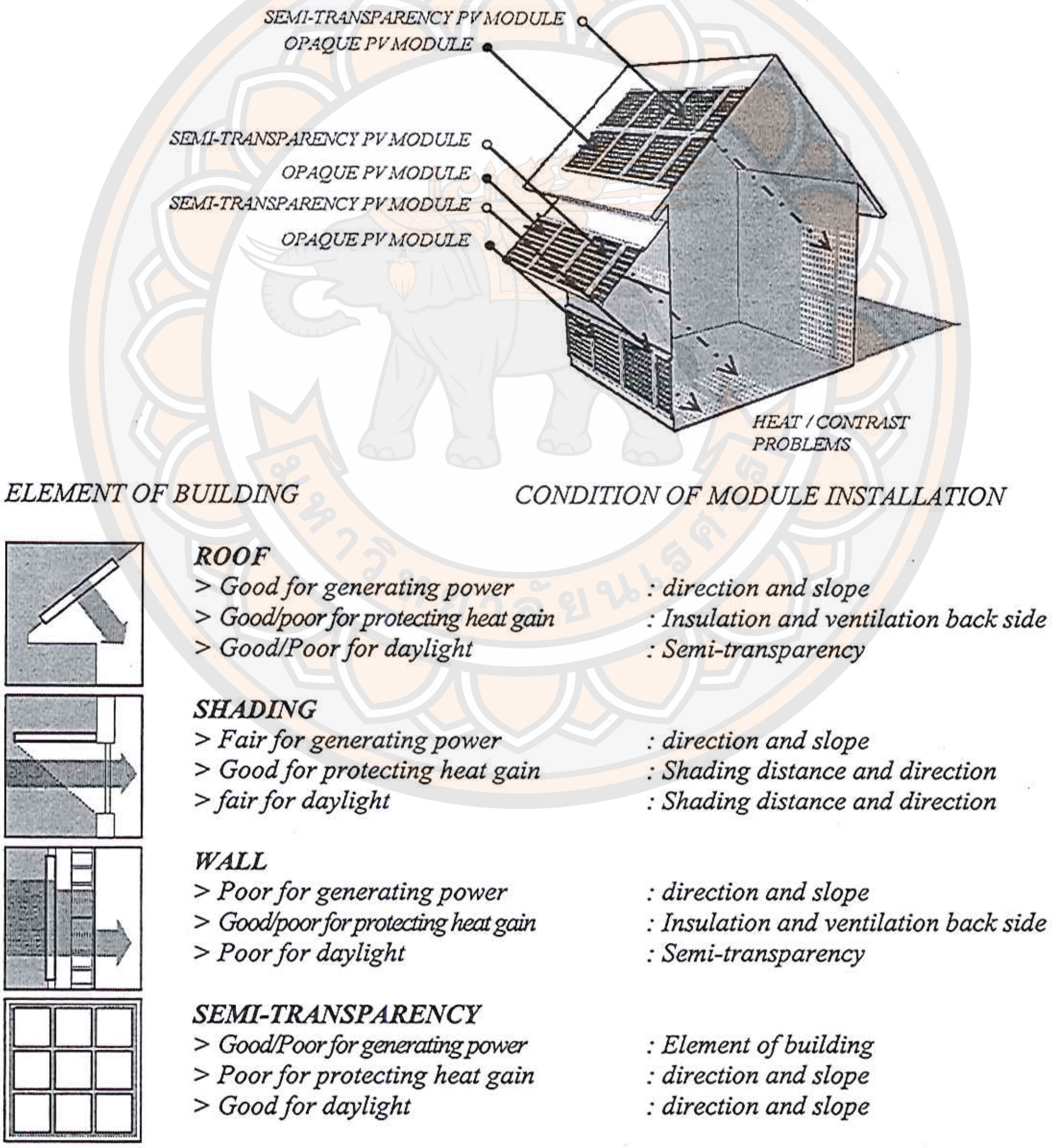

Figure 10 BIPV options for the tropical building design

11. The reduction of solar radiation on solar module plane

Solar modules installed on a vertical plane such as building wall (like the case of a shading device, or SIPV, under half sky according to Figure 11) diffuse sky radiation divided into 2 parts by shading of the building's vertical plane. The plane is a blocker of direct solar radiation for the period of time when the sun is behind the shading device. Solar radiation reflected with a wall plane above solar module will be more or less depending on reflectance of the reflector, which is different from installation on a flat plane without any covering.

Therefore, SIPV receives total solar radiation falling down against the solar module from beam radiation, half sky radiation, ground reflected radiation and building reflected radiation. This is due to the problem of shade effect from the building, which affects decreasing in electric current production. Therefore, SIPV contains problem of decreasing solar radiation caused by building itself.

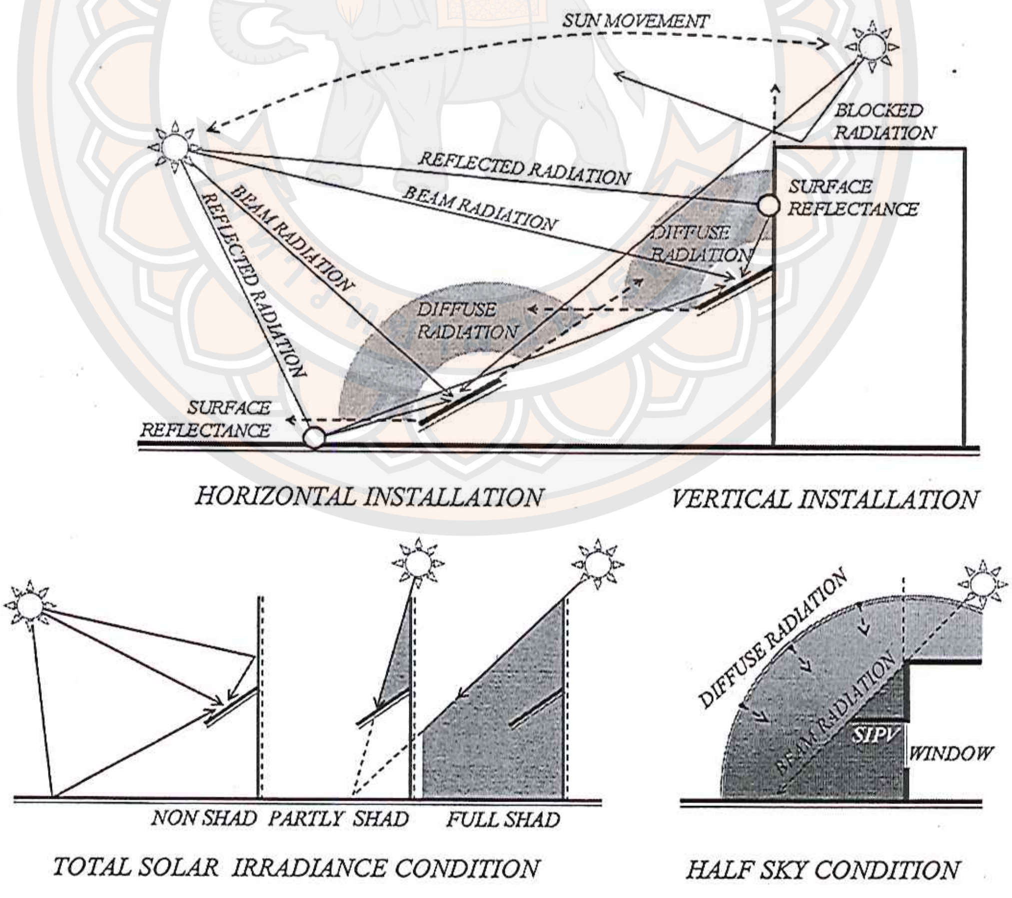

Figure 11 The effect of vertical installation

12. The investment of Photovoltaic system

The BIPV system is one type of building material capable of producing energy. The amount of produced energy depends on the amount of total solar radiation falling down on skin of the solar cells and area supporting solar radiation (both direct and diffused solar radiation). In the case of SIPV limited conditions than is the case on the roof unobstructed because it is material that depends on efficiency of electricity production and area of installation on the building. Plus, solar module is more expensive when compared to other materials or energy production technology, wind turbine technology, biomass technology and hydro turbine technology etc. as shown in Figure 12 below.

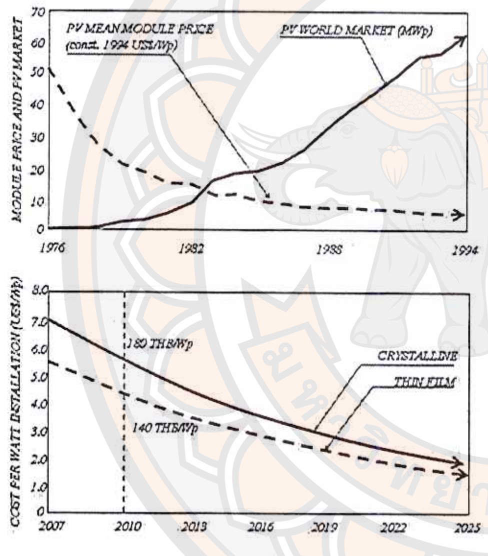

The present time, the cost decreases contentiously when the PV market increases contentiously too. And the trend of installation in the future is still increase, which affects the PV price as well.

The trend of the PV technology cost gradually reduces after 2010. For solar home system, 50 homes of PEA project in 2002 estimates the energy cost approximately 12 THB/kW-hr and the price is 190-220 THB/Wp.

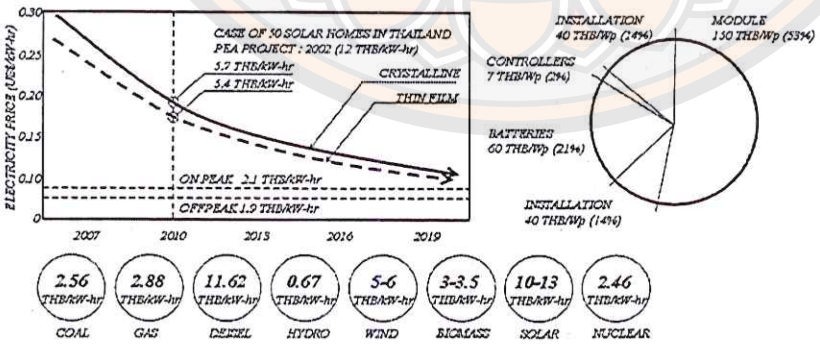

Figure 12 The PV pricing trends and electrical prices

Source: V. Napatra [35]; Banmuang [59]; John Schmitz [70]; Martin LaMonica [75]; Michael S. Davies [77]; United Nations University [91]

In 2010, price of crystalline silicon technology is higher than thin film technology's at about 180 THB/W_p and 140 THB/W_p respectively. Although photovoltaic technology results in cheap electricity bill of 5.4-5.7 THB/kWh and ratio of solar module price is at 53% of system price referred from example of investment to install in solar home project, BIPV provides more benefit than just produce electrical energy such as decreasing expenses of building envelope material, structure without using area to install. Especially, in case of SIPV which can reduce the use of energy in air conditioning system and lighting system. Therefore, it is considered an interesting advantage when comparing to disadvantages of producing process.

Conclusion of problems for research

SIPV is appliance for clean energy production, heat prevention and light control designed to use with windows in the condition of comfort zone regarding temperature and light and discerning out the window. The problems are as follows:

1. SIPV prevents heat from solar radiation coming into windows. However, it decreases a chance to receive daylight and perceive view outside the window.

2. SIPV cuts out some part of solar radiation due to installation on vertical plane with building as sunshade blacking solar radiation from getting in.

3. SIPV is producing electricity energy. However, it is still an expensive technology.

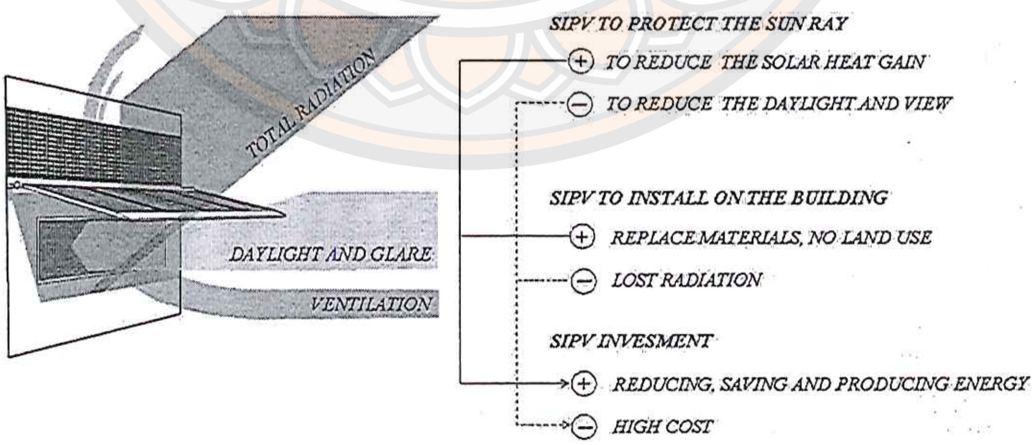

Figure 13 Advantages and disadvantages of SIPV

Conceptual design for problem solving

SIVP design aims to optimize installation to save total energy of building. The concepts are as follows:

1. To prevent direct solar radiation and part of diffuse radiation from half sky radiation

2. To adjust level of daylight shining in through the window to make most angles and least glare

3. To find direction, inclined angle and suitable installation to be able to produce most of energy from operation of solar module

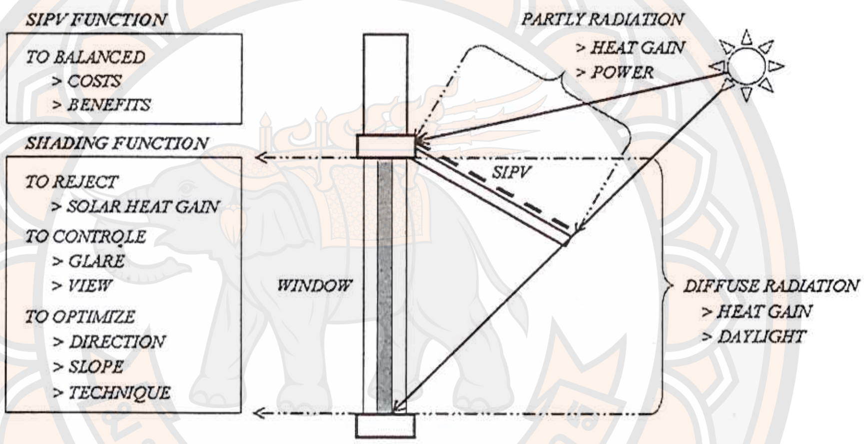

Figure 14 Integrative functions of SIPV

Purpose of research

1. To optimize shading to decrease heat gain and increase daylight usability of shading device integrated photovoltaic system

2. To optimize costs and benefits of shading device integrated photovoltaic system

Hypothesis

Shading device integrated photovoltaic system helps in reducing cooling load of air conditioning system and make a use of daylight to save energy from lighting load including creating a clear angle of buildings in Thailand.

Conceptual framework

This research focuses on designing shading device integrated photovoltaic system containing 4 steps as shown in Figure 15

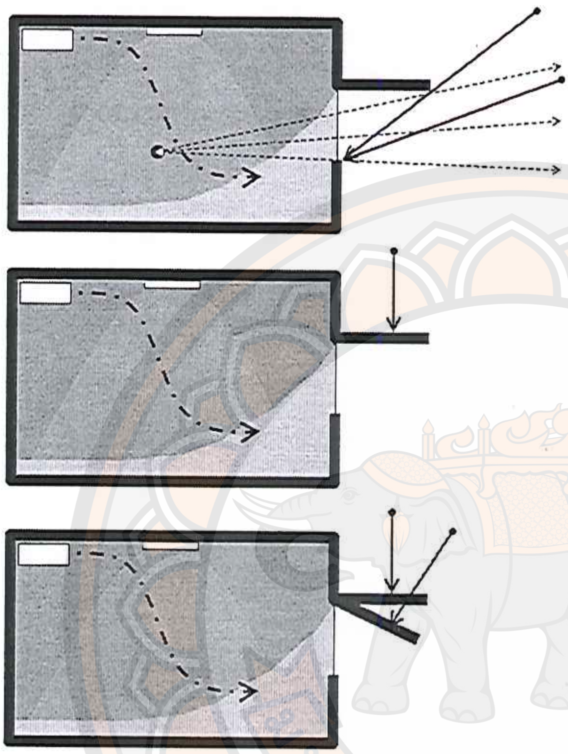

1. Optimization in preventing direct solar radiation in each direction and receiving daylight due to the outstretched part of shading device.

2. Calculation of total radiation falling down on inclined plane of shading device and efficiency resulting from condition of receiving solar radiation under half sky state.

3. The use of tracking technique to increase energy production and more opportunity for the view to be in sight which is suitable according to each period of time.

4. Economical optimization by using benefit and cost ratio and payback period.

Figure 15 4 steps of frame work

Research conditions

If it is for study experiment and analysis, there are 4 conditions as follows:

1. Design for Latitude of Thailand

2. Studying from models installed at SERT, Naresuan University, Pisanulok and Faculty of Architecture, Chiang Mai University, Chiang Mai, Thailand

3. Case study and data collection are the use of the solar module of amorphous silicon and poly crystalline silicon technologies belonged to SERT, Naresuan University, Pisanulok

4. Economic optimization from direct and indirect analysis

Benefits of research

Benefits of this research occurred from the idea of green building are as follows:

1. Building system can save the total energy of building by using shading device integrated photovoltaic system

2. The clear angle of windows comes from the design of shading device integrated photovoltaic system

3. The investment in shading device integrated photovoltaic system is worth and can receive payback in a short period of time

Key words

Key words for this research are such as

1. SIPV is Shading Device Integrated Photovoltaic System

2. Working space is room for general activities and 3.0 meters height measured from the floor to ceiling

3. Comfort space is room that dry air circulate and relative humidity are controlled at 25 °C and 55% RH respectively. Appropriate air conditioning system and lighting at the working plane is 300 lux minimum receiving artificial light and daylight coming through the window

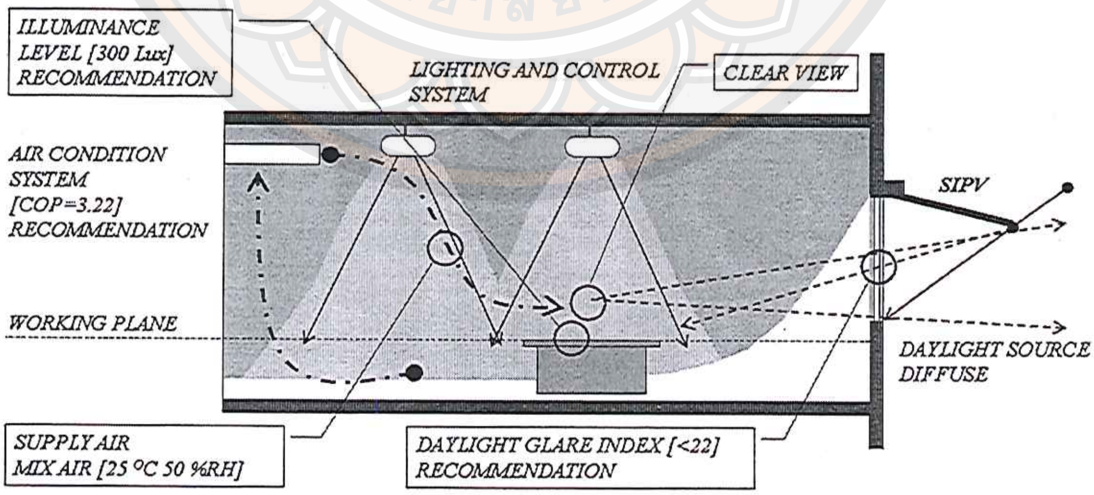

Figure 16 Key words of study design

CHAPTER II

REVIEW OF RELATED LITERATURE AND RESEARCH

Knowledge diagram

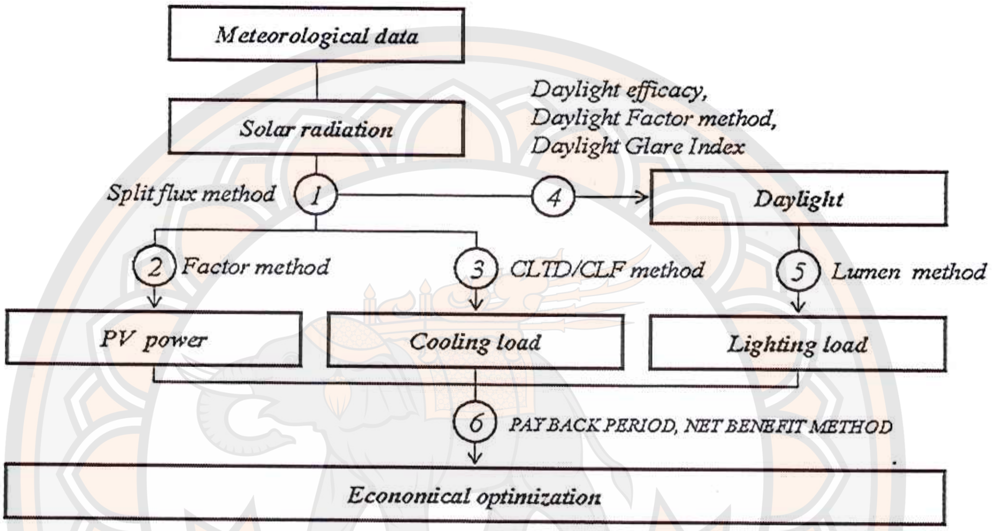

Figure 17 Diagram of knowledge for studing

Meteorological data

This study is related to solar energy and the climate of Thailand which has characteristics different from cold countries. Studying an actual database collected from area of interest was practiced to anticipate the values. The results were more accurate than using the default data of the equation value anticipation program. Metrological data for this research consists of global solar radiation, diffuse solar radiation and ambient temperature collected by the Thai Meteorological Department (TMD) and from the School of Renewable Energy Technology (SERT), where data is managed hourly for the whole year in the form of a typical meteorological year (TMY).

However, collected data is different every year depending on influences of phenomena such as monsoon, cold and warm current, etc. The data study was studied over 5 years in 2006-2010 as presented in Table 2.

Table 2 The weather data during the year

Year	Condition compare with normal year (average of 1971-2000)
2006	7% over for raining, almost hotter, 2 tropical cyclone
2007	4% over for raining, almost hotter, 3 tropical cyclone
2008	11% over for raining, almost hotter, 1 tropical cyclone and 3 closer
2009	4% over for raining, almost hotter, 1 tropical cyclone
2010	5% over for raining, all hotter, 1 tropical cyclone

Source: Thai Meteorological Department [86, 87, 88, 89, 90]

Solar radiation

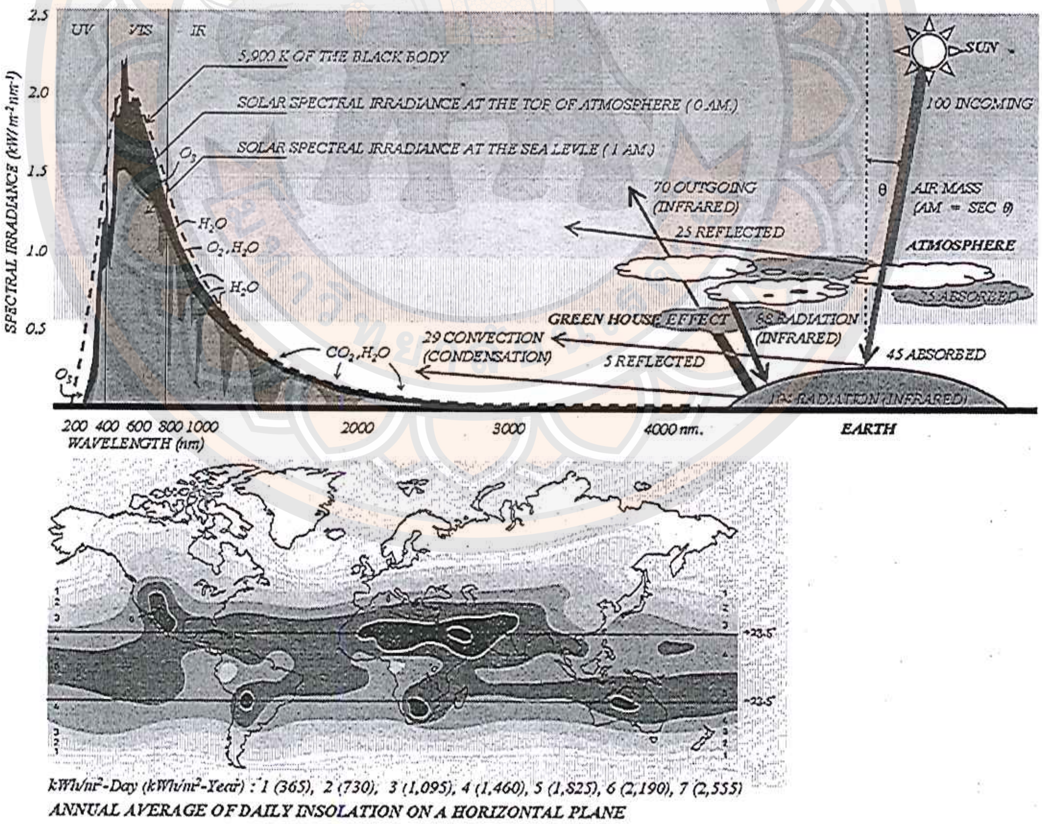

Figure 18 Solar insolation on earth

Source: Simon Roberts and Nicolo Guariento [27]; Learner, Annenberg [73]

The solar radiation, electromagnetic radiation passing through the earth's atmosphere down to the surface, about 45% is absorbed and 30% is reflected back. However, 25% is absorbed by atmosphere composed of ozone, carbon dioxide and water vapor.

In studying solar radiation, sun-earth angle was used for this research to estimate total irradiance on slope surface in both cases of a PV module and a glass window. As Thailand is located in a tropical zone with a large amount of vapor and dust in the air, variables regarding location and weather such as latitude, longitude, weather data and solar radiation should be considered in estimation of any values. Therefore, specific characteristics of design conditions will be revealed, as shown in Figure 19 explaining the process in solar irradiance calculation.

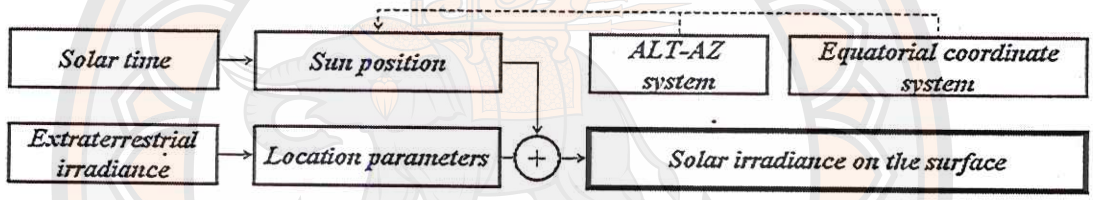

Figure 19 The calculation's process of solar irradiance on the surface

1. Solar time

Figure 20 shows the relation of earth-sun position, which is the system of positioning changed by the time of day. Solar time is calculated by the equation [19] as follows:

$$t_S = t_{SL} + (EOT / 60) + [(L_{SM} - L_{ON}) / 15] \quad \text{Eq. 1}$$

$$EOT = 9.87 \, SIN \, 2B - 7.53 \, COS \, B - 1.5 \, SIN \, B \quad \text{Eq. 2}$$

$$B = 360 \, [(N - 81) / 364] \quad \text{Eq. 3}$$

Table 3 The conversion of the day Number

Month (Day)	Day Number, *N*	Notes
January (31)	d	d is the day of the month
February (28)	d + 31	
March (31)	d + 59	Add 1 when leap year
April (30)	d + 90	Add 1 when leap year
May (31)	d + 120	Add 1 when leap year
June (30)	d + 151	Add 1 when leap year
July (31)	d + 181	Add 1 when leap year
August (31)	d + 212	Add 1 when leap year
September (30)	d + 243	Add 1 when leap year
October (31)	d + 273	Add 1 when leap year
November (30)	d + 304	Add 1 when leap year
December (31)	d + 334	Add 1 when leap year
	Days of Special Solar Interest	
Solar event	**Date**	**Day number, N**
Vernal equinox	March 21	80
Summer solstice	June 21	172
Autumnal equinox	September 23	266
Winter solstice	December 21	355

Note: Solstice and equinox dates may vary by a day or two. Also, add 1 to the solstice and equinox day number for leap years.

Source: John A. Duffie and William A. Beckman [18]

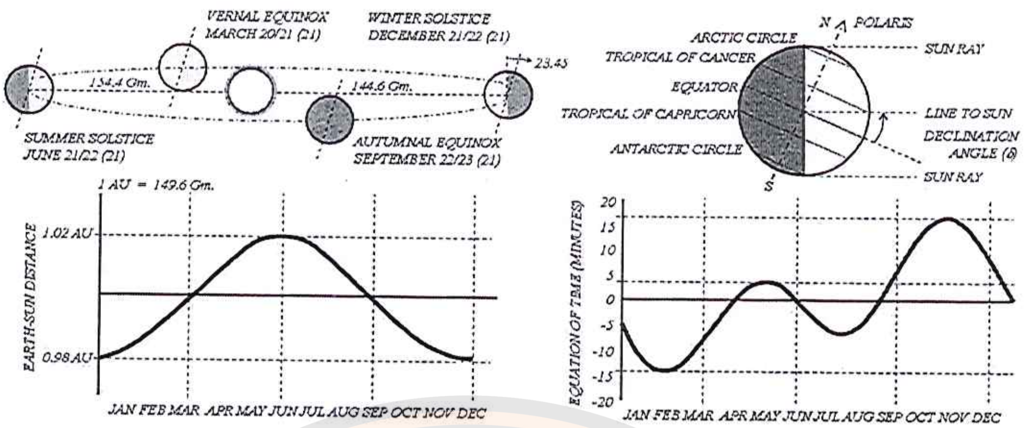

Figure 20 Orbit of the earth-sun and the equations of the relations

Source: American Society of Heating, Refrigerating and Air-Conditioning Engineers [2]; Kreider F. Jan and Curtiss S. peter [19]; William Stine and Michael Geyer [95]

2. Sun position

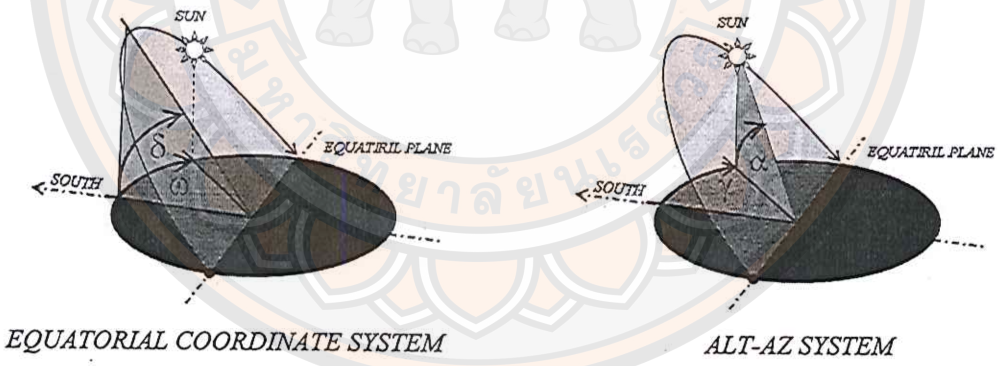

Figure 21 Co-ordinate systems of the Earth-Sun geometry

2.1 Equatorial coordinate system [19]

The coordinate system based on the celestial equator and the celestial poles are both defined in a similar manner to latitude and longitude on the surface of the earth, which is the equatorial coordinate system. This system defines the sun position with the hour angle that varies by the solar time and the declination angle that varies by the day number. Both are expressed as follows:

$$\omega = 15(t_S - 12) \qquad \text{Eq. 4}$$

$$\delta = 23.45\ SIN\ [360(284 + N)/365] \qquad \text{Eq. 5}$$

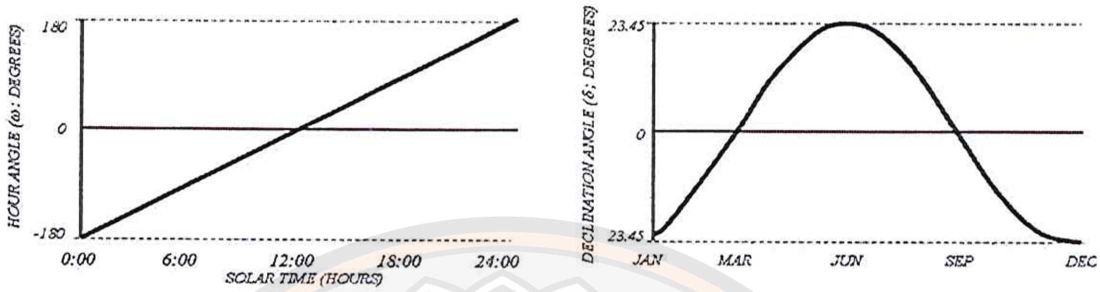

THE HOUR ANGLE COORDINATION *THE DECLINATION ANGLE COORDINATION*

Figure 22 Co-ordinate system of the equatorial coordinate system

2.2 ALT-AZ system [19]

ALT-AZ system [19], a local coordinate system, defines the sun position with the solar altitude angle that varies by the latitude location, the declination angle and the hour angle. Another is the solar azimuth, which varies by the declination angle and the hour angle, also. These are expressed as follows:

$$\theta_Z = COS^{-1}\ (COS\ \phi\ COS\ \delta\ COS\ \omega + SIN\ \phi\ SIN\ \delta) \qquad \text{Eq. 6}$$

$$\alpha = 90 - \theta_Z \qquad \text{Eq. 7}$$

$$\gamma = SIN^{-1}\ (COS\ \delta\ SIN\ \omega\ /\ SIN\ \theta_Z) \qquad \text{Eq. 8}$$

The sun path diagram is a tool used to design a shading device by specifying the altitude angle and the coordinates of time, such as the day and the solar time, in deciding the outstretched part of the shading device shown in both Figure 23 and Figure 24, which were simulated by Ecotect program.

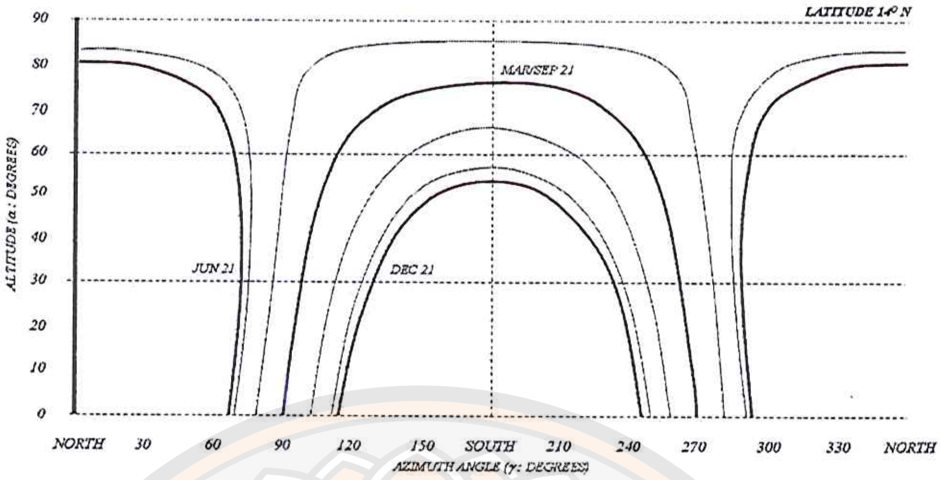

Figure 23 Co-ordinate system of the ALT-AZ system of the 14^O N latitude

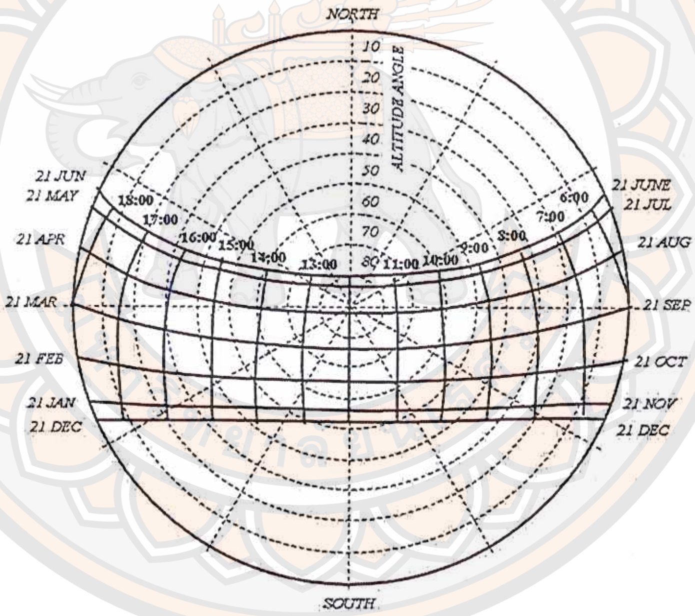

Figure 24 The sun path diagram of the 14^ON latitude

3. The extraterrestrial irradiance

Extraterrestrial irradiance is irradiance on a perpendicular plane outside the earth's atmosphere AM 0 with the constant of 1,367 W/m^2. It can be expressed by Eq.9 [2] as follows:

$$E_0 = 1{,}367\,[1 + 0.034\,COS\,(2\pi N / 365.25)] \qquad Eq.\ 9$$

4. Location parameter and hourly terrestrial irradiance

In Figure 18, the terrestrial irradiance on the earth's surface reduced by the mass of the atmosphere is divided into beam solar irradiance and diffuse solar irradiance from the sky presented by air mass (AM) definition as Eq. 10 [2]. The atmosphere is composed of dry air (such as N_2, O_2, and CO_2), inert gas, water vapor, and particles. This composition varies according to location and climate.

$$AM = SEC\ \theta_E \qquad Eq.\ 10$$

The ratio of diffuse solar irradiance to total solar radiance is used to estimate diffuse solar irradiance using data collected by the weather station of location needed for estimation. Janjai, S., et al. [16] presented the relative functions between the ratios of the diffuse irradiance and the total irradiance in the form of the hourly clearness index, K, as follows in Eq.11-14

$$E_d / E_t = 0.8004 + 1.7153\,K - 7.3459\,K^2 + 5.5780\,K^3\ ;\ CM \qquad Eq.\ 11$$

$$E_d / E_t = 0.6934 + 2.3406\,K - 8.0800\,K^2 + 5.6614\,K^3\ ;\ UB \qquad Eq.\ 12$$

$$E_d / E_t = 0.7091 + 1.8910\,K - 6.2693\,K^2 + 3.9744\,K^3\ ;\ SK \qquad Eq.\ 13$$

$$E_d / E_t = 0.6772 + 2.5680\,K - 8.8866\,K^2 + 6.3828\,K^3\ ;\ NP \qquad Eq.\ 14$$

Note: CM is Chiang Mai province
UB is Ubon Ratchathani province
SK is Son khla province
NP is Nakhon Pathom province

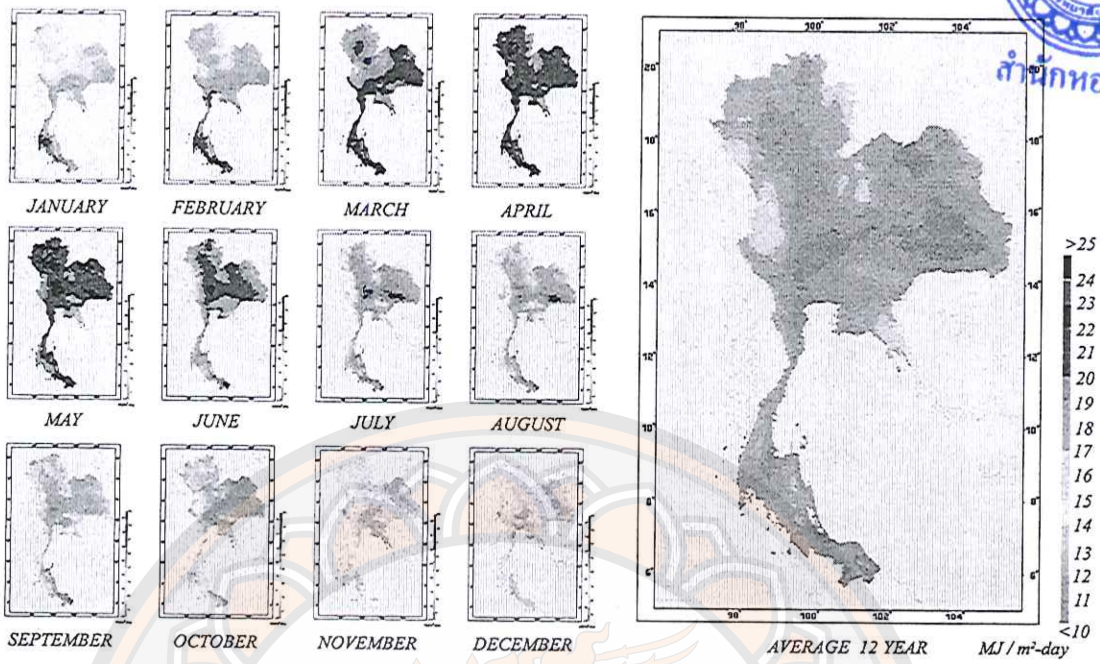

Figure 25 The solar maps of Thailand

Source: Department of Alternative Energy Development and Efficiency [65]

In Thailand, there is a solar map presentation by the Department of Alternative Energy Development and Efficiency (DEDE) and Faculty of Science, Silpakorn University [65] as shown in Figure 25.

5. Solar irradiance on the slope surface

ASHREA [2] presented the estimation of total irradiance on a slope surface shown in Eq.15 composing of the speech about beam solar irradiance, diffuse solar irradiance and ground reflected solar irradiance. However, the equation is based on a hypothesis named the isotropic sky model suggested by Hottel and Wortz (1942) and derived by Liu and Jordan (1963) as shown in Figure 26. However, the form of the anisotropic sky model is detailed in calculation more than the form presented by Hay and Davies (1980) consisting of horizontal sky term, the circum solar diffuse and the diffuse sky term. The form of the NDKR model (the Hay, Davises, Klucher, Reindl model) improved from the Hay and Davides model by Klucher (1979) and by Reindl, et al. (1990) had its composition divided further which is the horizontal sky term as shown in Figure 26.

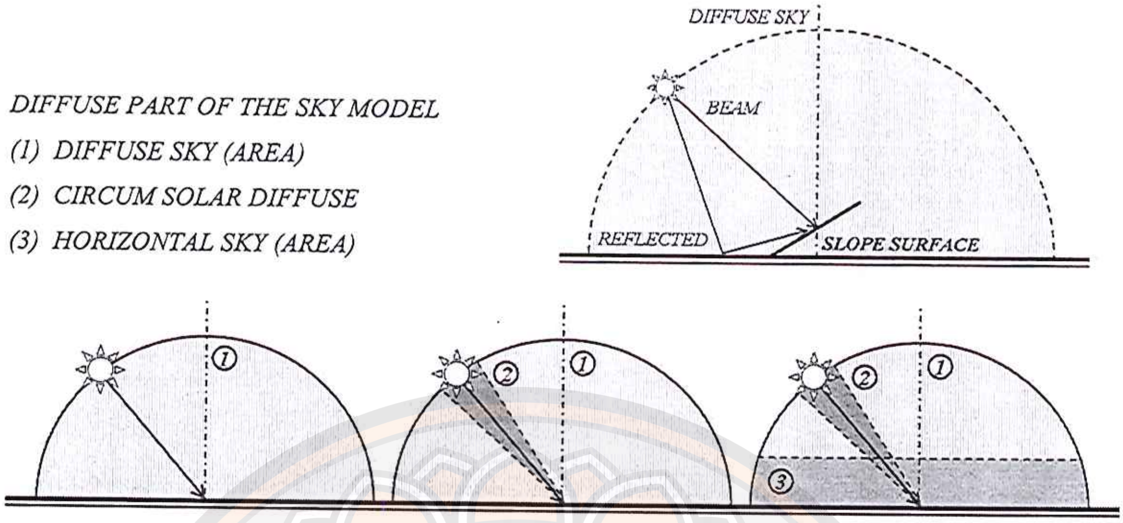

ISOTROPIC SKY MODEL (Eq15) ANISOTROPIC SKY MODEL(Eq16) HDKR SKY MODEL (Eq17)

Liu and Jordan (1963) Hay and Davies (1980) Klucher (1979)/ Reindl, et al. (1990)

Figure 26 The comparison of sky models

Source: John A. Duffie and William A. Beckman [18]

The anisotropic sky model was tested in estimation. As a result, it has a higher value than the isotropic sky model by about 7%. Also, the estimation of HDKR model was higher than the isotropic sky model by about 9% with the test of the same instance. However, the isotropic sky model is simpler in trying to understand and estimate. ASHREA suggested that the circum solar diffuse and horizontal sky were not significant for annual energy performance calculations and Jan F. Kreider, et al. [19] suggested that the accuracy of the isotropic model will usually be sufficient for building. Where A_i is an anisotropic index, is an indicator of solar beam transmission getting through the earth's atmosphere.

$$E_{tS\text{-}ISO} = E_b R_b + E_d R_d + \sigma_g E_G R_{rG} \quad \text{Eq. 15}$$

$$E_{tS\text{-}ANI} = (E_b + E_d A_i) R_b + (1 - A_i) E_d R_d + \sigma_g E_G R_{rG} \quad \text{Eq. 16}$$

$$E_{tS\text{-}HDKR} = (E_b + E_d A_i) R_B + (1 - A_i) E_d R_d [1 + f\, SIN^3(\beta/2)] + \sigma_g E_g R_{gr} \quad \text{Eq. 17}$$

$$R_b = COS\theta_i / COS\theta_Z \quad \text{Eq.18}$$

$$R_d = (1 + COS\beta)/2 \quad \text{Eq. 19}$$

$$R_{rG} = (1 - COS\beta)/2 \quad \text{Eq. 20}$$

$$A_i = E_{DN} / E_O \quad \text{Eq. 21}$$

$$f = E_d / E_G \quad \text{Eq. 22}$$

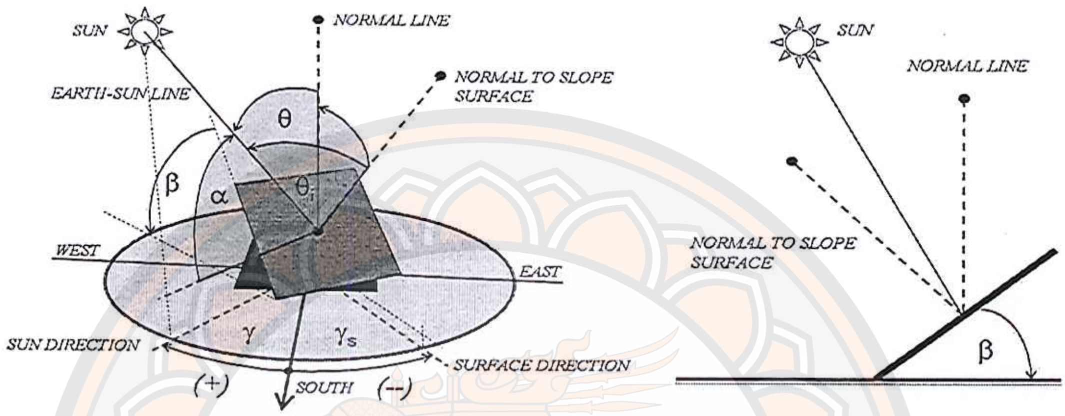

Figure 27 The geometry of earth-sun line on slope surface

Source: American Society of Heating, Refrigerating and Air-Conditioning Engineers [2]

ASHREA [2] presented equations such as Eq. 23-32 with variables A, B and C as determination of the solar irradiance intensity containing the A, B and C values shown in Table 4.

$$E_{tS} = E_{DN} COS\theta_i + E_d + E_{rG} \quad \text{Eq. 23}$$

$$E_{DN} = A / exp\,(B / SIN\alpha) \quad \text{Eq. 24}$$

$$Y = 0.55 + 0.437\, COS\theta_i + 0.313\, COS^2\theta_i \; ; COS\theta_i > -0.2 \quad \text{Eq. 25}$$

$$Y = 45 \quad ; COS\theta_i <= -0.2 \quad \text{Eq. 26}$$

$$E_d = CYE_d \quad ; \text{Vertical surface} \quad \text{Eq. 27}$$

$$E_d = CYE_d\,[(1 + COS\beta) / 2] \quad ; \text{Other slope} \quad \text{Eq. 28}$$

$$E_{rG} = E_{DN}\,[(C + SIN\alpha)\rho_g\,[(1 - COS\beta) / 2] \quad \text{Eq. 29}$$

$$COS\theta_i = SIN\delta\; SIN\phi\, COS\beta - SIN\delta\, COS\phi\, SIN\beta\, COS\gamma \quad \text{Eq. 30}$$

$$+ COS\delta\, COS\phi\, COS\beta\, COS\omega + COS\delta\, SIN\beta\, SIN\gamma\, SIN\,\omega$$

$$+ COS\delta\, SIN\phi\, SIN\beta\, COS\gamma\, COS\omega$$

$$COS\theta_i = SIN\theta_Z \, SIN\beta \, COS(\gamma_S - \gamma) + COS\theta_Z \, COS\beta \qquad Eq.\ 31$$

$$COS\theta_Z = COS\phi \, COS\delta \, COS\omega + SIN\phi \, COS\delta \qquad Eq.\ 32$$

Table 4 The relative data of extraterrestrial irradiance (the base year of 1964)

Month	E_0	EOT	Declination	A	B	C
(21st day)	W/m²	min	degrees	W/m²	Dimensionless ratio	
Jan	1416	−11.2	−20.0	1230	0.142	0.058
Feb	1401	−13.9	−10.8	1215	0.144	0.060
Mar	1381	−7.5	0.0	1186	0.156	0.071
Apr	1356	1.1	11.6	1136	0.18	0.097
May	1336	3.3	20	1104	0.196	0.121
June	1336	−1.4	23.45	1088	0.205	0.134
July	1336	−6.2	20.6	1085	0.207	0.136
Aug	1338	−2.4	12.3	1107	0.201	0.122
Sep	1359	7.5	0.0	1151	0.177	0.092
Oct	1380	15.4	−10.5	1192	0.16	0.073
Nov	1405	13.8	−19.8	1221	0.149	0.063
Dec	1417	1.6	−23.45	1233	0.142	0.057

For Thailand radiation data at the Bangkok station, 14°N latitude, during year 2009 was practiced estimation using ASHREA's equation determining reflectance of general ground surface at 0.2 [2] as shown in Figure 28. It was found that maximum solar radiation was 1,840 kW/ m^2 -Year at a slope surface of 20 degrees turning south. It decreased more than half when the slope at the angle was 70 degrees turning north between NW and NE.

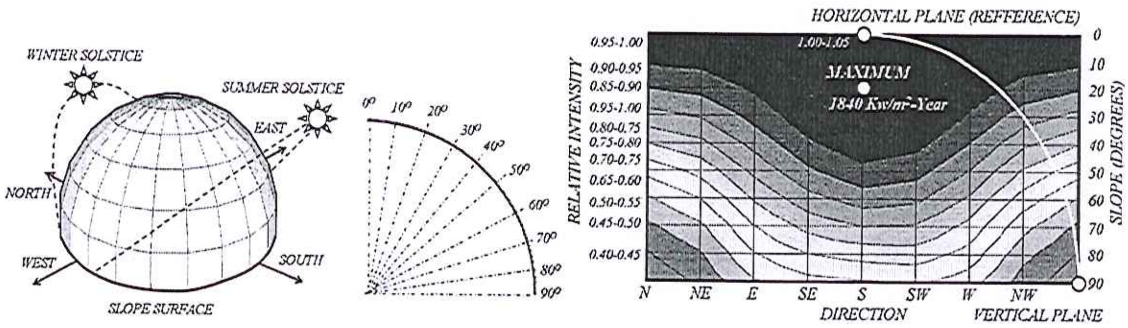

Figure 28 The relative intensity of annual solar irradiance of Thailand

Table 5 The relative intensity of annual solar irradiance on surface of Thailand

Slope	Direction							
(degrees)	N	NE	E	SE	S	SW	W	NW
Global	1.000	1.000	1.000	1.000	1.000	1.000	1.000	1.000
10	0.960	0.966	0.987	1.010	1.023	1.017	0.996	0.973
20	0.904	0.917	0.959	1.003	1.028	1.016	0.977	0.930
30	0.834	0.856	0.918	0.981	1.015	0.999	0.943	0.874
40	0.753	0.788	0.869	0.943	0.984	0.966	0.899	0.810
50	0.667	0.718	0.814	0.892	0.937	0.919	0.848	0.742
60	0.595	0.651	0.756	0.832	0.875	0.861	0.791	0.675
70	0.540	0.593	0.700	0.767	0.801	0.795	0.734	0.615
80	0.496	0.546	0.646	0.699	0.719	0.726	0.678	0.565
90	0.464	0.510	0.595	0.635	0.645	0.658	0.623	0.527

Note: initial data, global solar irradiance and diffuse solar irradiance collected hourly by TMD summed as the total 1,788 kW/m^2-Year that was compared with the estimated by the same process as the total 1,789 kW/m^2-Year, which was closely.

6. Solar irradiance on the tracking surface

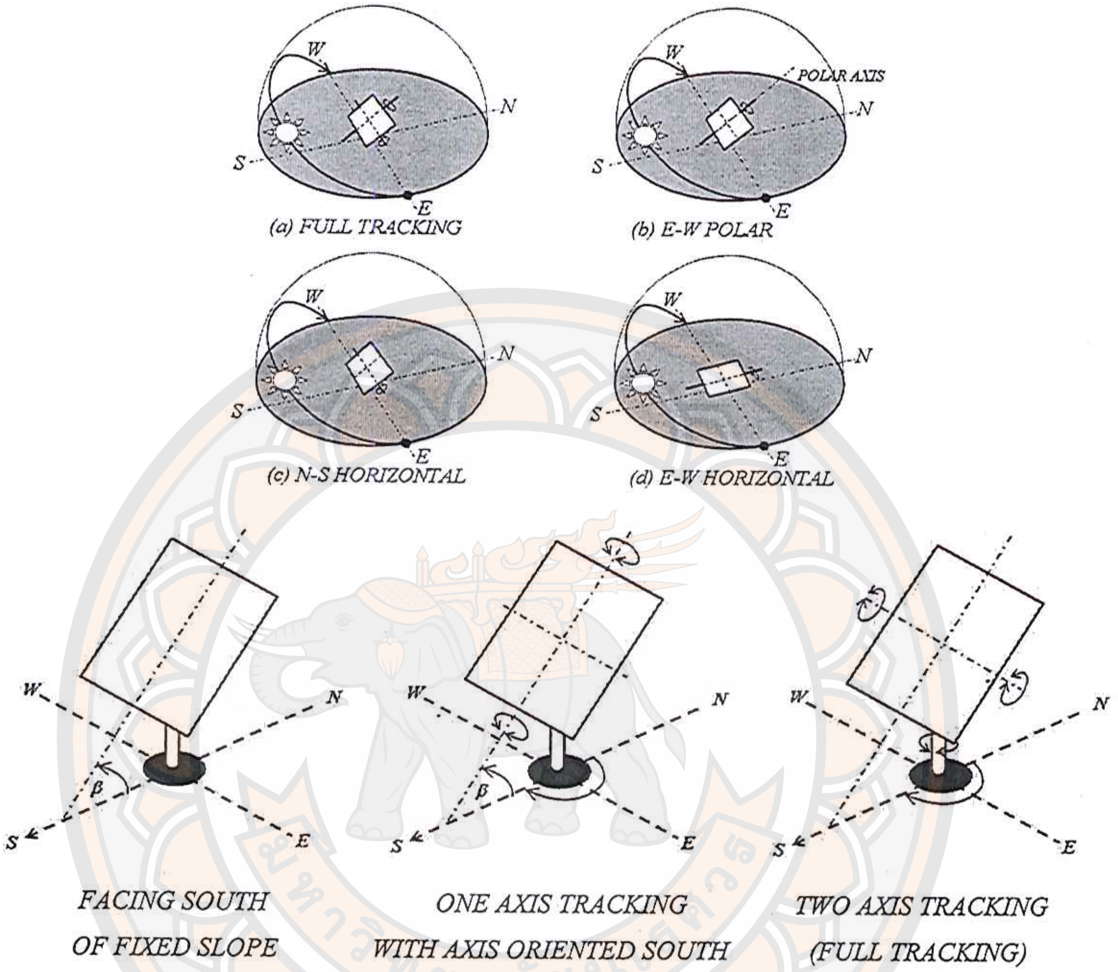

Figure 29 The type of PV tracking systems

Source: Magal, B.S. [22]

Tracking is the movement of the incident angle separated according to the pattern shown in Figure 29

6.1 Two axis tracking (a) [18, 22]

This movement function keeps the face to the sun at all times, as in Eq. 33.

$$COS\theta_i = 1 \qquad \text{Eq 33}$$

6.2 Fixed tilted with E-W tracking

6.2.1 Tilted N-S axis with tilted adjusted daily (like b) [18, 22]

The surface is a fixed slope on the N-S axis and rotated with the E-W axis, as in Eq.34 and the slope as in Eq.35.

$$COS\theta_i = SIN^2\delta + COS^2\delta\, COS\omega \qquad Eq.\ 34$$

$$\beta = |\phi - \delta|,\ if\ (\phi - \delta)>0\ ,\ \gamma_S = 0\ or\ if\ (\phi - \delta)<0\ ,\ \gamma_S = 180 \qquad Eq.\ 35$$

6.2.2 Polar N-S axis with E-W tracking (b) [18, 22]

The surface is a fixed slope on the N-S axis parallel to the axis of the earth, as in Eq. 36 and the slope as in Eq.37.

$$COS\theta_i = COS\delta \qquad Eq.\ 36$$

$$TAN\beta = TAN\phi\, /\, COS\gamma_S \qquad Eq.\ 37$$

6.3 Horizontal with tracking

6.3.1 Horizontal E-W axis with N-S tracking (c) [18, 22]

This movement is fixed parallel with the earth and tracking daily with the N-S axis, as in Eq. 38 of Duffie and Beckman (1991) and Eq. 39 of Meinel and Meinel (1976).

$$COS\theta_i = (1 - COS^2\delta\, SIN^2\omega)^{0.5} \qquad Eq.\ 38$$

$$COS\theta_i = ((SIN^2\delta + COS^2\delta\, COS^2\omega)^{0.5} \qquad Eq.\ 39$$

$$TAN\beta = TAN\theta_Z\, |COS\gamma| \quad ,if\ \gamma < 90,\ \gamma_S = 0\ or\ \ if\ \gamma > 90,\ \gamma_S = 180 \qquad Eq.\ 40$$

6.3.2 Horizontal N-S axis with E-W tracking (d) [18, 22]

This movement is fixed parallel with the earth and tracking all day with the E-W axis, as in Eq. 41 of Duffie and Beckman (1991) and Eq. 42 of Meinel and Meinel (1976) and slope as in Eq. 43.

$$COS\theta_i = (COS^2\theta_Z + COS^2\delta\, SIN^2\omega)^{0.5} \qquad Eq.\ 41$$

$$COS\theta_i = COS\phi\, COS\omega + COS\delta\, SIN^2\omega \qquad Eq.\ 42$$

$$TAN\beta = TAN\theta_Z / COS(\gamma_S - \gamma) / \ , if\ \gamma > 0,\ \gamma_S = 90\ or\ if\ \gamma < 0,\ \gamma_S = -90 \qquad Eq.\ 43$$

The comparison is estimated for 35° latitude with standard conditions shown in Figure 30

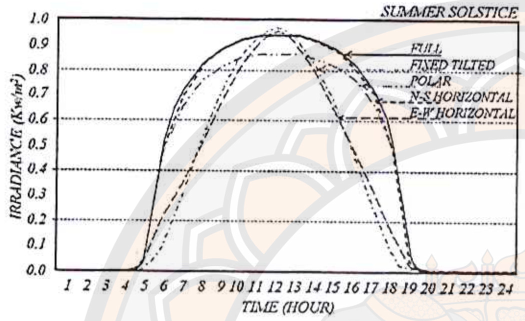

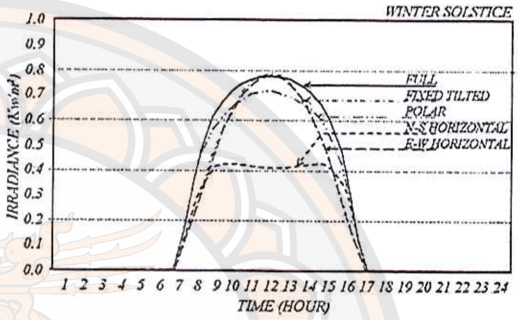

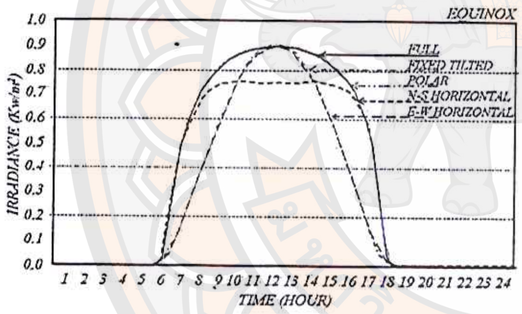

Mode	kWh/m^2			Percentage		
	E	SS	WS	E	SS	WS
Full T.	8.43	10.60	5.70	100	100	100
E-W polar	8.43	9.73	5.23	100	91.7	91.7
N-S H.	7.51	10.36	4.47	89.1	97.7	60.9
E-W H.	6.22	7.85	4.91	73.8	74.0	86.2

Note: E= Equinox, SS= Summer solstice, SW= Winter solstice

Figure 30 The solar irradiance of PV tracking systems

Source: Magal, B.S. [22]

Photovoltaic power system

This section reviews the energy produced by the photovoltaic system to be integrated with a shading device, which is a system used to convert the solar radiation as it is the heat source of air conditioning systems into electricity energy.

1. PV materials

The photoelectric process in semiconductor material studied and developed as many kinds of photovoltaic technologies can be ranged as shown in Figure 31. Composition of a PV module is shown in Figure 32. Well-developed technologies such as crystalline and amorphous silicon made up 85% of the market share. Both are made of silicon but with different procedures. One problem of PV technology was low efficiency conversion, so it was designed to have a composition that reduces received solar energy loss, for example, glass can be put on top of the solar module to trap light or reduce the degree of reflection with AR coating as shown in Figure 32.

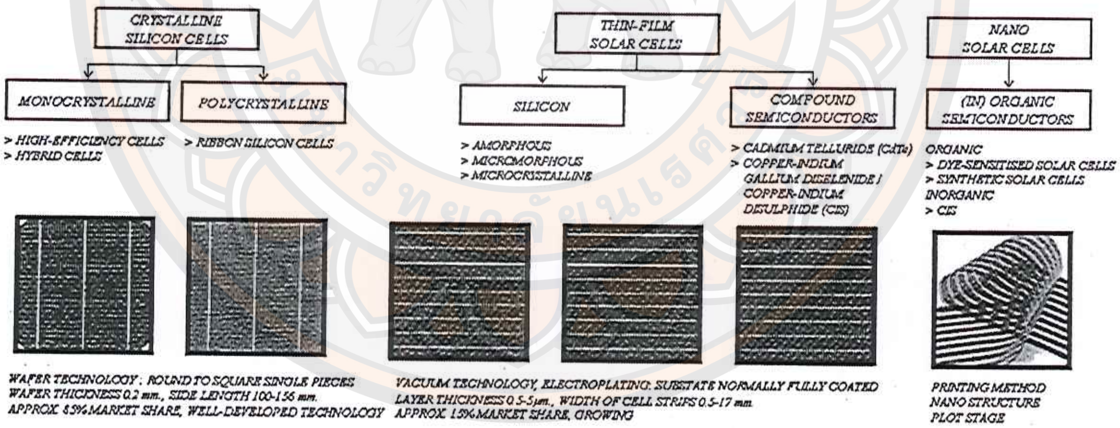

Figure 31 The classification of PV technologies

Source: Bernhard Weller, Claudia Hemmerle, Sven Jakubetz and Stefan Unnewehr [5]

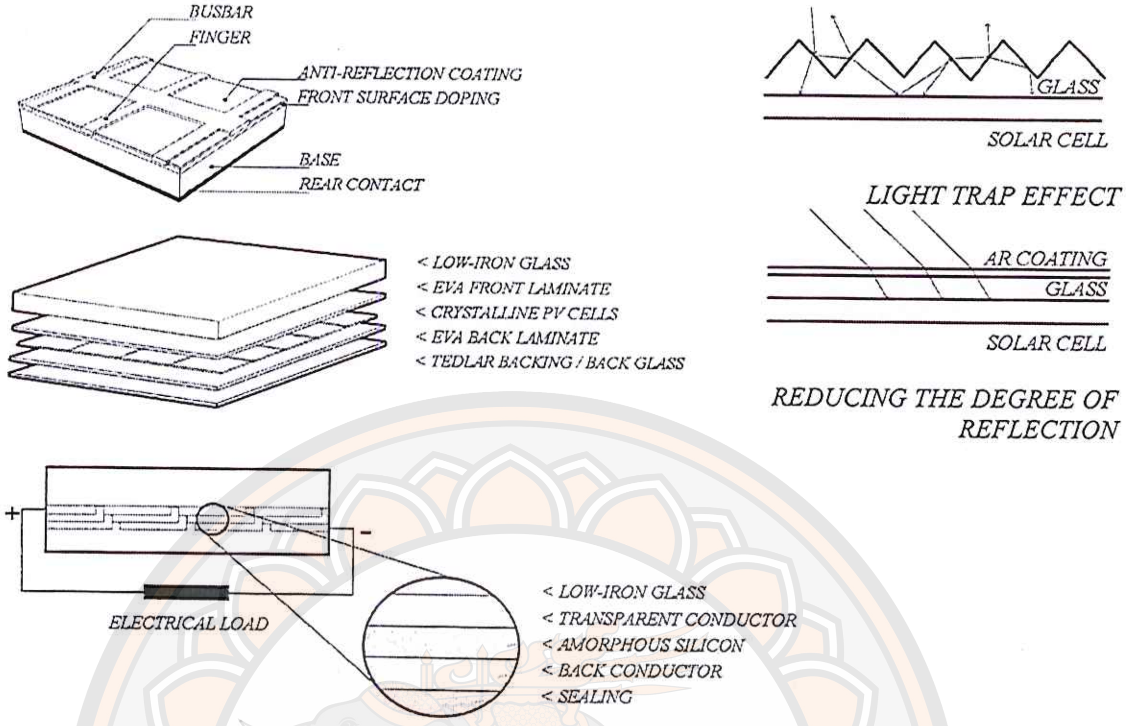

Figure 32 The components of PV module

Source: Bernhard Weller, Claudia Hemmerle, Sven Jakubetz and Stefan Unnewehr [5]; Simon Roberts and Nicolo Guariento [27]

2. PV module efficiency

PV modules are used in the production of electricity from light; it is a clean and renewable energy source. The conversion is caused from electrons and holds diffuse between the P-N junction depending on the energy band gap. However, the solar energy falling on the PV surface cannot convert to the electrical energy all, so the technology has low efficiency.

2.1 Spectral sensitivity

The efficiency of PV cells resulted from components of crystalline cells responding to the spectrum in a long-wave period better than thin-film cells. However, it responds less in a period of visible light as shown in Figure 33. C. Titiporn [54] found that in Thailand's climate, both technologies respond to energy production according to conditions of the sky, which change seasonally. Figure 34 shows the data collection for the study at SERT for 4 years.

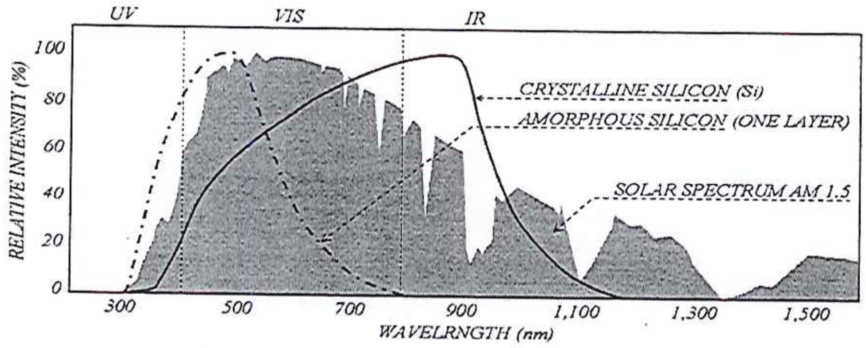

Figure 33 The relative intensity of PV materials

Source: Bernhard Weller, Claudia Hemmerle, Sven Jakubetz and Stefan Unnewehr [5]; Sterling, VA. [30]

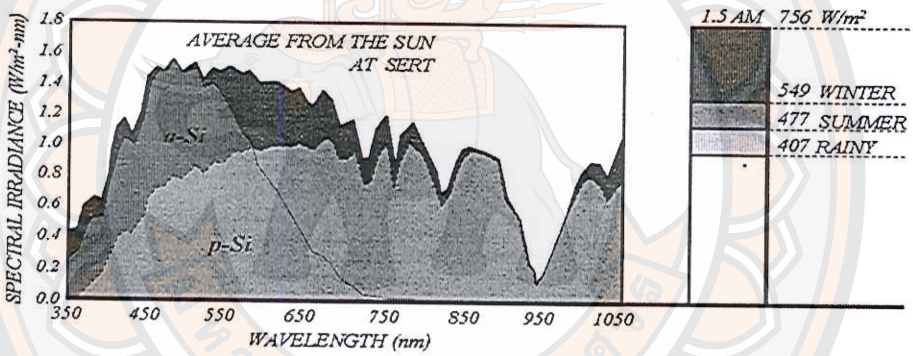

Figure 34 The responsive spectral irradiance of p-Si and a-Si in Thailand

Source: Bernhard Weller, Claudia Hemmerle, Sven Jakubetz and Stefan Unnewehr [5]

2.2 I-V curve characteristic and fill factor

Identity of PV was explained by the relation in the form of I-V curve (the character of PV unit can be expressed in the curve of I and V relationship) indicating efficiency and performance of each PV cell. It was tested using Standard Test Conditions (STC) such as module temperature at 25°C, solar irradiance on cell surface at 1,000 W/m^2 and 1.5 AM, or according to outdoor conditions determined by normal operating cell temperature (NOCT) conditions such as at 20° C, irradiance on cell surface at 800 W/m^2, wind velocity of 1.0 m/s and open back-side mounting.

Fill factor, FF, shown in Figure 35, in which proportion is reduced by the characteristic series resistance and shunt resistance affecting efficiency of a PV cell were able to be explained by using Eq. 44-47. FF of poly crystalline silicon and amorphous silicon was approximately 0.75-0.85 and 0.56-0.61, respectively [30].

$$\eta = P_o / P_i \qquad \text{Eq. 44}$$

$$= P / E_{tS} A_{PV} \qquad \text{Eq. 45}$$

$$= FF\, I_{SC}\, V_{OC} / P_i \qquad \text{Eq.-46}$$

$$FF = P_{MP} / I_{SC}\, V_{OC} \qquad \text{Eq. 47}$$

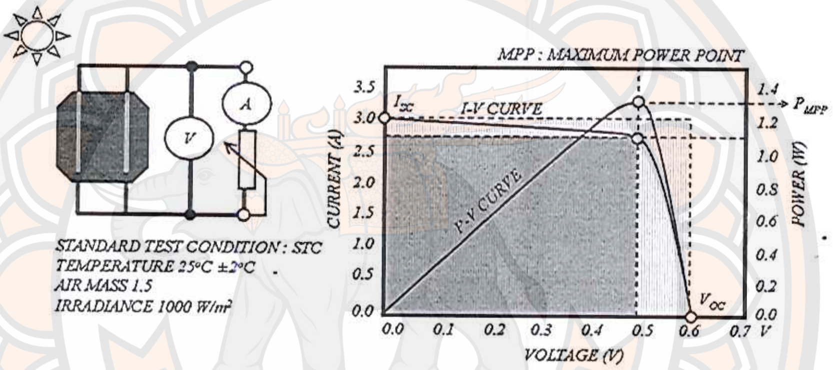

Figure 35 The curve characteristic and fill factor

Source: Simon Roberts and Nicolo Guariento [27]; Sterling, VA. [30]

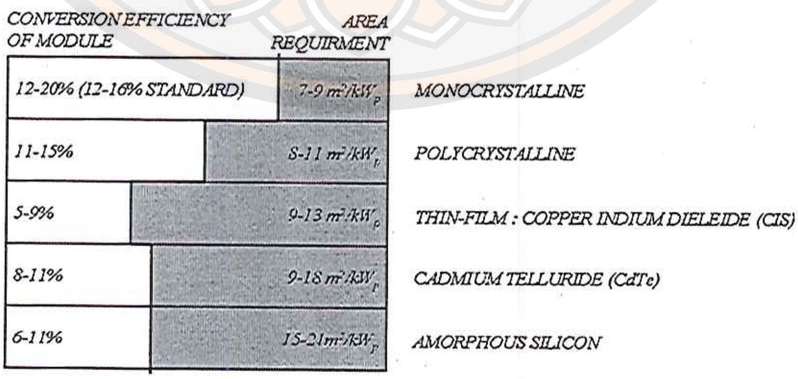

Figure 36 The conversion efficiency of module technologies

Source: Simon Roberts and Nicolo Guariento [27]; Sterling, VA. [30]

As for installation, the surface area of the panels is very impotent due to the limited area of the building surface and limited area suitable for solar radiation reception.

2.3 Module temperature effect

The diode model expressed in Eq. 48 [68] showed current: I which was varied according to cell temperature and voltage: V_{oc}. It also decreased with higher levels of temperature cell as shown in Eq. 49 [68].

$$I = I_0 [\exp(qV/nkT) - 1] - I_L \qquad \text{Eq. 48}$$

$$V_{OC} = (kT/q) \ln (I_{SC} / I_0) \qquad \text{Eq. 49}$$

Note: at 300.00 K (26.85°C), kT/q = 25.850 mV, the thermal voltage. at 298.15 K (25.00°C), kT/q = 25.693 mV

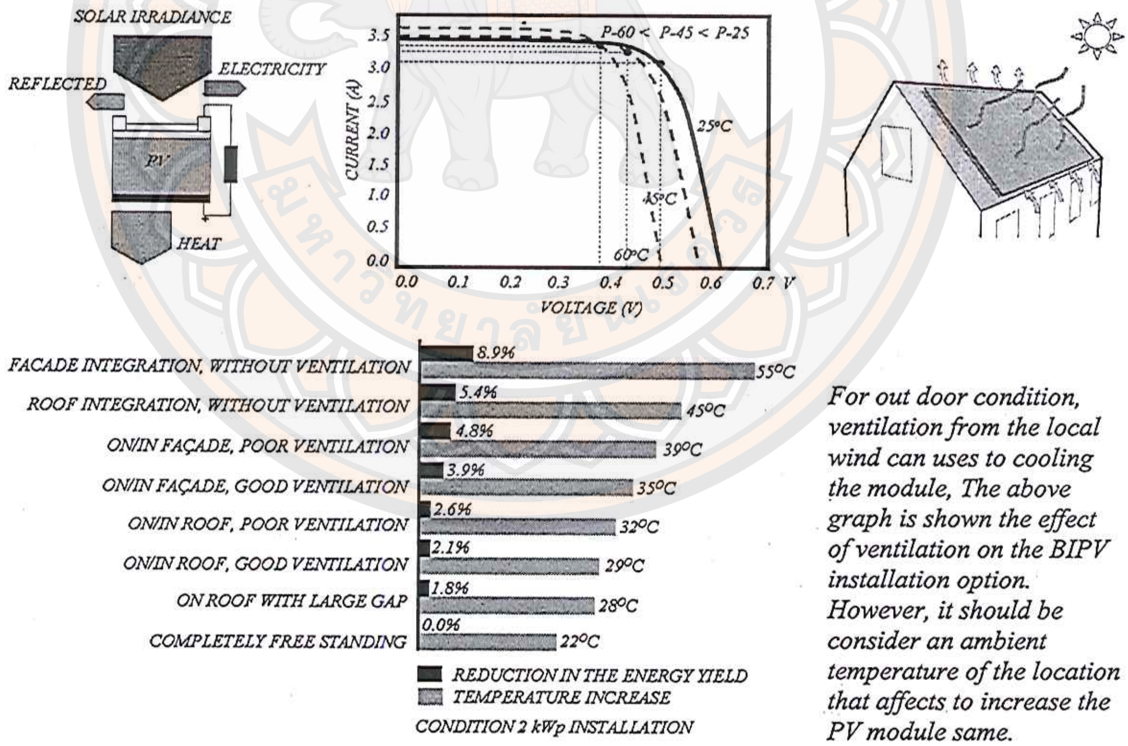

Figure 37 The module of temperature effect

Source: Simon Roberts and Nicolo Guariento [27]; Sterling, VA. [30]

The open circuit voltage slightly constant decrease as the irradiance change when the irradiance fall below 100 W/m² does the voltage break down and rapidly decrease, which likes the overcast sky condition.

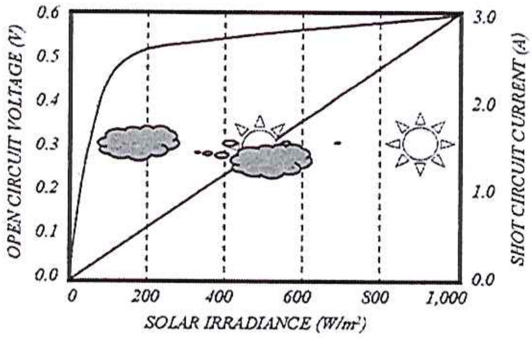

Figure 38 The sky condition and the PV electrical characteristics

Source: Sterling, VA. [30]

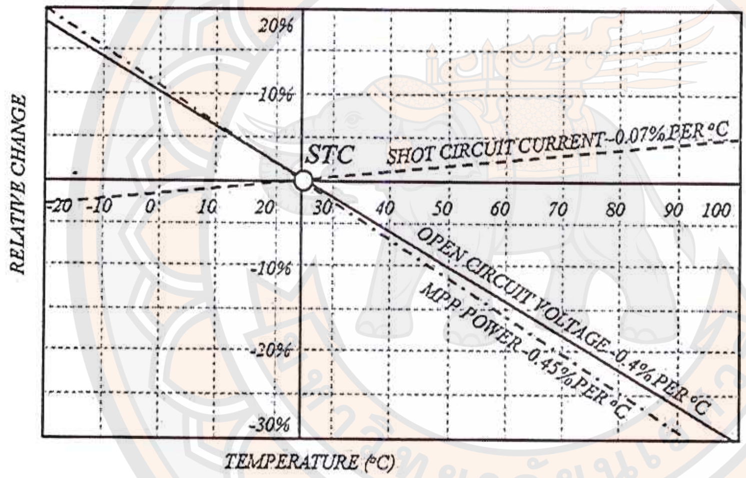

TEMPERATURE COEFFICIENT (% /°C)

CRYSTALLINE SILICON

-0.4 TO -0.5

AMORPHOUS SILICON

-0.21

CADMIUM TELLURIDE (CdTe)

-0.25

COPPER INDIUM GALLIUM SELENIDE (CIGS)

-0.32 to 0.36

Figure 39 The relative change of PV parameters

Source: Energy Market Authority and Building and Construction Authority [12]; Sterling, VA. [30]

The PV array, the group of PV modules, was installed on the roof or building surface, causing less ventilation than standalone PV array installation. It is the same as shading device installation. However, if a photovoltaic system were designed to be integrated into the system in a form of shading device, it would create better ventilation around the PV module. A comparison of the differences is shown in Figure 37.

3. The losses of PV system

Figure 40 illustrates the average the losses of a sample BIPV system and the temperature effects of different installations. In the case of a CIS warm façade, loss because of temperature was about 6% with no shadow effect. Roof-mounted installation losses due to temperature were about 3.5% and 2% from shadow effect. According to study cases, the most loss was from inverter operation was 10% and 7% respectively.

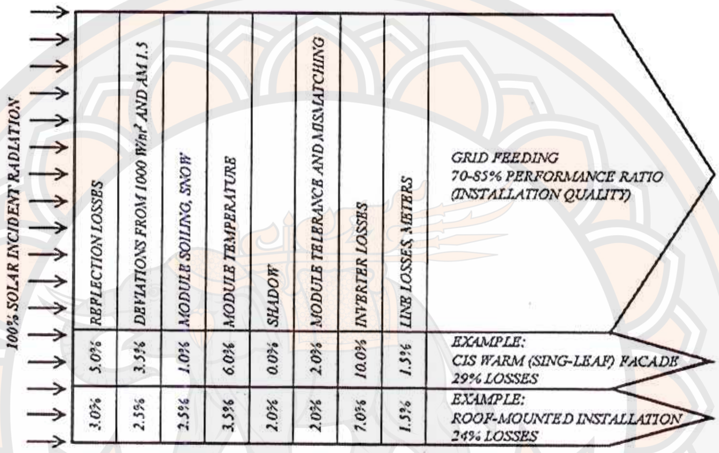

Figure 40 The energy loss and performance ratio for the PV installations

Source: Jesse Henson [17]

3.1 Shadow effect

For BIPVs in the city received partial shade on the PV cell connection shown in Figure 41 affected current or volt reduction according to cell connection.

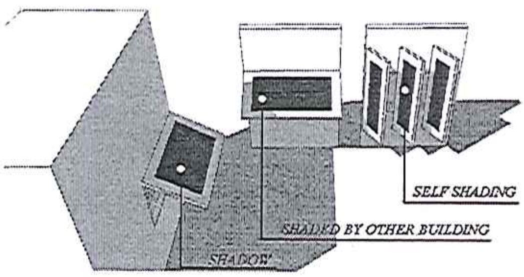

Figure 41 Shading effect on PV module

3.2 Degradation and Failure Modes

Degradation is a parameter that shows the stability and resistance to corrosion of the materials affecting the decreased efficiency or less electricity producing capacity of system operation or. Normally, the manufacturer guarantee is set at 20 years, which indicates the quality of bulk silicon PV modules currently being produced.

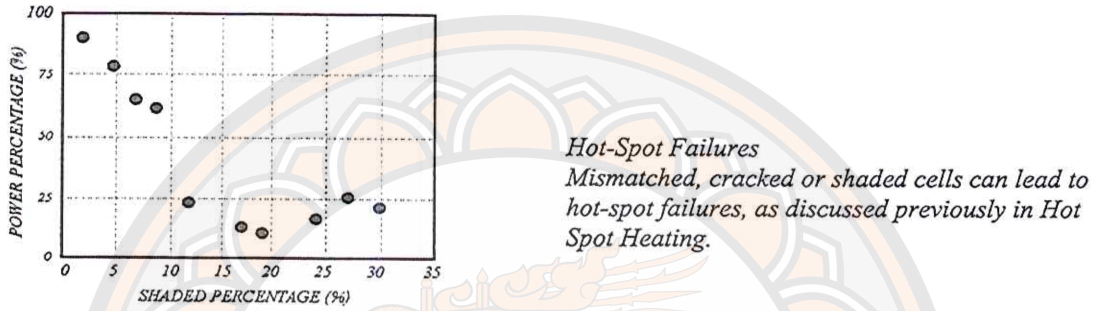

Figure 42 The relation of shading on the PV array and PV power

Source: Deo Prasad and Mark Snow [10]

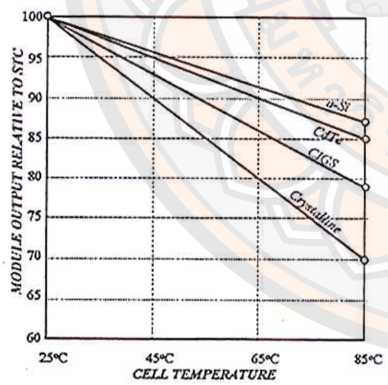

Technologies	*Temperature Coeficiency (%/°C)*
Crystalline	*-0.40 to -0.45*
CIGS	*-0.32 to -0.36*
CdTe	*-0.25*
a-Si	*-0.21*

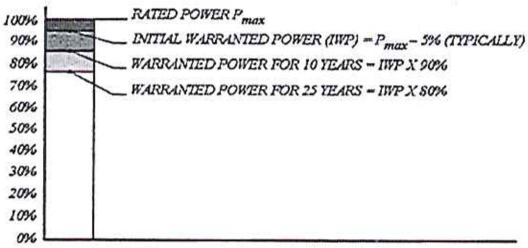

Figure 43 The PV efficiency drop

Source: Building and Construction Authority [63]

PV modules produces under STC have a limited power output warranty. Most manufacturers guarantee at least 90% of the minimum rated output for 10 years and 80% of the minimum rated output for 20-25 years. It should be noted that the minimum rated output is usually defined as 95% of the rated output to allow for manufacturing and measurement tolerances, which is illustrated in Figure 43.

3.3 Inverter efficiency

The inverter is the element in charge of converting electricity produced by the PV system and connects with the parallel or series PV module as shown in Figure 44. This component works under weather conditions affecting the efficiency depending on the severity of radiation. B. Tharika [53] found that 40% of energy content was produced from solar irradiance between 720 and 960 W/m^2 and 92% of the efficiency of the inverter for operation under Thailand radiation was more than 90%. However, energy content in solar irradiance between 0-350 W/m^2, which was a period of diffuse irradiance, created inverter efficiency at 20% causing negative results towards electrical energy production, as shown in Figure 45.

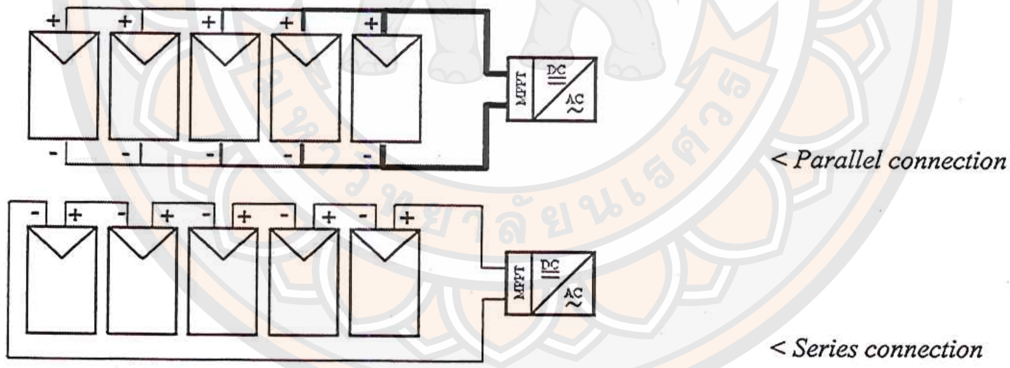

Figure 44 The connection of PV modules with an inverter

Source: Simon Roberts and Nicolo Guariento [27]

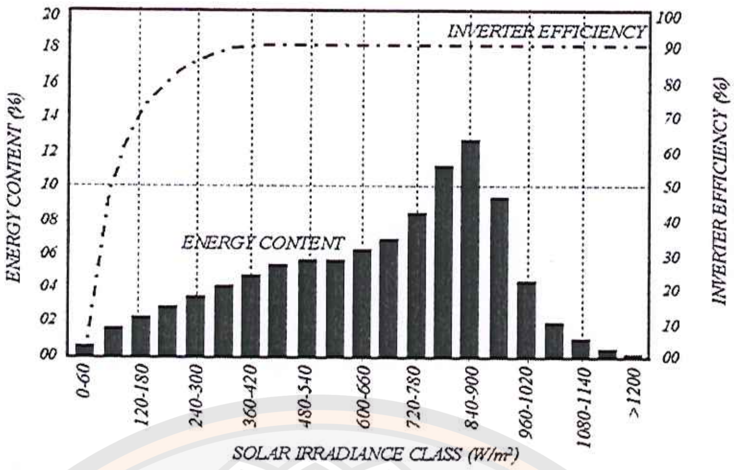

Figure 45 The comparison of the energy content and inverter efficiency

Source: Bunphan, Tharika [53]

4. BIPV design and installation

4.1 Construction and integration

A roof-mounted PV construction system is generally found functioning only as additional electrical energy production not for protection from the weather. The alternative is to place the module within the building envelope with the same function. For example, the function of a PV installation is to be weather proof cladding installed on the external wall. It is a design consideration in the case of a cold (double-leaf) façade and an integration option to create the highest level of benefit in regards to materials and construction. Its functions are weather protection, thermal insulation, sun shading and sound insulation. Therefore, it is an attractive choice for building design.

Figure 46 The constructional integration of building

Source: Bernhard Weller, Claudia Hemmerle, Sven Jakubetz and Stefan Unnewehr [5]

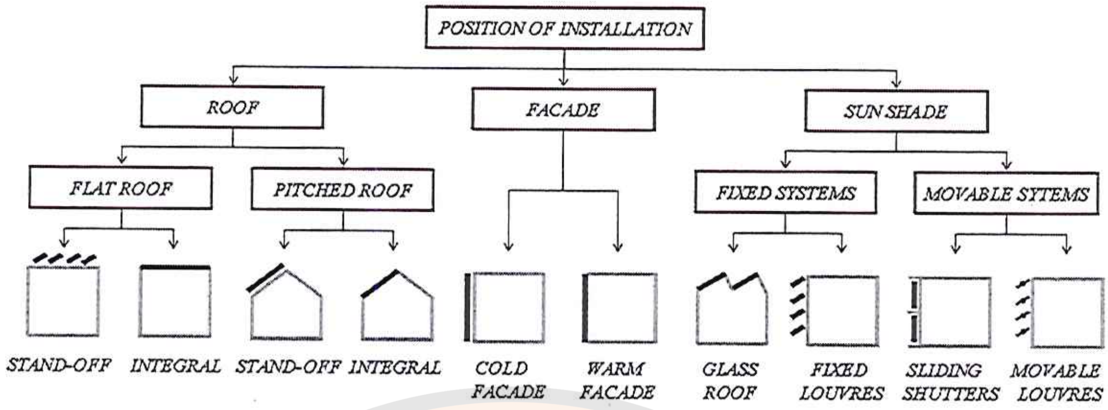

Figure 47 The principal installation options

Source: Bernhard Weller, Claudia Hemmerle, Sven Jakubetz and Stefan Unnewehr [5]

Integration as sun shade is classified into two types as illustrated in Figure 47. The fixed system is designed as a glass roof to decrease light coming into the building, which is good for daylight. Fixed louvers help in reducing heat coming into the building, which is good for thermal. In addition, movable systems are designed to control light and heat coming in the building using smaller modules.

Figure 48 describes the beneficial functions of transparent PV modules, which are generating, shading and lighting. Transparent PV options are used because of the need for daylight, causing the PV element to be more beneficial than just producing electricity, as shown in Figure 48. However, transparent PV cells had been developed from organic technology with less than 1.0% efficiency. Not long after that, MIT's team developed its efficiency to be 1.7% in the early-prototype solar cells [82].

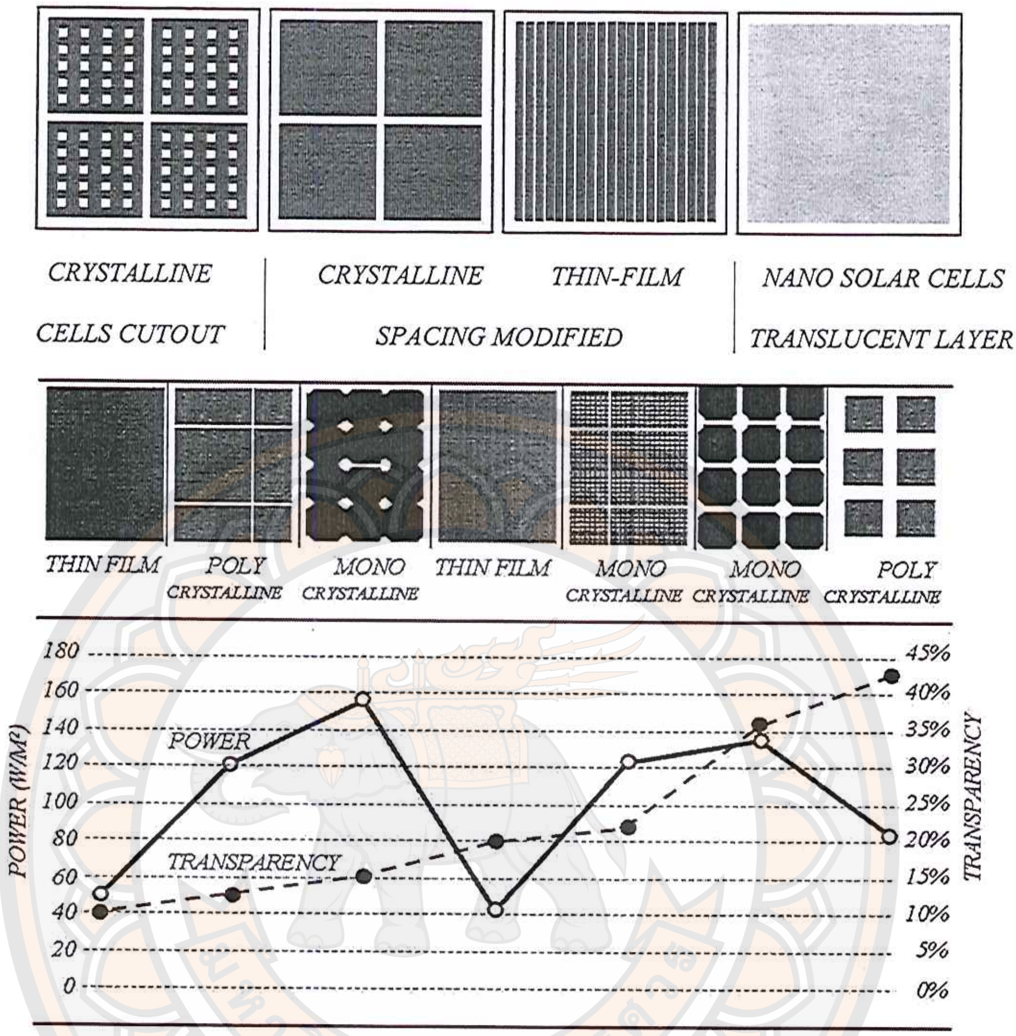

Figure 48 The types of transparent PV module

Source: Sapa build ing system ab offices [83]

4.2 BIPV potential in city

Performance of PV is considered low if installed is in the city. This is a result of the shade from the high buildings around the modules. Nevertheless, there are the cases of tall dominant buildings having no block. Figure 49 shows the different results between BIPV installed on the roof and BIPV installed on a façade. It was found that a tilted angle of the roof gained more benefit than a tilted angle of the façade or vertical wall.

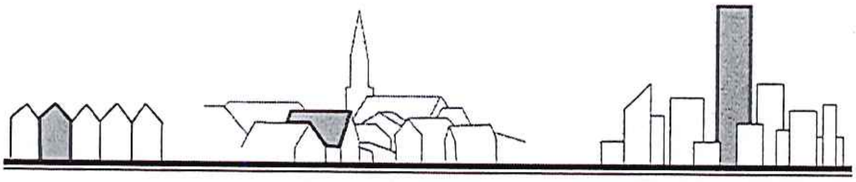

Figure 49 The relation between PV and the surroundings

Source: Bernhard Weller, Claudia Hemmerle, Sven Jakubetz and Stefan Unnewehr [5]

Table 6 Rules of thumb for BIPV potential

Solar architectural rules of thumb for BIPV potential			
	on ROOF		on FAÇADE
Ground floor area	1 m^2	Base of BIPV potential in relative terms	1 m^2
Gross area	1.2 m^2	Ratio gross area / ground floor area	1.5 m^2
	60%	Suitable building envelope parts taking in to account construction, historical and shading elements, including vandalism factor	20 %
Architecturally Suitable area	0.72 m^2	Ratio architecturally suitable area / ground floor area	0.3 m^2
	55%	Suitable building envelope parts taking into account sufficient solar yield	50 %
Solar architecturally Suitable area	0.4 m^2	Ratio solar architecturally suitable area / ground floor area (Utilisation factor)	0.15 m^2

Source: Deo Prasad and Mark Snow [10]

5. Case study of shading integrated

5.1 Installation case study

5.1.1 Galleria Naviglio

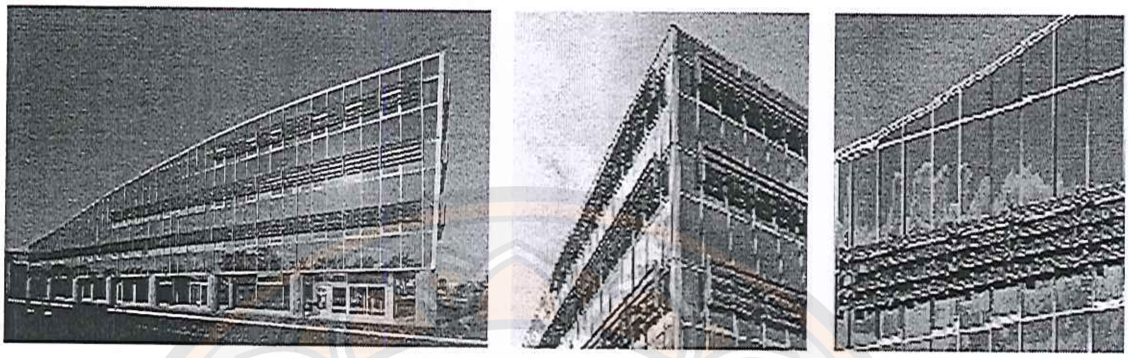

Complex office, shops, apartment, Faenza, Italy (latitude 44.3°N)

PV installation type : Mono crystalline

Shading Type tilted 70° azimuth South East and North East

Total 21 kW_p η-PV array 7.8% – 9.2%, η-PV system 7.0 – 8.2 PR 34%

PR 33.88% (Estimation)

Figure 50 Photovoltaic system of Galleria Naviglio

Source: Simon Roberts and Nicolo Guariento [27]

5.1.2 Photovoltaic System Research Center

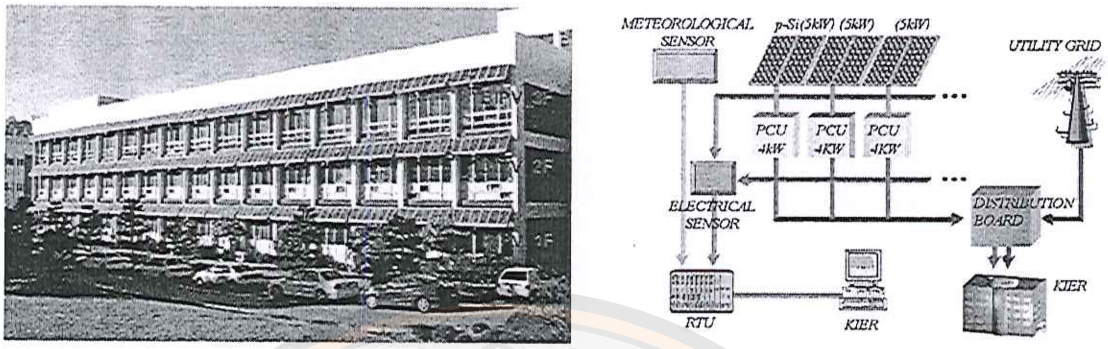

Korea Institute of Energy Research, Taejeon, South Korea (latitude 36°N)

PV installation type : Poly crystalline (50 W_p module)

Shading Type tilted 60° azimuth -10 degrees (South East)

Total 15.00 kW_p η-PV array 7.8% – 9.2%, η-PV system 7.0 – 8.2 PR 65% – 76%

3^{th} Floor 5.28 kW_p PR 76.1%

2^{nd} Floor 4.87 kW_p PR 70.1%

1^{st} Floor 4.48 kW_p PR 65.3%

Figure 51 Photovoltaic system of Research Center

Source: Yu, G.J., So, J.H., Jung, Y.S., Kang, G.H. and Choi, J.Y. [52]

5.1.3 Samsung Institute of Engineering and Construction Technology

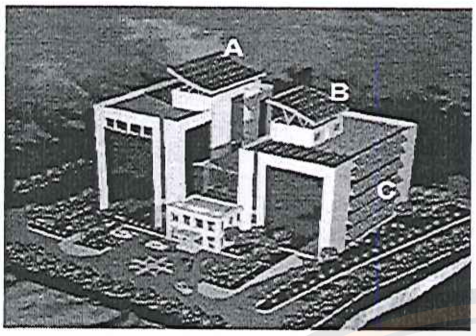

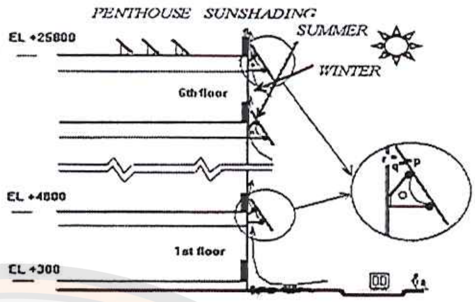

ELEVATION

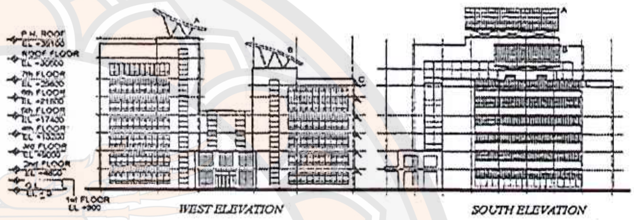

RISER DIAGRAM

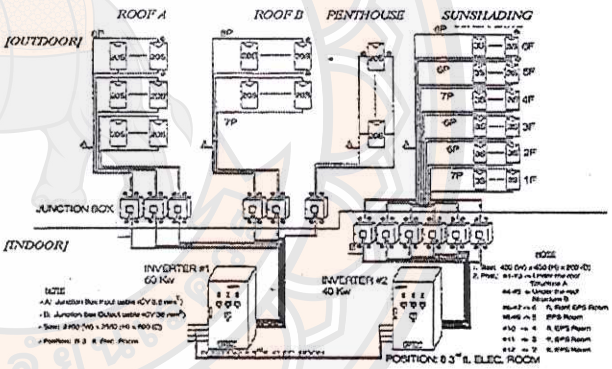

Korea Institute of Energy Research, Taejeon, South Korea (latitude 37.3°N)

PV installation type : Mono crystalline

Shading Type tilted 55.5°(for aesthetic) azimuth 0 degrees (South)

Total 40 kW_p (C : shading) η-PV module 14% , PR 25% – 40% (PR of Array yielded)

Cloudy day PR 40.59% module temperature 27.6 °C

Normal day PR 39.21% module temperature 39.5 °C

Sunny day PR 25.94% module temperature 43.5 °C

Figure 52 Photovoltaic system of SIECT

Source: Seung-Ho Yooa and Eun-Tack Lee [48]

Overall, BIPV installed on a building façade with the proper tilt angle causes more electrical energy production than vertical slope installation. The temperature of the module was less because of the better ventilation. In contrast, the performance was reduced if the installation was at a lower level because of buildings shade covering the modules.

5.2 The optimization of shading type research

5.2.1 Tilt of shading type in Hong Kong in reducing energy consumption

L.L. Sun and H.X. Yang [44] found that the impact of the tilt angles on the energy performance of the shading-type BIPV claddings is analyzed by calculation method in terms of annual electricity generation and annual cooling load reduction for a building. The study, as seen in the Figure 53, showed the annual energy generation was at the highest level at the slope angle of 20° while the local latitude of Hong Kong is around 22.3°N. Combining electricity generation and cooling load reduction, it can be concluded that the optimum tilt angles for the first type of shading-type BIPV claddings vary from 30 degrees to 50 degrees, while the optimum tilt angle for the second type is 0 degrees.

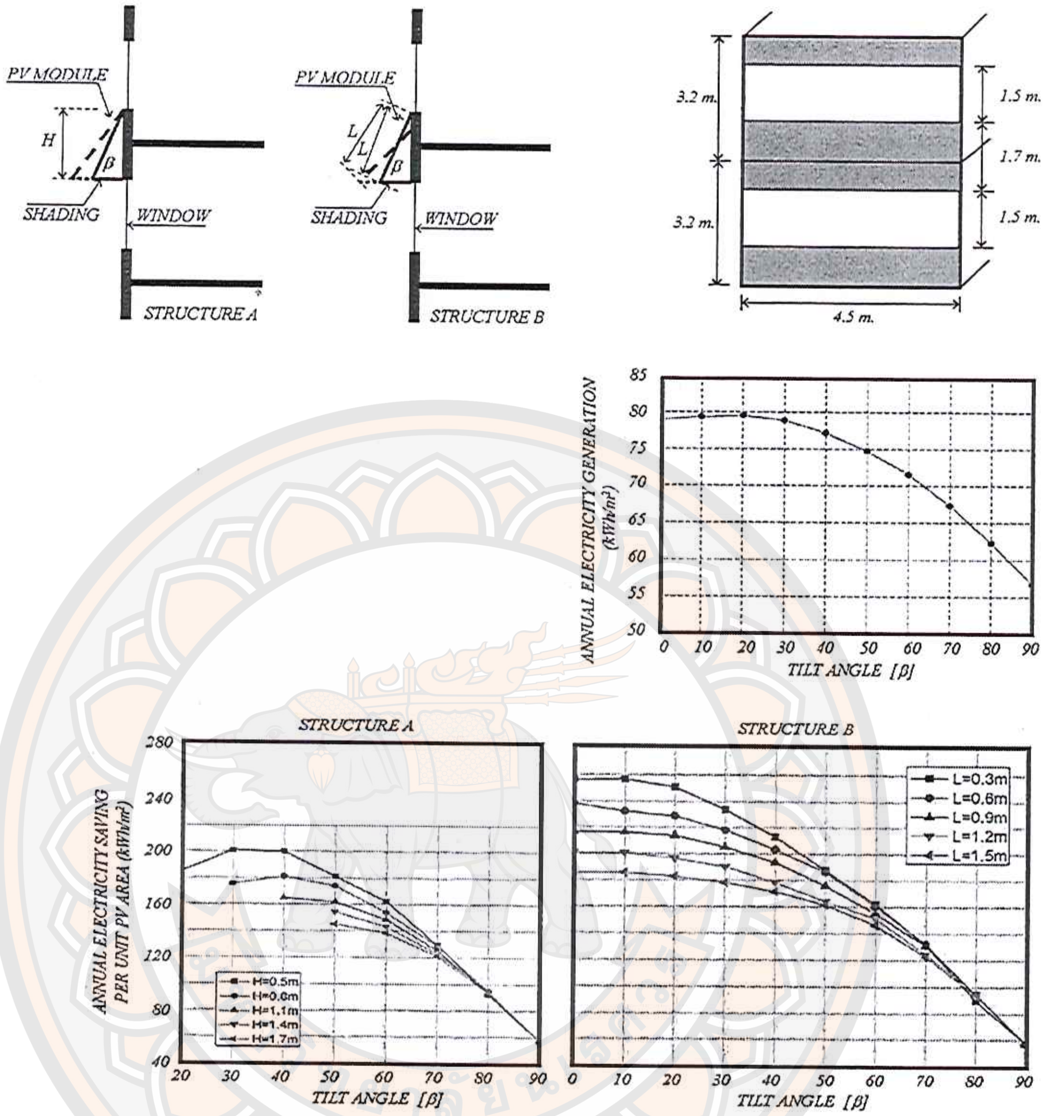

Figure 53 The study of L.L. Sun and H.X. Yang

Source: L.L. Sun and H.X. Yang [44]

5.2.2 Tilt of shading type in Taiwan

C.L. Chenga, C.Y. Chanb and C.L. Chen [7] found that the impact of the tilt angles on the energy performance of the shading-type was analyzed by regression method in a form of ratio of irradiance from slope surface to irradiance from flat surface from six locations in Taiwan. The results are shown in Figure 53, stating that the best tilt angle was between 0-30 degrees while the range of the location latitude was between 22-25 degrees.

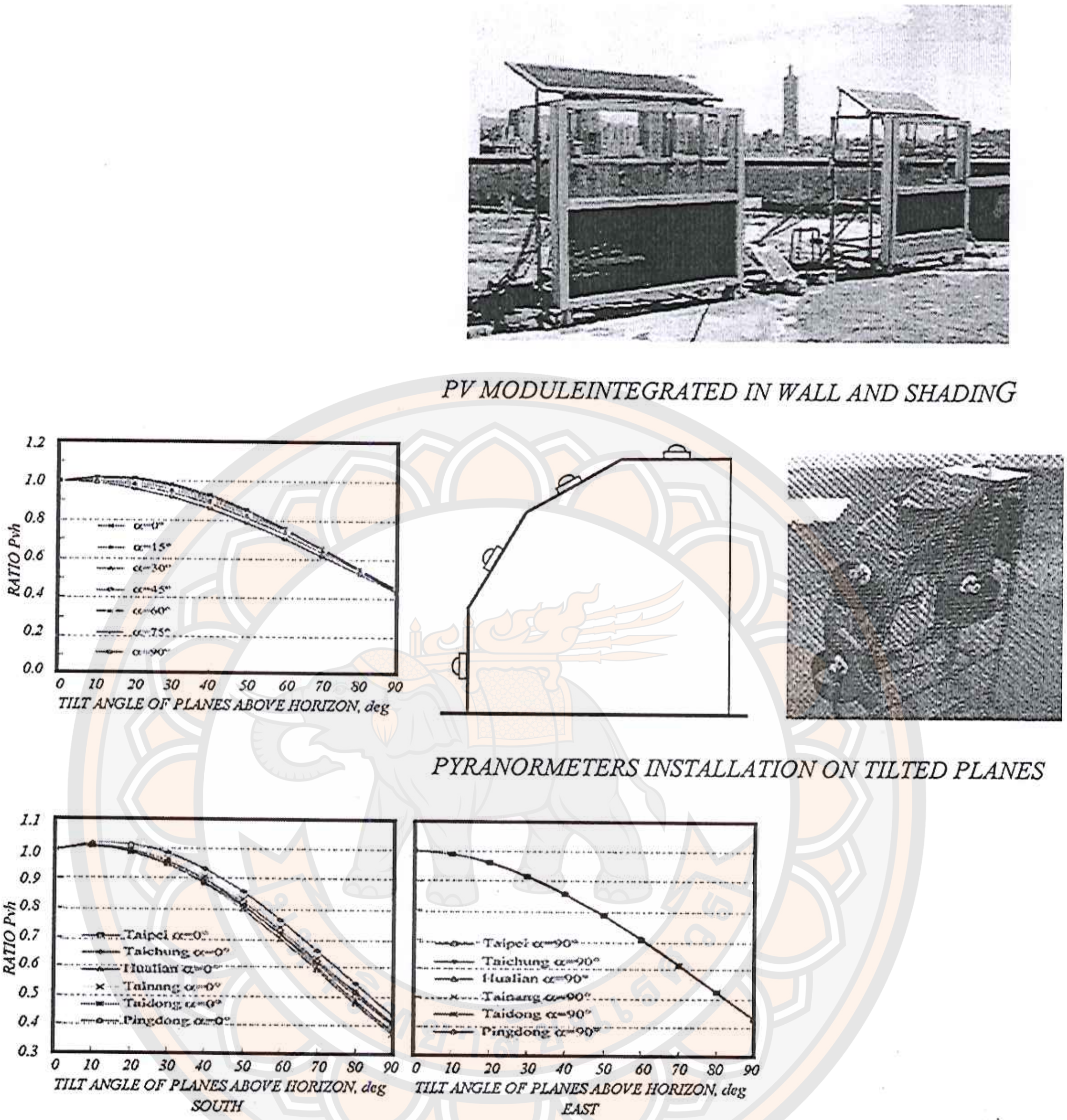

Figure 54 The study of C.L. Chenga, C.Y. Chanb and C.L. Chen

Source: Chao-Yu Chan [7]

5.2.3 E. Chanipat [55] found that the impact of the tilt angles on the energy performance of the shading-type was analyzed by computer simulation method, in the form of ratio of irradiance from slope surface to irradiance from flat surface in Bangkok, 14° latitude, on the southeast and the south as shown in Figure 54 stating that the best tilt angles were at 7 degrees and 12 degrees, respectively.

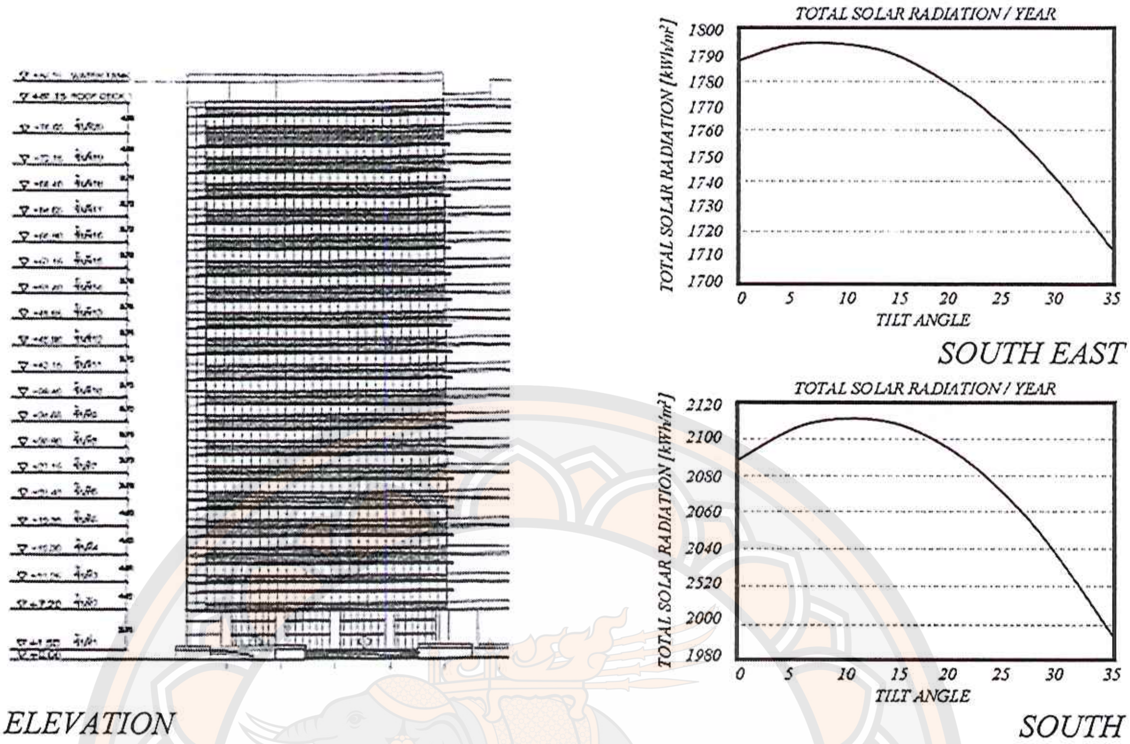

Figure 55 The study of E. Chanipat

Source: Euvananont, Chanipat [55]

5.2.4 S. Wanchart [56] found that the impact of the tilt angles on the energy performance of the louver type was analyzed by using comparison in the form of room temperature, internal illumination and power output of the PV generator in Bangkok, 13.5° latitude, on the south as shown in Figure 56 stating that the best tilt angles were at 7 degrees 22°.

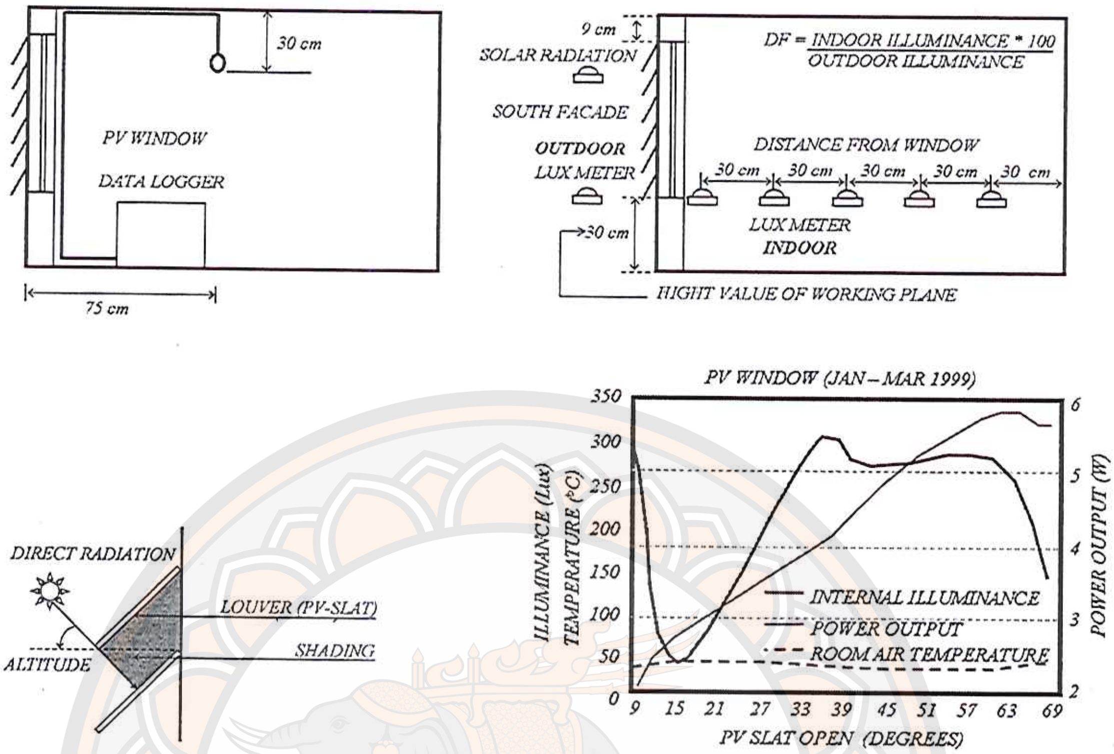

Figure 56 The study of S. Wanchart

Source: Supheng, Wanchart [56]

Conclusions of study showed the result of shading slope, according to the rule of thumb, depends on the latitude of each buildings location. Installation of different shading devices caused different results. The installation of a louver caused shade on the solar module due to the vertical overlapping.

The result parameter to design
1) The direction of PV module cause of the sun path.
2) The shading slope cause of latitude and building obstruction.
3) The half sky effect cause of building obstruction.
4) The shad of upper shading cause of shading obstruction.

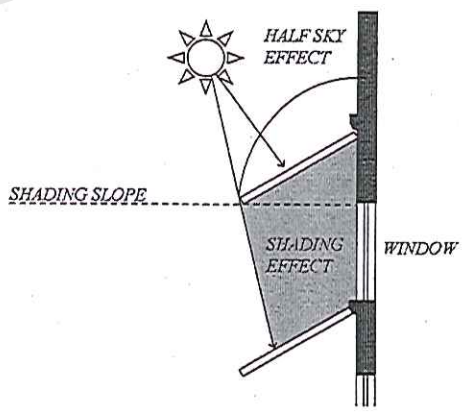

Figure 57 Summary of case studies

Cooling load

Solar heat gain from the solar radiation is protected by the shading device that is integrated with the photovoltaic system. Cooling shown in Figure 58 resulted from heat transfer in the forms of heat conduction, convection and radiation from air conditioning system by using electricity.

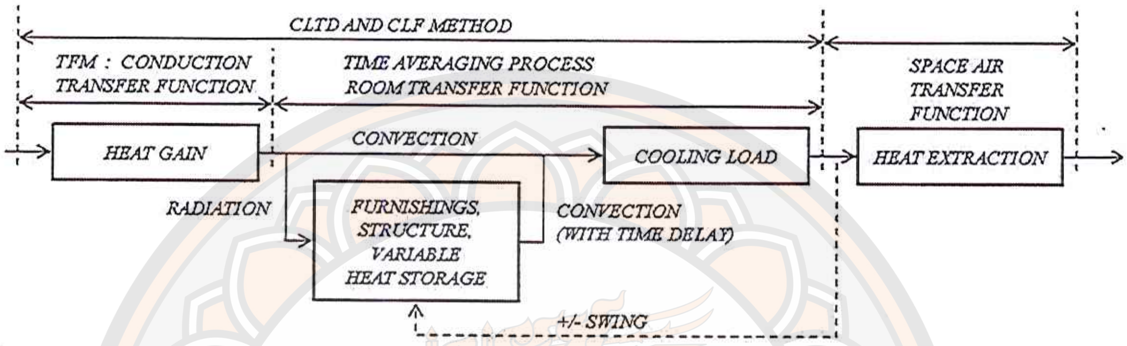

Figure 58 The procedure for calculating cooling load

Source: American Society of Heating, Refrigerating and Air-Conditioning Engineers [1]

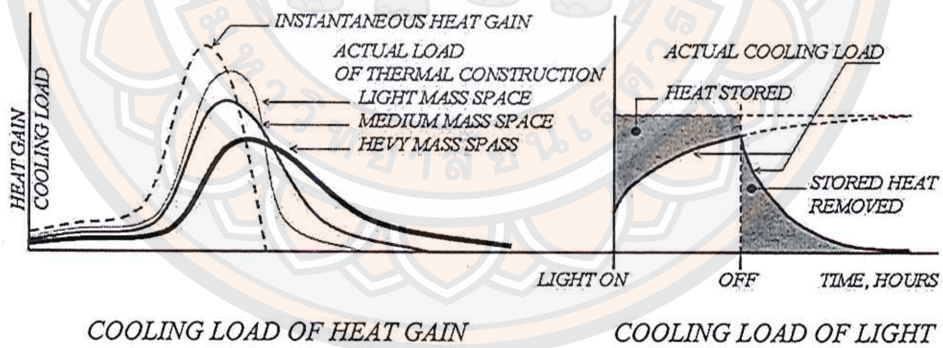

Figure 59 Heat delay of thermal construction and light

Source: American Society of Heating, Refrigerating and Air-Conditioning Engineers [1]

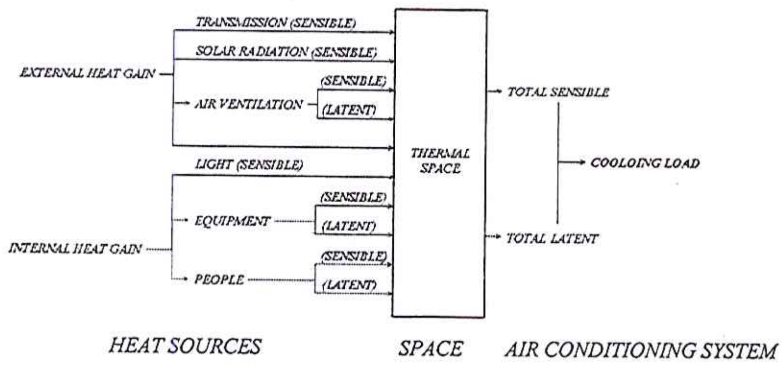

Figure 60 Cooling load calculations of sensible and latent heat

ASHREA [1] presented the CLTD and CLF methods used to estimate cooling coil load, as shown in Figure 58, which serves one or more conditioned space. CLTD method or Cooling Load Temperature Differential and CLF or Cooling Load Factors are steps in calculating cooling load from heat transferring through building envelop from both opaque and transparent parts and from internal heat load, as shown in Figure 60. This method includes the effect of time delay caused by thermal storage of materials, as shown in Figure 59. However, the scope of this research is only in the matter of fenestration and light sources, as shown in Figure 61.

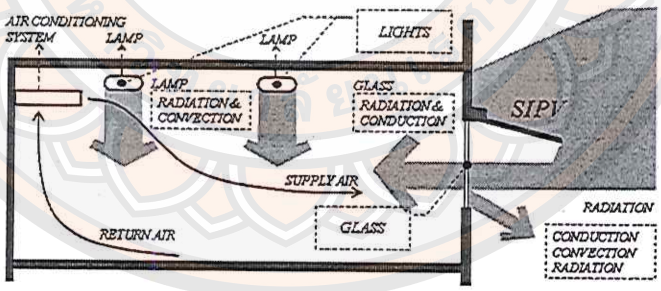

Figure 61 The components of heat load

The conditions of SIPV performance appraisal in cooling load is divided into 2 parts: cooling load because of glass and because of light bulbs.

1. Glass affects SIPV performance because heat is a part of the solar radiation that goes through the glass into the cooled space via conduction and radiation. It varies according to the properties of the glass and shading effect. It is calculated using equation as follows:

$$q_{cond} = (A)(U)(CLTD) \qquad Eq.\ 50$$

$$q_{rad} = (A)(SHGF)(CLF)(SC) \qquad Eq.\ 51$$

$$SC = SHGC(SC) \qquad Eq.\ 52$$

$$U = 1/R_T \qquad Eq.\ 53$$

$$R_T = R_o + dx_1/k_1 + dx_2/k_2 + dx_3/k_3 + \ldots + dx_n/k_n + R_{gap} + R_i \qquad Eq.\ 54$$

CLTD, parameters are changed by outside and inside air temperature, which is calculated for an inside temperature of 25.5°C and outdoor maximum temperature of 35°C with an outdoor daily range of 12°C. Table 7 remains approximately correct for the other outdoor maximums of 34°C to 39°C and other outdoor daily ranges from 9°C to +19°C, provided the outdoor daily average temperature remains approximately 29.4°C. If the room air temperature is different from 25.5°C and/or the average daily outdoor temperature is different from 29.4°C, the following rules apply:

1.1 For room air temperature less than 25.5°C, subtract the difference.

1.2 For average daily outdoor temperature less than 29.4°C, subtract the difference between 29.4°C and the daily average temperature; if greater than 29.4°, add the difference.

Table 7 Cooling Load Temperature Differences (CLTD) of clear glass

Solar time	(h)	1	2	3	4	5	6	7	8	9	10	11	12
CLTD	(°C)	1	0	-1	-1	-1	-1	-1	0	1	2	4	5
Solar time	(h)	13	14	15	16	17	18	19	20	21	22	23	24
CLTD	(°C)	7	7	8	8	7	7	6	4	3	2	2	1

Source: American Society of Heating, Refrigerating and Air-Conditioning Engineers [1]

SHGF, the maximum Solar Heat Gain Factor, varied by orientation, latitude and month, as shown by the comparison in Table 8. The maximum solar heat gain factor for externally shaded glass (based on a ground reflectance of 0.2) is shown in Table 9.

Table 8 Maximum Solar Heat Gain Factor, W/m^2, for 14°N latitude of glass

	Orientation					
month	N	NE/NW	E/W	SE/SW	S	H
Jan	96.5	186.5	674.0	785.5	601.0	804.5
Feb	105.5	317.0	735.0	724.0	453.0	885.0
Mar	112.0	454.0	751.0	610.5	261.5	927.5
Apr	124.5	552.5	716.0	460.5	134.0	913.5
May	176.5	604.0	673.5	348.5	127.5	886.5
Jun	222.5	618.5	648.5	298.0	127.5	869.0
Jul	186.5	596.5	658.0	336.0	131.0	871.0
Aug	131.0	539.5	689.5	438.5	296.5	890.0
Sep	115.5	435.5	719.0	588.5	261.5	897.5
Oct	105.5	312.5	710.0	700.5	441.5	867.5
Nov	98.0	186.5	662.5	773.0	591.5	798.0
Dec	93.0	138.5	639.0	796.5	645.5	763.5

Source: American Society of Heating, Refrigerating and Air-Conditioning Engineers [1]

Table 9 Maximum Solar Heat Gain Factor, W/m^2, externally shaded

	Orientation					
month	N	NE/NW	E/W	SE/SW	S	HOR
Jan	98	98	107	117	120	50
Feb	107	107	114	120	123	50
Mar	114	117	123	126	123	60
Apr	126	130	133	129	126	76
May	137	142	142	129	126	88
Jun	142	148	145	129	126	98
Jul	142	145	148	133	129	98
Aug	133	136	145	136	133	88
Sep	117	120	129	133	129	73
Oct	107	107	120	126	126	60
Nov	101	101	107	120	123	54
Dec	95	95	101	114	117	47

Source: American Society of Heating, Refrigerating and Air-Conditioning Engineers [1]

Table 10 The Cooling Load Factor for glass without interior shading

Solar time	Orientation								
h	N	NE	E	SE	S	SW	W	SW	HOR
1	0.23	0.07	0.07	0.09	0.12	0.15	0.15	0.14	0.16
2	0.2	0.06	0.06	0.08	0.11	0.14	0.13	0.12	0.14
3	0.18	0.06	0.06	0.07	0.09	0.12	0.11	0.11	0.12
4	0.16	0.05	0.05	0.06	0.08	0.1	0.1	0.09	0.11
5	0.14	0.04	0.05	0.05	0.07	0.09	0.09	0.08	0.09
6	0.34	0.21	0.18	0.14	0.08	0.09	0.09	0.09	0.11
7	0.41	0.36	0.33	0.26	0.11	0.1	0.09	0.1	0.16
8	0.46	0.44	0.44	0.38	0.14	0.12	0.1	0.11	0.24
9	0.53	0.45	0.5	0.48	0.21	0.13	0.11	0.13	0.33
10	0.59	0.4	0.51	0.54	0.31	0.15	0.12	0.14	0.43
11	0.65	0.36	0.46	0.56	0.42	0.17	0.13	0.16	0.52
12	0.7	0.33	0.39	0.51	0.52	0.23	0.14	0.17	0.59
13	0.73	0.31	0.35	0.45	0.57	0.33	0.19	0.18	0.64
14	0.75	0.3	0.31	0.4	0.58	0.44	0.29	0.21	0.67
15	0.76	0.28	0.29	0.36	0.53	0.53	0.4	0.3	0.66
16	0.74	0.26	0.26	0.33	0.47	0.58	0.5	0.42	0.62
17	0.75	0.23	0.23	0.29	0.41	0.59	0.56	0.51	0.56
18	0.79	0.21	0.21	0.25	0.36	0.53	0.55	0.54	0.47
19	0.61	0.17	0.17	0.21	0.29	0.41	0.41	0.39	0.38
20	0.5	0.15	0.15	0.18	0.25	0.33	0.33	0.32	0.32
21	0.42	0.13	0.13	0.16	0.21	0.28	0.27	0.26	0.28
22	0.36	0.11	0.11	0.14	0.18	0.24	0.23	0.22	0.24
23	0.31	0.09	0.1	0.12	0.16	0.21	0.2	0.19	0.21
24	0.27	0.08	0.08	0.1	0.14	0.18	0.17	0.16	0.18

Source: American Society of Heating, Refrigerating and Air-Conditioning Engineers [1]

CLF, the Cooling Load Factor, varies by orientation, mass of construction, and effect interior shaded, which is shown in Table 9 to Table 11 for general cases of medium construction (100-mm concrete exterior wall, 100-mm concrete floor slab). It was estimated as mass per unit of floor area at 340 kg/m2.

SHGC, the Solar Heat Gain Coefficient, varies by the properties of glass and the incident angle. It was shown in Table 11.

R, Resistance value, varies by the properties of glass and air film both inside and outside of the glass, as shown in Table 12.

Table 11 The Solar Heat Gain Coefficient of glass

		SHGC						
		Center of glazing properties : Incidence angles						
	VT	Normal, 0	40	50	60	70	80	Hemisphere Diffuse
clear glass	0.90	0.86	0.84	0.82	0.78	0.67	0.42	0.78

Source: American Society of Heating, Refrigerating and Air-Conditioning Engineers [1]

Table 12 The resistance value of air

	Resistance value of air						
The property of glass surface	Air gap mm.						
	inside	5	6	7	10	13	outside
High radiation emission	0.120	0.084	0.091	0.097	0.110	0.119	0.044
Low radiation emission	0.299	0.167	0.196	0.208	0.278	0.345	-

Source: American Society of Heating, Refrigerating and Air-Conditioning Engineers [1]

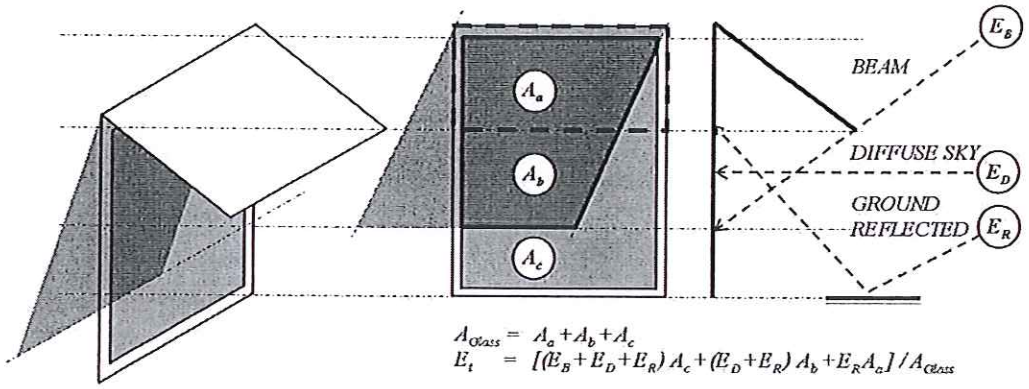

Figure 62 The shading area on the glass under shading device

SC, the Shading Coefficient, varies by the effect of effective shading in reducing the beam and diffuse radiation on the glass as shown in Figure 62. It calculated following Eq. 55.

$$SC = E_{twS} / E_{tw} \qquad \text{Eq. 55}$$

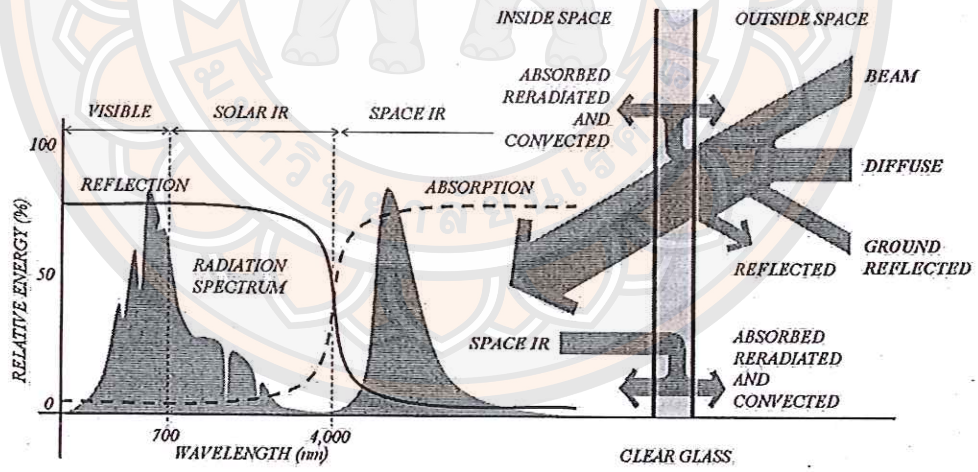

Figure 63 The heat transfer of the solar ray

Source: Lechner, Norbert [20]

2. Lights also affect SIPV performance. The internal cooling load varies by the light fixture type, supply and return ventilation, space furnishing and thermal structure. It can be calculated as follows:

$$q_{el} = (H\,G_{el})(CLF_{el}) \quad \text{Eq. 56}$$

$$H\,G_{el} = (W_l)(F_{ul})(F_{sa}) \quad \text{Eq. 57}$$

CLF_{el}, the Cooling Load Factor of the light, should be considered 1.0 when the cooling system operates only during the occupied hours; but if not under this condition, it should be considered as shown in Table 13 to 15 in the case of lights being on for 8 hours.

Table 13 "a" coefficient

"a"	Furnishings	Air supply and return	Type of light fixture
0.45	Heavyweight, simple furnishings, no carpet	Low rate; supply and return below ceiling (V <= 2.5)	Recessed, not vented
0.55	Ordinary furniture, no carpet	Medium to high ventilation rate; supply and return below ceiling or through ceiling grill and space (V >= 2.5)	Recessed, not vented
0.65	Ordinary furniture, with or without carpet	Medium to high ventilation rate or fan coil or induction type air-conditioning terminal unit; supply through ceiling or wall diffuser; return around light fixtures and through ceiling space (V <= 2.5)	Vented
0.75 or greater	Any type of furniture	Ducted returns through light fixtures	Vented or free-hanging in air stream with ducted returns

Note: V is the room air supply rate in liters per second per square meter of floor area

Table 14 "b" classification

Room envelope construction1 (mass of floor area, kg/m^2)	Room air circulation and type of supply and return[2]			
	Low	Medium	High	Very high
50 mm wood floor (50)	B	A	A	A
75-mm concrete floor (200)	B	B	B	A
150-mm concrete floor (370)	C	C	C	B
200-mm concrete floor (590)	D	D	C	C

Note: 1. Floor covered with carpet and rubber pad; for a floor covered only with floor tile, take the next classification to the right in the same row.

2. These values are defined as follows:

2.1 *Low*: low ventilation rate -- minimum required to cope with cooling load from lights and occupants in interior zone. Supply through floor, wall, or ceiling diffuser. Ceiling space not vented and h = 2.3 $W/m^2\ {}^oC$, where h = inside surface convection coefficient used in calculation of b.

2.2 *Medium*: Medium ventilation rate, supply through floor, wall, or ceiling diffuser. Ceiling space not vented and h = 3.4 $W/m^2\ {}^oC$

2.3 *High*: Room air circulation induced by primary air of induction unit or by fan coil unit. Return through ceiling space and h = 4.5 $W/m^2\ {}^oC$

2.4 *Very high*: High room air circulation used to minimize temperature gradients in a room. Return through ceiling space and h = 6.8 $W/m^2\ {}^oC$

Table 15 Cooling Load Factor when lights are on for 8 hour

"a"	45				55				65				75			
"b"	A	B	C	D	A	B	C	D	A	B	C	D	A	B	C	D
h_{off}	Cooling Load Factor after lights are turned on															
1	0.02	0.07	0.11	0.14	0.01	0.06	0.09	0.11	0.01	0.04	0.07	0.09	0.01	0.03	0.05	0.06
2	0.46	0.51	0.55	0.58	0.56	0.6	0.63	0.66	0.66	0.69	0.72	0.73	0.76	0.78	0.80	0.81
3	0.57	0.56	0.58	0.60	0.65	0.64	0.66	0.67	0.73	0.72	0.73	0.74	0.80	0.80	0.81	0.82
4	0.65	0.61	0.60	0.61	0.72	0.68	0.68	0.68	0.78	0.75	0.75	0.75	0.84	0.82	0.82	0.82
5	0.72	0.65	0.63	0.62	0.77	0.71	0.70	0.69	0.82	0.77	0.76	0.76	0.87	0.84	0.83	0.83
6	0.77	0.68	0.65	0.63	0.82	0.74	0.71	0.70	0.86	0.80	0.78	0.77	0.90	0.85	0.84	0.83
7	0.82	0.71	0.67	0.64	0.85	0.76	0.73	0.71	0.88	0.82	0.79	0.77	0.92	0.87	0.85	0.84
8	0.85	0.74	0.69	0.65	0.88	0.79	0.75	0.72	0.91	0.84	0.8	0.78	0.93	0.88	0.86	0.84
9	0.88	0.77	0.71	0.66	0.90	0.81	0.76	0.72	0.93	0.85	0.82	0.79	0.95	0.89	0.87	0.85
10	0.46	0.34	0.28	0.22	0.37	0.28	0.23	0.18	0.29	0.22	0.18	0.14	0.21	0.15	0.13	0.10
11	0.40	0.30	0.30	0.20	0.30	0.30	0.20	0.20	0.20	0.20	0.20	0.10	0.20	0.10	0.10	0.10
12	0.30	0.28	0.25	0.21	0.24	0.23	0.20	0.17	0.19	0.18	0.16	0.13	0.13	0.13	0.11	0.10
13	0.24	0.25	0.23	0.20	0.19	0.20	0.19	0.17	0.15	0.16	0.15	0.13	0.11	0.11	0.10	0.09
14	0.19	0.22	0.22	0.20	0.16	0.18	0.18	0.16	0.12	0.14	0.14	0.13	0.09	0.10	0.10	0.09
15	0.15	0.20	0.20	0.19	0.13	0.16	0.17	0.16	0.10	0.13	0.13	0.12	0.07	0.09	0.09	0.09
16	0.12	0.18	0.19	0.19	0.10	0.15	0.16	0.15	0.08	0.12	0.12	0.12	0.06	0.08	0.09	0.08
17	0.10	0.16	0.18	0.18	0.08	0.13	0.15	0.15	0.06	0.10	0.11	0.11	0.05	0.07	0.08	0.08
18	0.08	0.15	0.17	0.18	0.07	0.12	0.14	0.14	0.05	0.09	0.11	0.11	0.04	0.07	0.08	0.08
19	0.06	0.13	0.16	0.17	0.05	0.11	0.13	0.14	0.04	0.08	0.10	0.11	0.03	0.06	0.07	0.08
20	0.05	0.12	0.15	0.16	0.04	0.10	0.12	0.13	0.03	0.08	0.10	0.10	0.02	0.05	0.07	0.07
21	0.04	0.11	0.14	0.16	0.03	0.09	0.11	0.13	0.03	0.07	0.09	0.10	0.02	0.05	0.06	0.07
22	0.03	0.10	0.13	0.16	0.03	0.08	0.11	0.13	0.02	0.06	0.08	0.10	0.02	0.04	0.06	0.07
23	0.03	0.09	0.12	0.15	0.02	0.07	0.10	0.12	0.02	0.06	0.08	0.10	0.01	0.04	0.06	0.07
24	0.02	0.08	0.12	0.15	0.02	0.06	0.10	0.12	0.01	0.05	0.07	0.09	0.01	0.04	0.05	0.07

Note: h_{off} is the number of hours after lights are turned on.

a is coefficient.

b is classification.

Lights bulbs diffusing heat and light radiation because of energy conversion showing the loss of fluorescent lamps affect the calculation of cooling load as shown in Figure 64.

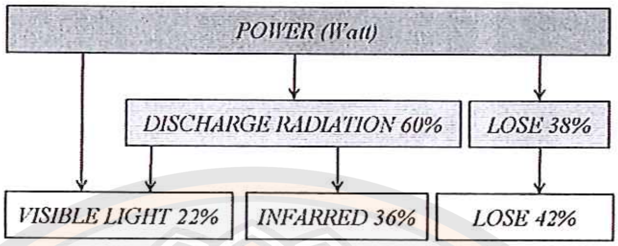

Figure 64 The heat conversion of a fluorescent lamp

Source: B. Sulee [3]

Daylight

1. Measurement light units

Daylight consists of UV, VIS and IR, which enters via the window and affects comfort in the living space in need for illuminance level and contrast for visualization. This can be measured in terms of light parameters, as shown in Figure 65 and Eq.58-60.

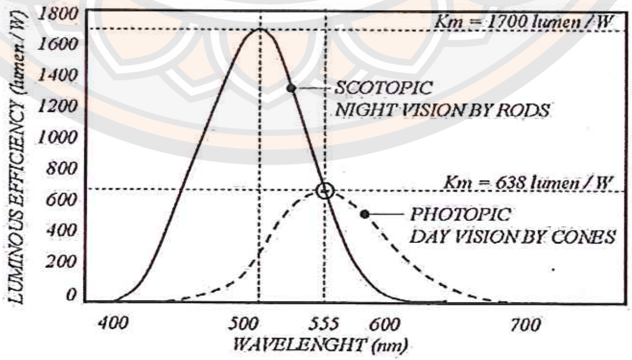

Figure 65 Human eye sensitivity and luminous efficiency

Source: Williamson, S. J. and Cummins, H. Z. [37]

$$F = 4\pi CP \qquad Eq.58$$

$$L = \rho E / \pi \qquad Eq.59$$

$$L = \tau E / \pi \qquad Eq.60$$

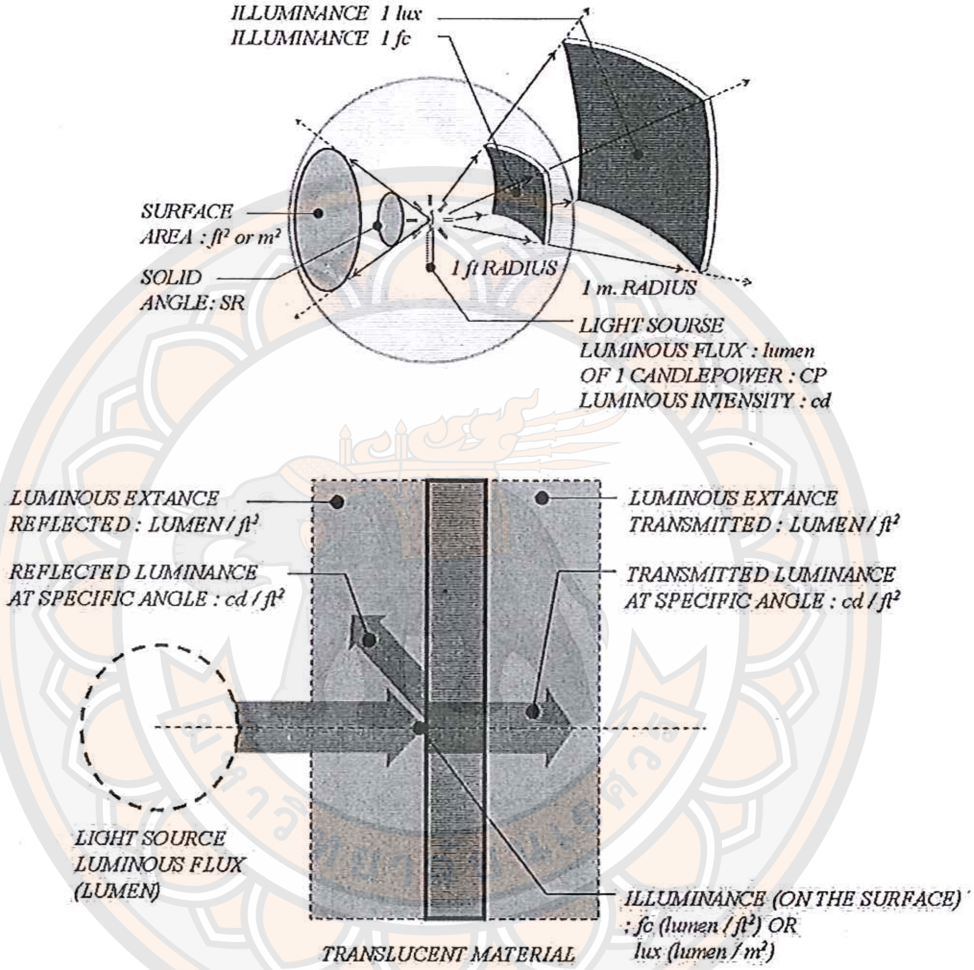

Figure 66 The measurement in term of light

Source: Egan, M. David [11]

2. Sky condition and sky model

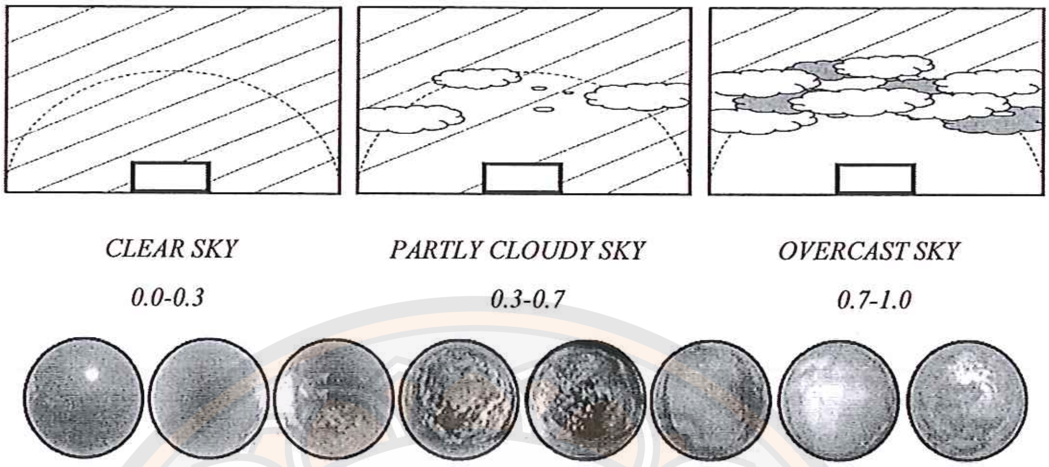

Figure 67 The sky condition

The sky conditions influencing the amount of daylight inside the building are separated into 3 forms: clear sky, partly cloudy sky and overcast sky. The differences are determined by cloud ratio, as shown in Figure 64, 65, 66 and Figure 67.

2.1 Uniform sky model

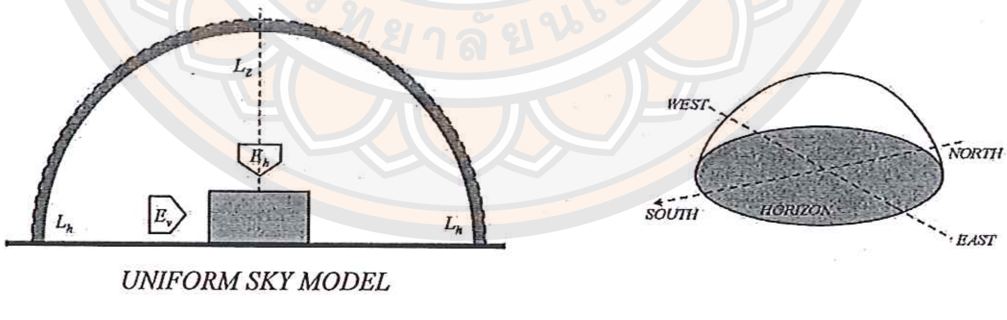

Figure 68 Uniform sky model

Source: Cowan, Henry, J. [9]

This module appears in constantly luminous daylight with a luminous value of 0.5 at the vertical view.

$$E = \pi L \qquad Eq.61$$

$$E_h = \pi L \qquad Eq.62$$

$$E_v = (1/2)\,\pi L \qquad Eq.63$$

2.2 Overcast sky model

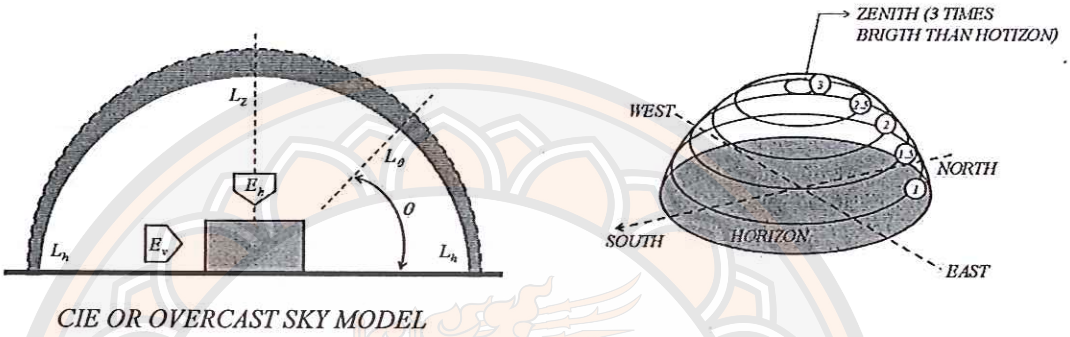

Figure 69 Overcast sky model

Source: Cowan, Henry, J. [9]

$$L_\theta = (1/3)\,L_Z\,(1 + 2\sin\theta) \qquad Eq.64$$

$$L_h = (1/3)\,L_Z \qquad Eq.65$$

$$E_h = (7/9)\,\pi L_Z \qquad Eq.66$$

$$E_v \approx L_Z \qquad Eq.67$$

This module shows maximum luminosity at the horizontal plane, which will be decreased to 1/3 at the vertical view.

2.3 Clear sky model

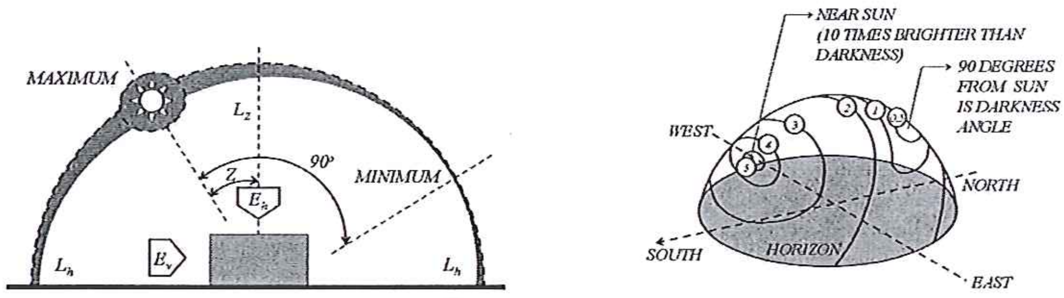

CLEAR SKY MODEL

Figure 70 Clear sky model

Source: Cowan, Henry, J. [9]

$$L_\theta = \frac{(1-e^{-0.32/\sin\theta})(0.91+10e^{-3a} + 0.45\cos^2 a)\, L_Z}{0.274(0.91+10e^{-3Z}+0.45\cos^2 Z)} \qquad Eq.68$$

$$L_\theta = \text{constant} ;\ 15 < \theta < 90 \qquad Eq.69$$

$$= L_Z / \sin\theta \qquad Eq.70$$

$$= L_Z / \sin 15^o = 3.86\, L_Z \qquad Eq.71$$

This module shows maximum luminosity at the sun position and minimum luminosity at 90 degrees measured from the maximum point.

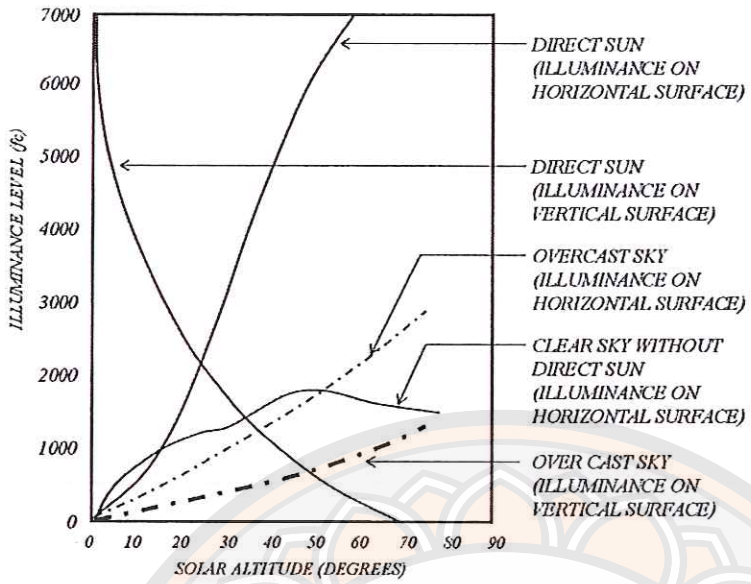

< The vertical surface was received the illuminance around a half compare with the horizontal surface.

Figure 71 The illuminance level comparison

Source: Egan, M. David [11]

Figure 71 explains natural light under weather conditions comparing illuminance due to the fact that location of solar attitude is related to direction of vision towards the daylight source or window.

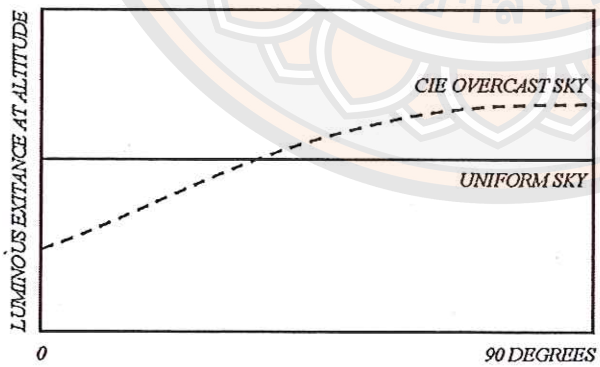

< The Uniform sky has luminous constantly around the average of the overcast sky model.

Figure 72 The comparison between uniform sky and overcast sky models

Source: Cowan, Henry, J. [9]

3. Efficacy of daylight

As shown in Figure 73, Daylight is a light source with high efficacy compared to artificial light sources, containing the approximate values of 120 lumen/Watt for average sky, 150 lumen/Watt for clear sky, and below 120 lumen/Watt for average sky with sun rays.

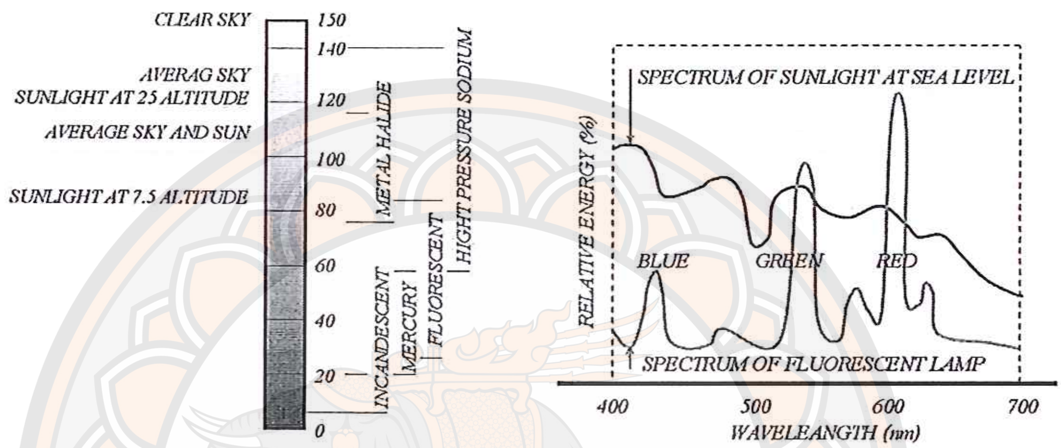

Figure 73 The efficacy of daylight and artificial light sources

Source: M. David Egan and Victor W. Olgyay [21]

4. Day lighting design

Daylight Factor, DF, is the method for prediction by math models described in Eq.72-73 for lumen method and Eq.74-76 for experimental method. In experimental study, a mirror box was used to collect data, as shown in Figure 75. A mirror box is a tool that reproduces an overcast sky. However, if the data collection was meant to come from the real sky, then a clear sky or overcast sky should be considered. As for a partly cloudy sky, it is easily changeable, unstable and difficult to study.

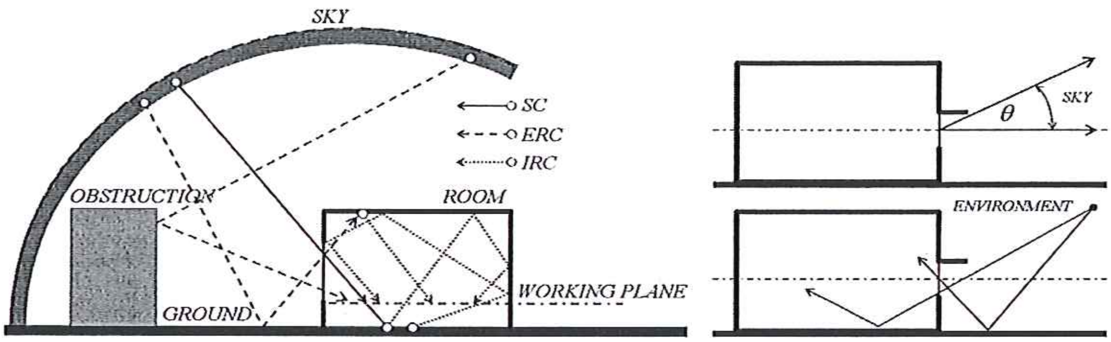

Figure 74 The daylight part into the room

Source: Cowan, Henry, J. [9]

$$DF_{av} = C\,A_W\,\tau\,MF\,(GBC)\,/\,A_t\,(1 - \rho_{av}) \qquad Eq.72$$

$$DF_{av} = A_t\,\tau\,MF\,(GBC)\,[\,(C/A_L)+(C\,\rho_L + 0.05\rho_U)/A_t\,(1 - \rho_{av})] \qquad Eq.73$$

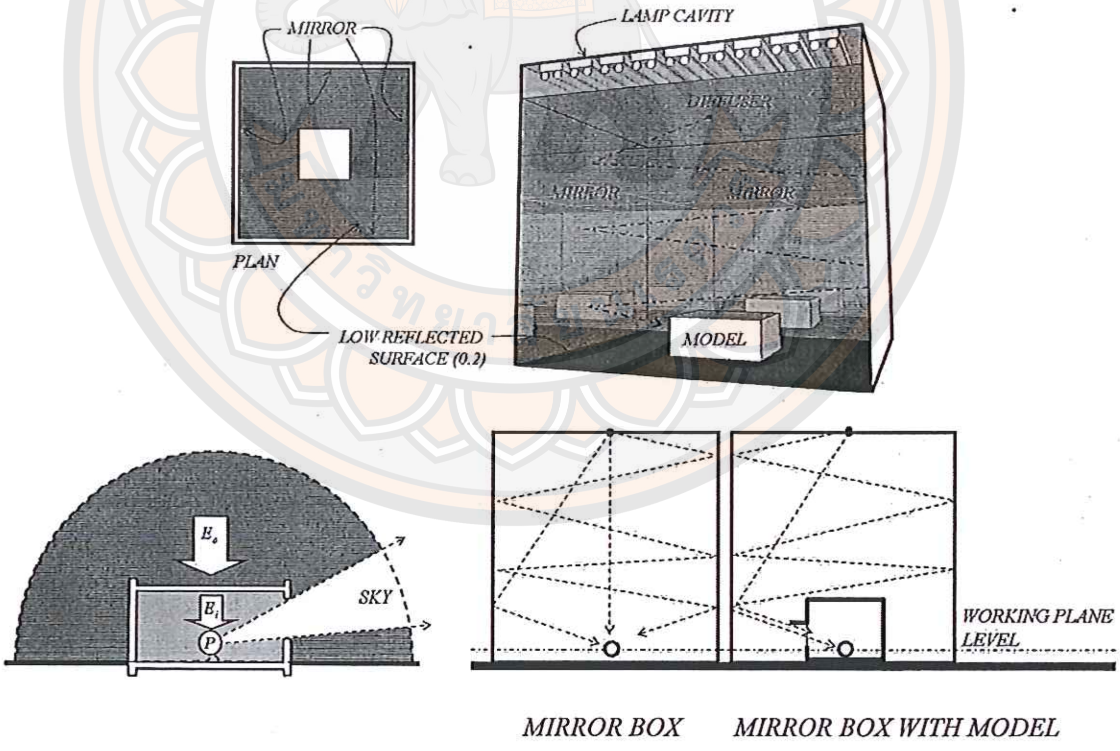

Figure 75 The mirror box explanation

Experimental methods including the mirror box or real sky used to evaluate daylight factor will apply physical model with enough scale to enter light sensors in each position on the working plane. However, in the case study under real sky conditions, the thing that should be watched out for is the shade of clouds blocking out the sun light and the amount of clouds in the sky. The data collection should be only for light from the sky, not direct solar radiation.

$$DF = E_i / E_o \qquad Eq.74$$

$$DF = SC + IRC + ERC \qquad Eq.75$$

$$E_i = DF(E_{sky}) \qquad Eq.76$$

5. Illumination on the working plane

Illuminance is light measured on the plane which, in this study, was the working plane at a height of 0.75 m varying according to need in usability. The suitability is shown in Table 2, 3, 4, 5, 6, 7, 8, 9, 10, 11, 12, 13, 14 and Table 15 compared using numbers of standards such as Thai building code, French CIE standards, American IES standards to DF suitable for each type of activity.

Table 16 The comparison of illumination standards

Working plane	Building code (Lux)	CIE (Lux)	EIS (Lux)	DF (%)
General area	300	150-200-300	200-300-500	5
Meeting	300	300-500-750	200-300-500	5
Office working	300	300-500-750	500-750-1,000	5
Walking area	200	50-100-150	50-75-100	2
Parking area	50	50-100-150	50-75-100	2

Note: CIE is The International Commission on Illumination (The Commission Internationale de I'Eclairage).
EIS is Illuminating Engineering Society of North America.

Source: Benjamin Stein and John S. Reynolds [4]; I, Kasadit [15]; Srisutapan, A and T. Panjira [29]

Lighting systems were designed to be proper for usability and the amount of electric power per unit of utility space according to type of building in need of energy saving. Details from building law for energy conservation are defined in Table 17. The aforementioned values resulted from design and determination of type of light bulb with reflector, type of ballast and light control such as on/off technique or dimming technique to create usability as long as needed, especially with daylight.

Table 17 The maximum power of lighting system defined by building code

Building type	Average power (W/m^2)
Education, Office	14
Shopping center, Rental shop, Theater	18
Hotel, Residential, Hospital	12

6. Daylight Glare Index

Glare is one of the qualitative indicators affecting usability in relation with angles as shown in Figure 76. In this research, windows are a light source causing glare when looking out the window which changes throughout the day, as shown in Figure 77 by the calculation of daylight glare index (DGI) using Eq.77-85. Glare is an important parameter affecting usability when gazing out a window. The discomforting glare occurs when the light source coming through the window is much brighter than requirement for sensation of the eyes. Disabling glare occurs when the light affects the ability to see. Conditions of differences of light in the form of contrast ratio were suitable at 3:1, which was the ratio of the viewing area to ambient area, 10:1 for the ratio of the viewing area to background area, and 50:1 for ratio of the highlighted object to the ambient area [21]. However, Hopkinson presented the GI, Glare Index, in 1960 and was supported by a field study in 1970 that expressed GI as Eq.77-85 [8]. Then it was modified from dGI to DGI as described by Eq.86.

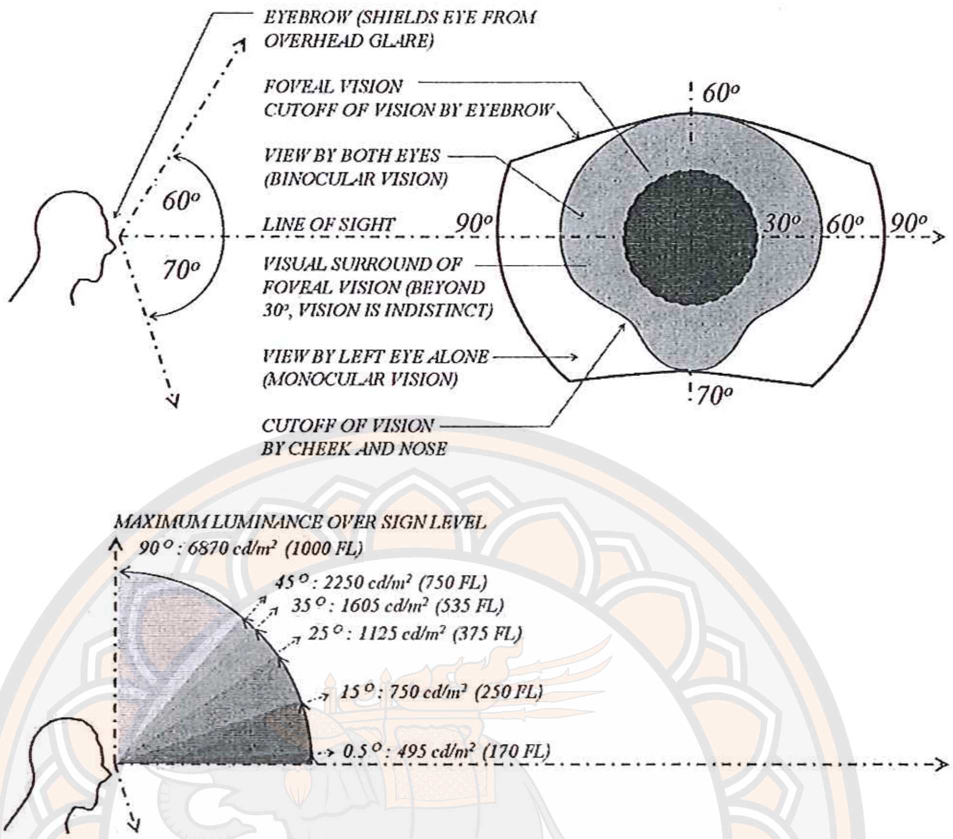

Figure 76 The eyes view and luminance sensation

Source: Claude L. Robbins [8]; Flynn, John E., Kremers, Jack A., Segil, Arthur W. and Staffy Gary R. [13]; M. David Egan and Victor W. Olgyay [21]

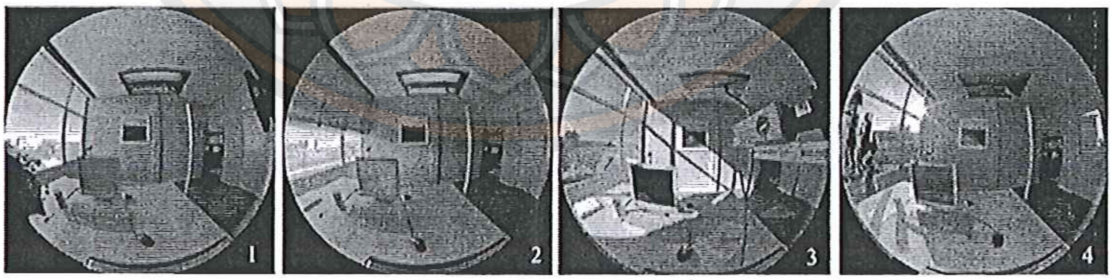

Figure 77 The glare effect from the side window

Source: Andersen, Marilyne [58]

Hopkinson model

$$dG = 11\{(L_s^{1.6})(\Omega^{0.8})/L_b+[(0.07(\omega^{0.5})(L_a)]\} \quad Eq.77$$

$$L_a = 0.3178\,E_a \quad Eq.78$$

$$L_s = (E_{sp}/V)(T_g/0.85) \quad Eq.79$$

$$L_b = [(IRE + ERE)/\pi](z)(T_g/0.85) \quad Eq.80$$

$$z = (1.9785 \ln E_H) - 15.9164 \quad Eq.81$$

$$v = 0.8536\,e^{0.0733A} \quad Eq.82$$

$$L/d = w/d \quad Eq.83$$

$$L/d = I/d \quad Eq.84$$

$$dGI = 10 \log_{10}\Sigma dG \quad Eq.85$$

Parameter A is the angle between the direction of view of the eyes and the center of the aperture.

Modified model

$$DGI = dGI - (x+y) \quad Eq.86$$

$$dGI = 12.02\,e^{(0.0309)(GI)} \quad ;\ for\ 10 < GI < 28 \quad Eq.87$$

$$x = (E_{dGI}^{-0.459})(100\,F_{dGI}^{3.148}) \quad Eq.88$$

$$F_{dGI} = D_{max}\{1+[E_{dGI}2 / E_{co}(E_{co} - 2E_{max})]\} \quad ;\ E_{dGI} < E_{co} \quad Eq.89$$

$$= [(2D_{max;})/(E_{co} - 2E_{max})](E_{dGI} - E_{max}) \quad ;\ E_{dGI} < E_{co} \quad Eq.90$$

$$y = (10\,x\,\rho_r) - 5 \quad ;\ 0.3 < \rho_r < 0.9 \quad Eq.91$$

Table 18 The Daylight Glare Index category

Illuminance category		DGI_{max}
General lighting throughout spaces		
Public spaces with dark suroundings	A	24
Simple orientation for short temporary visits	B	26
Working spaces where visual tasks are only occasionally performed	C	22

Source: Benjamin Stein and John S. Reynolds [4]; Claude L. Robbins [8]; Watson, Donald [36]

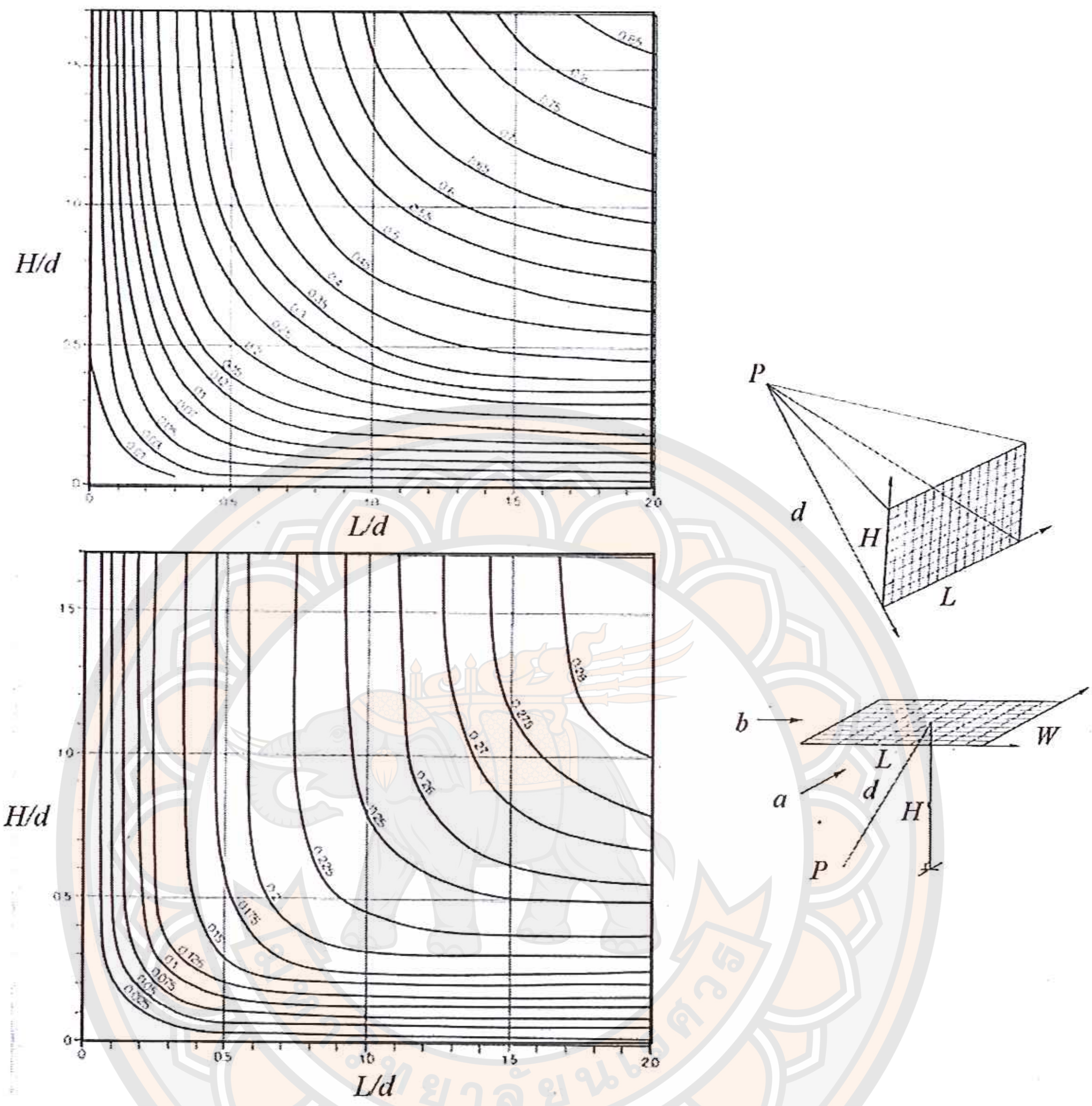

Figure 78 The eye parameters of Daylight Glare Index

Source: Claude L. Robbins [8]

Parameter D_{max} is the maximum fraction of the Standard Work Year (SWY) during which daylight can be used to replace or supplement electric light.

Table 19 Comparison between glare indexes (GI and DGI)

Degree of perceived glare	GI	DGI
Just perceptible	10.0	16
	13.0	18
Just acceptable	16.0	20
Borderline between comfort and discomfort	18.5	22
Just uncomfortable	22.0	24
	25.0	26
Just intolerable	28.0	28

Source: Claude L. Robbins [8]

7. Lighting design

The Lumen method is the light calculation method used to find sizes and arrangement of light bulbs. In uniform distribution design, the value estimation was a result from Eq.92-96 presented by IES standards [21].

$$F = (E)(A) / (CU)(LLD)(LDD) \quad Eq.92$$

$$CU = (5h_C)[(L + W) / (L \times W)] \quad Eq.93$$

$$CCR = (5h_{CC})[(L + W) / (L \times W)] \quad Eq.94$$

$$RCR = (5h_{RC})[(L + W) / (L \times W)] \quad Eq.95$$

$$FCR = (5h_{FC})[(L + W) / (L \times W)] \quad Eq.96$$

Light control is one of the strategies for saving lighting energy to be able to use energy as needed. It includes switches for on-off or dimming considering the amount of daylight, as shown in Figure 81 stating the results of using the strategies.

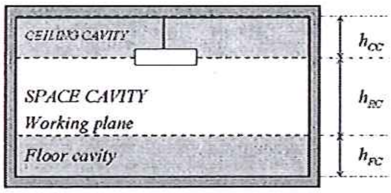

< The separate cavity of the lighting effect.

Figure 79 The spaces cavity of lighting

Source: M. David Egan and Victor W. Olgyay [21]

< The efficiency of lighting need include the reflector what it concentrates the light though the working plane.

Figure 80 The sample, Radial batwing, of light reflector distribution

Source: Benjamin Stein and John S. Reynolds [4]

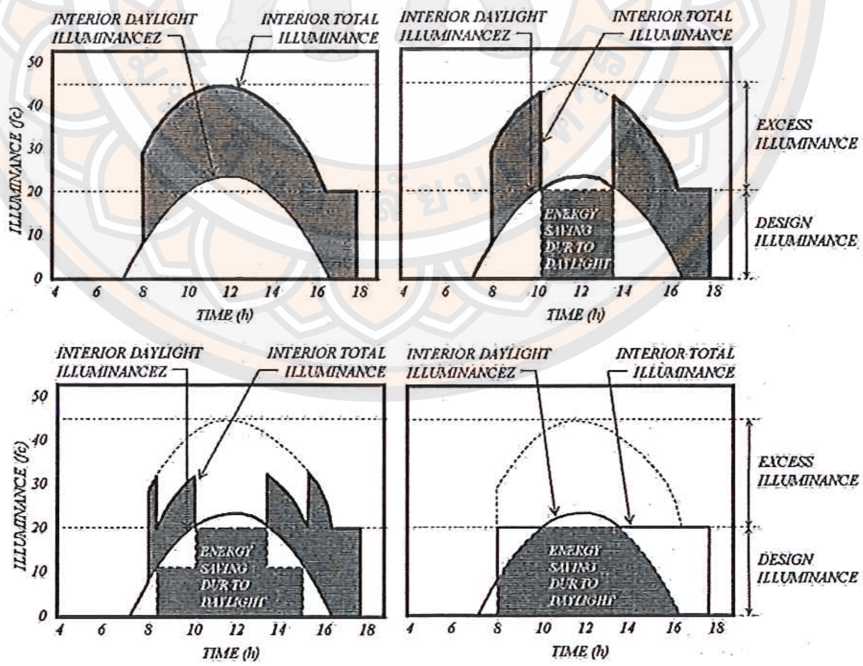

Figure 81 lighting control techniques

Source: Moor, Fuller [25]

Economic

1. Initial cost and life cycle cost

General PV systems are standalone system and grid connected system. The difference between the two mentioned systems is the battery element, which is easier to maintain and able to generate energy more reliably because it does not depending on an energy storage system leading to increasing system cost. When batteries and controller were excluded, its price ratio was about 23% of the system cost combined with saving labor for installation, structure, land used and building materials replaced with PV modules. This is the difference of the BIPV system.

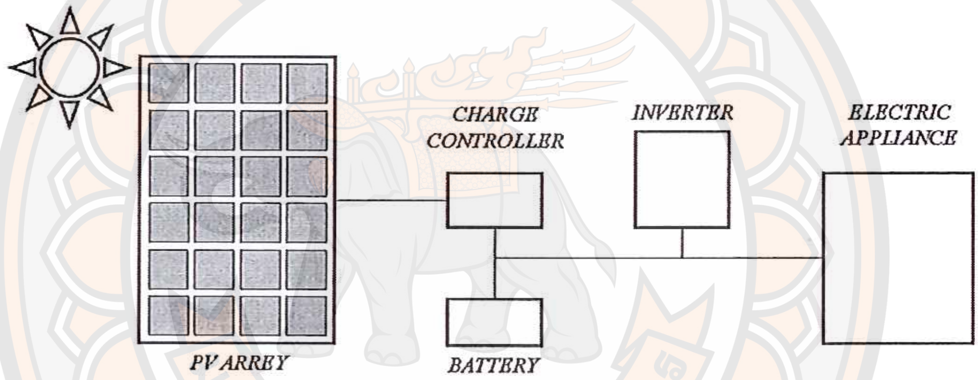

Figure 82 Stand alone PV system

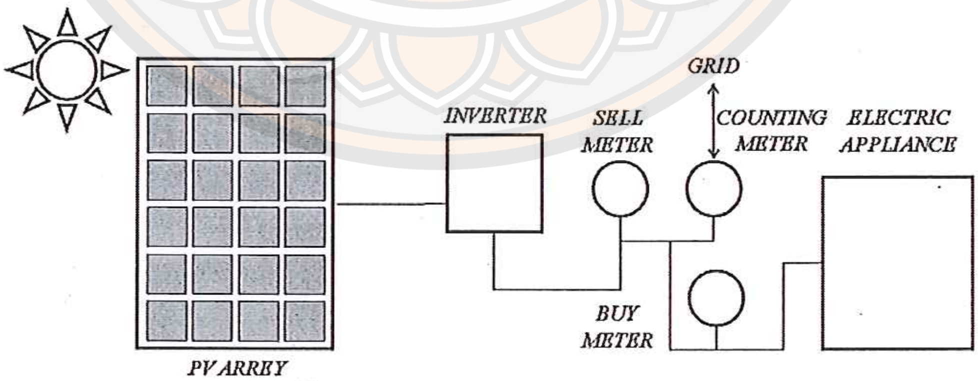

Figure 83 Grid connected PV system

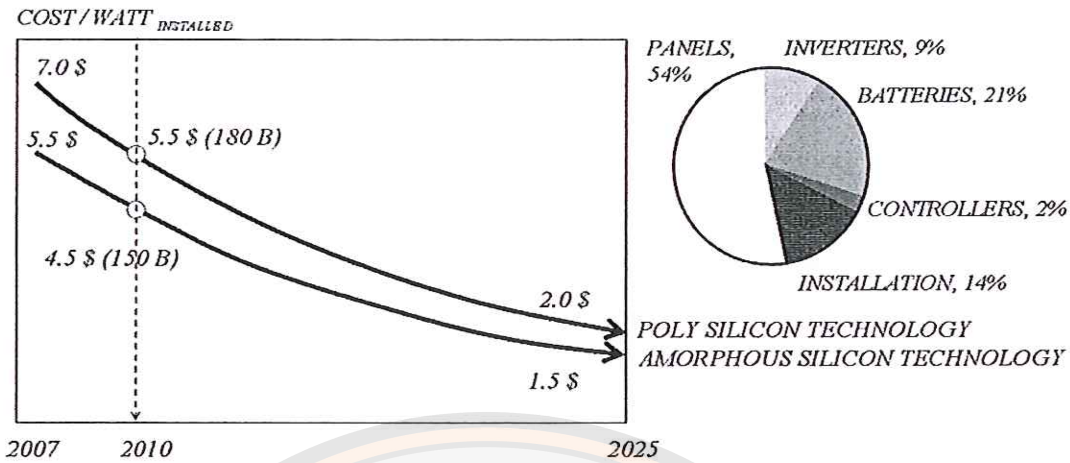

Figure 84 The trend of PV systems cost

Source: LaMonica, Martin [72]; Pearson, Chris [81]

The life cycle cost of a PV system is around 25 years guaranteeing only the PV modules integrated with the building envelope. Its life cycle operation is possibly more than 25 years including maintenance costs as a part of operation. Nevertheless, PV modules are expensive compared to general building materials as shown in Figure 85. The price could be lower when compared to some other types of decorative material. Besides, it is beneficial in clean energy generation concerning the environment. However, the cost of shading in the Thai market is estimated around \$30-\$60 per m^2.

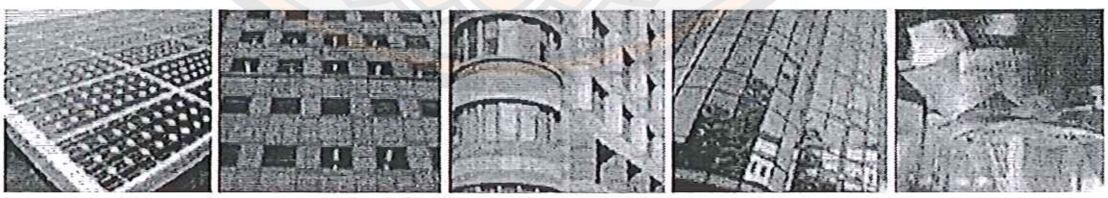

PV panel	Polished stone	Stone	Glass	Stainless steel
\$500-\$1500	\$2400-\$2800	\$800+	\$560-\$800	\$280-\$400

(These material costs were over investment for Thailand market in the present time.)

Figure 85 The comparison of material costs per square meter in 2002

Source: International Energy Agency [69]

2. Economical evaluation

The benefits of BIPV systems consist of 2 levels. First is the direct economic impact causing the decrease of construction material costs, electricity costs, enhancing power quality and reliability and providing tax credits. Second is the indirect economic impact due to environmental emissions reduction. For electrical costs, it is able to reduce energy used in air conditioning systems, save energy in lighting systems and produce energy used to replace energy from the grid. Therefore, to optimize investment, the costs and expected benefits must be acknowledged containing indicators as follows:

2.1 Payback period and break-event analysis

This method is used to predict the year that the benefits and costs will be equal. The break-even is used to compare the design solution for the final decision.

2.2 Benefits-Costs ratio (B/C)

This method converts to the present value of cost by using the present-worth method shown in Eq.98. Then, B/C and the results of comparison between benefits and costs leading to the investment decision are considered.

$$Payback = PVB / PVC \qquad Eq.97$$

$$P = F[1/(1+i)^t] \qquad Eq.98$$

$$PVB = \Sigma[B/(1+i)^t] \quad \text{, during } t=1 \text{ to the last year} \qquad Eq.99$$

$$PVC = K + \Sigma[C/(1+i)^t] \quad \text{, during } t=1 \text{ to the last year} \qquad Eq.100$$

$$B/C = PVB/PVC \qquad Eq.101$$

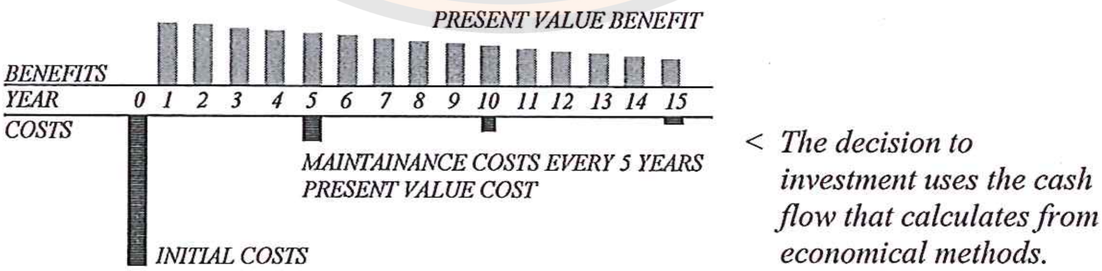

Figure 86 An example of cash flow model

Summary of the review

From the study, it can be concluded and shown in Figure 87 to lead to design a studying process as below:

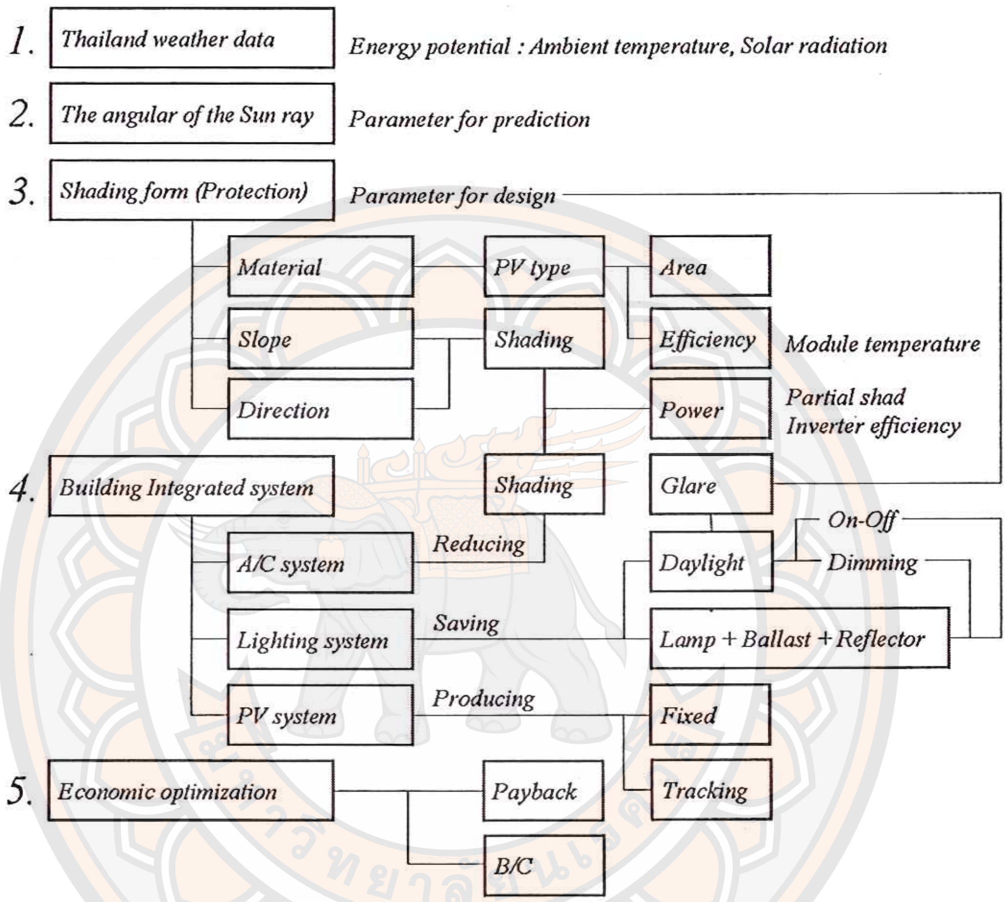

Figure 87 The summary review of the literature

1. Thailand has an solar energy potential average of about 5 kWh/m^2-Day, which is enough for investment.

2. Thailands latitude is between 6-20 degrees and longitude is between 97-101degrees, considering Bangkok, 14 degrees, as the center of Thailand.

3. Parameters affecting energy generated from PV systems include PV technology, slope and direction of PV module installation, which are needed to avoid the shade covering the area of the solar module.

4. The benefits of shading devices integrated with photovoltaic system include reduction of air conditioning system, electricity saving of lighting system and energy generation from the PV system.

5. Shading devices integrated with photovoltaic system can reduce cost of building and be more beneficial than general installation, which only generates energy. Therefore, it is more attractive for investment.

CHAPTER III

RESEARCH METHODOLOGY

Study plan

SIPV is an integrated system appliance consisting of shading, daylight control and electricity production. It depends only on one energy resource which is solar radiation from the sun and sky shining down on shading devices.

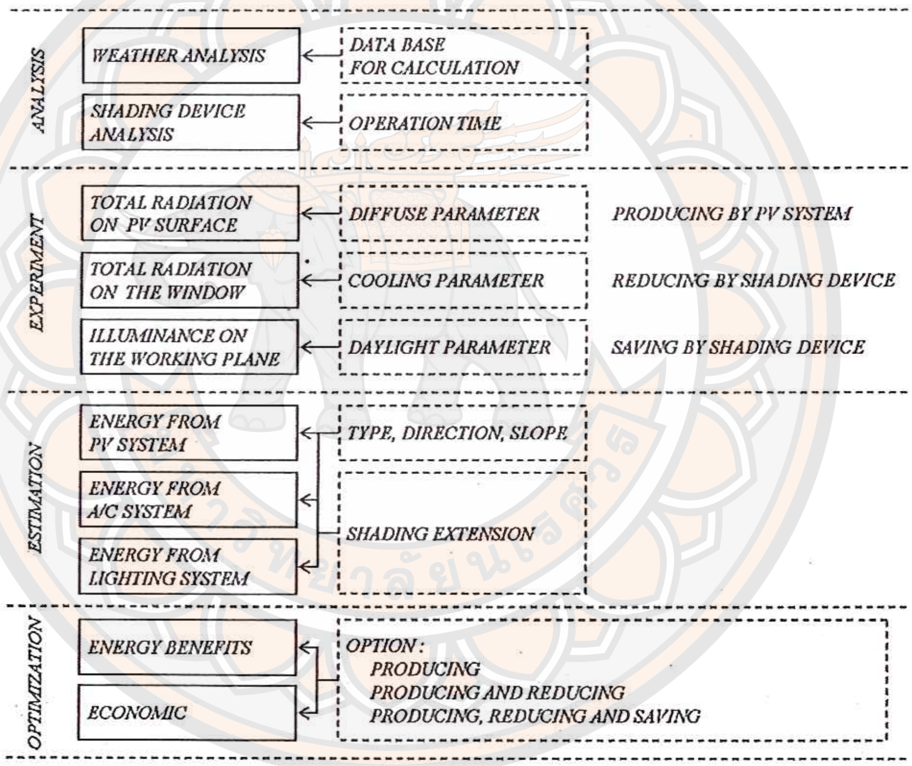

Figure 88 The study diagram

The process of this research trying to search for ideas of designing shape and installation of SIPV with energy suitability is divided into parts as follows:

1. The analysis part is to search for weather database referred to calculation, form of shading device and period of appraisal

2. The experiment part is to improve equations for value calculation in order to make it suitable according to the conditions of system installation

3. The estimation part is to estimate energy values in all kinds of systems annually in order to acknowledge all influences due to the design

4. The optimization part is to look for forms that create the highest level of energy saving in the conditions of establishing the most possible angles and avoiding glare effects. It is also concerning appraisal in the matter of economics to make the highest level of value

The definitions

1. The window functions

The function of a window is to be a source of natural daylight connecting the view between inside and outside. This research is to study only windows being a light channel considering data of heat radiation, daylight and area for view angles, as shown in Figure 89

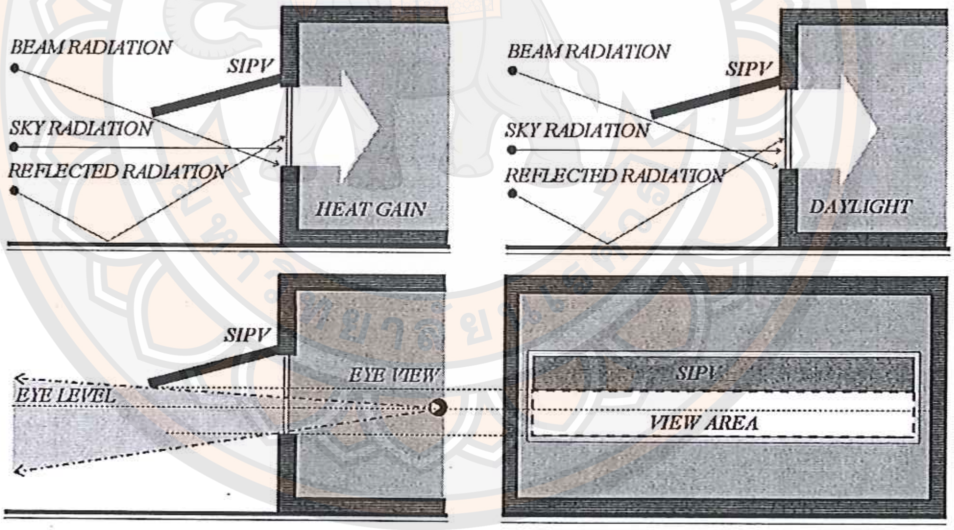

Figure 89 The window functions

2. The shading functions

The functions of shading are to reduce the amount of direct solar radiation and diffuse solar radiation. However, radiation reflecting from the ground still gets in. For estimating the value of received solar heat gain from both heat and light, the isotropic sky model is used.

2.1 The function of preventing heat from solar radiation is shown in Figure 90

2.2 The function of light control is shown in Figure 91

This does not consider direct solar radiation due to determination of design conditions to fully prevent direct solar radiation in the period of time of consideration.

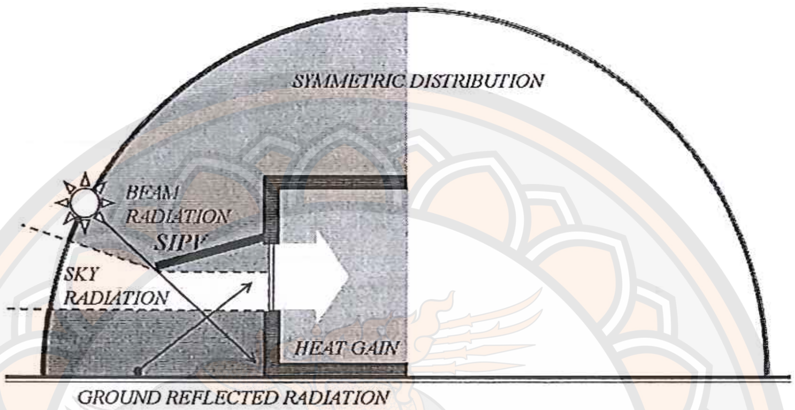

Figure 90 The shading function to protect the sun

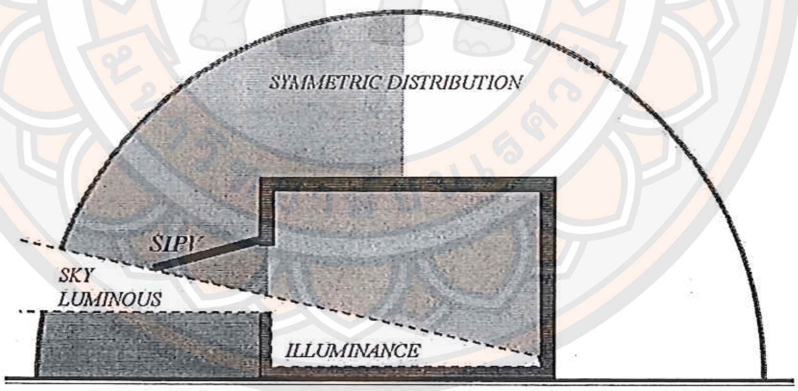

Figure 91 The shading function to control the luminous source

3. The generator function

The function of a solar module is to generate energy by transforming solar radiation into electricity. It depends on direction and inclined angle of the module. The hypothesis of this study is that the total energy produced resulting from the system is able to be used continuously by using a dummy load of a building and having no barriers in front of or on the solar module.

4. The benefits of SIPV

The benefits of SIPV are integrated advantages between shading devices, light control devices and energy production devices as shown below:

4.1 Reducing heat gain from solar radiation in a pattern of cooling load of the air conditioning system (The only focus is on glass under the pattern of shading device and direction of window).

4.2 Saving electricity of lighting systems by using control systems of on-off or dimming techniques under the pattern of shading device and direction of the window.

4.3 Producing electricity by converting solar radiation into electricity due to shading device installation.

5. Benefit options and conditions of study time

There are 3 patterns of benefits the change according to shape as follows:

Option 1; the producing option is the benefit from electricity production.

Option 2; the producing and reducing option is the benefit resulting from electrical energy production and reducing the cooling load of the air conditioning system.

Option 3; the producing, reducing and saving option is the benefit resulting from electrical energy production, reducing the cooling load of the air conditioning system, and saving energy in lighting system due to the use of daylight.

Data collection of this study was in the daytime during 8.00-16.00 for the suitable reasons presented in chapter IV. It is also because the time is suitable for the use of air conditioning systems to create the comfort zone. The consideration to operate the mentioned matter for 365 days was for the highest level of benefit.

Parameter and experimental setting

The study of optimization in SIPV design can be concluded as shown in Figure 92 which is separated into 4 main parts as below:

Part A is to study conditions of parameters depending on location, direction, tilt angle, and technique of PV module setting.

Part B is to collect data on the parameters from the experiments in the matter of total solar irradiance on slope surface, relation of daylight and relation of cooling load because of shading devices outside and inside the building, using basic equation improvement.

Part C is the estimation from calculation appearing in annual energy consumption, reflecting benefits due to light prevention and the use of daylight, and by using an improved equation to respond to the first purpose.

Part D is economic estimation to respond to the second purpose.

In parameter determination, the reference of standard value and use in the real situation should be considered.

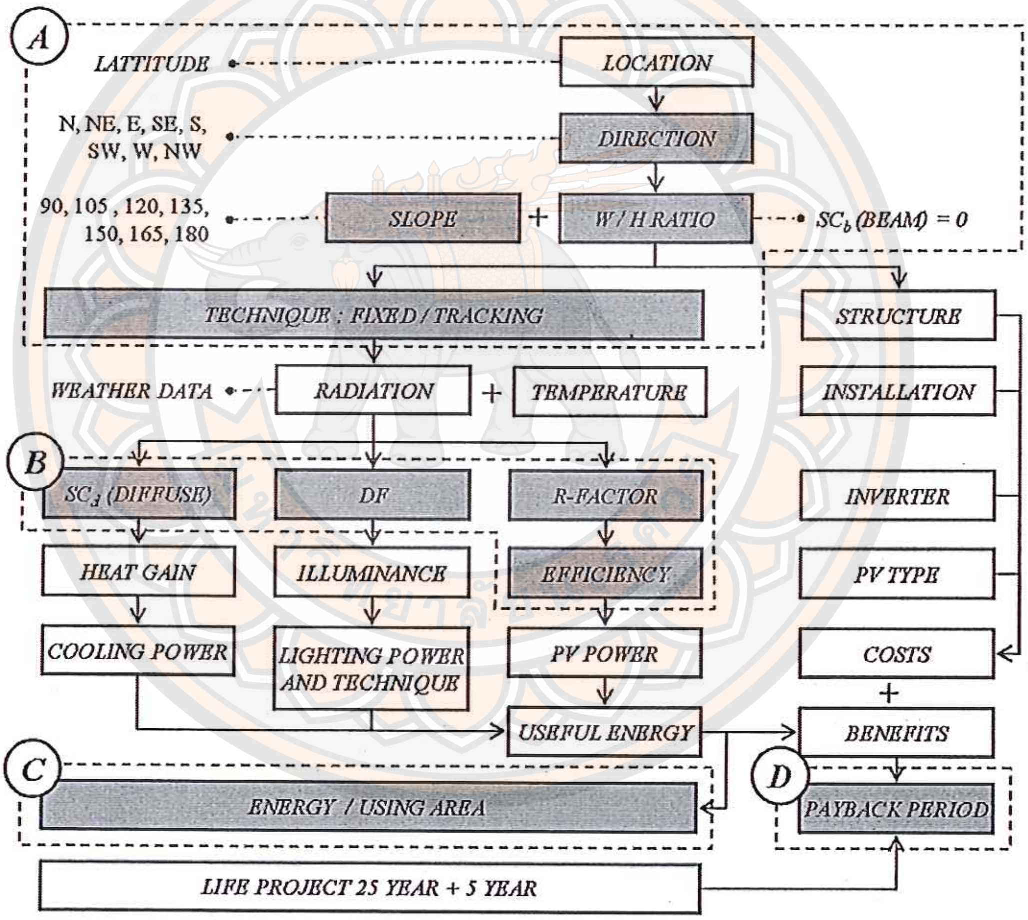

Figure 92 The flow diagram of parameters

1. The form of SIPV parameters

To respond with solar prevention in the form of shading coefficient, the shading coefficient value should be zero for the full-functioned beam solar radiation prevention for the whole period considered and for suitability in avoiding shade on the solar module, as shown in Figure 93. Therefore, a horizontal shading device was designed instead of a vertical module, which causes overlapped shading more easily.

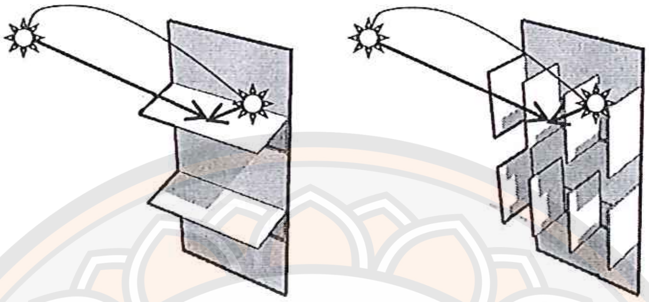

Figure 93 The shelf shading of the horizontal and vertical shading device

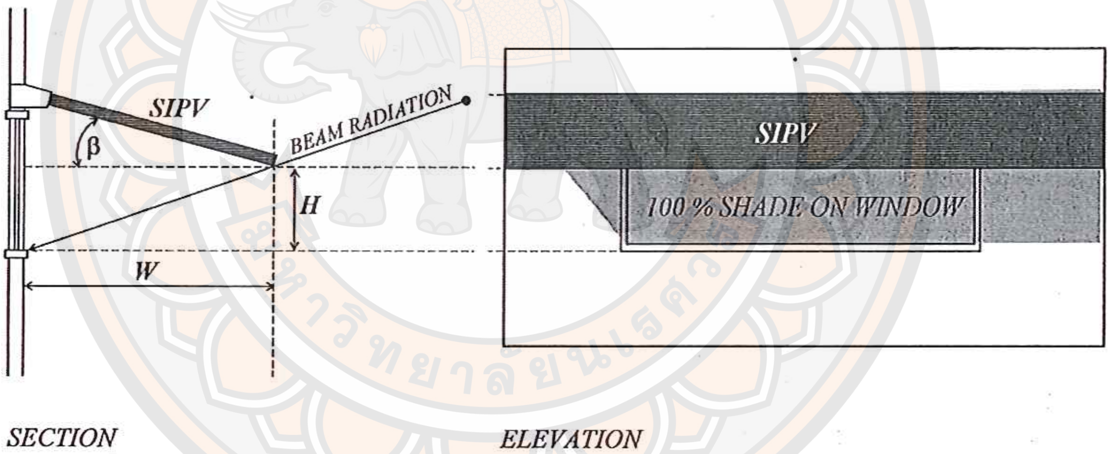

Figure 94 The study form of SIPV

The research specified a form of SIPV considering the outstretched part of the module which affects the shading coefficient used in calculation of the cooling load of the air conditioning system and the daylight factor used in calculation of illuminance on the working plane. The details are as follows:

1.1 Shading extending ratio (W/H): W is the extending part of the shading device and H is the height of the clear window under the horizontal shading device. The relation is shown in Figure 94.

1.2 The shading coefficient of the beam radiation can be found in the form of direct solar radiation on the glass plane. The comparison was the ratio of with shading device to without shading device. The shading coefficient of the diffuse radiation can be found in the form of diffuse solar radiation on the glass plane. The comparison was the ratio of with shading device to without shading device.

1.3 Tilt angle of the shading device was compared to a flat plane as shown in Figure 94.

1.4 Directions used for shading device installation were North, North East, East, South East, South, South West, West and North West.

2. SIPV installation parameter

From part A in Figure 95, the forms of SIPV were installed in 2 patterns: fixed and tracking patterns. Each installation technique was a study to optimize installation for practical use as a building shading device. The details of the study were as below:

2.1 The fixed SIPV, shown in Figure 95

2.2 The tracking SIPV, shown in Figure 96

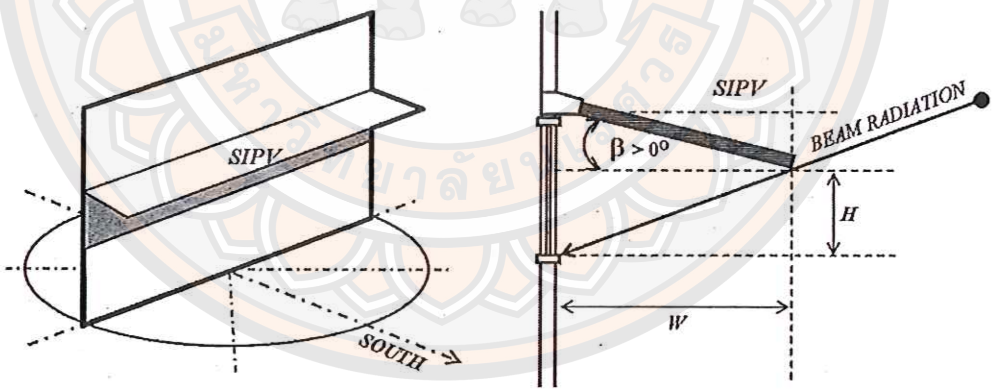

Beam radiation protection during operation time : 100% ($SC_b = 0$)

Direction : N,NE, E, SE, S, SW, W and NW

Slope (β) : 90, 105, 120, 135, 150, 165 and 180

Figure 95 The condition of the fixed SIPV technique

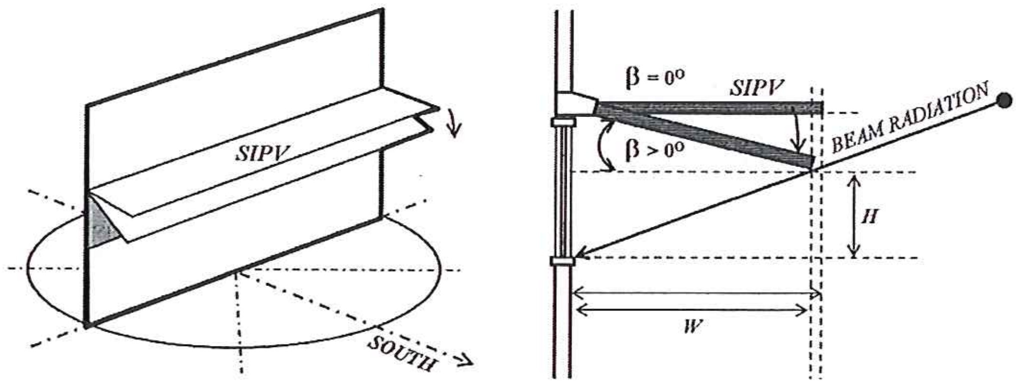

Beam radiation protection during operation time : 100% (SCb = 0)

Direction : Some direction that are optimized

Slope (β) : Tracking follow from the window function

Figure 96 The tracking condition of SIPV

3. Constant parameters

To estimate, constant parameters were calculated to determine energy of air conditioning systems, light systems and energy generation systems as shown in Figure 97. The parameters used in system design are as follows:

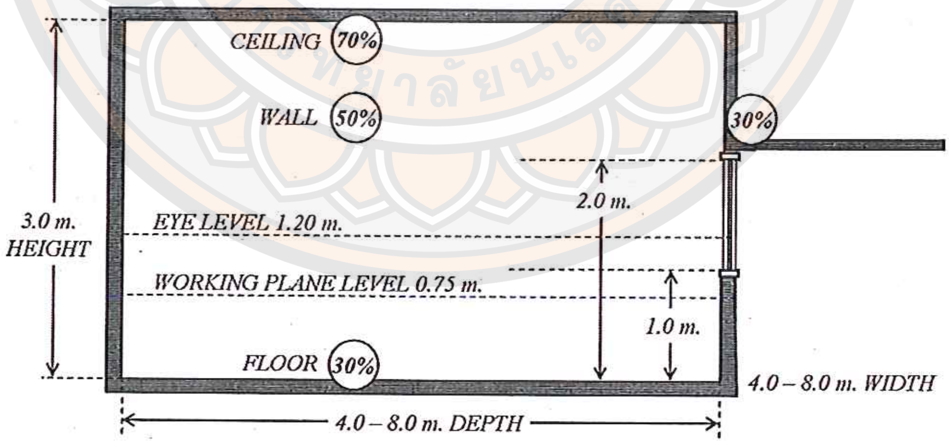

Figure 97 The constant parameters of the working space

3.1 PV technologies are a type installed for study and data collection at SERT since 2005 consisting of 2 types as shown in Figure 98.

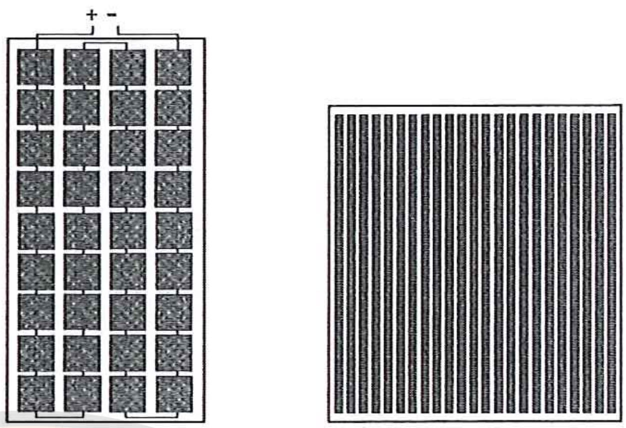

Technology	*Polycrystalline Silicon (p-Si)*	*Amorphus Silicon (a-Si)*
Power of installation (W_p)	*80*	*54*
Area (m^2, dimension)	*0.64,*	*0.85*
Weight (kg)	*N/A*	*N/A*
Efficiency (STC)	*11.53*	*5.74*
Temperature coefficient	*N/A*	*N/A*
Frame / substrate	*Aluminium / White plastic sheet*	*N/A*

Figure 98 The PV technologies of the study

3.2 The air conditioning system gained a Coefficient of Performance (COP) of 3.22 referred from the law of energy conservation in buildings in Thailand. In medium mass construction, the internal temperature system operation was determined at above 25°C.

The thickness of clear glass was also determined at 6 mm with overall heat transfer coefficient (U) at 5.874 W/m^2-°C, solar heat gain coefficient (SHGC) at 0.73 and visible transmittance at 0.88.

3.3 The lighting system consisted of T5 fluorescent 28 W bulbs with a loss of Ballast Electronic 4 W installed and a bat wing reflector. The coefficient of utilization were as follows:

LLD=0.95, LDD=0.90, Fsa=1.14, Ful=0.85

Design conditions were at the minimum of 300 lux, and the working plane was at 0.75 m according to the standards of light design for a general working area. The light control techniques used were on-off and dimming techniques.

4. Room parameters

To calculate the energy of air conditioning systems and light systems, it is necessary to specify the size of the using area. For lighting system design for rooms with different sizes, the number of light bulbs needs to be decided according to different Lumen method calculation. The primary scope of the study was determined to design a general room with 4 m, 6 m and 8 m width of A dimension which is the same to room B dimension with depths of 4 m, 6 m and 8 m. the size and number of light bulbs is shown in Figure 99 and Table 20. To specify the size of the room relation of A x B, there are 9 cases in total.

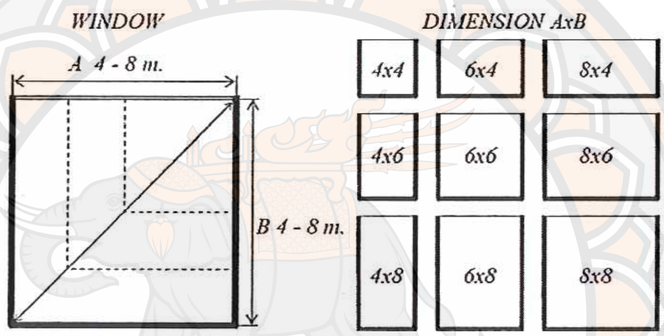

Figure 99 The dimension of study rooms

Table 20 The lighting installation by lumen method

Room dimension A x B	Direction A	Direction B
R 4x4	2 Lamp	3 Lamp
R 4x6	2 Lamp	4 Lamp
R 4x8	2 Lamp	5 Lamp
R 6x4	3 Lamp	3 Lamp
R 6x6	3 Lamp	4 Lamp
R 6x8	3 Lamp	5 Lamp
R 8x4	5 Lamp	2 Lamp
R 8x6	5 Lamp	3 Lamp
R 8x8	5 Lamp	4 Lamp

Experimental installation

The experiment can be divided into 3 parts as follows:

1. PV generator production

The main equation for calculation under the isotropic sky model was able to be explained in accordance with Eq. 15, which is the basic equation used in calculating total irradiance on a sloped surface under the isotropic sky model. The parameters of the mentioned equation were improved in the diffuse radiation factor and added in terms of solar radiation due to the reflection of the building wall. It is because of the difference of installation from the formal basis, as shown in Figure 100.

$$P_{SIPV} = \eta_{inv}\,\eta_{SIPV}\,E_{t\text{-}SIPV} \qquad Eq.102$$

$$E_{t\text{-}SIPV} = (R_b)E_G + (R_{sd}\,R_d)E_d + (R_{rG})E_G + (R_{rB})\,E_V \qquad Eq.103$$

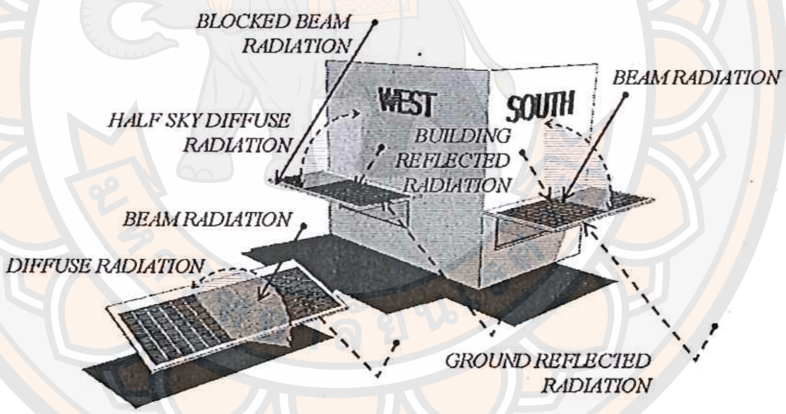

Figure 100 The difference of the installation effects

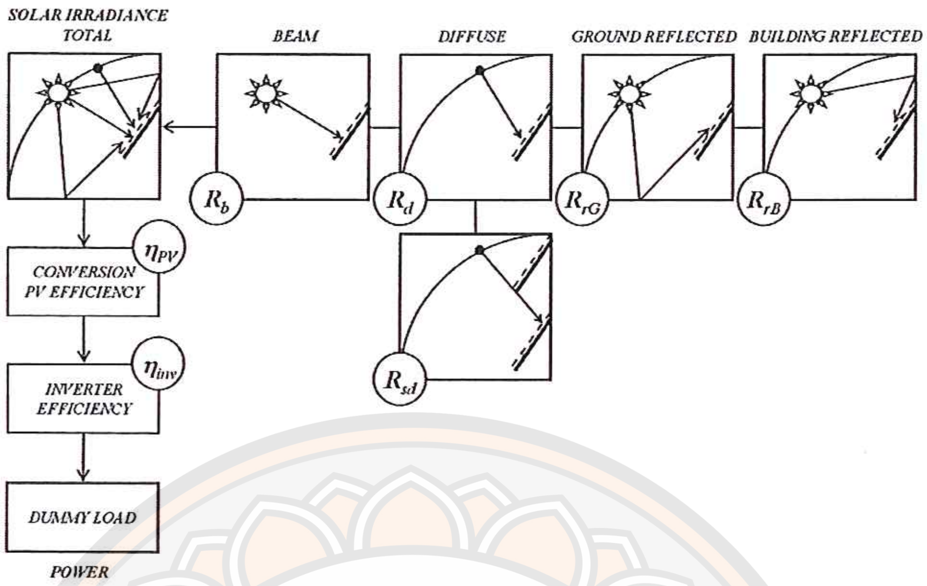

Figure 101 The relative factor of the power from SIPV system

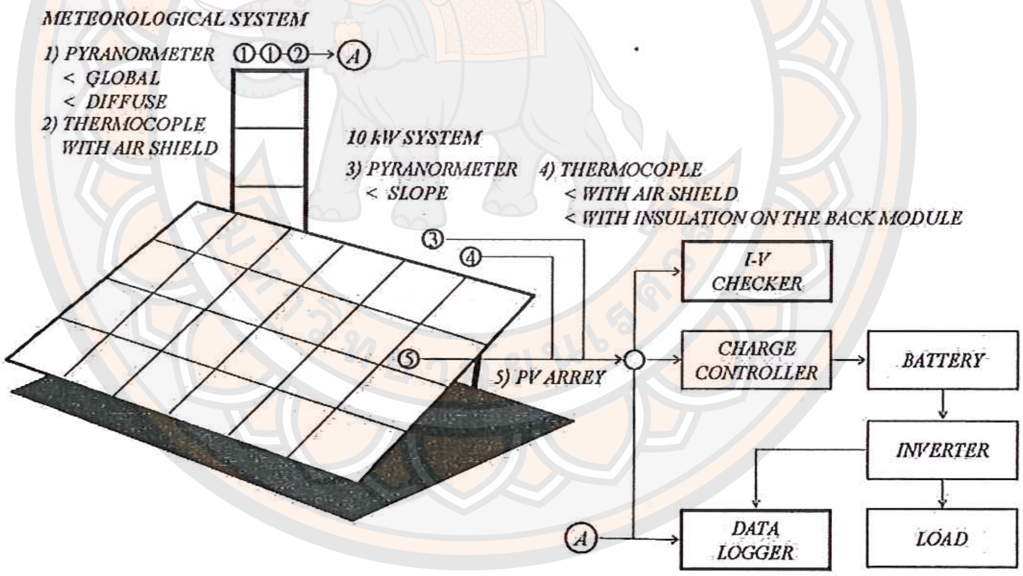

Sensors	*Data collected*	*Logger*	*Data collected*
Global pyranormeter	E_G	*I-V checker*	E_{tS}, T_{amb}, T_m, I, V
Diffuse pyranormeter	E_d	*Data logger*	E_G, E_D, E_{tS}, T_{amb}, I, V
Slope pyranormeter	E_{tS}		
Thermocopple with air shield	T_{amb}		
Thermocopple with insulation	T_m		

Figure 102 The PV system at SERT

The parameters of solar radiation in part A (shown in Figure 102) were solar radiation and weather condition data collected by a data logger attached to sensors. These parameters include the following:

1.1 Module temperature (T_m)

Module temperature was used to study the effects of temperature on PV array efficiency in both cases of amorphous silicon technology and polycrystalline silicon technology and parameters were analyzed by regression analysis using least square curve fitting to be used in prediction in the form of linear curve as shown in Eq.104.

$$T_m = aX_1 + bX_2 + c \qquad Eq.104$$

The information recorded was from meteorological information about weather and solar radiation for a 10-kW electrical system, as shown in Figure 102.

1.2 PV efficiency case of full sky condition (η_{PV})

Electricity converted from solar radiation depends on PV system efficiency. The experiment was analyzed by regression equation and was used to predict the value by the linear curve equations shown in Eq.105. The information collected was from meteorological information about weather and solar radiation for a 10-kW electrical system, as shown in Figure 102.

$$\eta_{PV} = aX_1 + bX_2 + c \qquad Eq.105$$

1.3 PV efficiency case of half sky condition (η_{SIPV})

In this case, the PV module received some part of solar radiation while there is an existence of air temperature similar to the case of having no shade. This experiment, therefore, was to analyze the relation of current and volt via the relation between I-V curve and P-V curve at STC, at solar irradiance of 1,000 W/m^2 containing cell temperatures at 25°C and air mass at 1.5. Then it is managed to adjust the parameters of solar irradiance, ambient temperature, and module temperature which were predicted due to Eq.104 from the case of half sky condition to find the predicting equation from the trend line according to regression analysis as shown in Eq.106. The information collected was from meteorological information about weather and solar radiation for a 10-kW electrical system, as shown in Figure 102.

$$\eta_{SIPV} = aX_1 + bX_2 + c \qquad Eq.106$$

1.4 Efficiency of the inverter system (η_{inv})

The information on efficiency of inverter systems was from the research belonging to Tharika Bunpan [53]. Efficiency of the inverter system depending on solar irradiance leads to the process of building data analyzed via a linear curve regression equation to be used in prediction using linear curve regression analysis as presented in Eq. 107.

$$\eta_{inv} = aX + c \qquad Eq.107$$

1.5 Efficiency of Power degradation for a long period (η_D)

It is considered from the guarantee of the production company leading to create a linear curve predicting equation as shown in Eq.108.

$$\eta_D = aX + c \qquad Eq.\ 108$$

1.6 Coefficient of solar reflectance (ρ)

Experimental materials tested included white wall and dark wall substitutes in order to cut out factors of reflection in unwanted directions as much as possible by measuring spectral solar irradiance, as shown in Figure 103, at wavelengths of 350-1050 nm. Spectroradiometer was used in record to find solar irradiance reflection from calculating the ratio of spectral solar irradiance reflecting from material skin to direct spectral solar irradiance averagely through wavelength.

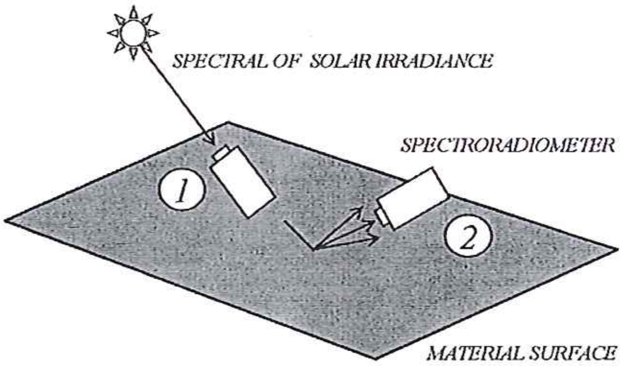

The measurement of spectral irradiance, position of the meter against the surface being measured and slowly retract the meter to a position 10 centimeter.

Figure 103 The experiment of the reflectance value

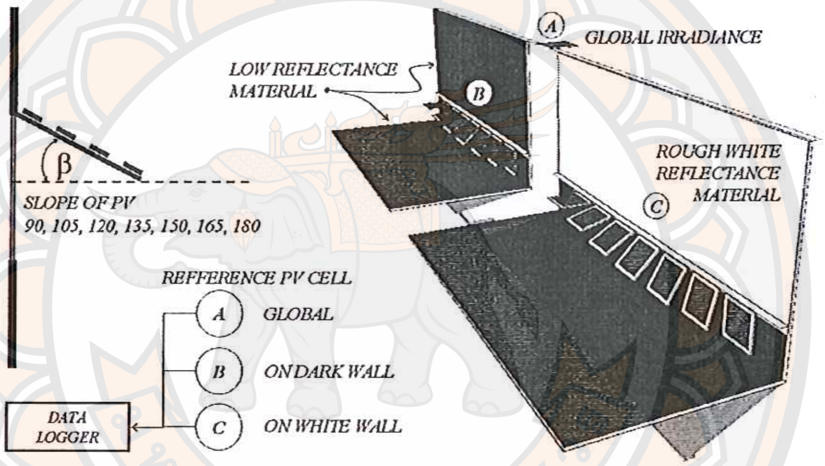

Figure 104 The experimental installation of the relative factors

1.7 Relative diffuse radiation factor (R_d) and relative reflected radiation factor (R_{rB}) falling down on solar module

General building envelope can reflect solar radiation in the form of diffuse radiation reflection due to the rough envelope, unlike glass, resulting in an unclear direction of solar radiation and affecting visual comfort. In Thailand, buildings are controlled by the Building Control Act, B.E. 2522 (1979), assigning the reflection on the envelope of high-rise building or large building not more than 30%, as shown in Figure 105 (above) indicating spectral solar irradiance reflecting from a white wall, from which solar reflectance can be calculated equivalent to 38%. Figure 105 (below) indicates a dark wall, from which solar reflectance can be calculated equivalent to 4% throughout the wavelength of 350-1050 nm.

The installed experiment reflecting black low solar irradiance as shown in Figure 104 was to cut out factors of solar irradiance reflecting from the floor as much as possible leading to study only part of the solar irradiance from the sky. In the case of the white wall, it was used to compare influence as a result of reflection when compared to the dark wall with low solar reflectance. The experiment was installed at SERT, Naresuan University, Thailand for 2 consecutive weeks in February 2011.

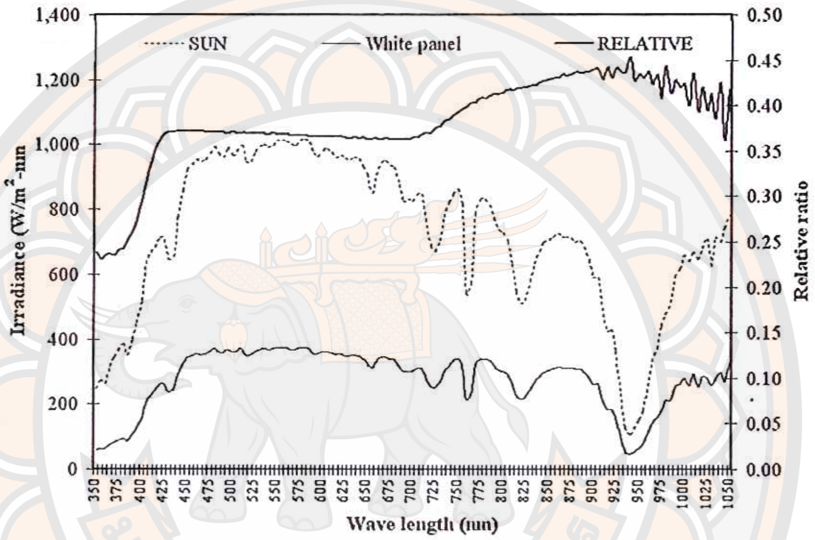

White panel

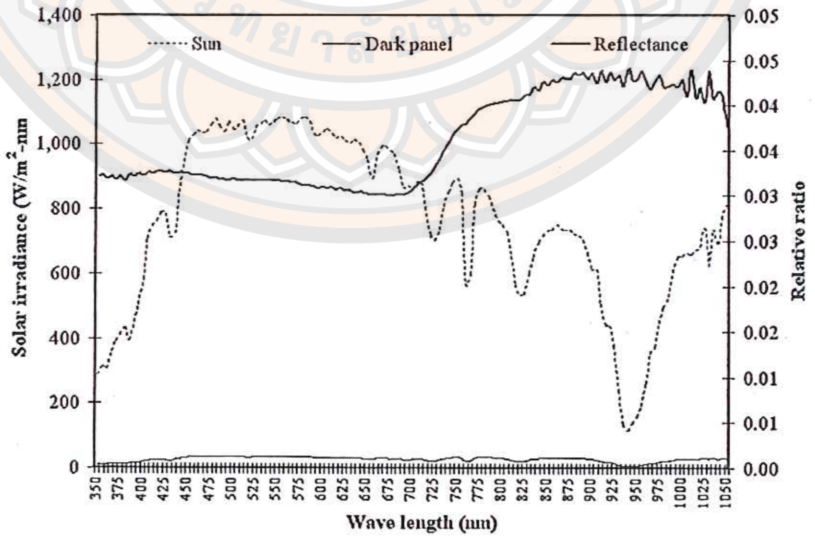

Dark panel

Figure 105 The solar reflectance experiments of the white and dark panel

The equipment set was placed towards North and West in a period of no direct solar irradiance to collect only diffuse data. It was also placed towards West and South in case of direct solar irradiance appearance to collect data compared to reflectance of solar irradiance.

The relative diffuse radiation factor: R_d was to be calculated from the ratio of receiving diffuse solar irradiance on the reference cells with different tilt angles to the reference cells with tilt angles on a horizontal plane (or 0 degree) in the condition of half sky equivalent to 0.5 compared to full sky on the dark plane.

The relative reflected radiation factor: R_{rB} was calculated from the ratio of receiving solar irradiance reflected from the white wall on the reference cells with different tilt angles to the reference cells with different tilt angles located on the same angles on the dark plane and compared to reference cell with tilt angle of 90 degrees, equivalent to 1.0.

Both experiments were analyzed by calculating the average data change according to solar attitude and creating an equation to predict it. A regression equation was analyzed by least square curve fitting to be used in prediction via a linear curve as shown in Eq.109 and Eq.110 respectively.

$$R_d = m(X) + C \qquad \text{Eq. 109}$$

$$R_{rB} = m(X) + C \qquad \text{Eq. 110}$$

1.8 Relative diffuse radiation factor under self shading: (R_{sd})

For vertical self-shading SIPV installation, as shown in Figure 106, relative diffuse radiation was decreased by view angles opened towards the sky according to each case of installation with the outstretched part and distance between modules. Direct solar irradiance was also decreased due to shade of SIPV modules covering each other as shown in Figure 106, indicating that the reference cells installed on the dark vertical plane provided low levels of solar irradiance reflectance to reduce the influence of reflectance by using electric measurement in the form of mV, which is the ratio between covered lower module (B) and uncovered upper module (A) in every case of change in extended distance (W) and covered distance (S) under clear sky and overcast sky. This experiment was installed at the Faculty of Architecture, Chiang Mai University, Thailand from July to September 2011.

The experiment was analyzed by calculating average data change according to extended distance and covered distance between vertical modules to compare the decrease of diffuse solar irradiance in each design.

$$R_{sd} = mX + C \qquad Eq.\ 111$$

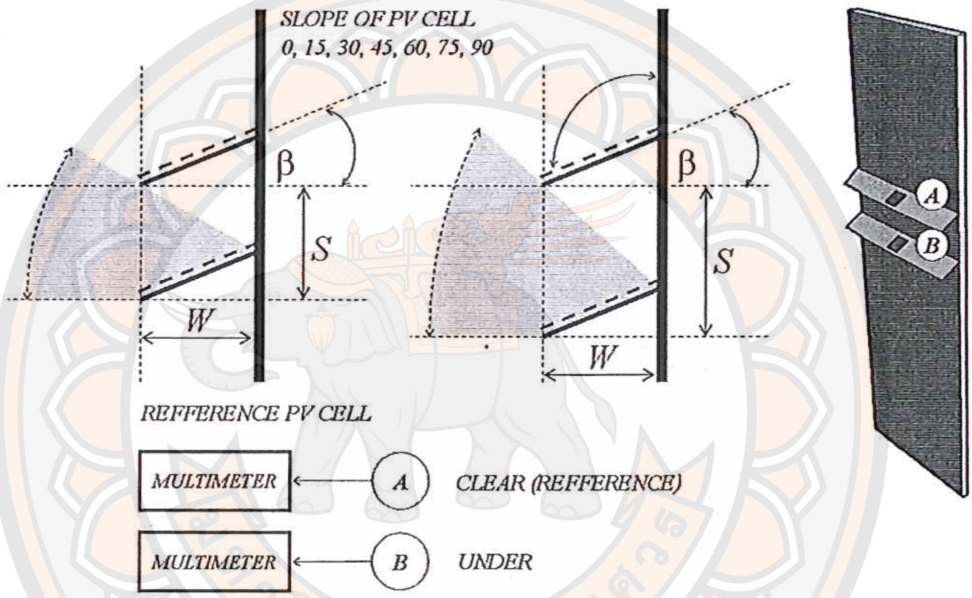

Figure 106 The relative factor of diffuse radiation under the SIPV

2. The daylight factor (DF)

The CIE sky model was used in calculation. The DF method was used in illuminance level estimation on the working plane in buildings and separated for consideration into 2 groups, namely the sky component: SC and internal reflected component: IRC without considering the external reflected component: ERC. Illuminance level on the working area inside the room is the sum total of SC and IRC, as shown in Figure 107. In addition, data collection was used to calculate the mean DF, as shown in Eq.112.

$$DF = C\text{ ; vary by distance of the dept of working space} \qquad Eq.\ 112$$

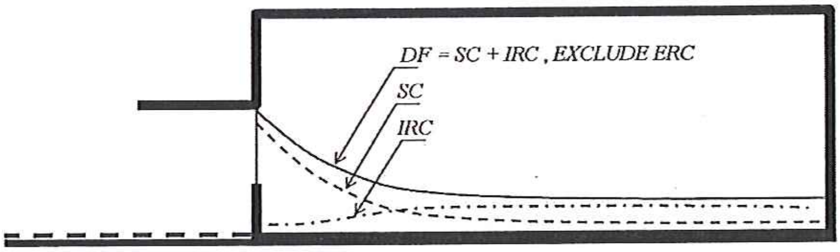

Figure 107 The combination of the daylight components

2.1 The sky component of the daylight factor (SC)

Influence from sky was shown in the form of SC. The experimental models were at the scale of 1:15 in measure of illuminance level at all levels of length shown in Figure 108 under clear sky and overcast sky. Inside wall models were painted black providing low solar irradiance reflectance to reduce the influence of IRC. In addition, illuminance levels in the buildings were measured and collected at all distances. It was also compared to the model's exterior in the case of having no covering and being under a band ring to confute the value gained from direct solar irradiance. The experiment was located at Faculty of Architecture, Chiang Mai University, Thailand from July to September 2011.

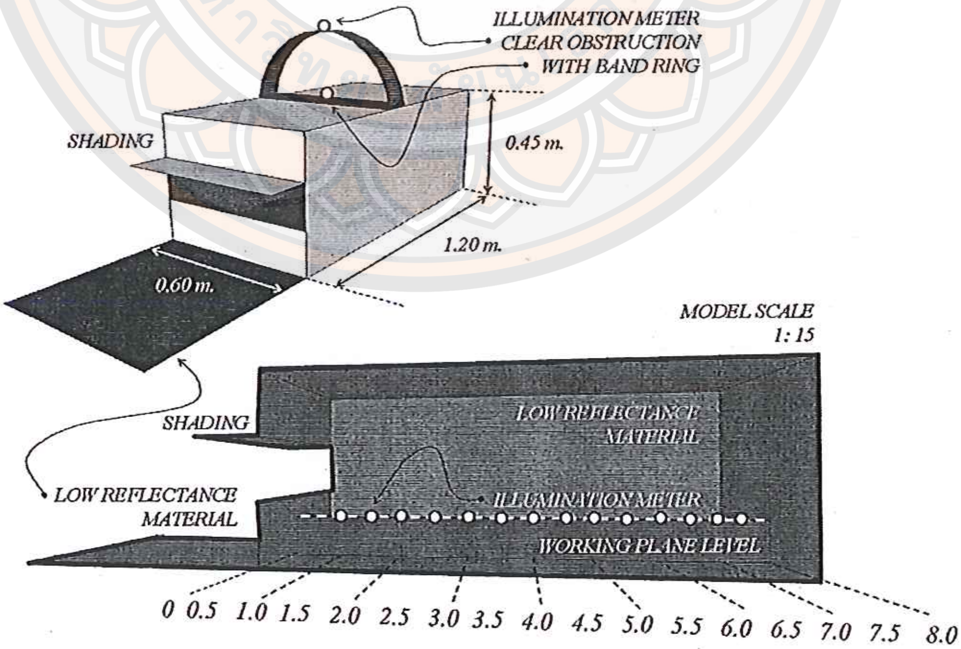

Figure 108 The sky component experiment

2.2 The internal reflected component of the daylight factor (IRC)

It is an experiment using a model at the scale of 1:20 which is smaller due to the limitation of the mirror box, the tool used for reproduction of an overcast sky, as shown in Figure 109. The model contains ceiling material, internal walls and flooring with reflectance ability at 70%, 50% and 20%, respectively. The experiment was kept in a laboratory at the Faculty of Architecture, Chiang Mai University, Thailand.

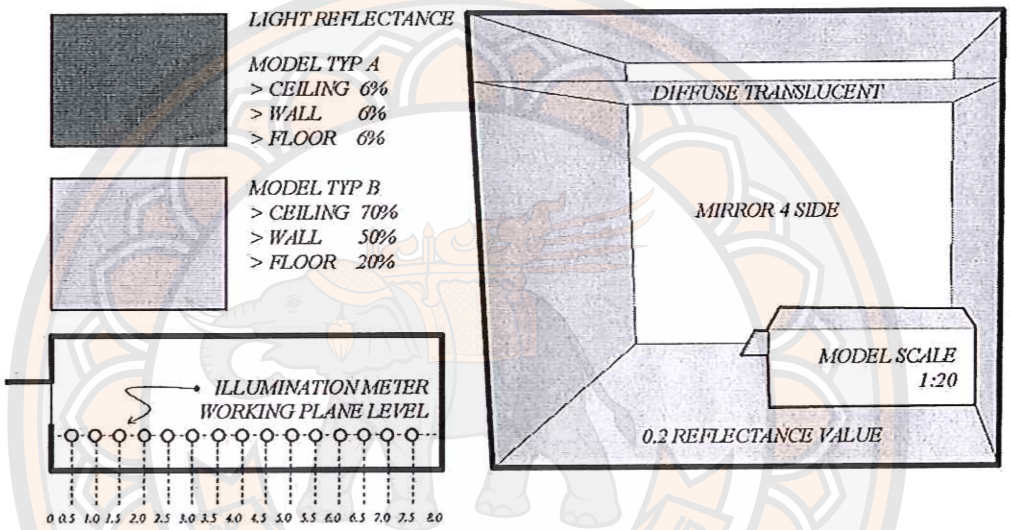

Figure 109 The internal reflected component experiment

3. The shading coefficient of the diffuse radiation (SC_d)

The W/H ratio of SIPV can prevent direct solar irradiance, which is related to Cosine's law and some part of diffuse irradiance using view factors. SIPV in this study was determined to have fully prevented direct solar irradiance. Therefore, the experiment was a study of SC_d only.

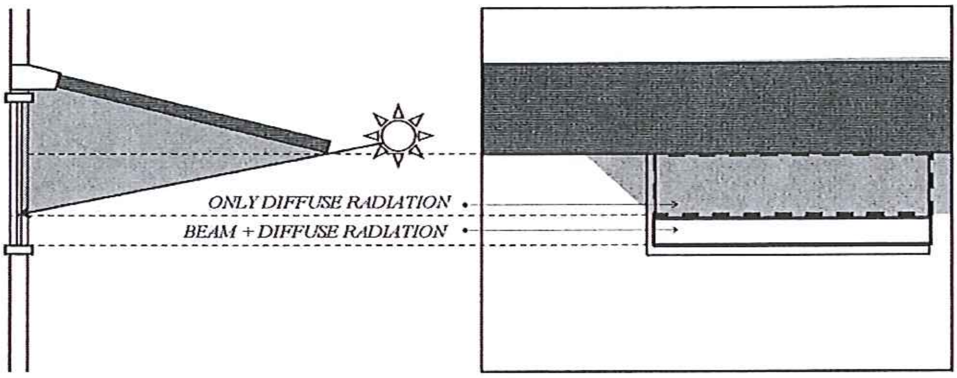

Figure 110 The shading effect from the beam and the sky

The model shown in Figure 111 was used in an experiment to compare forms of shading devices with ratios of W/H installed on the dark wall and dark floor providing low solar irradiance reflectance to eliminate influence of reflected irradiance as much as possible. Collected data from the reference cells was compared as a ratio of being under the shading device to having no shading device. The experiment was located at SERT, Naresuan University, Thailand for two consecutive weeks constantly in February 2011. An equation was created for prediction through analyzing the regression equation using least square curve fitting, which was used in linear curve prediction, as shown in Eq.113.

$$SC_d = m(W/H) + C \qquad Eq.\ 113$$

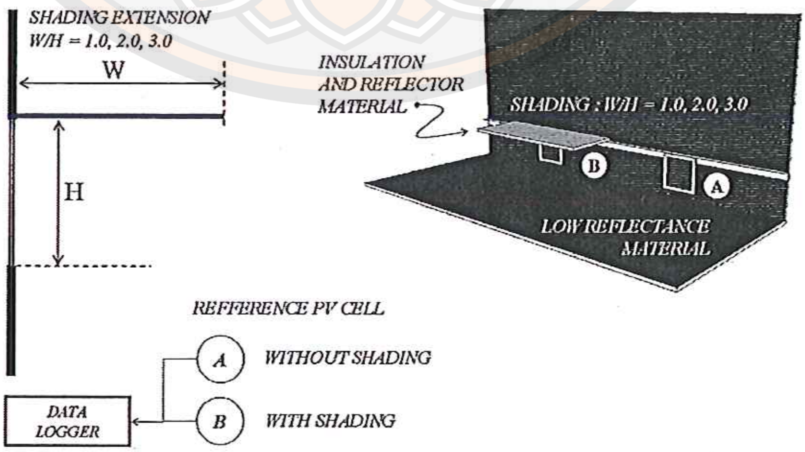

Figure 111 The Shading Coefficient of the diffuse radiation experiment

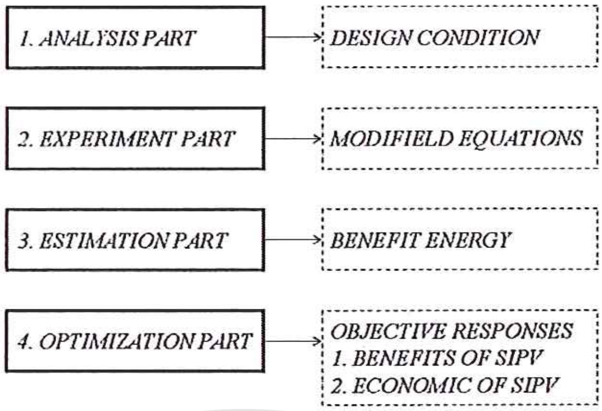

Figure 112 Summary of the study process

Summary of the study process

The study process can be divided into 4 parts as follows:

1. The analysis part is to search for condition of SIPV design and database concerning weather and solar radiation

2. The experiment part is to determine and study .parameter by improving every factors used in calculation of energy of air conditioning system, lighting system and energy generation system

3. The estimation part is to estimate annual energy consumption in every system

4. The optimization part is to prove objectives from study in order to design proper SIPV system

CHAPTER IV

RESULTS AND DISCUSSION

Study process

There are 2 objectives in this research as follows: first is to optimize heat reduction and light usage in buildings. Second is to optimize in economics due to the usability of Shading Device Integrated Photovoltaic system, study process as shown in Figure 113.

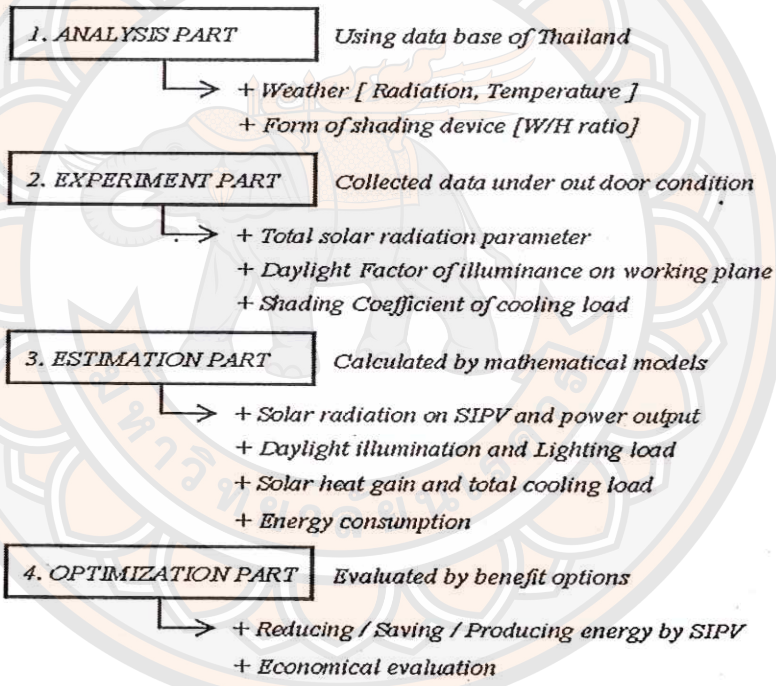

Part 1; Analysis is to study data on solar irradiance and weather including the forms of shading devices proper for direct solar irradiance prevention.

Part 2; Experiment is to study parameters used in equation of calculating total radiation, daylight factor and shading coefficient.

Part 3; Estimation is to study estimation of developed equation to predict benefit concerning energy gained from SIPV installation.

Part 4; Optimization is to study benefit and expenses in SIPV investment to evaluate worthiness and study objectives response.

Figure 113 The study process diagram

Analysis part

1. Solar radiation and weather data in Thailand

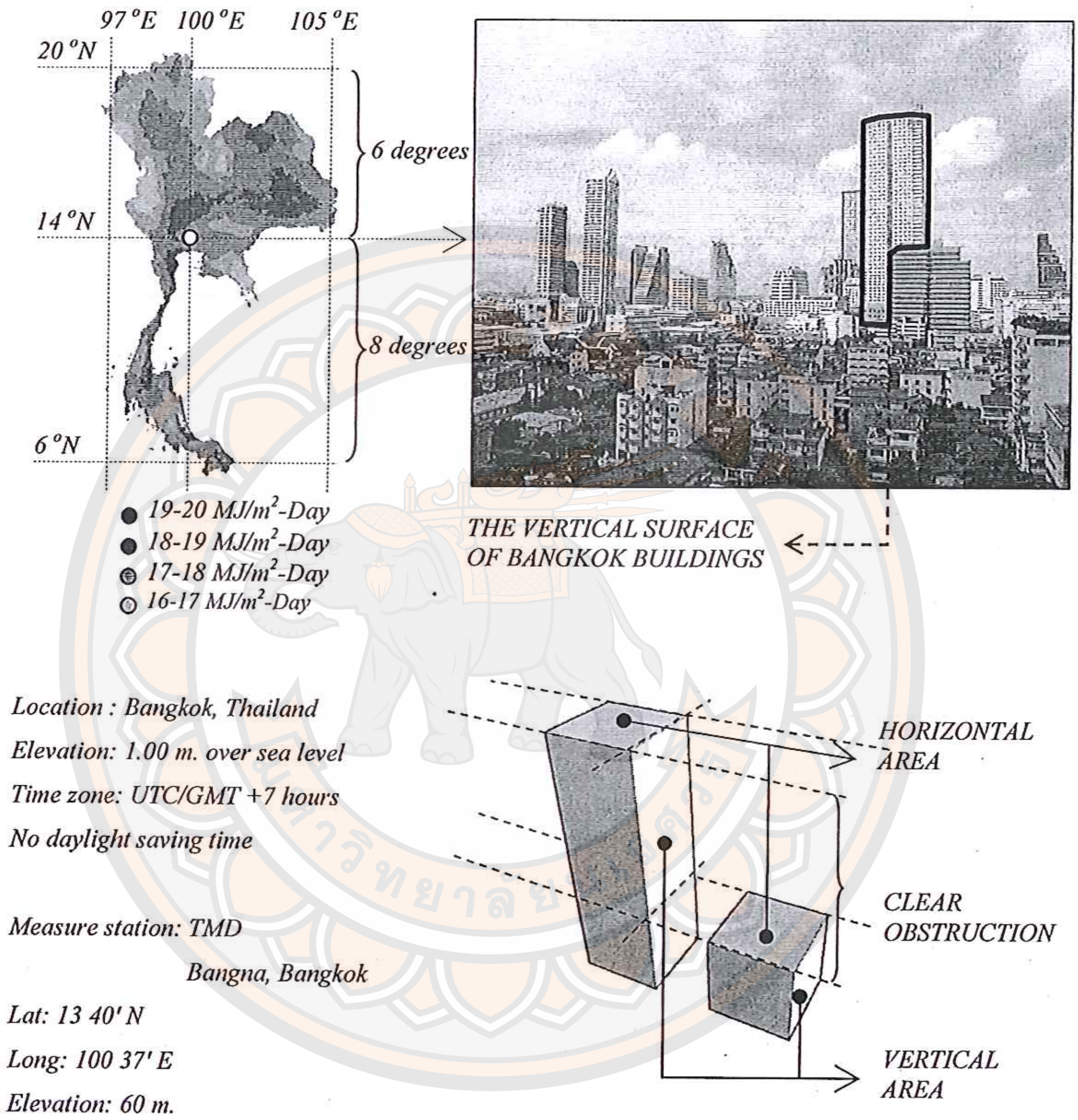

Figure 114 The represented city of Thailand location

Source: Department of Alternative Energy Development and Efficiency [65]

Bangkok as a hub representing Thailand appears to have a large amount of building envelopes receiving more of solar radiation than buildings in other cities. Buildings in Bangkok consist of high-rise buildings with vertical surface rather than horizontal surface. Shading devices and high-performance glass are needed for solar heat gain prevention as presented in Figure 114 showing Bangkok location with image of the city on geographical territories gaining solar radiation averagely 18-19 MJ/m^2-Day.

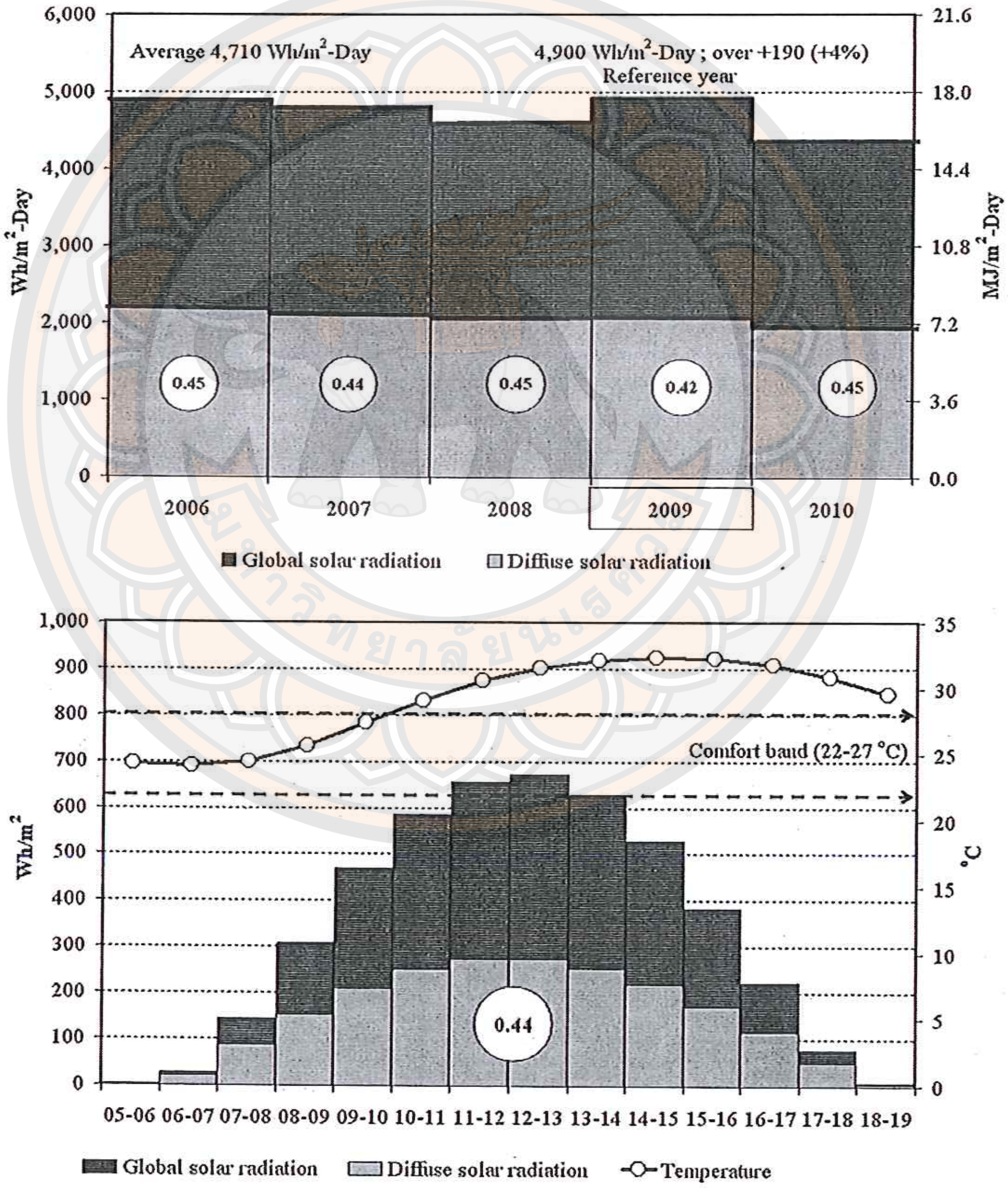

Figure 115 Average solar radiation and air temperature of Bangkok

During 2006-2010, solar radiation data of Bangkok shown in Figure 115 (Top) showed ratio of solar diffuse radiation at 42%-45%. In 2009, ratio of solar diffuse radiation was about 42% and total solar radiation was about 4,900 Wh/m^2-Day which was higher than the average of the total data 4% or about 190 Wh/m^2-Day. Figure 115 (below) shows the comparison between the hourly average of solar radiation and air temperature concerning comfort zone of between 22-27 °C. It is found that the temperature was higher than comfort zone after 10.00 A.M. and remained for the whole day.

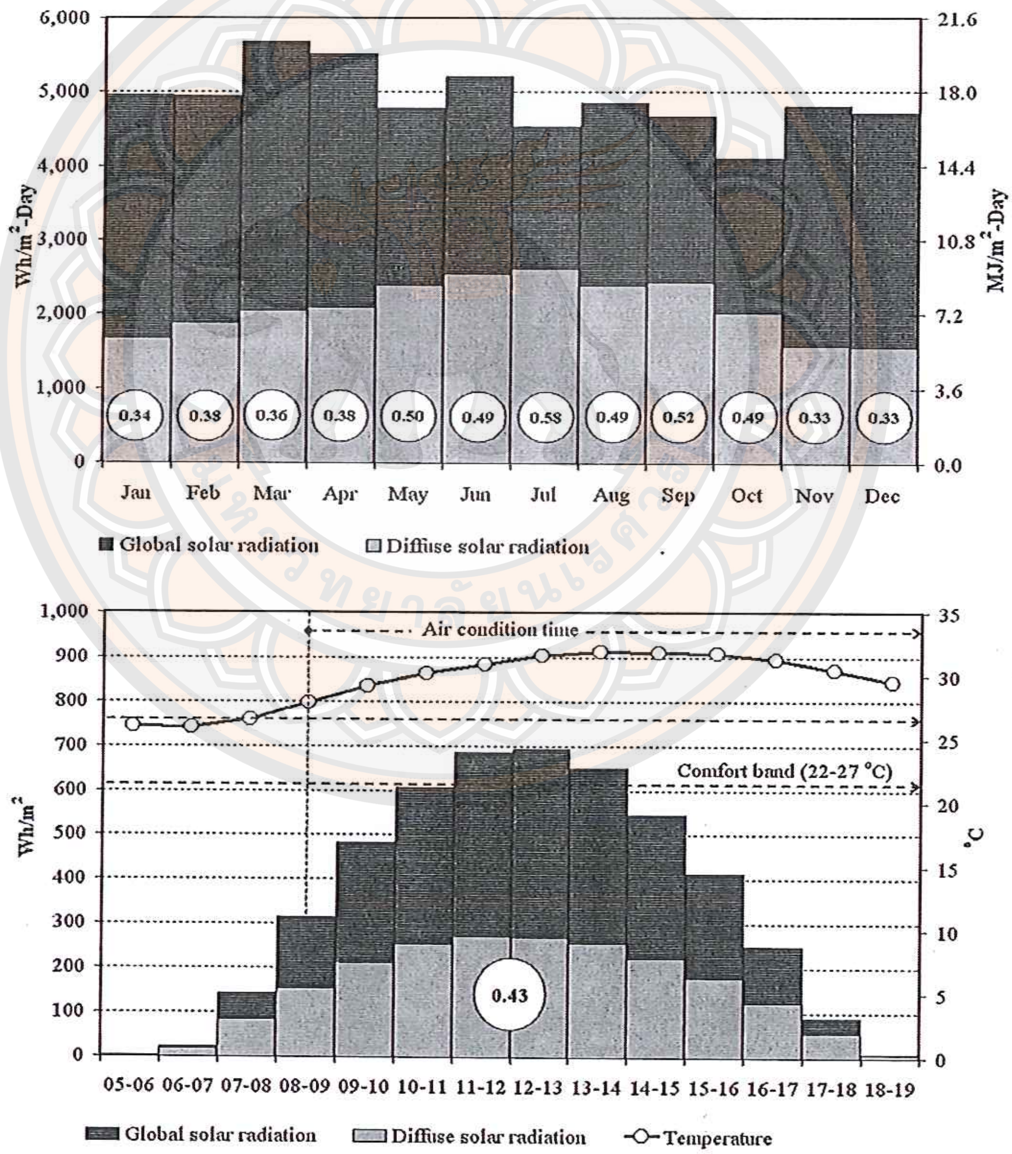

Figure 116 Average radiation and air temperature of Thailand in 2009

Data collected in 2009 was used as database being referred for calculation as shown in Figure 116 (top). It presented ratio of solar diffuse radiation in each month. It is found that in rainy season; May-September, contained high ratio of solar diffuse radiation, which is sometime higher than direct solar radiation, due to the declination moving towards north of equator line resulting in low energy from direct solar radiation with module installation turning towards south. In contrast with other months with declination encircling towards south, it was corresponded with data from other years during 2006-2010. In Figure 116 (below), the conclusion was to have suitable period of air conditioning systems start working from 8.00 A.M. to create comfort zone consistent to general working hour.

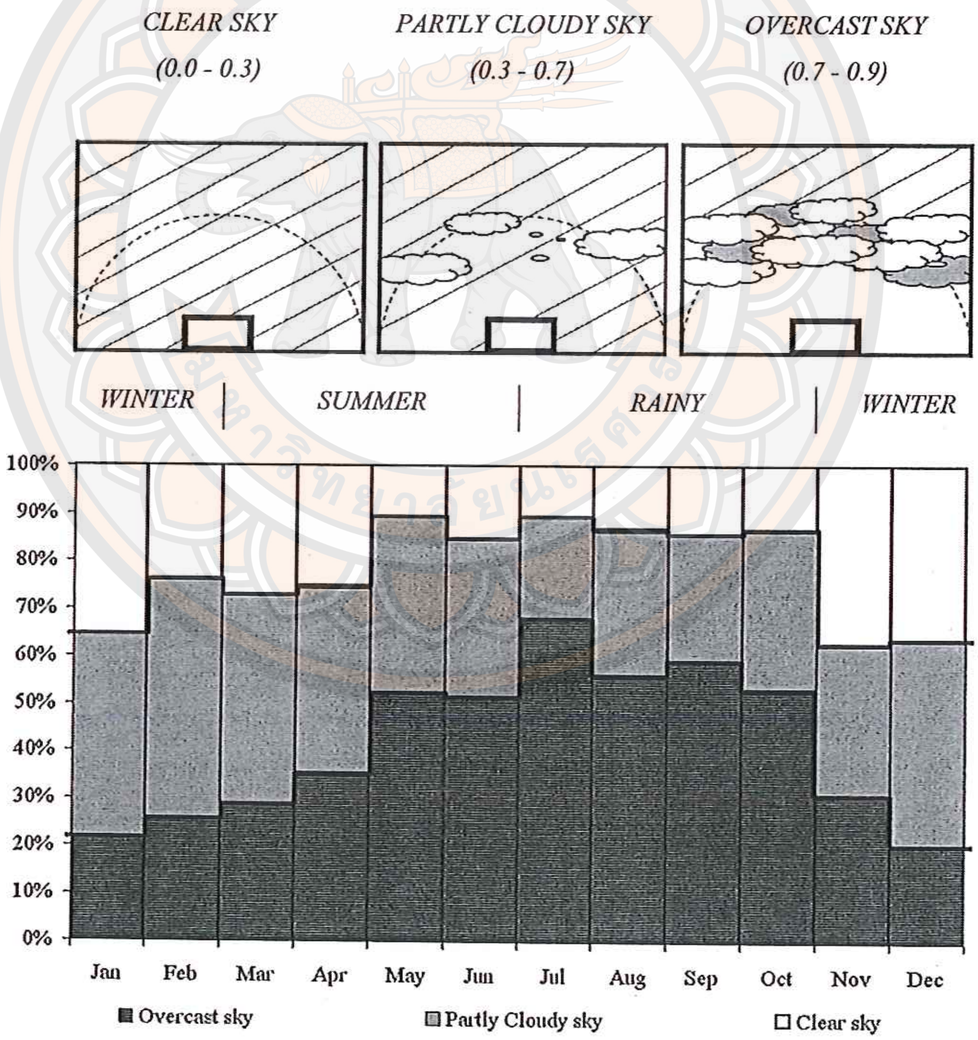

Figure 117 Average ratio of diffuse solar irradiance to total solar irradiance

In Figure 117, shows ratios of solar radiation according to sky conditions in 2009 divided into 3 seasons as follows:

1. Summer season between February and May
2. Rainy season between May and October
3. Winter season between October and February

Most of solar radiation ratio shows appearances of sky component with partly cloudy sky and overcast sky in rainy season affecting total solar radiation on solar module

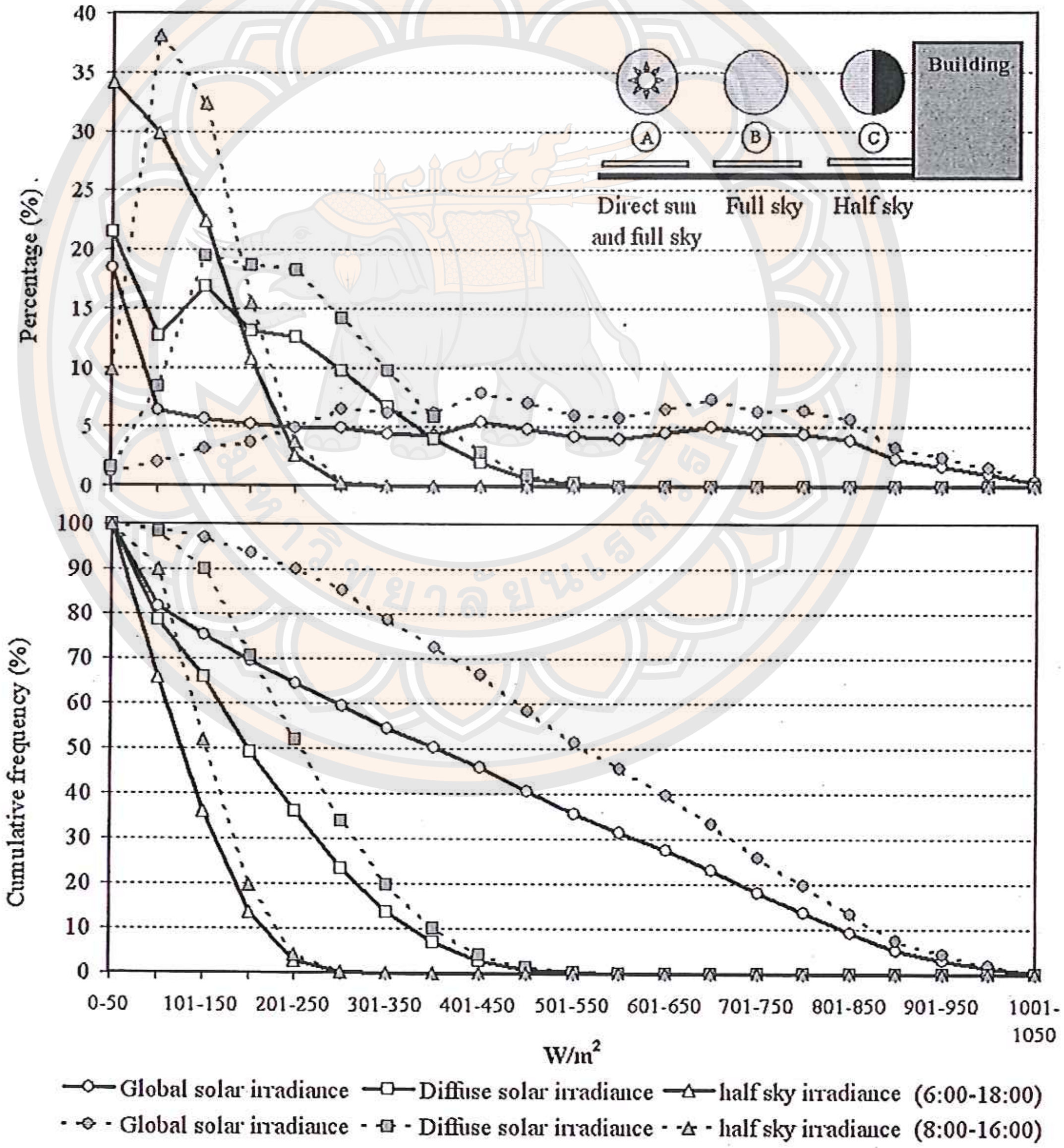

Figure 118 The frequency and cumulative frequency of solar irradiance in 2009

As Figure 118 shows frequency of solar irradiance reception on the condition of sky component, it is found that 8.00-16.00 mostly provides low solar diffuse radiation. It is said the same way that 80% of the mentioned time provides solar irradiance not less than 300 W/m^2 in the case of diffuse radiation under full sky and 150 W/m^2 in the case of diffuse radiation under half sky. Figure 118 (below) shows influence of diffuse radiation is mostly quite low.

Therefore, total solar irradiance in case of SIPV under half sky was probably reduced about 25% due to the fact that 50% was direct solar radiation and 50% more of diffuse radiation was reduced by building shade.

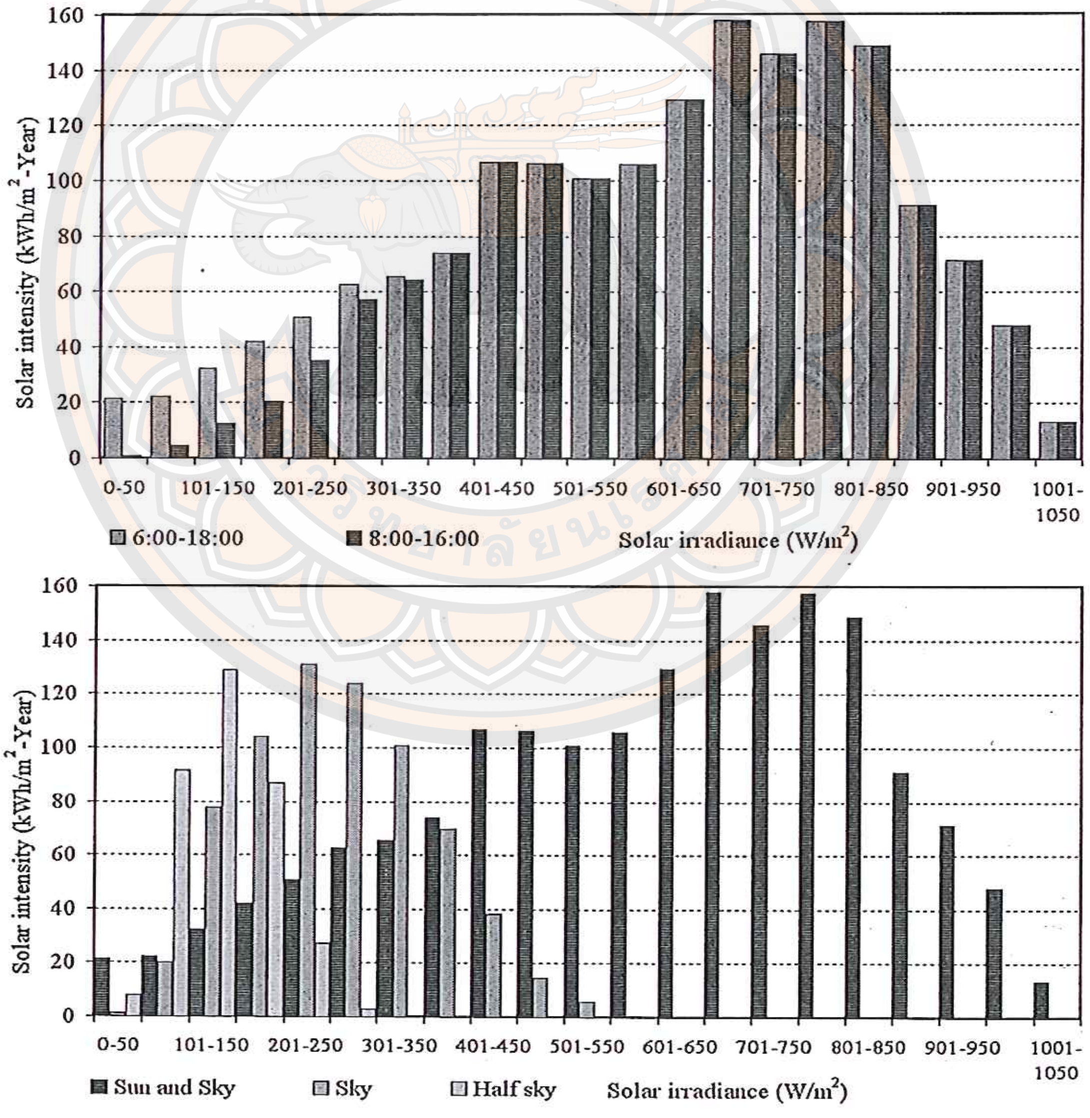

Figure 119 The solar intensity of Bangkok in 2009

The highest level of solar intensity was about 150 kWh/m^2-Year in the case of global solar irradiance in the period of total solar irradiance between 700 and 800 W/m^2. The highest level of solar intensity was about 130 kWh/m^2-Year in the case of half sky in the period of diffuse solar irradiance between 100 and 150 W/m^2 as shown in Figure 119 and Figure 120 presenting that more than 65% of midday at 8.00 A.M. provides temperature of more than 27°C.

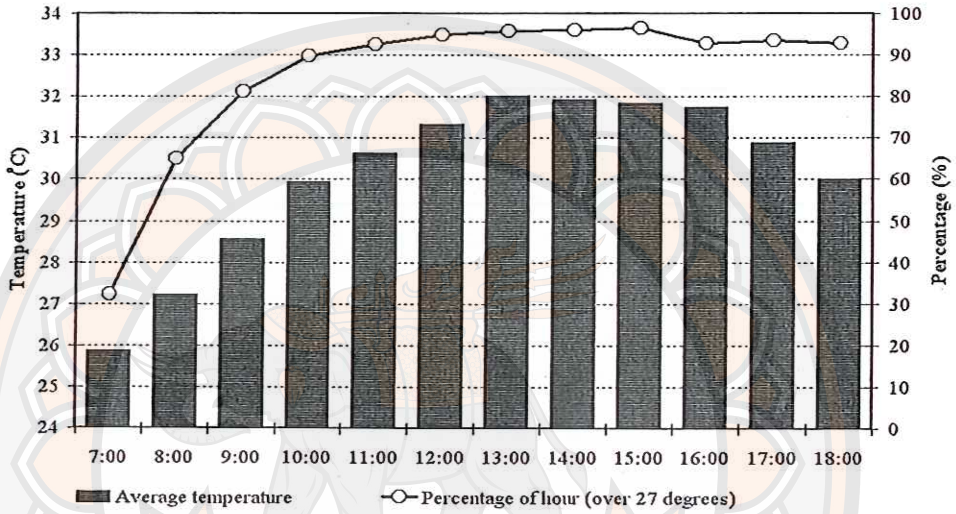

Figure 120 Average and percentage of air temperature

In conclusion, appearances of data of 2009 used in calculation in the period of SIPV operation are as follows:

1. In the case of half sky, most diffuse irradiance was at about 150W/m^2 resulting in sum total per year of about 130 kWh/m^2

2. To design shading to prevent direct solar radiation in basic step, the suitable time to start should be at 8.00 A.M. according to the use of air conditioning system. It is because of temperature higher than comfort zone

2. Ratio of outstretched part of shading devices at latitude 14° north

In designing horizontal shading devices with outstretched part to prevent direct solar radiation, it is changed according to profile angle which is uprisen angle perpendicular to wall where considered. In this study, 8.00-16.00 was considered in direct solar radiation prevention as it is working hours with thermal uncomfortable condition. In Figure 121 shows total solar irradiation falling down on vertical surface like window provides value as low as diffuse radiation in the period containing the highest level of the day as it is considered non-severe. However, sunlight prevention until 17.00 P.M. can reduce more heat with the design of more outstretched part of shading devices due to the low value of the sun's uprisen angle.

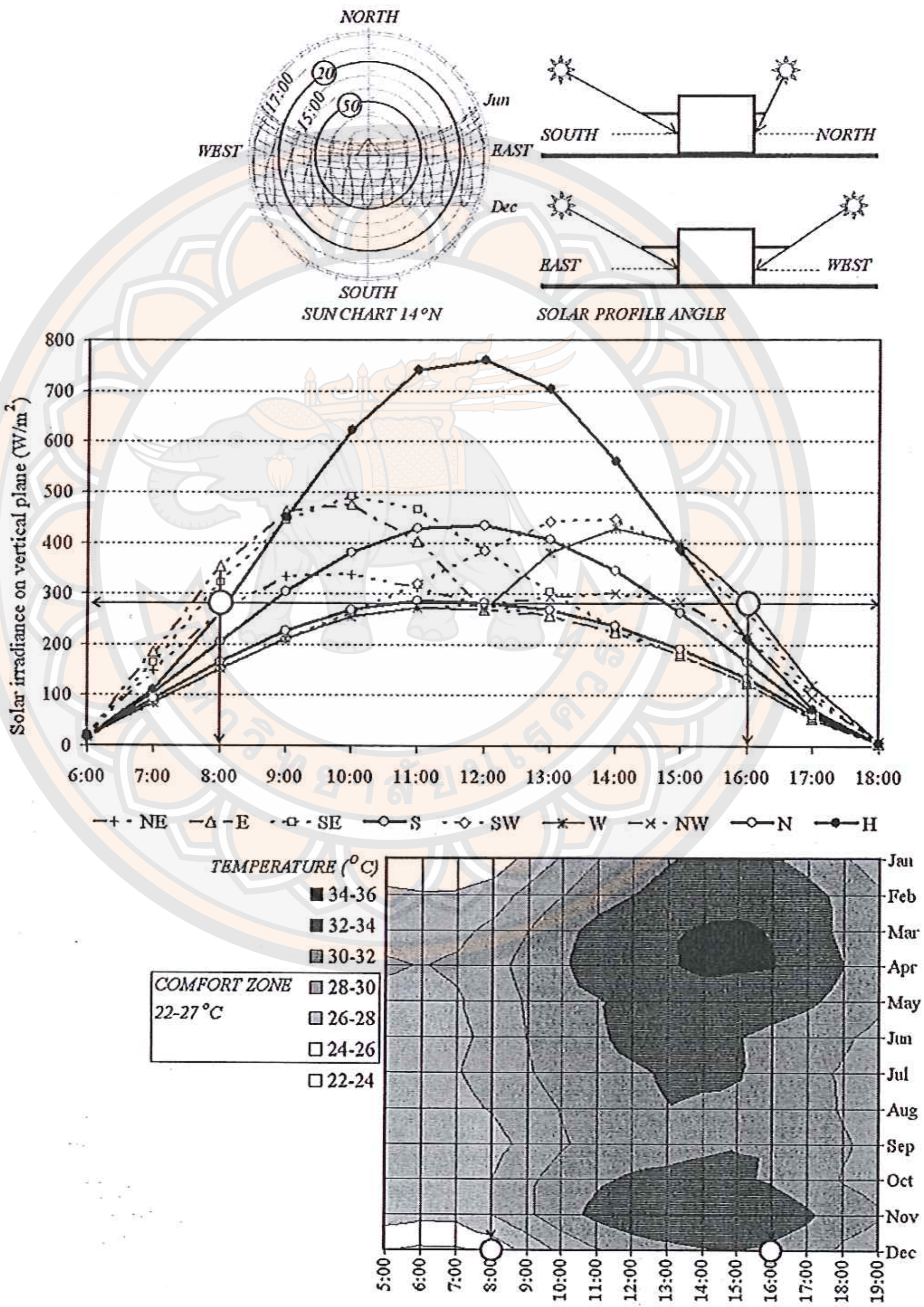

Figure 121 The analysis of shading time for thermal comfort

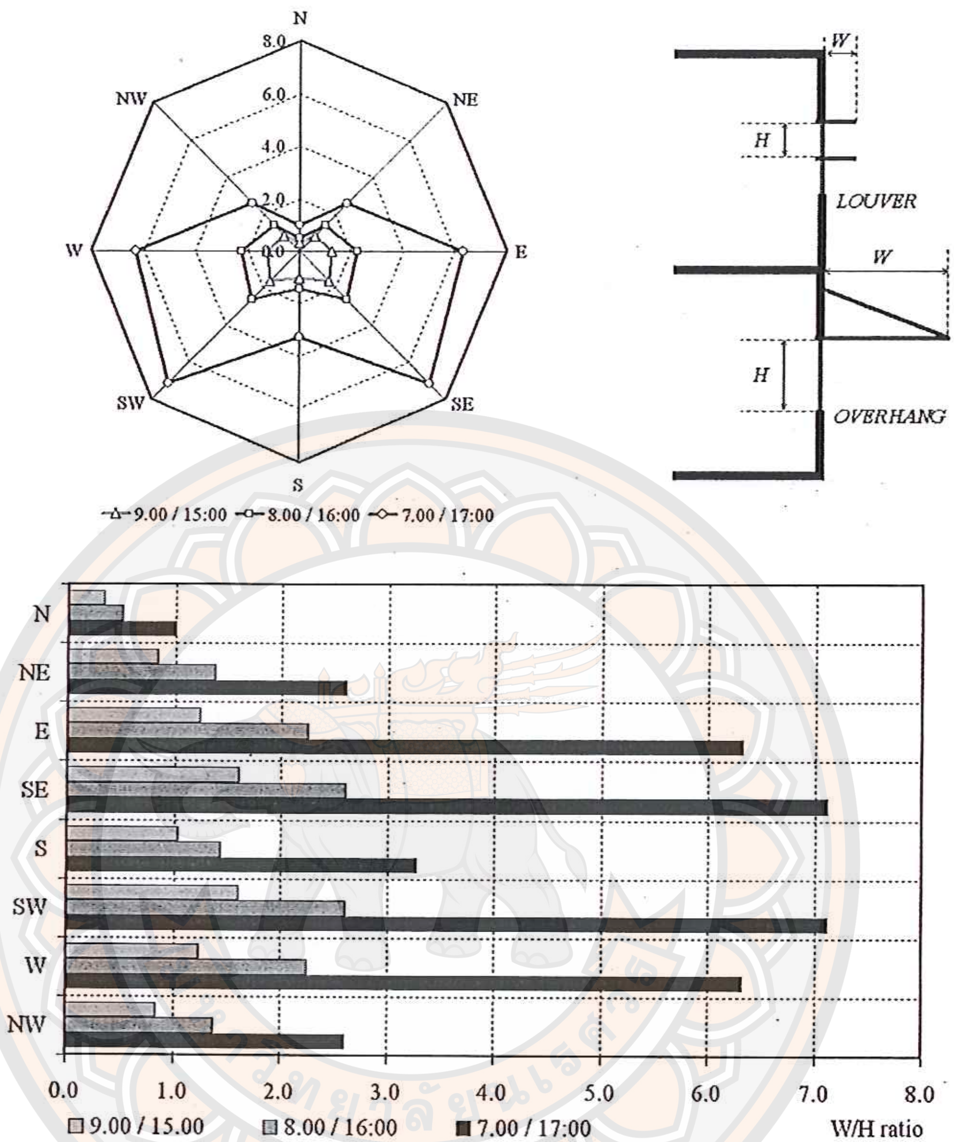

Figure 122 The shading extension ratio

Shading in both cases of over hang and louver can specify their forms from W/H ratio as shown in Figure 122 which is dimension indicating the ability in sunlight prevention resulting in SC_b equivalent to 0.0. In cooling time, outstretched part W should be corresponded according to position or solar attitude. Outstretched part design during 9.00-15.00 is a little bit shorter that during 8.00-16.00 unlike during 7.00-17.00 with outstretched part of shading devices is increasing more than needed affecting structure, budget and depletion of area around building. Therefore, the suitability in shading devices design is limited only during 8.00-16.00.

3. Solar tracking of shading devices

Solar tracking depending on solar altitude indicates that the angle of system being installed in some directions is adjusted at not more than 20 degrees which is considered a few when compared to the need of maintenance. The installations are such as N, NE and NW as shown in Figure 123 (top).

When considering the area of angle throughout the windows due to the shading devices according to W/H ratio, it is found that in the case of fixed installation, there is open angle area more than 60% unlike the case of installation turning towards N, NE, NW and S and the case of tracking installation which there are more angle area than fixed installation. The comparison is shown in Figure 123.

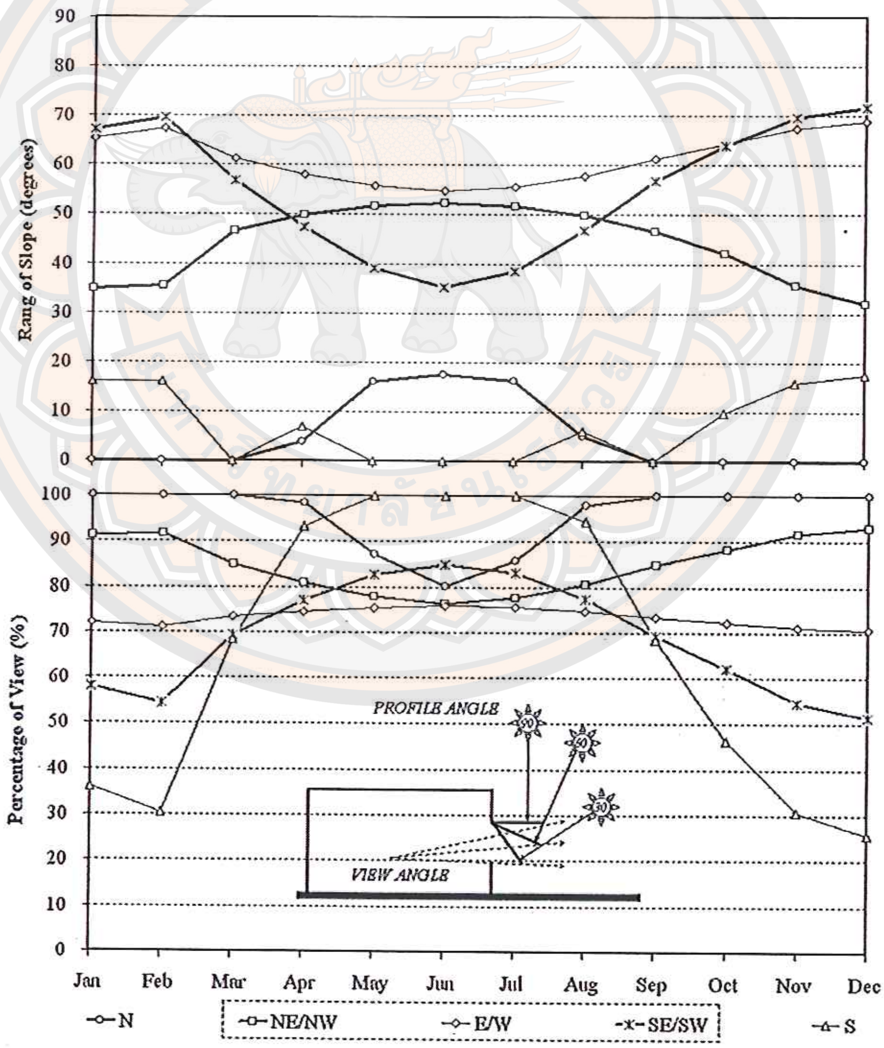

Figure 123 The clear view height of tracking effect

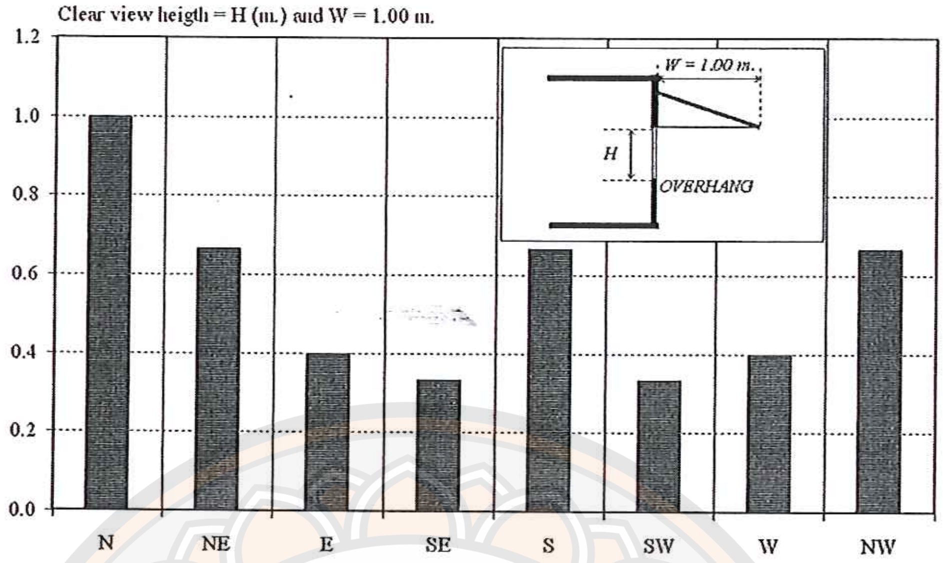

Figure 124 The clear view height of fixed effect

4. Summary of the analysis part

The summary of analyzing the forms of shading devices design

4.1 Weather and solar irradiance data of 2009 are used in analysis and estimation

4.2 Shading devices is designed to have outstretched part during 8.00-16.00. It is for suitability to avoid having unnecessary outstretched part and correspond to working hours

4.3 The design is determined to have outstretched part of shading devices according to ratio W/H in each direction as follows: N=0.5, NE/NW=1.5, E/W= 2.5 and S=1.5 for fixed installation as shown 4-12

4.4 For tracking design, outstretched part should be short due to structure. It should also be installed in E/W, SE/SW and S

Experiment part

1. Total solar irradiance on slope surface [Chapter III; page 100-103]

1.1 Diffuse solar irradiance factor under half sky condition

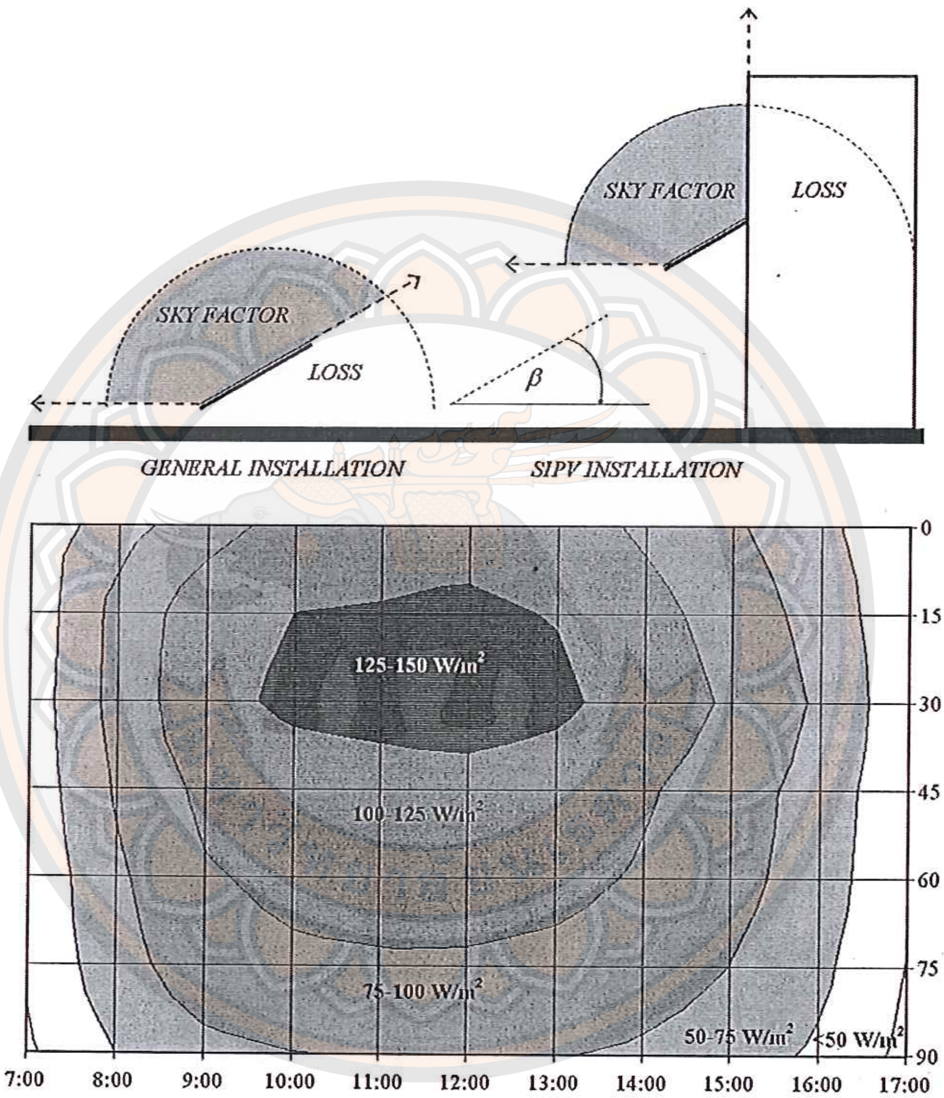

Figure 125 The collected data of the diffuse solar irradiance from the half sky

Half sky condition only diffuse solar radiation as shown in Figure 125. The result of experiment found that SIPV's tilt angle at about 15-45 degrees is the angle receiving the most of solar irradiance. It is also a hilltop sloping down towards the ground at more or less angle in every period of different solar altitude. The most value of angle is at noon where the position of the sun is at the highest.

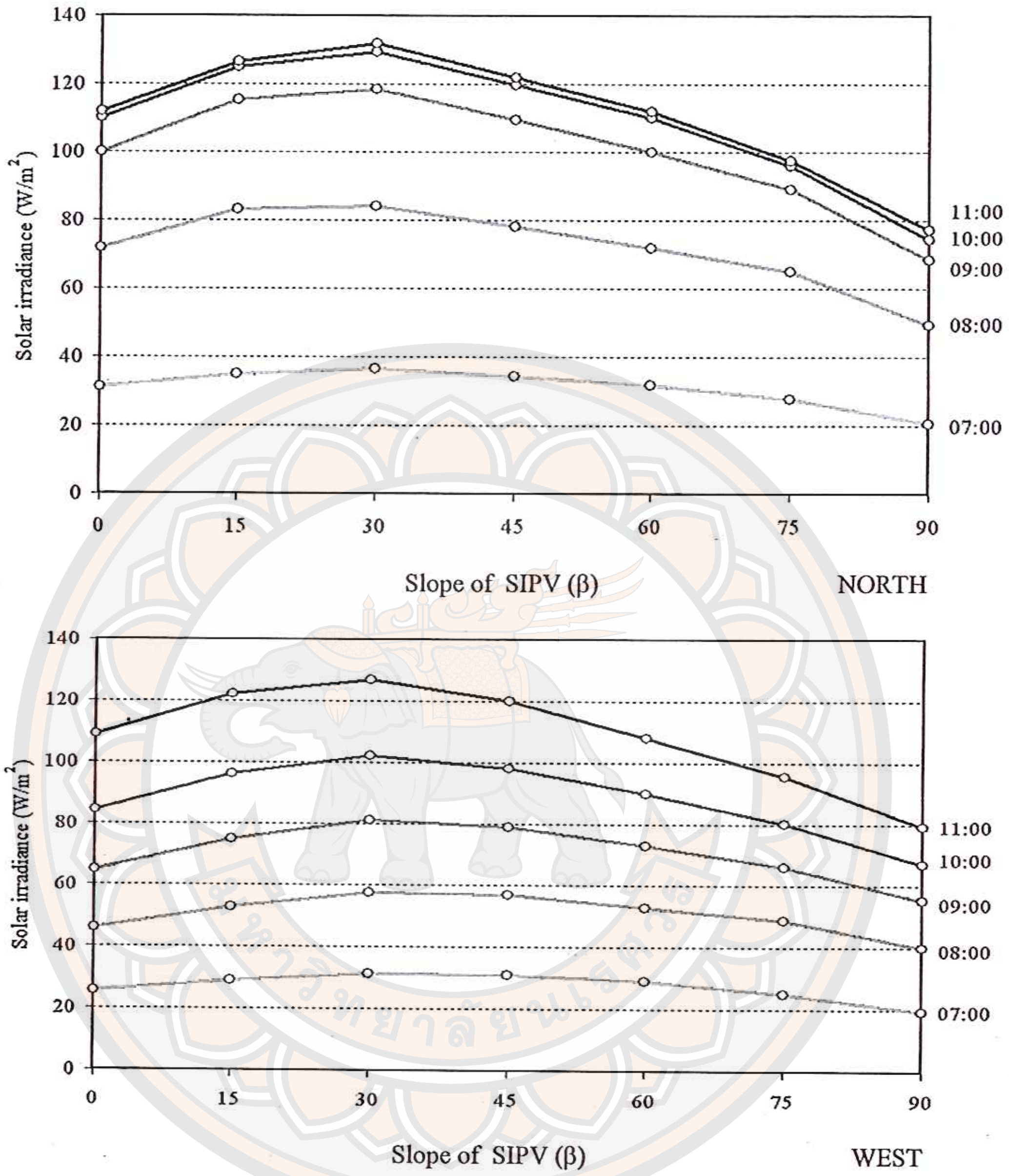

Figure 126 The diffuse solar irradiance comparison of every SIPV slope

Figure 126 shows solar irradiance in each period during 7.00 to 11.00. In the case of half sky turning towards north and west, it is found that tilt angle at 30 degrees is at the highest level in every case and decreases when there is other more or less angles. The difference is clear when the solar altitude is high.

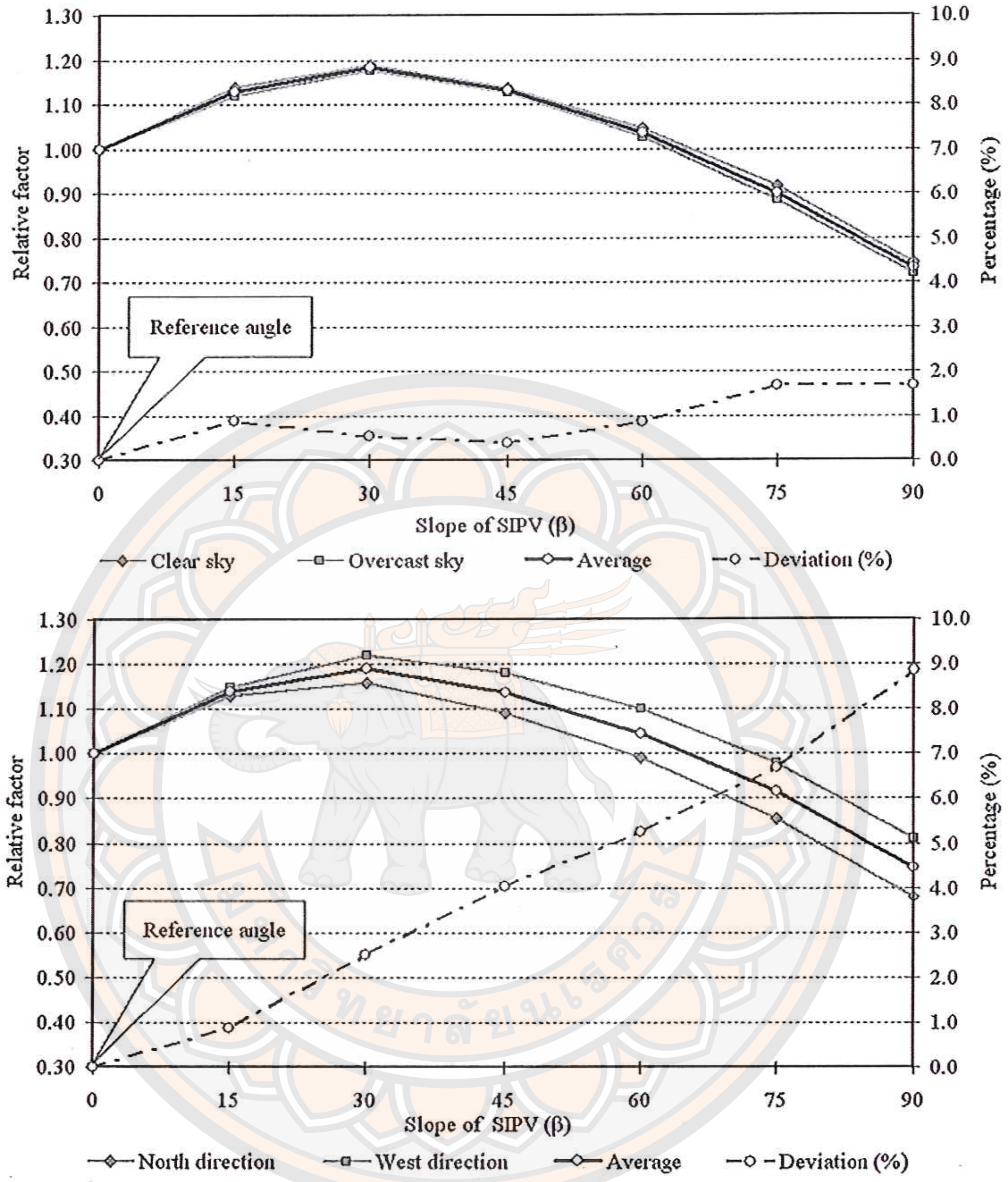

Figure 127 The diffuse solar irradiance comparison of sky condition

Figure 127 shows the relation of the ratio of diffuse radiation of every tilt under half sky compare with the tilt angle of 0 degrees or horizontal surface in case of clear sky and overcast sky. In the top Figure shows the difference not more than 2% unlike the below Figure which is the comparison between sky direction showing the more difference but not exceed 9%. In every case, the differences will increase at the high tilt angle.

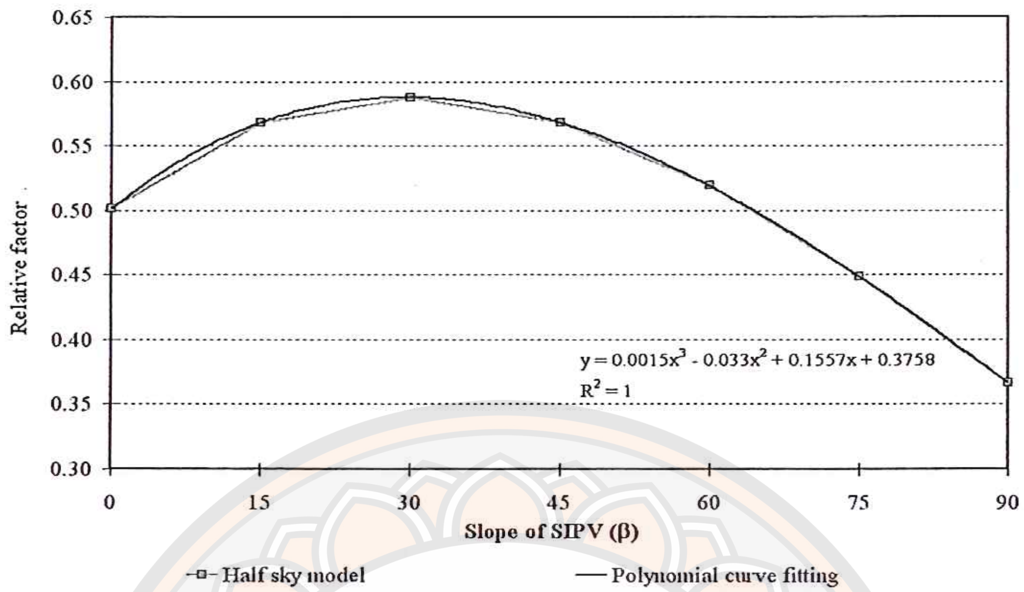

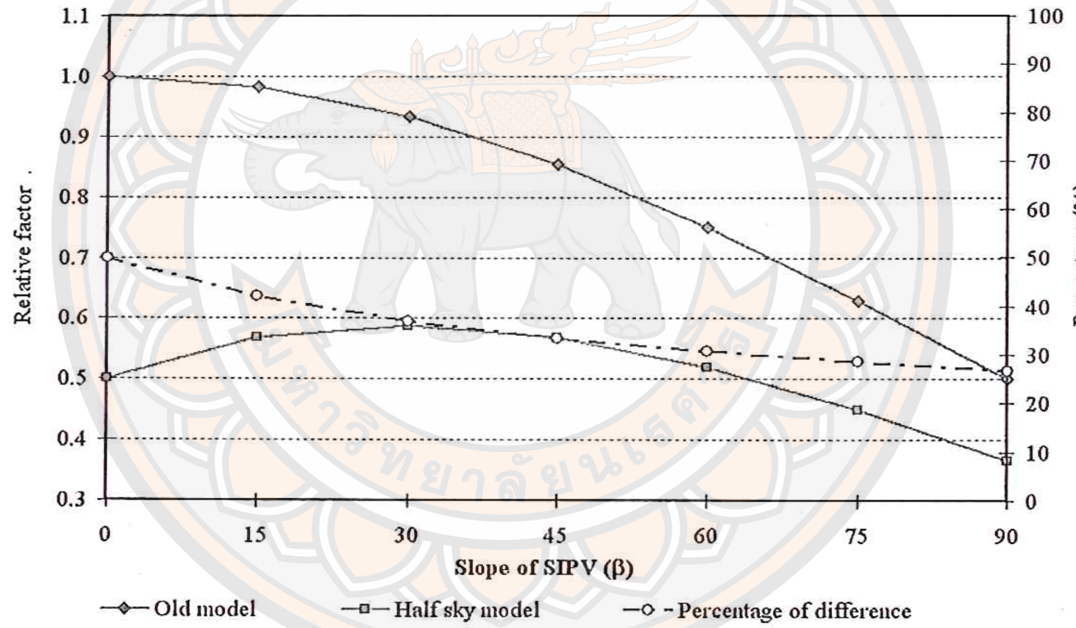

Figure 128 Math models of half sky condition and full sky condition

Figure 128 on top shows the averaging of data gained from analysis under conditions of all sky types. Below Figure shows the comparison with full sky condition at tilt angle of 0 degrees or flat surface with the value of 1.0 in the case of full sky and the value of 0.5 in the case of half sky. It indicates that in the case of half sky have clear differences in the matter of amount and the position of the highest value. The mentioned relation will be created as equation to predict.

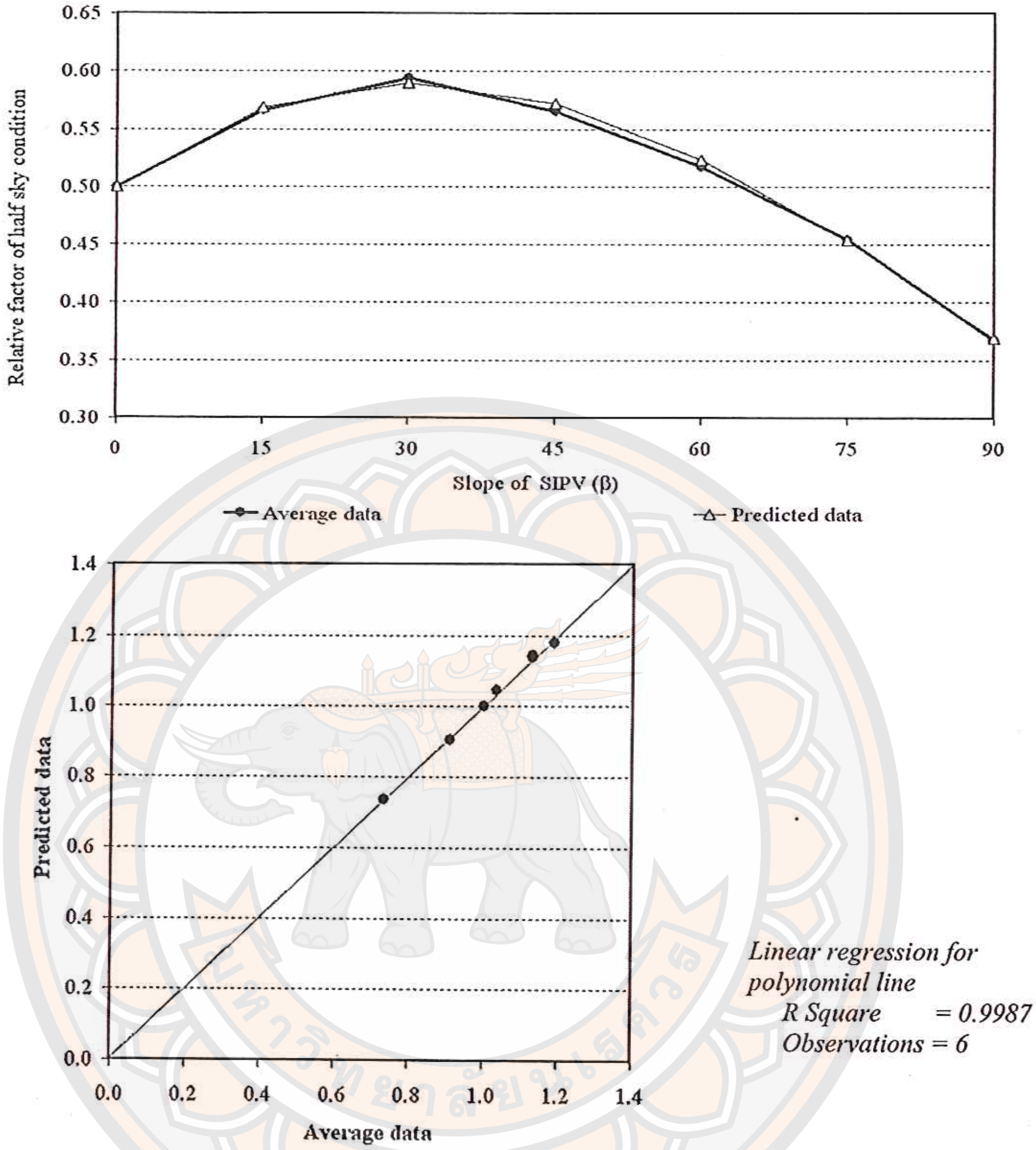

Figure 129 The evaluation of half sky model

$$R_d = 0.5(1+\cos B)\ ;\ \textit{for full sky} \qquad \text{Eq.109}$$

$$R_d = -0.0015A^3 + 0.0330A^2 + 0.1557A + 0.3758;\ \textit{for half sky} \qquad \text{Eq.109}$$

$$A = (15+\beta)/15$$

The diffuse solar irradiance of half sky model shown in Figure 129 indicates that the highest value is about 0.59 at tilt angle of 30 degrees appeared in a form of polynomial line multiply by 3. The coefficient of determination, R^2, of this model is at 0.9987 as Eq. 109.

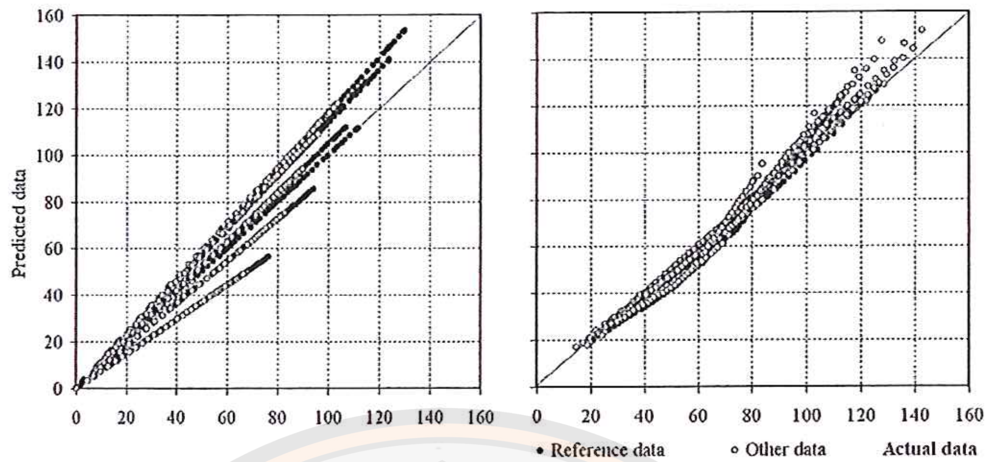

NORTH WEST

Figure 130 The comparison between predicted data and actual data

Table 21 The evaluation of the solar diffuse irradiance under half sky model

	North		West	
	Reference data	Other data	Reference data	Other data
	Feb 6th 2010	Feb 7th 2010	Feb 3rd 2010	Feb 2nd 2010
Observation	11,550.00	12,600.00	10,320.00	10,080.00
RMSE	10.75	10.10	3.92	4.55
NRMSE	15.29%	17.00%	5.72%	6.40%
MBE	2.91	2.62	-1.54	0.18
NMBE	4.14%	4.41%	-2.25%	0.26%
R square	0.9360	0.9407	0.9849	0.9857

Comparing with data from other days not data used in analysis with root mean square error (RMSE) and the mean bias error (MBE) as shown in Table 21, it can be explained that sky condition in the west can be used to predict the value much closer than in the north. However, there are reasons according to the site of installation to collect data with the different environment

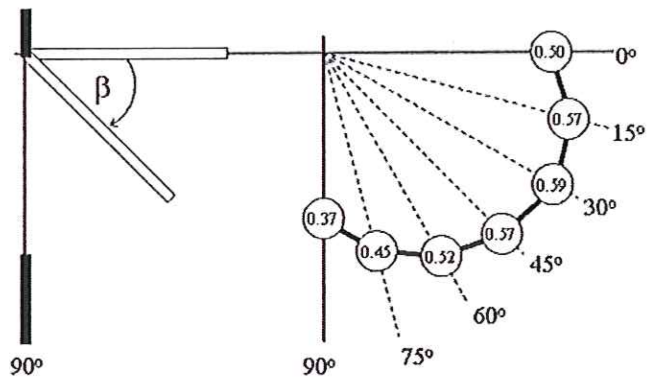

Figure 131 The diffuse solar irradiance explanation of half sky condition

1.2 Reflected solar irradiance factor from the buildings surface

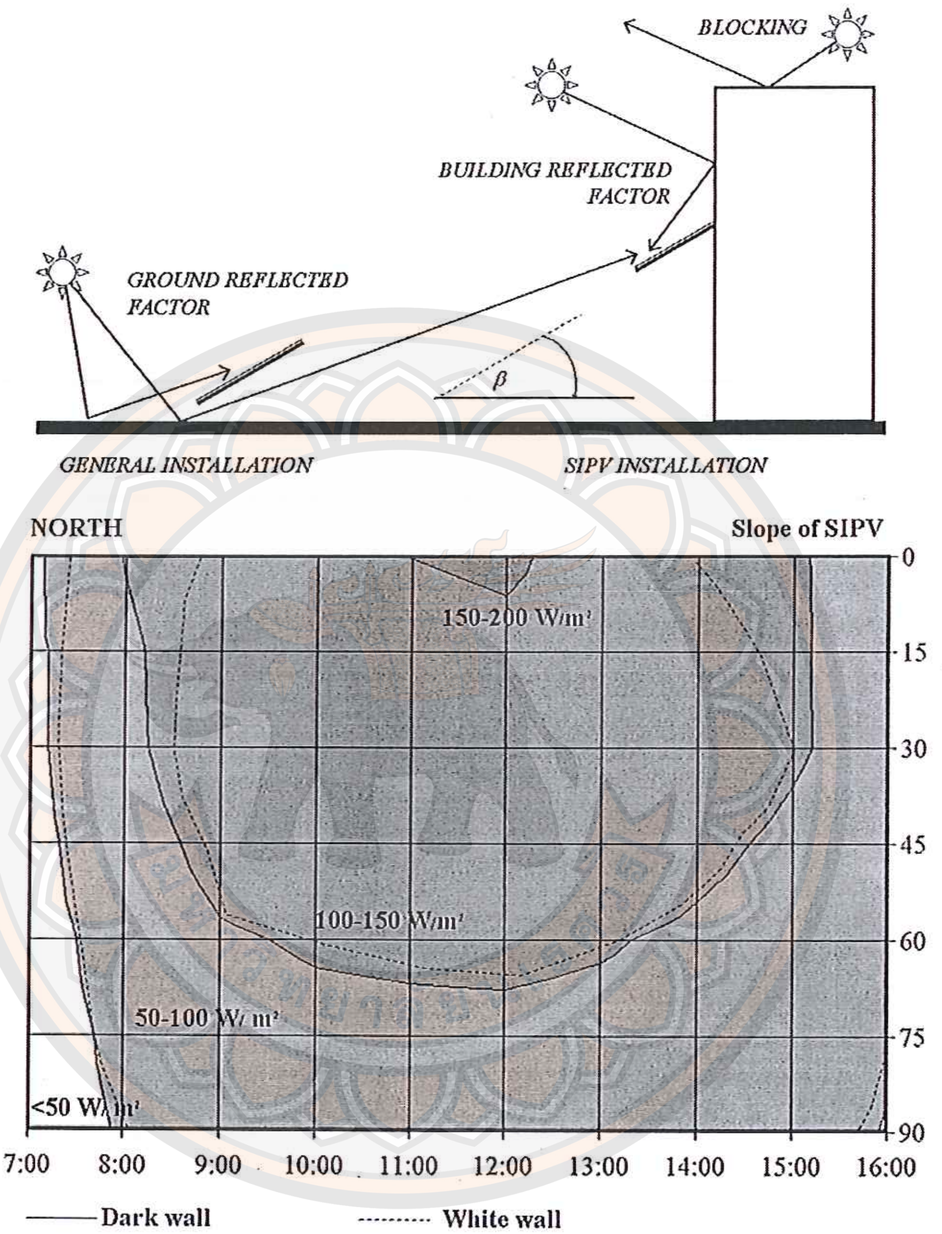

Figure 132 The collected data of the reflected solar irradiance from the North sky

Building envelope on top of SIPV shown in Figure 132 and Figure 133 found that SIPV with tilt angle at 0 degrees or horizontal plane can receive most of solar irradiance in every cases of sky turning towards every direction and lesser when SIPV slopes to make angle wider. This factor is only a few.

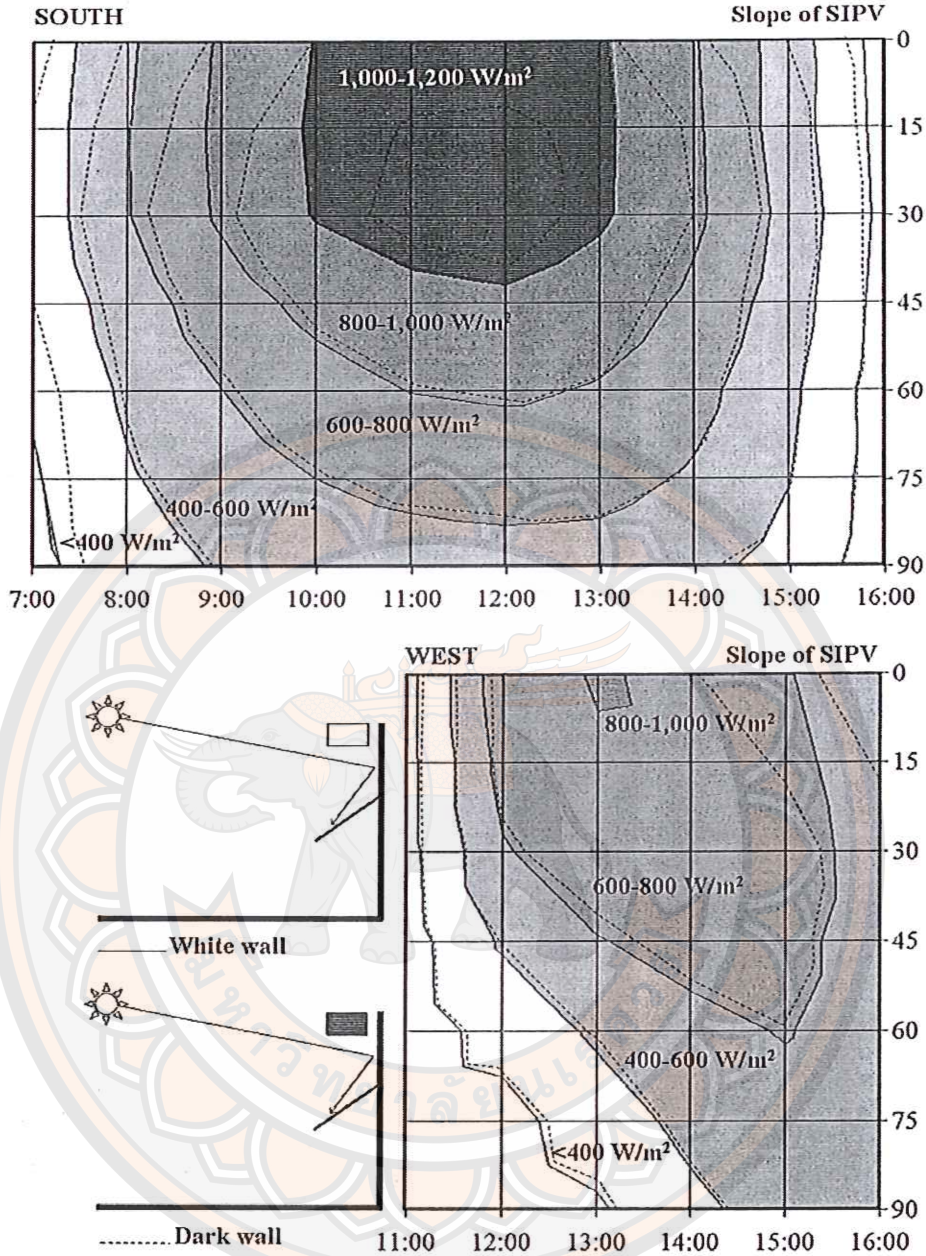

Figure 133 The collected data of the reflected solar irradiance from the South and West sky

Although building envelope can affect the increase of solar irradiance on SIPV module, it affects a little in the case of experiment showing solar radiation reflectance at 38% and lesser when consideration is accordance with law containing the suitability of solar radiation reflectance at 30% in order to make buildings a non-heat source and non-light pollution to nearby buildings.

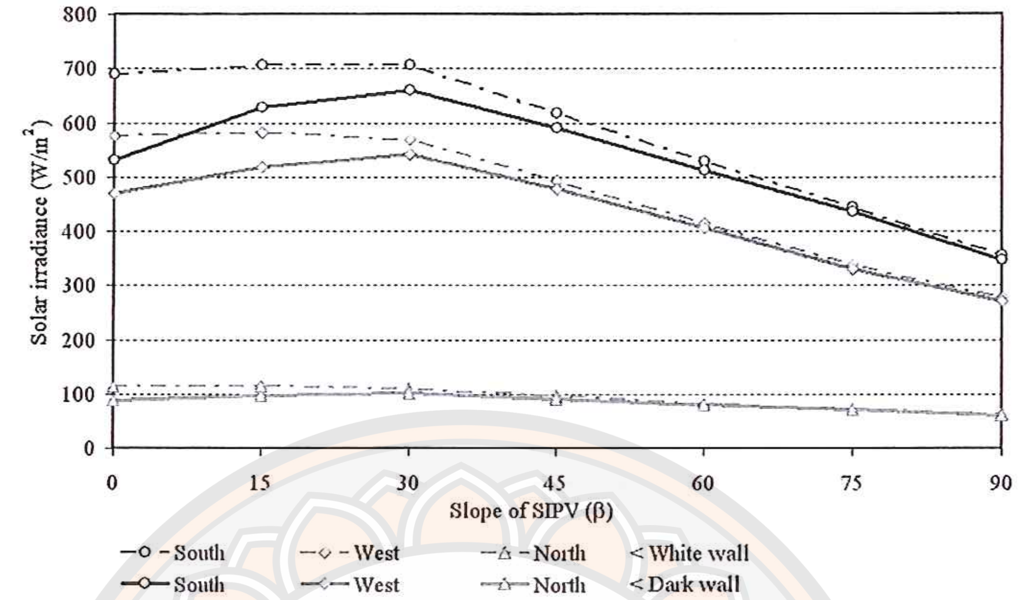

Figure 134 The solar reflected irradiance of the white and the dark panel

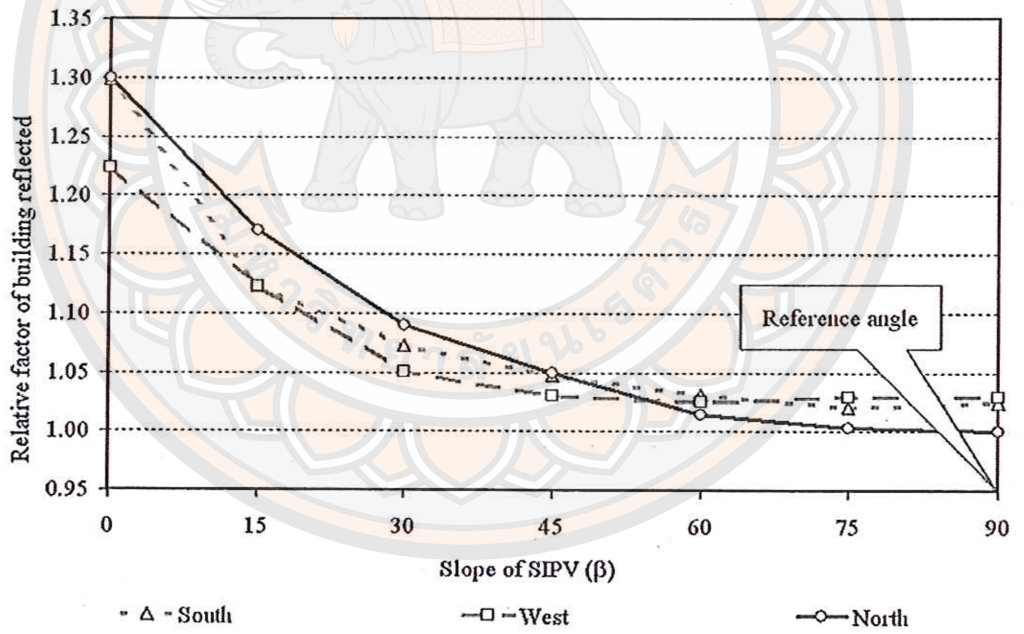

Figure 135 The reflected solar irradiance comparison of the sky conditions

Figure 134 shows the experimental result of solar radiation falling down on SIPV both white and black wall. Figure 135 shows the result in a form of ratio of reflectance compared to directions of sky such as South and West and in a form of average value by considering solar radiation reflectance at 38%.

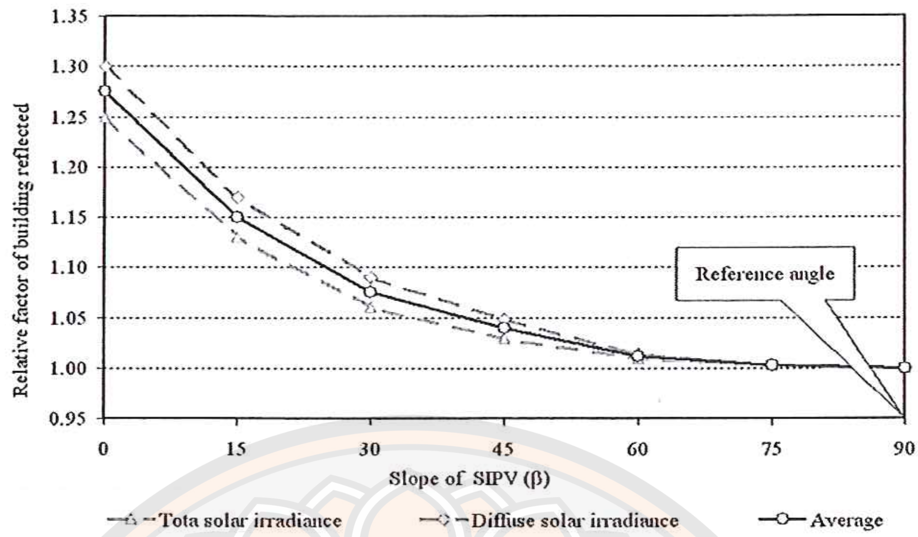

Figure 136 The building reflected trend of the solar irradiance conditions

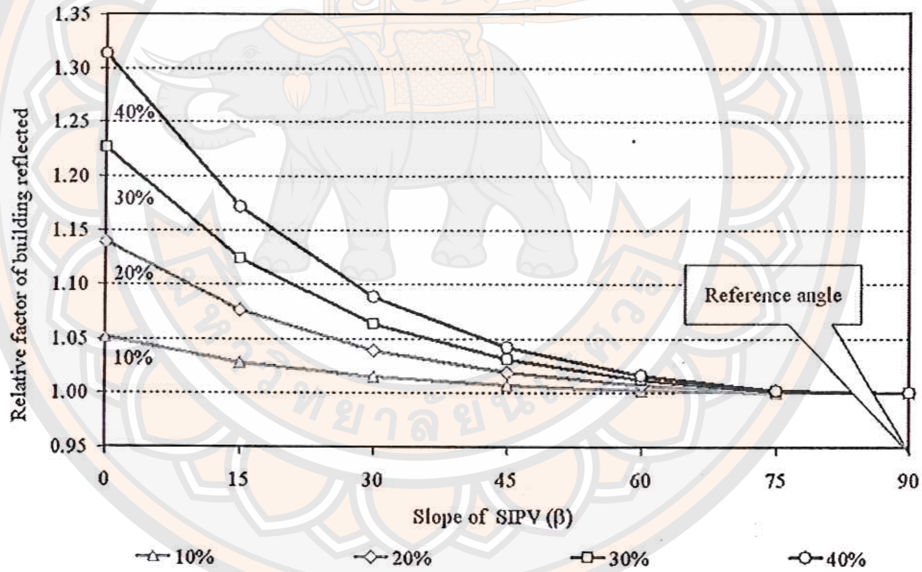

Figure 137 The building reflected trend of every the solar reflectance

The comparison of total solar irradiance reflectance in the case of sky on the West and diffuse solar irradiance reflectance in the case of sky on the North shown in Figure 136 result in the same type of characteristics. Figure 137 shows the comparison of the ratio to estimate in the case of solar radiation reflectance qualifications of building envelope materials between 10%-40% according to qualification of color and building material generally sold in market.

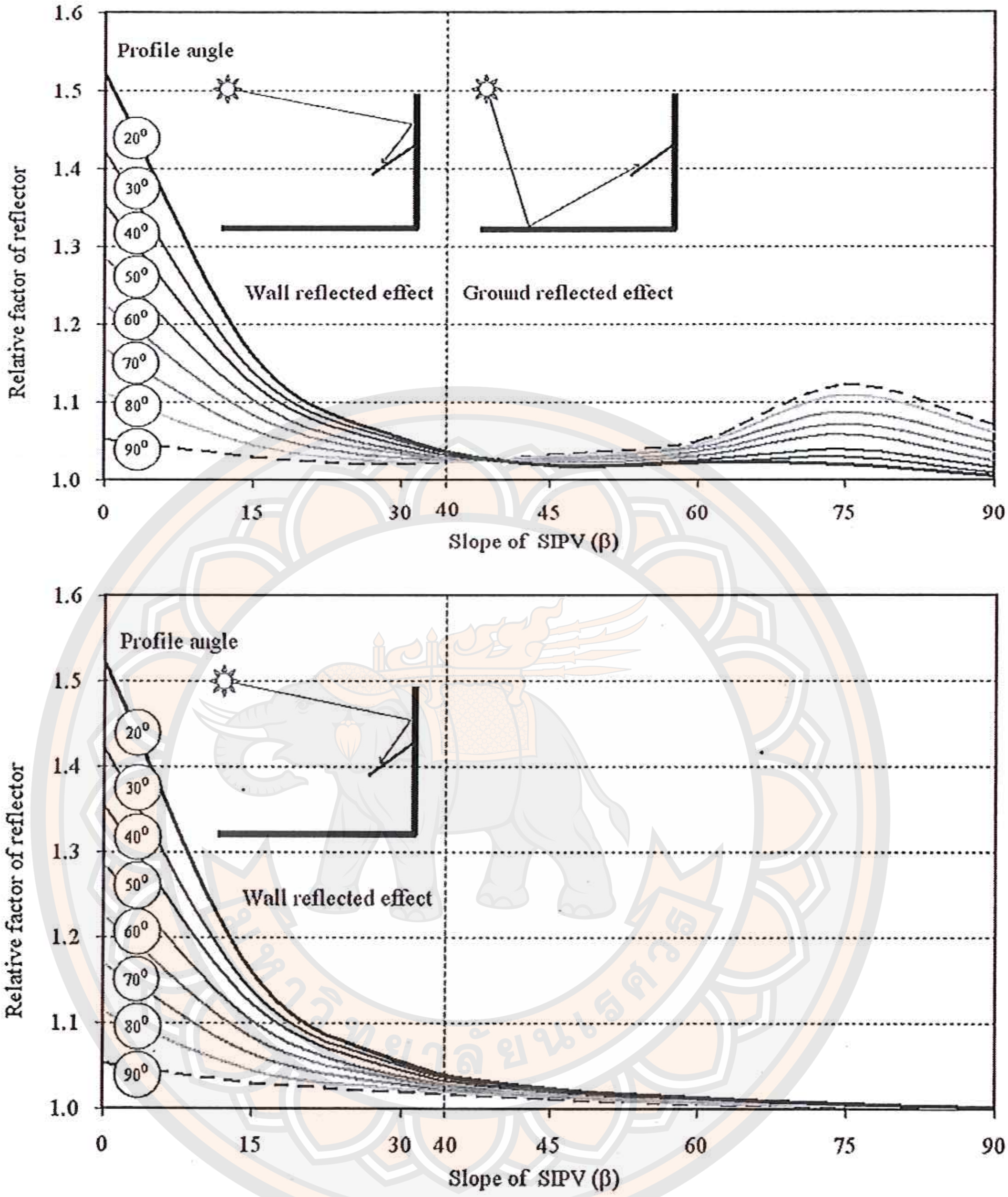

Figure 138 The relative factor of every profile angle and every SIPV slope

Figure 138 (top) shows solar irradiance reflectance factor in each period of time according to solar altitude. Besides, Figure 138 (below) shows the consideration to improve data of angle from 45 degrees to 90 degrees in order not to have factor of solar irradiance reflecting from ground surface to create suitability according to trend line.

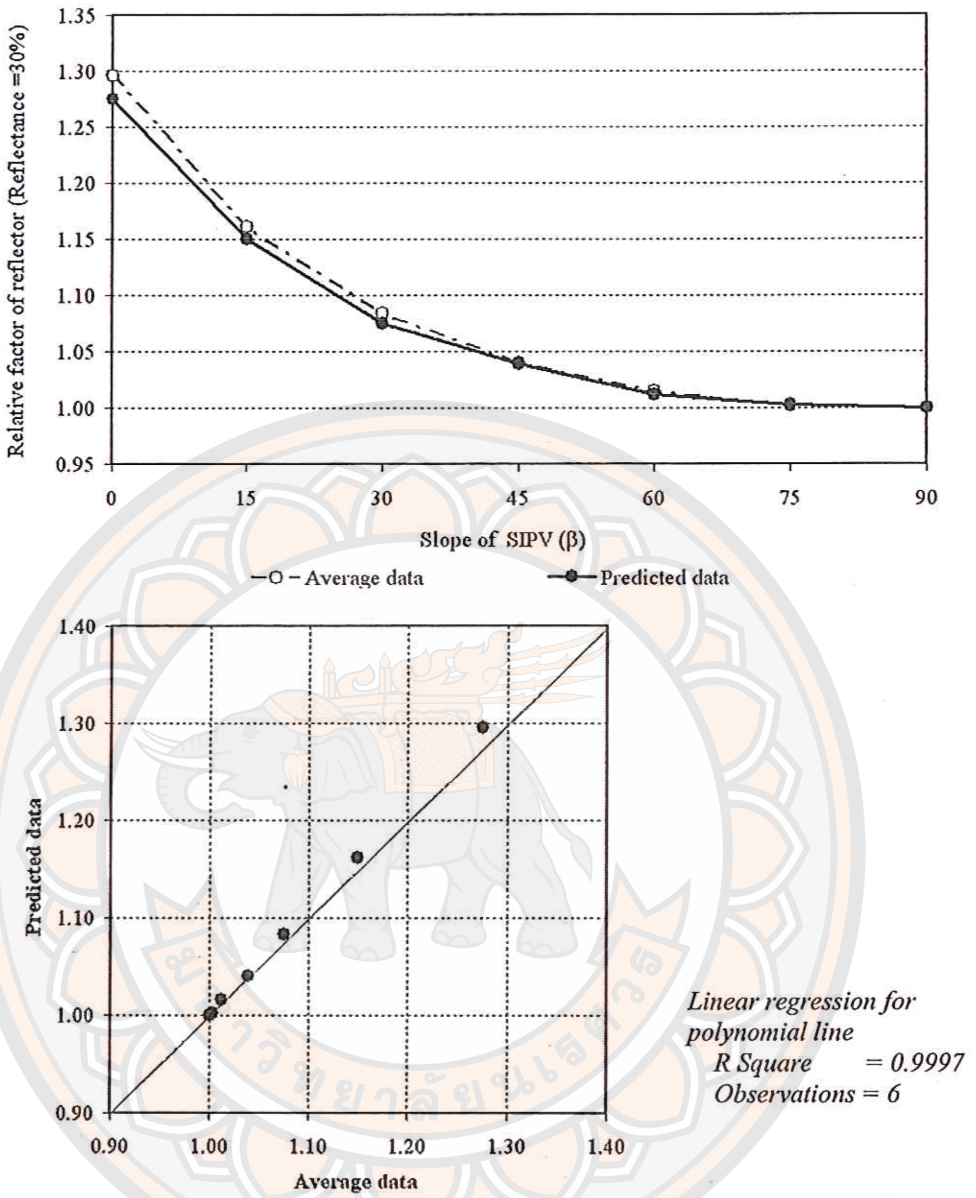

Figure 139 The evaluation of building reflected model

$$R_{rB} = 0.0003A^4 - 0.0029A^3 + 0.0153A^2 - 0.0278A + 1.0154 \qquad Eq.110$$

$$A = (105-\beta)/15$$

The building reflective model as shown in Figure 139 shows the highest value is at tilt angle of 0 degrees and value is decreasing rapidly in a curve of polynomial line as well as shows the reliability in a form of the coefficient of determination, R^2, at 0.9997.

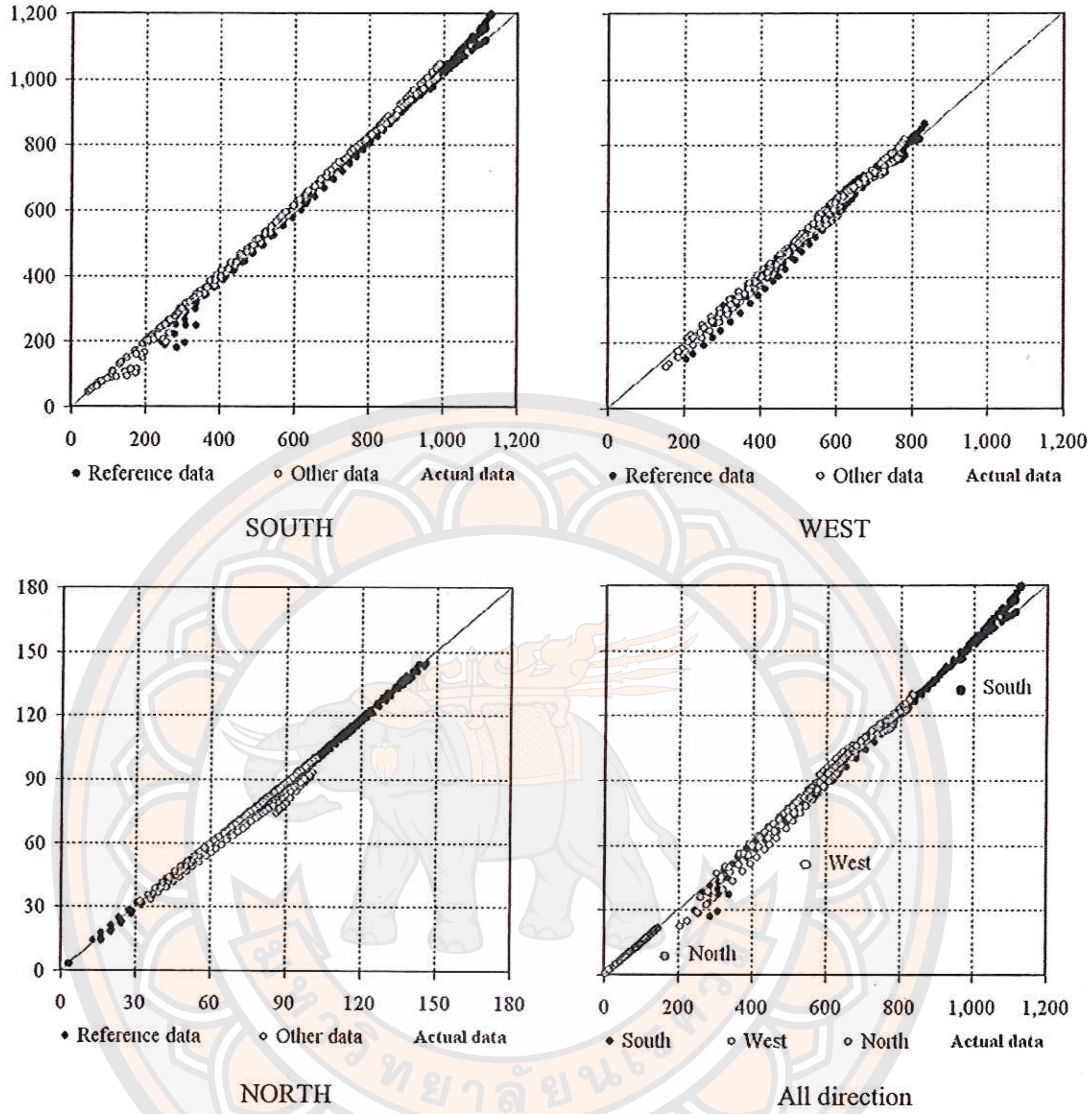

Figure 140 The comparison between predicted data and actual data

Table 22 The evaluation of the building reflected model

	Reference data	Other data	Reference data	Other data
	West		South	
	Feb 3rd 2010	Feb 2nd 2010	Feb 8th 2010	Feb 5th 2010
Observation	5940	6420	7200	7200
RMSE	23.27	16.11	21.96	30.26
NRMSE	3.84%	3.09%	4.13%	3.74%
MBE	5.6071	4.7228	7.7054	12.4975
NMBE	0.9254%	0.9047%	1.4484%	1.5440%
R square	0.9875	0.9938	0.9961	0.9981
	North		All direction	
	Feb 6th 2010	Feb 7th 2010	Feb 6th 2010	Feb 7th 2010
Observation	6600	6600	19740	19740
RMSE	1.91	4.63	22.32	16.35
NRMSE	2.16%	5.86%	4.40%	4.33%
MBE	-1.5186	-3.5981	5.7379	3.1435
NMBE	-1.7140%	-4.5560%	1.1313%	0.8327%
R square	0.9991	0.9739	0.9977	0.9984

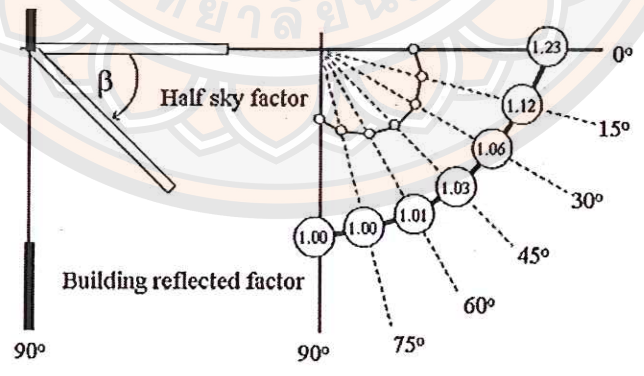

Figure 141 The reflected solar irradiance explanation of half sky condition

Comparing to data from other days which is not data used in analysis with root mean square error (RMSE) and the mean bias error (MBE) as shown in Table 22 explains that values of all sky conditions can be predicted similarly.

The comparison of diffuse solar irradiance factor and the building solar reflectance in each installation with all kind of tilt angles of SIPV as shown in Figure 142 presents that both have the different highest values. However, if the calculation result in a form of annual solar radiation on SIPV is being compared, it is found that at the tilt angle of 30 degrees provides the highest value due to a few factor of solar irradiance reflectance as shown in Figure 143.

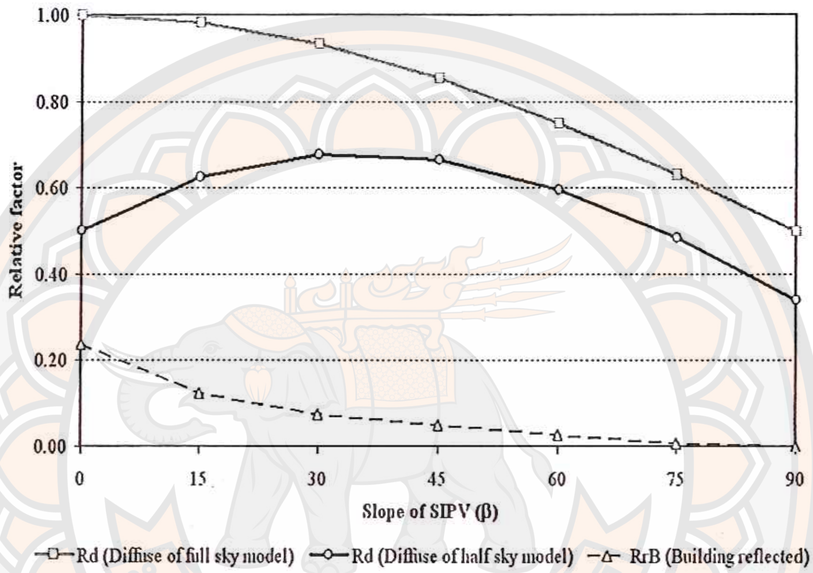

Figure 142 The comparison of experimental models

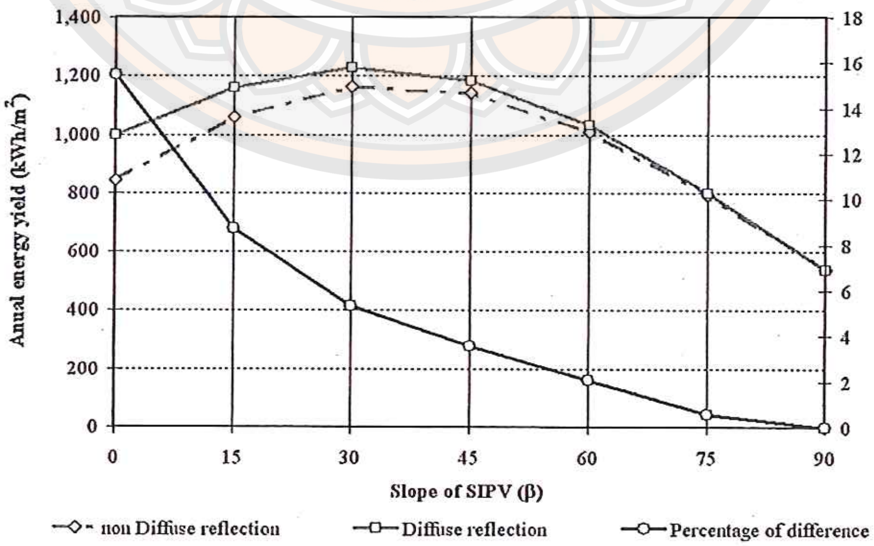

Figure 143 The effect of building reflected and diffuse solar irradiance

1.3 Factors of overlapped SIPV installation

SIPV is solar module installed on vertical plane of building. It has one disadvantage indicating that when another PV array is installed down below being covered by the array on the top, it results in the below one receives less solar irradiance both direct and diffuse irradiance. Figure 144 and Table 23 shows the relation of the decrease due to installation with outstretched part and distance according to all kind of vertical planes in both cases of clear sky and overcast sky. The values are changed because of opened angle allowing to see the sky and trends of both sky conditions are similar.

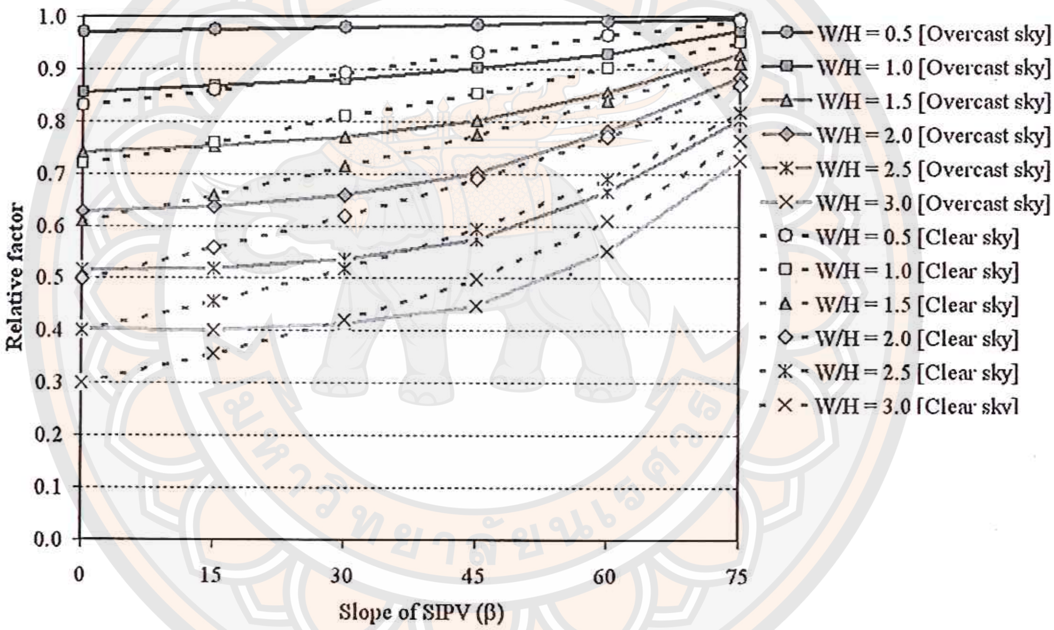

Figure 144 The relative factor of stack effect

Table 23 The relative factor of stack effect

	Slope					
W/H	**90**	**75**	**60**	**45**	**30**	**15**
Clear sky						
0.5	0.83	0.86	0.89	0.93	0.96	0.99
1.0	0.72	0.76	0.81	0.85	0.90	0.95
1.5	0.61	0.66	0.72	0.78	0.84	0.91
2.0	0.50	0.56	0.62	0.69	0.77	0.87
2.5	0.40	0.46	0.52	0.60	0.69	0.82
3.0	0.30	0.36	0.42	0.50	0.61	0.76
Overcast sky						
0.5	0.97	0.98	0.98	0.99	0.99	1.00
1.0	0.86	0.87	0.88	0.90	0.93	0.97
1.5	0.74	0.75	0.77	0.80	0.85	0.93
2.0	0.63	0.64	0.66	0.70	0.78	0.88
2.5	0.52	0.52	0.54	0.58	0.67	0.81
3.0	0.40	0.40	0.41	0.45	0.55	0.73

2. Efficiency of PV module [Chapter III; page 100-103]

2.1 Module temperature effect of solar irradiance in the case of full sky condition

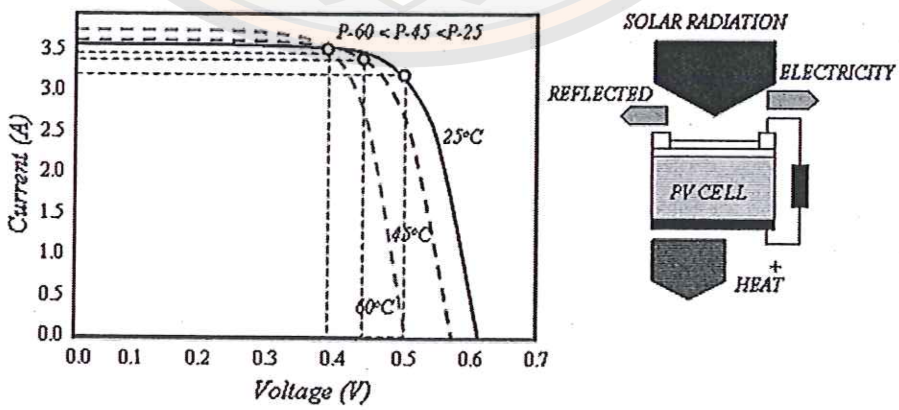

Figure 145 The effect of module temperature

In this part is to find efficiency of PV which is changed by PV module temperature. However, PV module temperature is altered according to solar irradiance and whether as shown in Figure 145. This is because the installation in outdoor condition according to quality of thermos, heat reflecting and heat transferring materials. As a result, there is a difference between both mentioned cases of installations as shown in Figure 146.

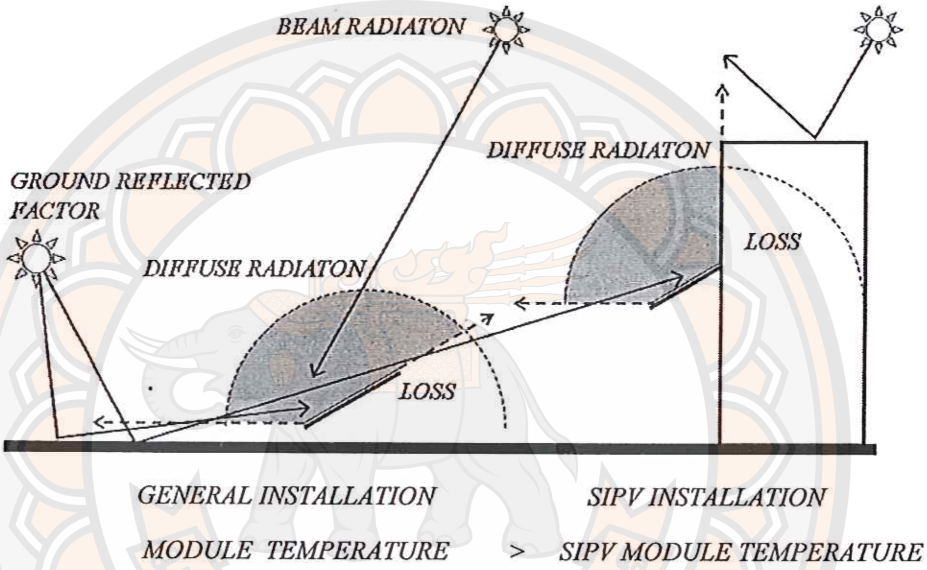

Figure 146 The comparison of the PV installation

PV is material with low heat radiation reflectance capable of collecting only a few amount of solar irradiance because of its thinness and non-insulator. This results in heat on skin of module causing lower efficiency. In the case of half sky, the effect of solar irradiance is lesser while effect of whether is being equally received.

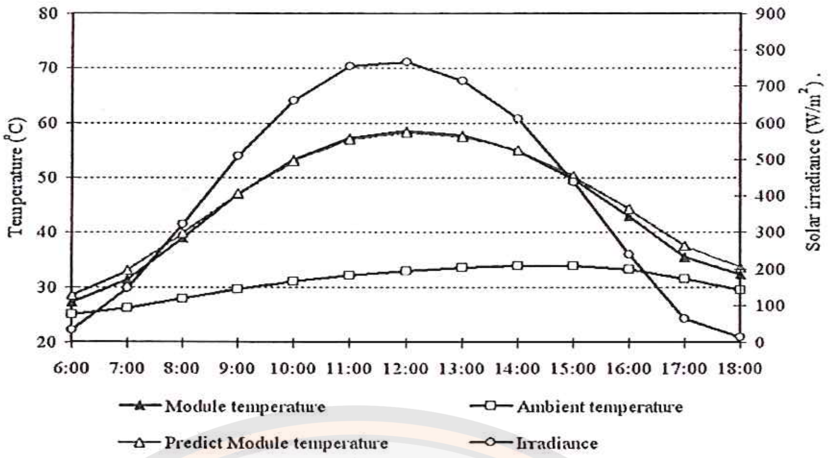

Amorphous silicon

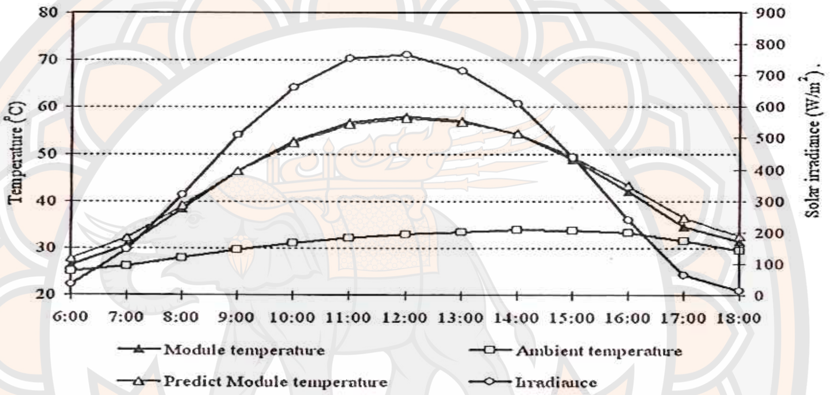

Polycrystalline silicon

Figure 147 The comparison of the module temperature, solar irradiance and ambient temperature

$$Tm_{a\text{-}Si} = -2.9564 + (1.2249\ T_{amb}) + (0.0271\ I_{tT}) \quad Eq.104$$

R Square = *0.9456*

Observations = *29,483 ; during 2007*

$$Tm_{p\text{-}Si} = -3.3869 + (1.2055\ T_{amb})+(0.0276\ I_{tT}) \quad Eq.104$$

R Square = *0.9460*

Observations = *29,482 ; during 2007*

Figure 147 shows that both technologies have similar module temperature in the case of experiment under full sky condition. It is found that the temperature is changed by solar irradiance and because of effect of weather causing the low decrease of module temperature as the solar irradiance is supposed to decrease more in the evening. From using the equation gained from regression analysis, the values of both technologies can be predicted similar to the actual data.

2.2 PV module efficiency under full sky condition

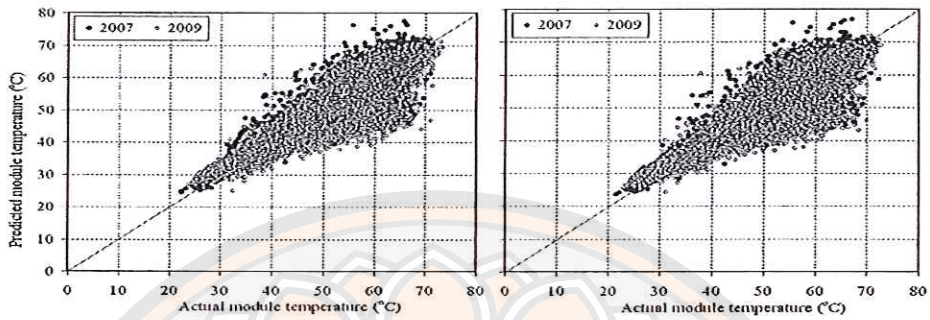

Amorphous silicon technology Polycrystalline silicon

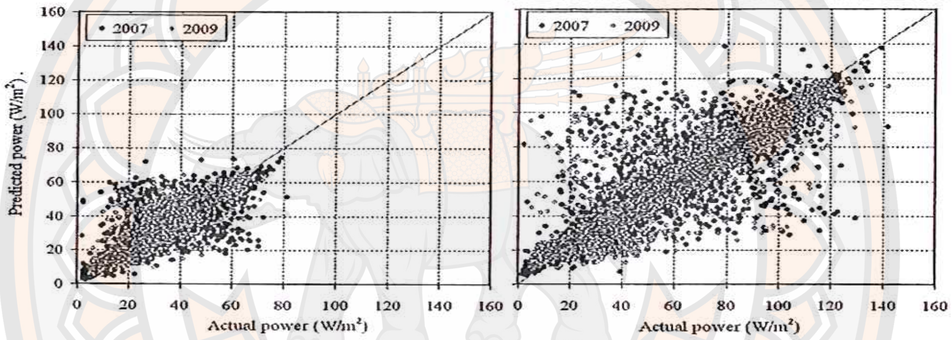

Amorphous silicon technology Polycrystalline silicon

Figure 148 The comparison between predicted data and actual data

Table 24 The evaluation of the module temperature models

	Module temperature				**Power**			
	Amorphous silicon		Polycrystalline silicon		Amorphous silicon		Polycrystalline silicon	
	2007	2009	2007	2009	2007	2009	2007	2009
Observations	17,487	21,020	17,487	21,020	17,487	21,020	17,487	21,020
RMSE	2.9833	3.8660	3.1114	3.8053	4.2269	3.2557	7.1870	6.2038
NRMSE	5.7580	7.6252	6.0899	7.6333	12.7638	10.6719	11.9829	10.8979
MBE	-0.0635	-1.9004	-0.1128	-1.8130	0.1080	0.1322	-0.0341	-1.2394
NMBE	-0.1226	-3.7483	-0.2208	-3.6367	0.3262	0.4333	0.0568	-2.1773
Rsquare	0.9115	0.8764	0.9061	0.8787	0.9266	0.9478	0.9323	0.9486

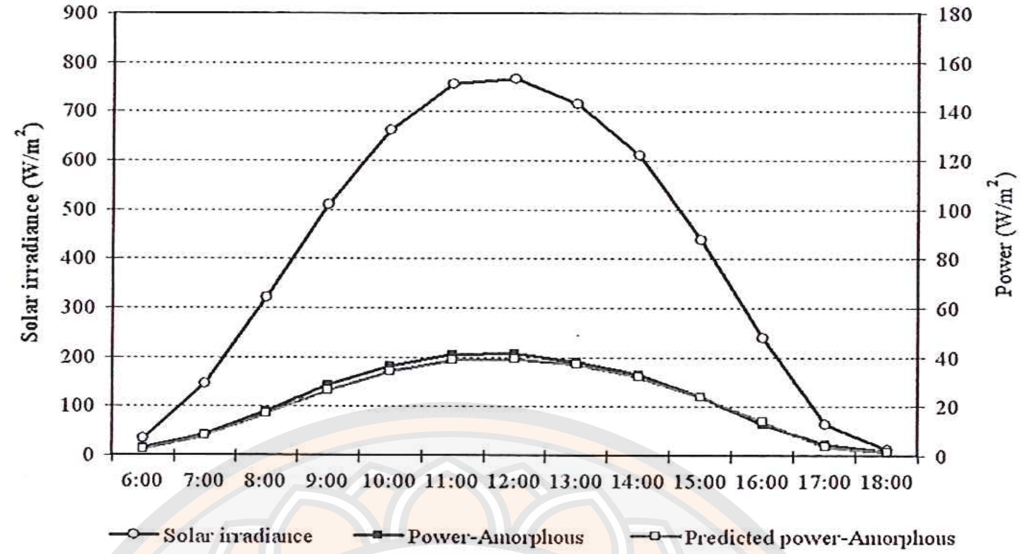

Amorphous silicon technology

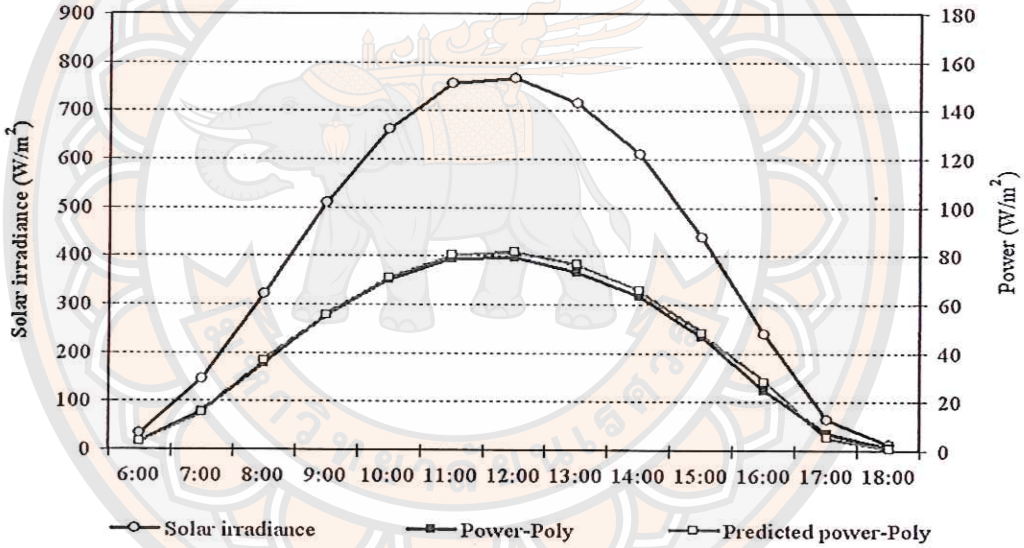

Polycrystalline silicon

Figure 149 The power prediction by the mathematical models

Comparing to data from other years which is not data used in analysis with root mean square error (RMSE) and the mean bias error (MBE) as shown in Table 24 explains that the equation can be used in prediction and with database from different other years. From the data disperse shown in Figure 148 of both technologies, it is found that the disperse rather provides a clear linear trend in both cases of module temperature and produced power.

Figure 149 shows result of comparison due to the use of equation to predict the values of both solar cells technologies as shown in Eq. 105 and database of 2009.

$$\eta_{a\text{-}Si} = [-5.8527 + (0.2659\ T_m) + (0.0446\ E_{tT})]\ /\ E_{tT} \qquad Eq.105$$

R Square = *0.8978*

Observations = *19,445 ; during 2007*

$$\eta_{p\text{-}Si} = [-1.9995 + (0.2207\ T_m)+(0.0893\ E_{tT})]\ /\ E_{tT} \qquad Eq.105$$

R Square = *0.9043*

Observations = *21,209 ; during 2007*

2.3 Module efficiency under half sky

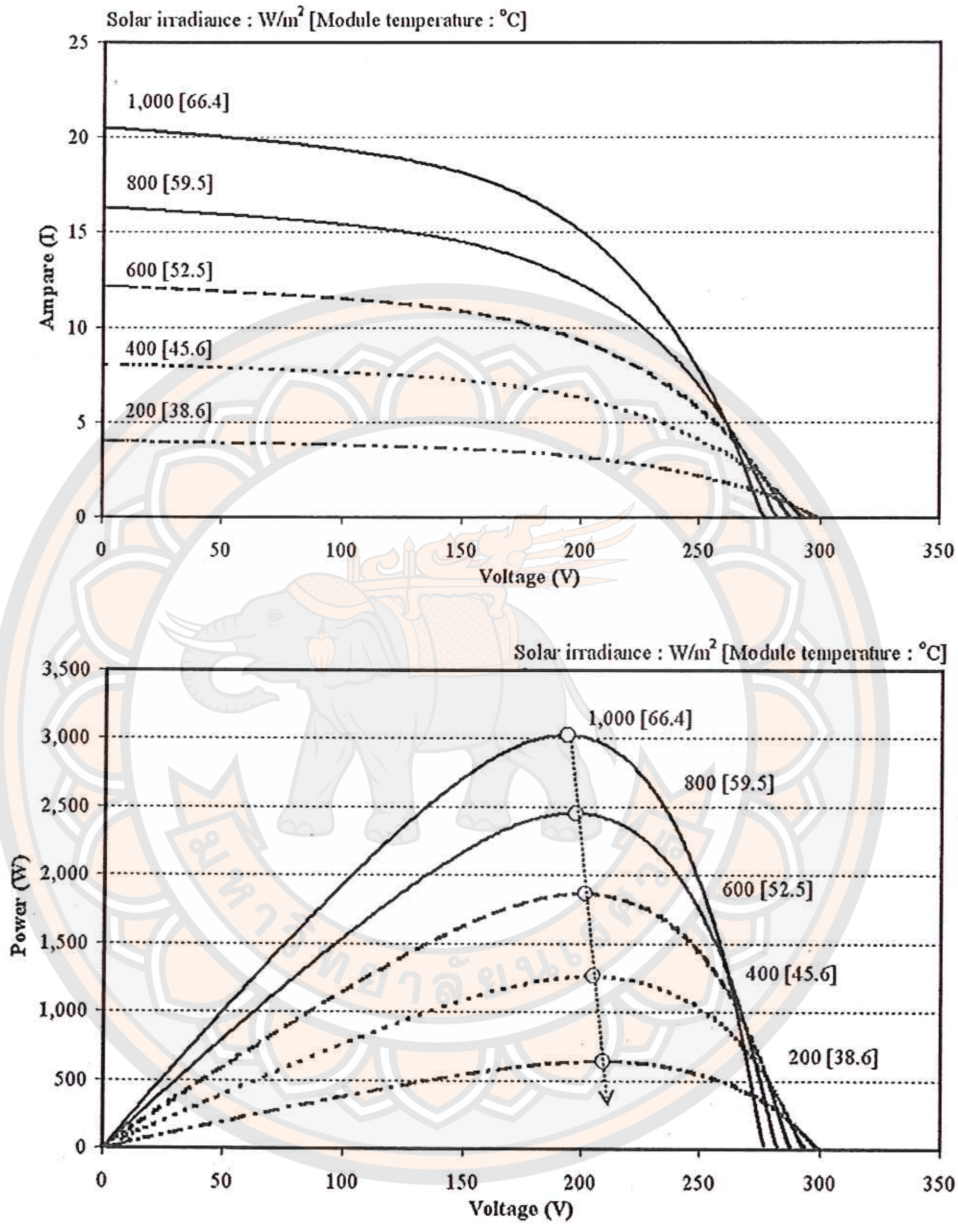

Figure 150 The characteristic curves of amorphous silicon technology

Figure 150 shows the comparison of solar irradiance change and module temperature change in the forms of I-V curve and P-V curve of amorphous silicon technology. It is found that the highest value of electric power at curve of each condition tends to decrease as a linear.

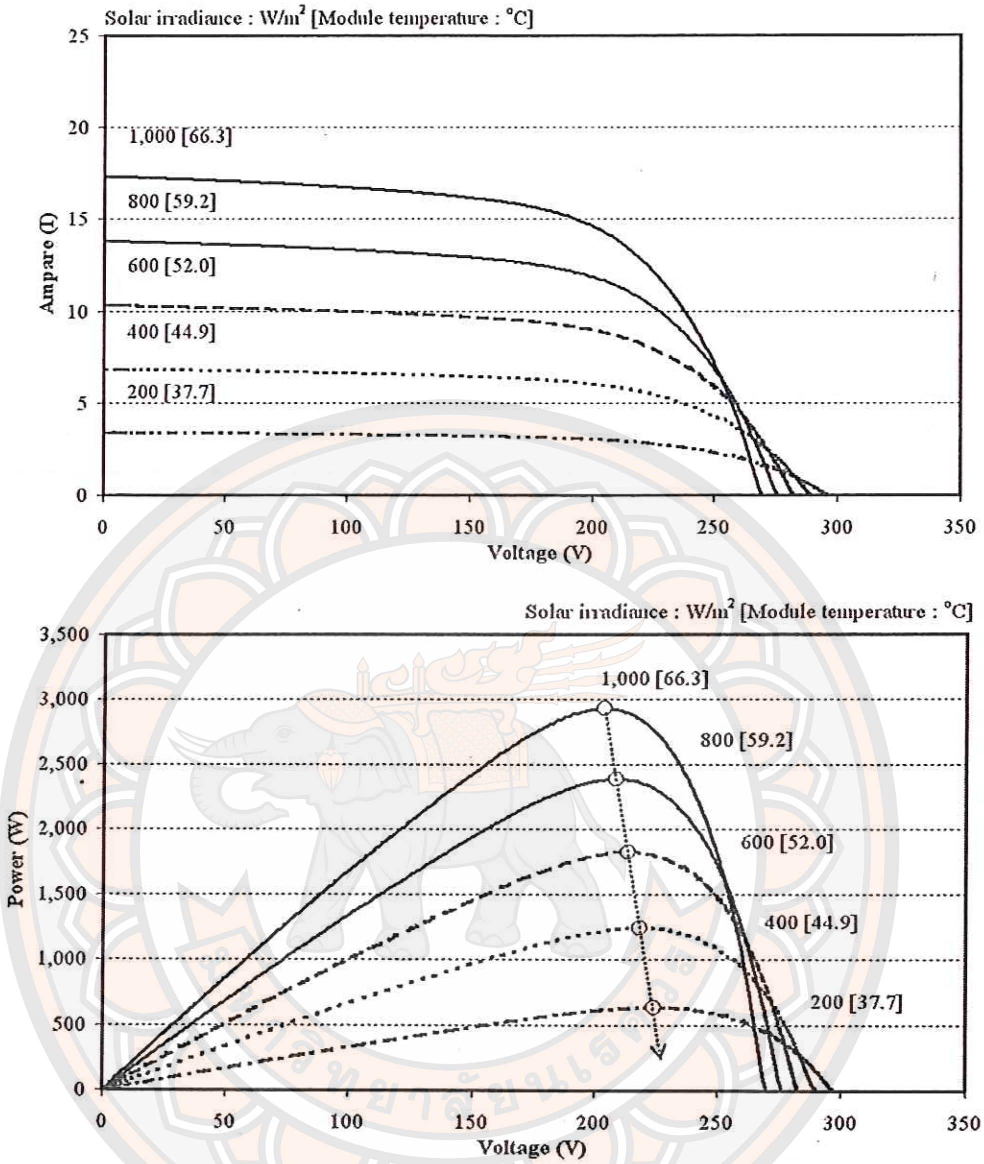

Figure 151 The characteristic curves polycrystalline silicon technology

Figure 151 shows the comparison of solar irradiance change and module temperature change in the forms of I-V curve and P-V curve of polycrystalline silicon technology. It is found that highest value of electric power at curve of each condition tends to decrease as linear with a little difference of line slope.

When the period of Solar irradiance at 50-300 W/m^2 and air temperature between 20°C to 36°C as shown in Figure 152, it is found that the period of the change in polycrystalline silicon module efficiency is more than Amorphous silicon technology.

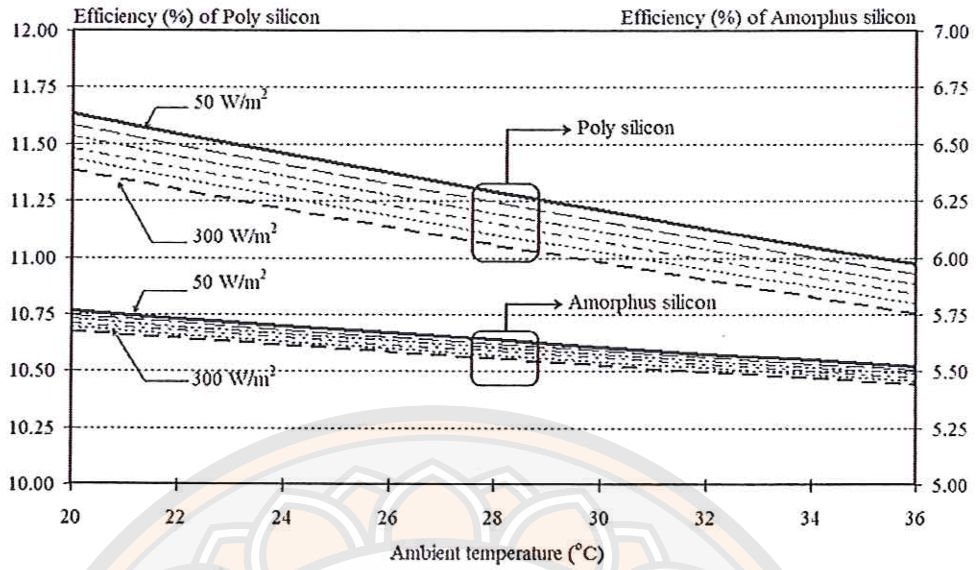

Figure 152 The module temperature effect under half sky condition

$$Eff_{a\text{-}Si} = 6.0709 - 0.0003\, I_{tT} - 0.0148\, T_{amb} \qquad Eq.106$$

$$R^2 = 0.9995$$

Observations = 54 ; during 2008

$$Eff_{p\text{-}Si} = 12.4671 - 0.0009\, I_{tT} - 0.0402 T_{amb} \qquad Eq.106$$

$$R^2 = 0.9993$$

Observations = 54 ; during 2008

Figure 153 shows the prediction of PV efficiency compared to solar irradiance. Figure 154 shows the comparison of ambient temperature; the Eq. 105 is used in the case of full sky and Eq. 106 is used in the case of half sky. It is found that in Polycrystalline silicon, p-Si, efficiency is clearly changed according to solar irradiance and in Amorphous silicon, effect of temperature is shown. From the increase by the trend of ambient temperature, it is found that efficiency of both technologies under half sky is more stable than full sky condition.

Therefore, the power change of solar cells technology contains two following factors in prediction: solar irradiance and ambient temperature. The gained math models will be separately used in prediction according to solar irradiance receiving and solar cells technologies.

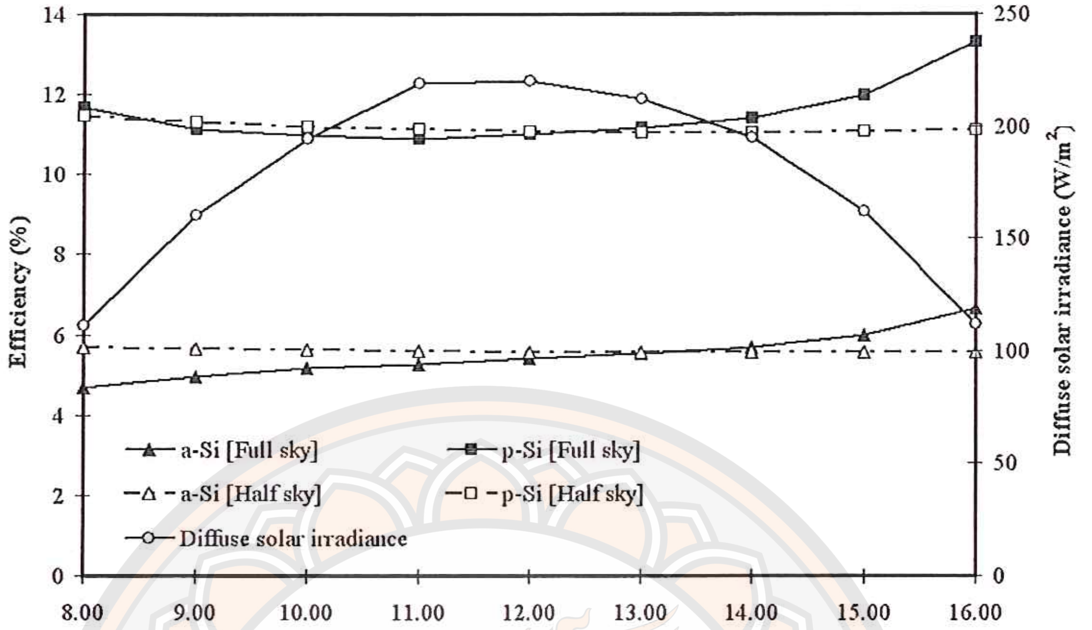

Figure 153 The comparison between the PV efficiency and the solar irradiance

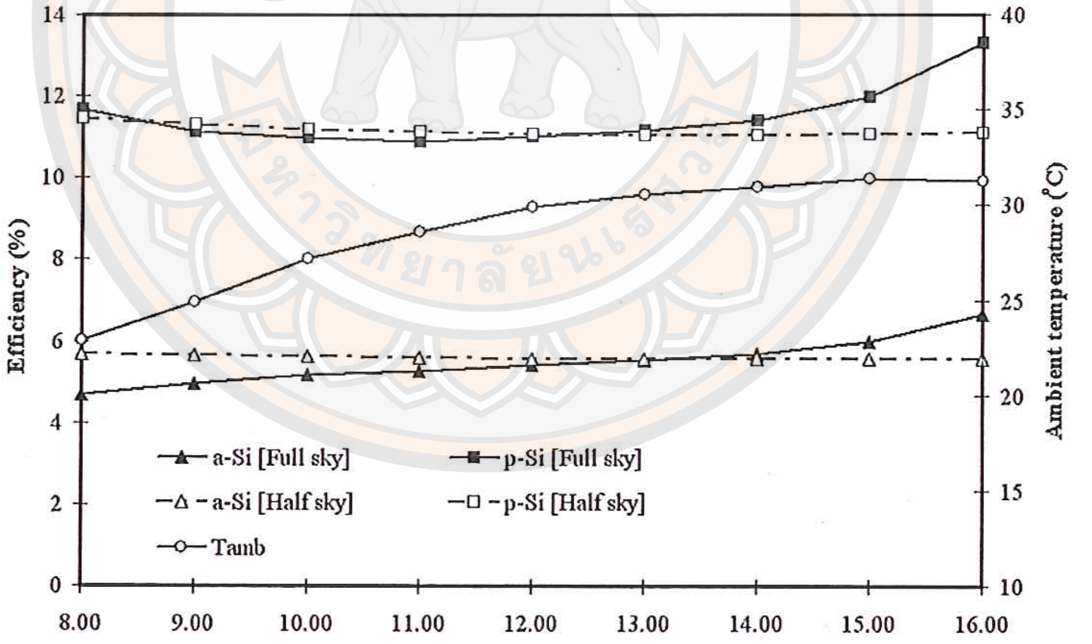

Figure 154 The comparison between the PV efficiency and the ambient temperature

3. The efficiency of inverter under out door condition

The experiment using B. Tarika's [53] research data analysis as shown in Figure 155 and the improvement of equation used in prediction by using regression analysis technique as shown in Figure 156, it is found that inverters can work well or have high efficiency when receiving total solar irradiance more than 600 W/m^2 which is not half sky case.

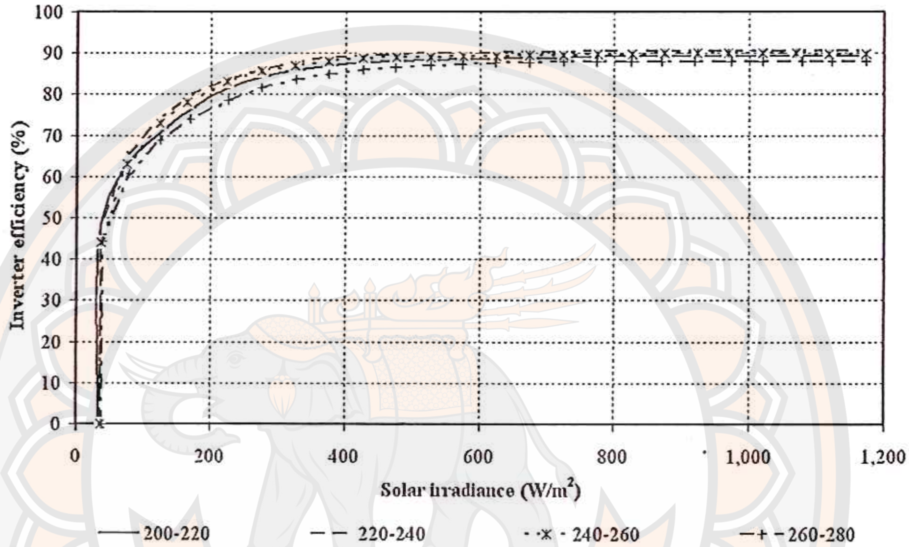

Figure 155 The efficiency of inverter operation between 200 V and 280 V

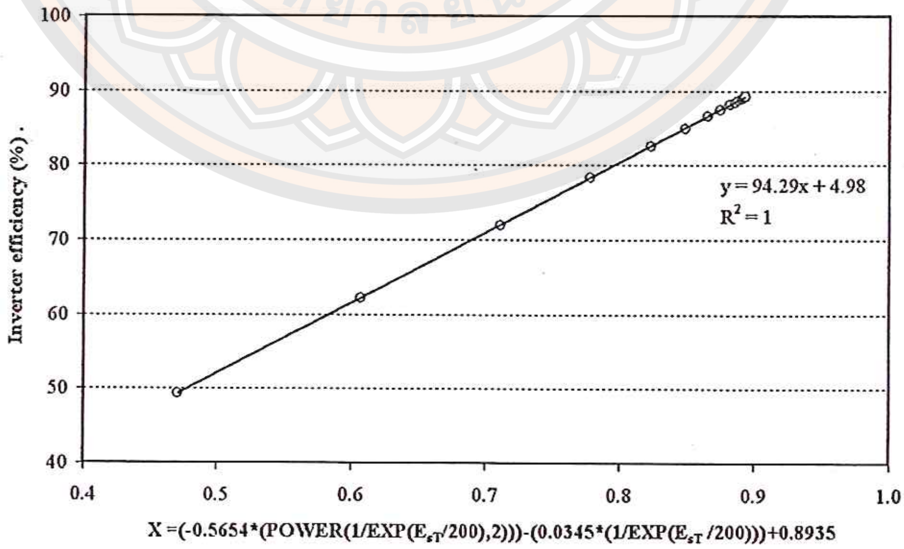

Figure 156 The relation between efficiency and modified solar irradiance

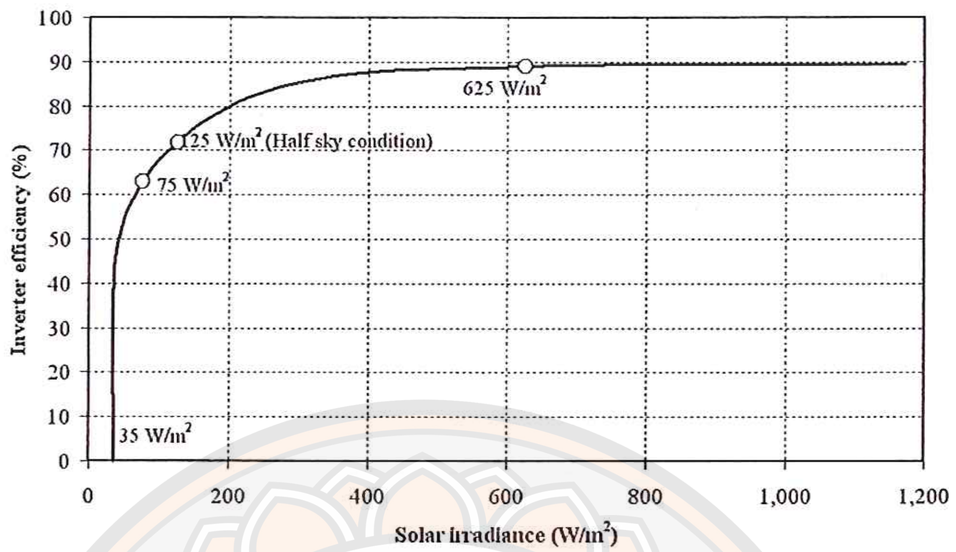

Figure 157 The predicted line of inverter efficiency

$$\eta_{inv} = 0.0498 + 0.9429(X) \quad Eq.107$$

$$X = (-0.5654x((1/exp(E_{t}S/200))^2))-(0.0345x(1/exp(E_{t}S\ /200)))+0.8935$$

Figure 157 shows efficiency of inverters operation. It is found that the highest efficiency is at about 90%, at 625 W/m². While half sky condition at 125 W/m² has about 72% of efficiency and cannot work well at 35 W/m². It can be said that the operation under full sky condition will have efficiency from 85% to 90% corresponding to the operation of shading devices during 8.00-16.00. In addition, inverters' operations have low efficiency when there is low solar irradiance before 8.00 or after 16.00.

4. Daylight Factor (DF) [Chapter III; page 104-105]

4.1 The Sky Component (SC)

Figure 158 shows the data comparison between the case of with shading devices at W/H=0.3 and without shading devices at W/H=0 in various period of time. It is found that the collected data tends to be similar in every period of time including the case of clear sky as shown in Figure 158. In Figure 159, trend of the overcast sky is more different.

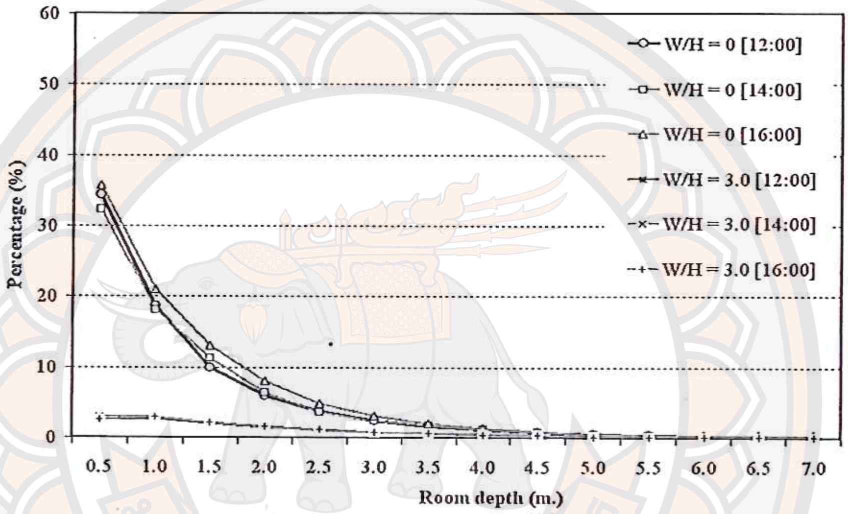

Figure 158 The SC comparisons of clear sky condition

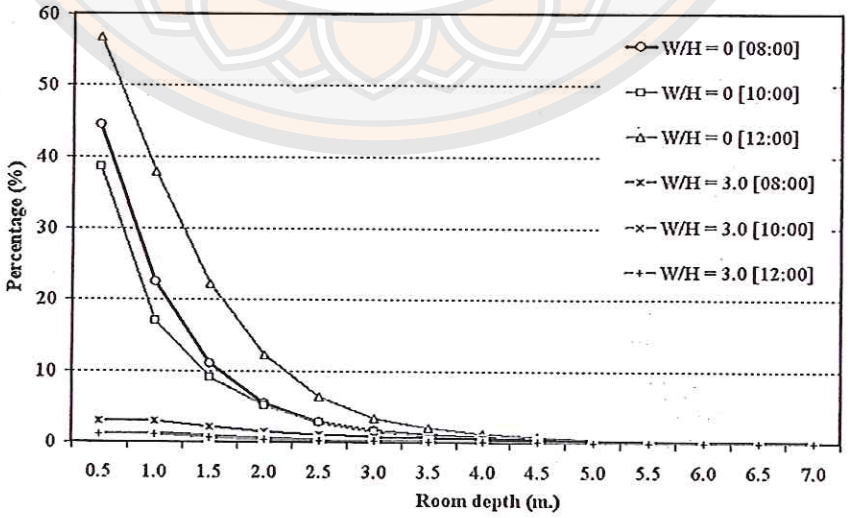

Figure 159 The SC comparisons of overcast sky condition

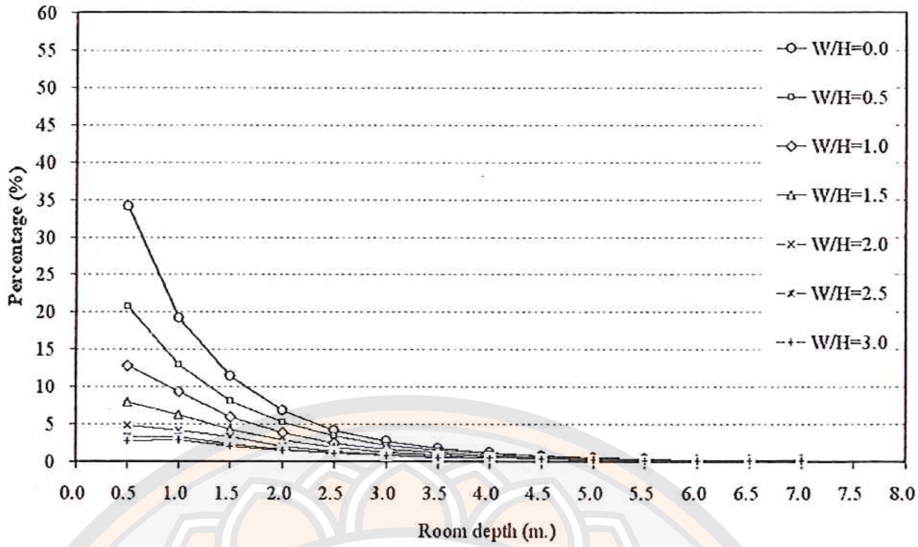

Figure 160 The SC comparison every W/H ratio of clear sky condition

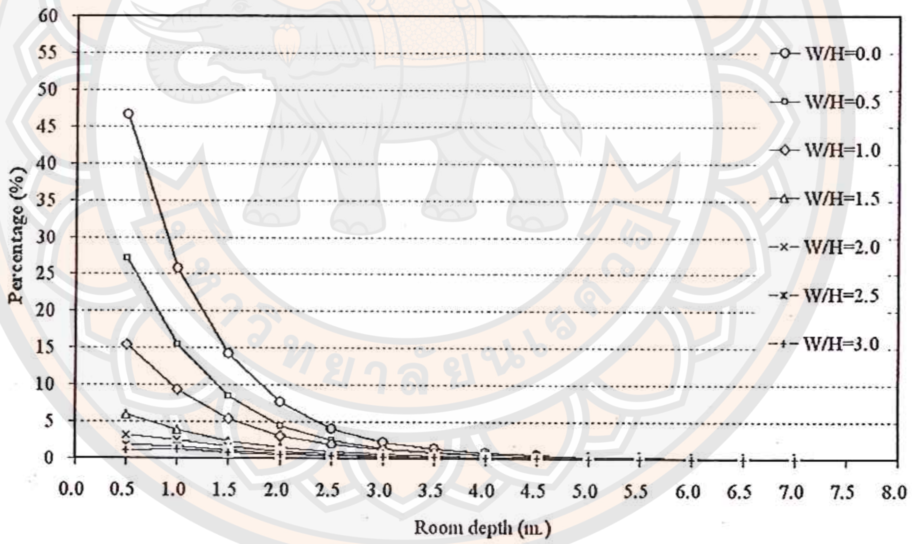

Figure 161 The SC comparison every W/H ratio of overcast sky condition

Both sky conditions have similar trends by receiving daylight which is decreased according to W/H ratio of shading devices and rapidly decreased where there is a long distance from window causing the similar values at the distance about 4 times of window height.

4.2 The Internal Reflected Component (IRC)

The Mirror box was used in this experiment to reproduce overcast sky in order to find effect of reflectance of room surface within the buildings. The comparison is between normal surface model and dark surface model with qualification of low reflectance as shown in Figure 162. When the gained IRC ratio being confuted, it is found that the trend of high value is the area close to window but it will not rapidly decrease and have different effect through the depth of the room.

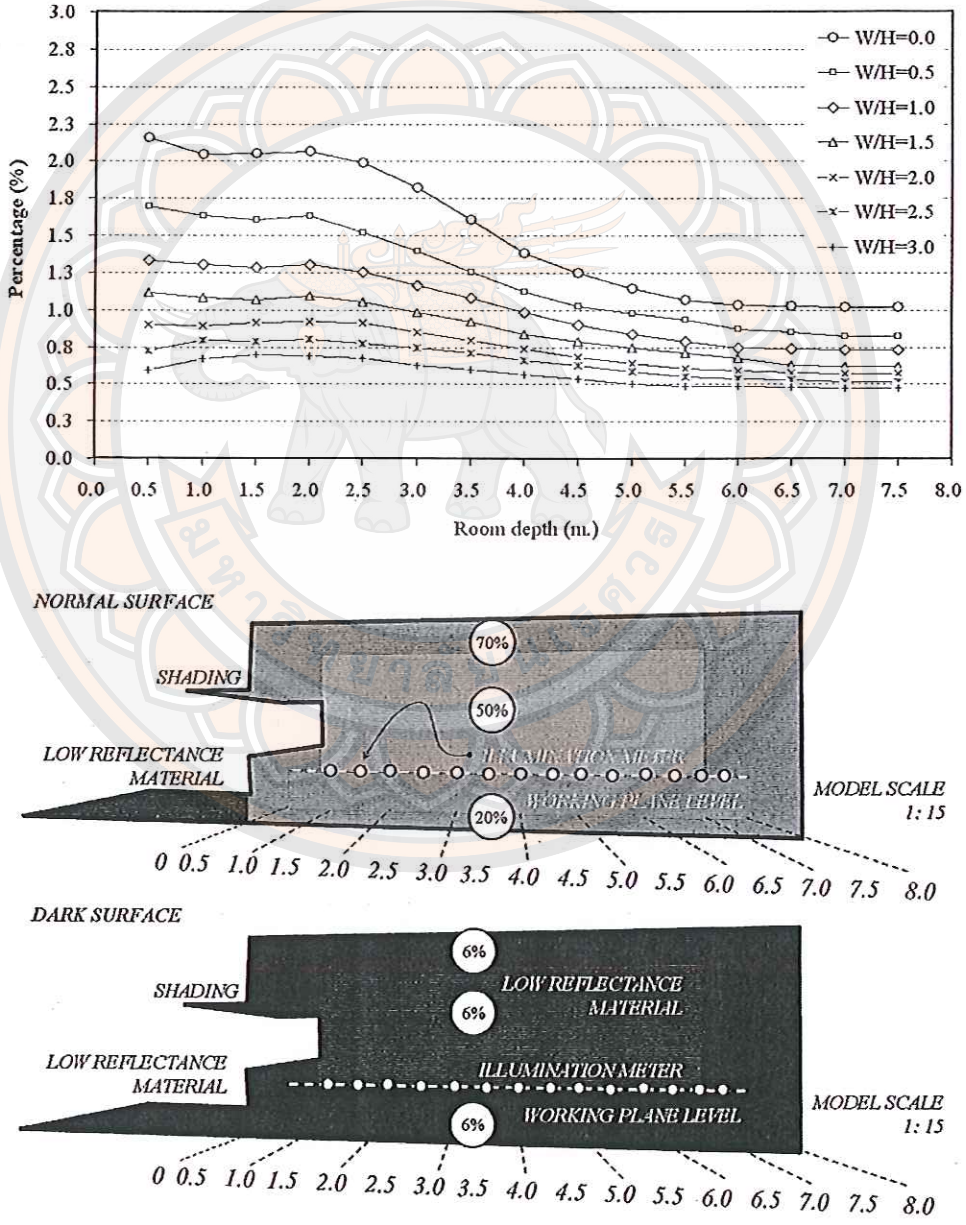

Figure 162 The IRC every W/H ratio of mirror box condition

4.3 Total Daylight Factor (DF)

For the usability, clear sky case is considered in estimation due to the fact that it is the condition allowing SIPV to work normally as shown in Figure 163. Sum total of SC and IRC is shown in Table 25 in every forms of W/H of shading devices in each position of distance from the window using Eq.112.

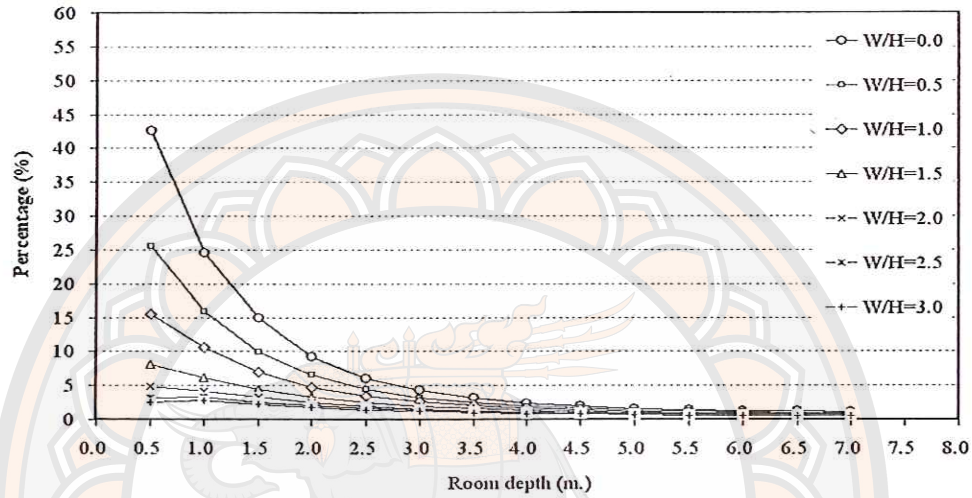

Figure 163 The DF every W/H ratio of average sky condition

Table 25 The SC and IRC every W/H ratio of average sky condition

SC							**Room dept**							
W/H	**0.5**	**1.0**	**1.5**	**2.0**	**2.5**	**3.0**	**3.5**	**4.0**	**4.5**	**5.0**	**5.5**	**6.0**	**6.5**	**7.0**
0.0	40.37	23.90	14.1	6.99	4.01	2.54	1.92	40.37	23.90	14.14	6.99	4.01	2.54	1.92
0.5	22.52	14.25	9.34	5.11	3.29	2.49	2.06	22.52	14.25	9.34	5.11	3.29	2.49	2.06
1.0	12.81	8.28	5.72	3.35	2.49	1.77	1.49	12.81	8.28	5.72	3.35	2.49	1.77	1.49
1.5	7.20	4.86	3.48	2.19	1.53	1.22	1.06	7.20	4.86	3.48	2.19	1.53	1.22	1.06
2.0	4.08	3.00	2.23	1.48	1.07	0.86	0.78	4.08	3.00	2.23	1.48	1.07	0.86	0.78
2.5	2.47	1.84	1.46	0.94	0.73	0.62	0.57	2.47	1.84	1.46	0.94	0.73	0.62	0.57
3.0	1.59	1.24	1.00	0.69	0.53	0.46	0.42	1.59	1.24	1.00	0.69	0.53	0.46	0.42
IRC	**0.5**	**1.0**	**1.5**	**2.0**	**2.5**	**3.0**	**3.5**	**4.0**	**4.5**	**5.0**	**5.5**	**6.0**	**6.5**	**7.0**
0.0	2.16	1.70	1.33	1.11	0.90	0.73	0.59	2.16	1.70	1.33	1.11	0.90	0.73	0.59
0.5	2.04	1.63	1.31	1.08	0.89	0.79	0.67	2.04	1.63	1.31	1.08	0.89	0.79	0.67
1.0	2.05	1.60	1.28	1.07	0.91	0.79	0.70	2.05	1.60	1.28	1.07	0.91	0.79	0.70
1.5	2.06	1.63	1.30	1.09	0.92	0.80	0.69	2.06	1.63	1.30	1.09	0.92	0.80	0.69
2.0	1.99	1.52	1.25	1.05	0.91	0.78	0.67	1.99	1.52	1.25	1.05	0.91	0.78	0.67
2.5	1.82	1.39	1.17	0.98	0.85	0.75	0.63	1.82	1.39	1.17	0.98	0.85	0.75	0.63
3.0	1.60	1.25	1.08	0.92	0.79	0.71	0.60	1.60	1.25	1.08	0.92	0.79	0.71	0.60

5. The Shading Coefficient of diffuse radiation (SC_d) [Chapter III; page 107]

SC_d is a value indicating shading coefficient. From the result of experiment, the comparison is between sky in the North shown in Figure 164 (top) and West shown in Figure 164 (below) by testing with shading devices with 3 types of W/H ratio as follows: 1.0, 2.0 and 3.0. The results shows that two sky conditions provide similar experiment result and when compared as SC_d as shown in Figure 165 by considering the average between 2 sky curve to be used in creating predicting equation and to conclude as a constant for each W/H ratio of shading devices as shown in Table 26.

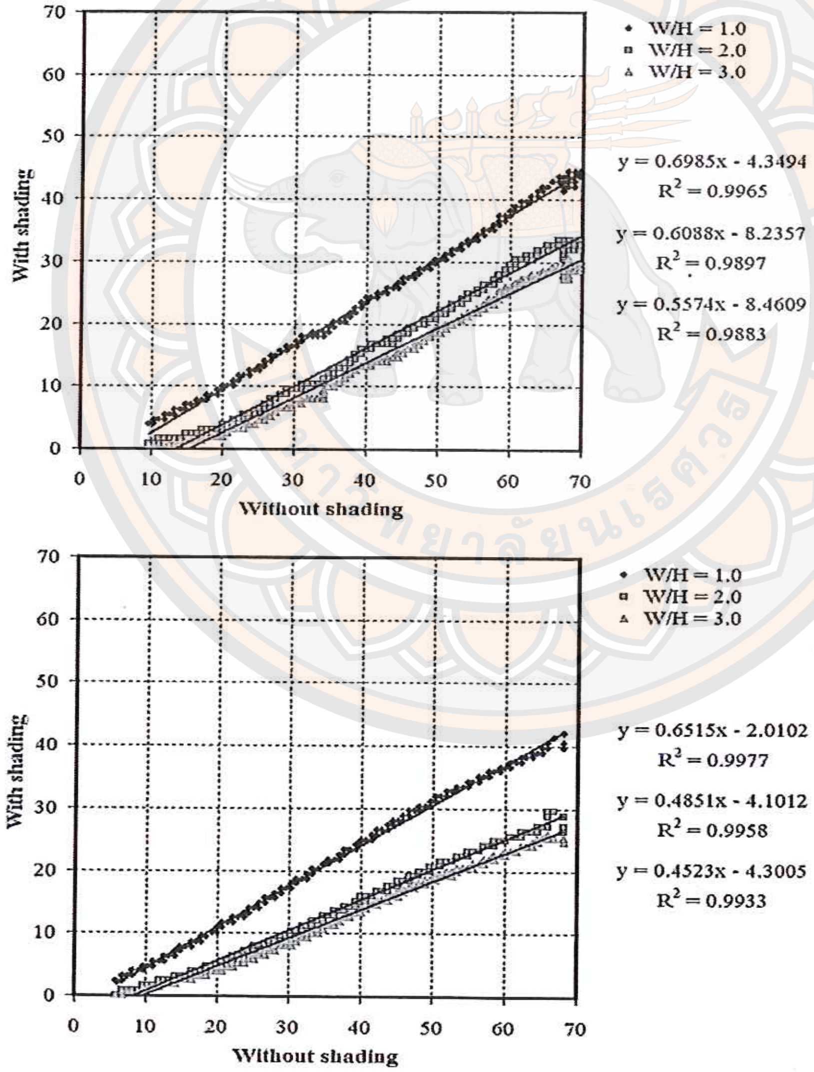

NORTH

WEST

Figure 164 The solar irradiance ratio with shading to without shading

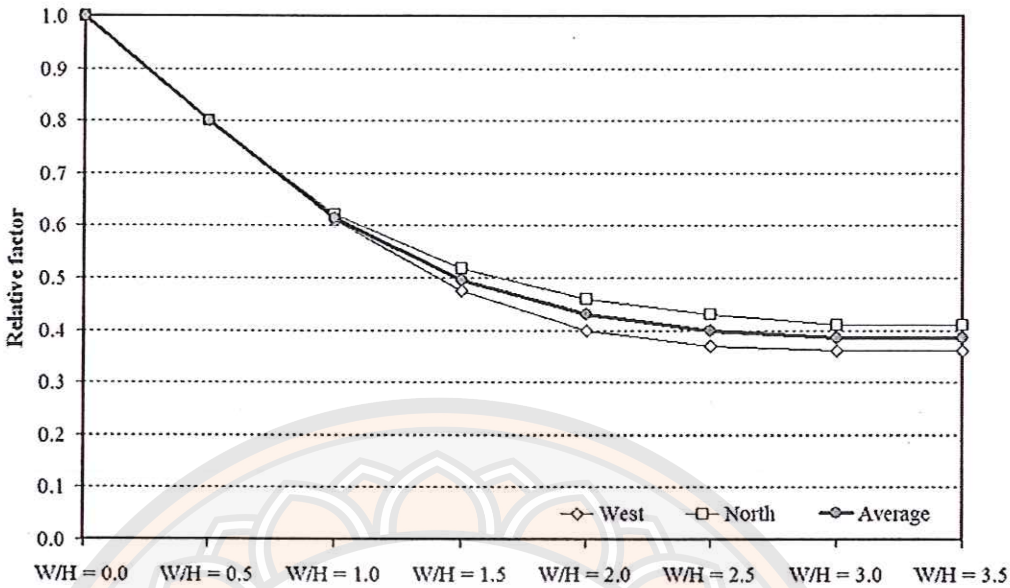

Figure 165 The Shading Coefficient of diffuse radiation comparisons

Table 26 Shading Coefficient of diffuse radiation (SC_d)

	Shading Coefficient of diffuse radiation (SC_d)			
		Clear sky		**Overcast sky**
W/H	**North**	**West**	**Average**	
0.0	1.00	1.00	1.00	1.00
0.5	0.80	0.80	0.80	0.52
1.0	0.62	0.61	0.62	0.30
1.5	0.52	0.48	0.50	0.21
2.0	0.46	0.40	0.43	0.15
2.5	0.43	0.37	0.40	0.13
3.0	0.41	0.36	0.39	0.13
3.5	0.41	0.36	0.39	0.13

However, trend of SC_d in the case of clear sky is a little lower than the case of overcast sky. It is also found that SCd of W/H ratio at more than 2.5 is quite stable and tends not to decrease staying permanently at about 0.39 which means no matter how much longer the shading devices are, SC_d will not decrease.

Figure 166 shows the comparison of clear sky condition and overcast sky condition. It is found that SC_d is different. Due to the fact that overcast sky might affect cooling load quite a little and it doesn't need to open air conditioning system. This research is, therefore, considering using clear sky condition in estimation. The equation created by using regression analysis is linear equation with R square at 0.9995.

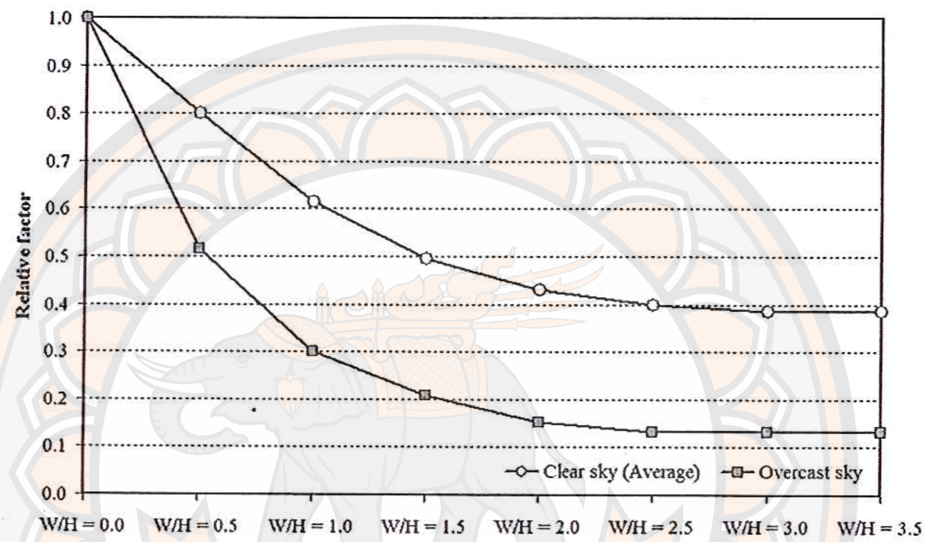

Figure 166 The comparisons between clear sky and overcast sky conditions

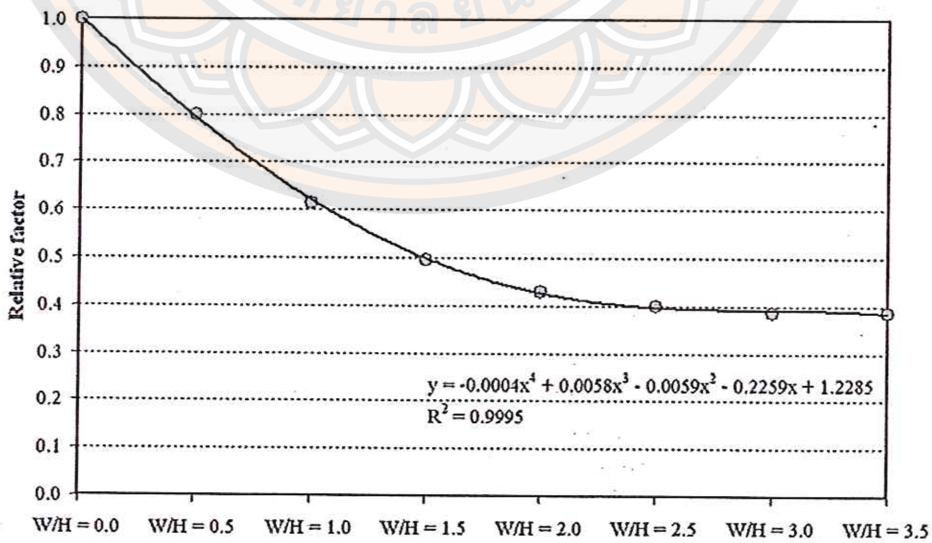

Figure 167 The Shading Coefficient of diffuse radiation trend

$$SC_d = 0.0004\,X^4 + 0.0058\,X^3 - 0.0059\,X^2 - 0.2259X + 1.2285 \qquad Eq109$$

$$X = 2(W/H) + 1$$

6. Summary of the experimental part

It is the study to improve equation for prediction of energy systems as follows:

6.1 To predict total solar irradiance using basic equation of ASHRAE (ASHREA's equation) improved by Eq.109 and Eq.110 in the case of SIPV design

6.2 To predict electric power using equations gained from experiment. Eq.105 is for the case of half sky condition as it is when total irradiance consists of beam radiation and sky irradiance. Eq.106 is for the case of half sky as it is when total irradiance consists of only sky irradiance

6.3 To predict electric power from using inverter by using Eq.107

6.4 To predict electric energy used for the whole 30 years and during 8.00 to 16.00

6.5 To predict illuminance level on working plane using Eq.112

6.6 To predict shading coefficient for shading devices located in each direction using Eq.113

Estimation part

The study in this part is to estimate from improved equation in order to predict the use of energy in air conditioning, light and SIPV energy production systems.

1. The total solar irradiance on slope surface

Procedure in estimation of total solar irradiance on slope surface is shown in Figure 168 using Eq.109 and Eq.110 in improving ASHREA's equation.

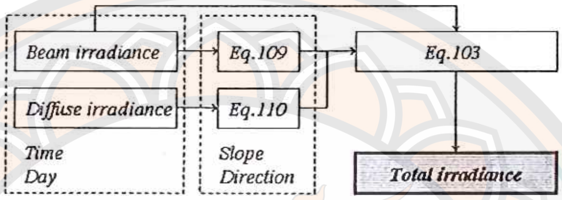

Figure 168 The process of total solar irradiance on slope surface calculation

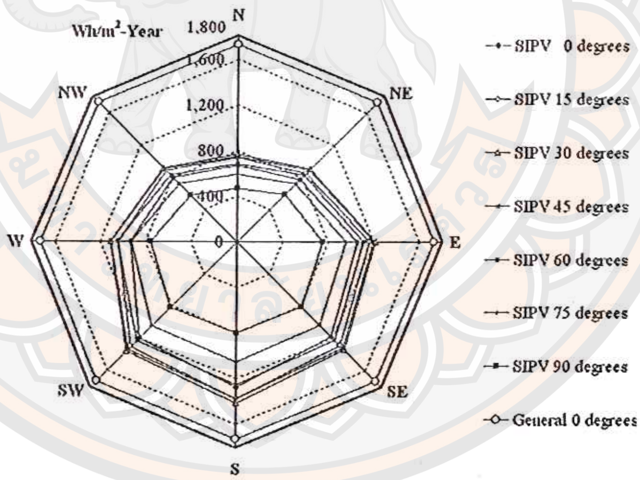

Figure 169 The estimation of the total solar irradiance on slope surface

From annual solar radiation falling down on SIPV plane in each direction and angle, it is found that SIPV in the south makeing tilt angle of 30 degrees to horizontal plane receives the highest level of annual solar radiation. The installation on the East, South East, South, South West and West should be considered due to the similar high values clearly unlike the installation on the North East, North and North West as shown in Figure 169.

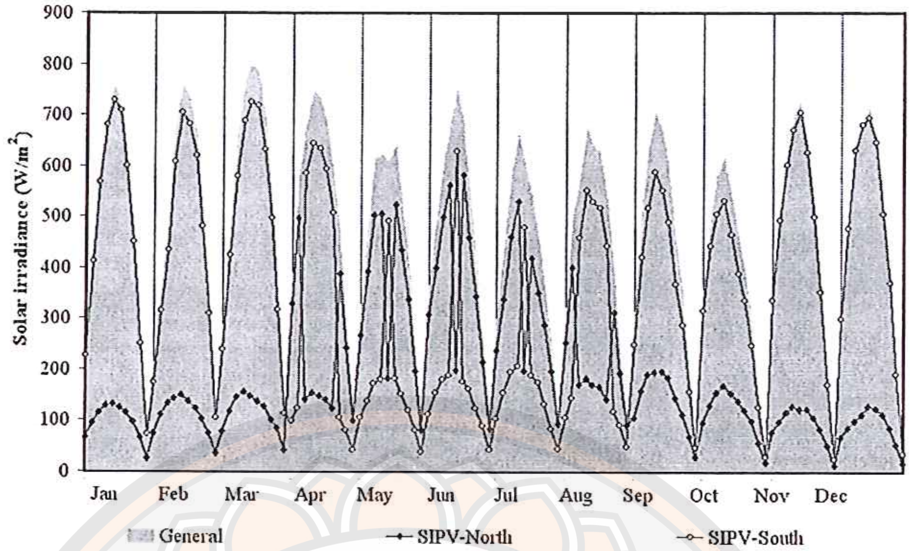

Figure 170 The total solar irradiance on slope surface of N and S

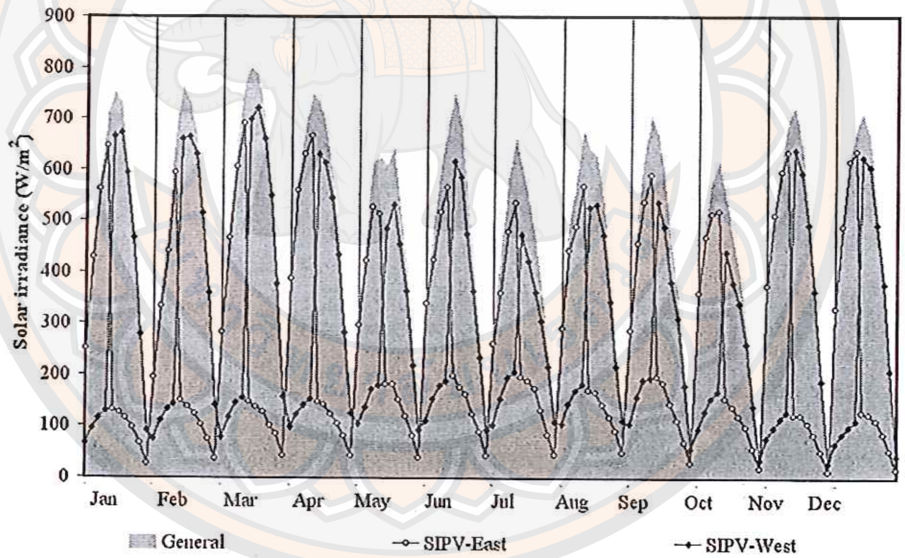

Figure 171 The total solar irradiance on slope surface of E and W

Hourly solar irradiance shown in Figure 170 and Figure 171 of SIPV is to compare PV regular installation on horizontal surface turning towards south which is considered as the best case. It is found that in the cases of North and South, the values are decreased in month of sun position getting behind the buildings. In addition, in the cases of East and West, the values are decreased in the afternoon and in the morning respectively.

In the cases of North East / South East and North West / South West, the values are also decreased due to lesser shade of building than in the cases of North, South, East and West as shown in Figure 172 and Figure 173 respectively.

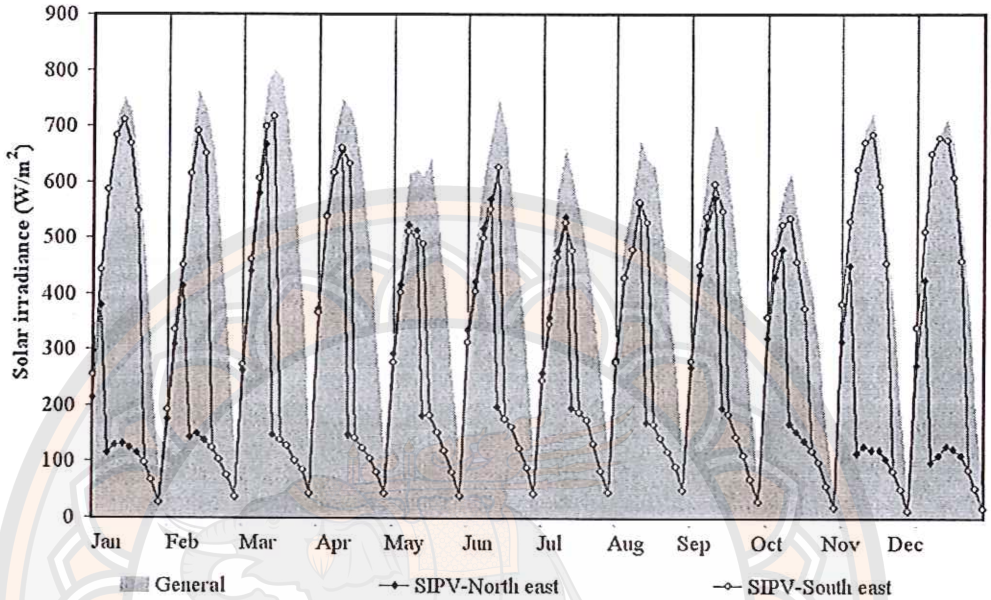

Figure 172 The total solar irradiance on slope surface of NE and SE

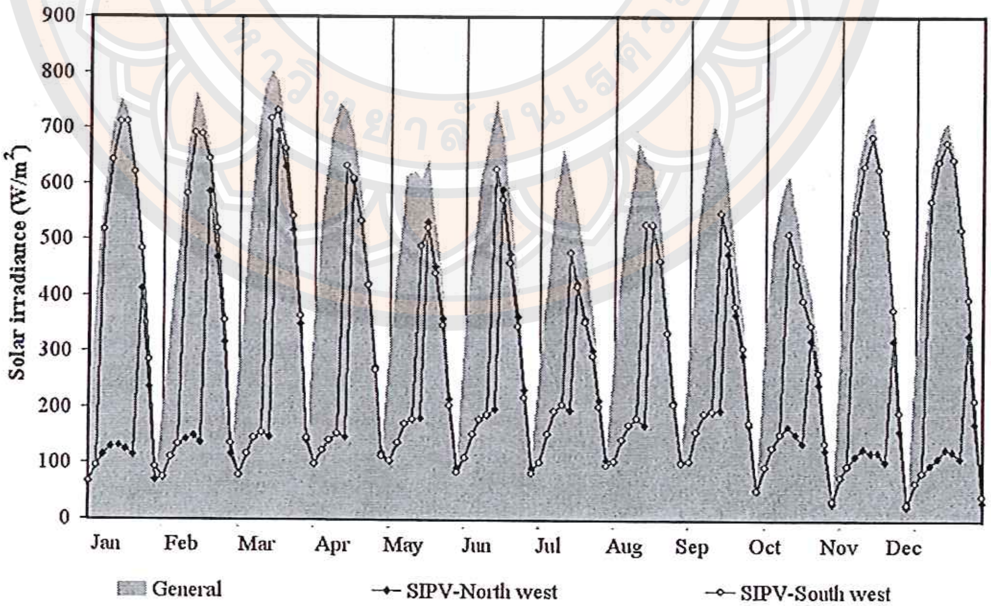

Figure 173 The total solar irradiance on slope surface of NW and SW

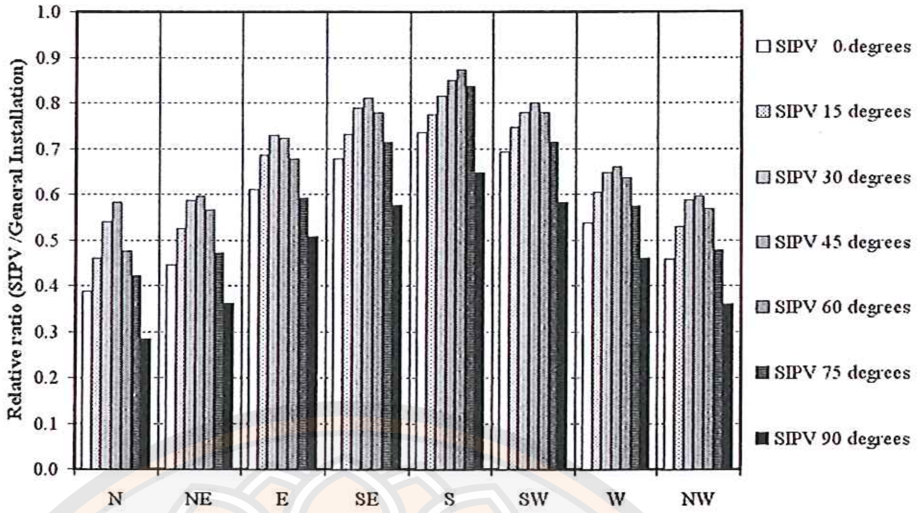

Figure 174 The annual solar radiation ratio of general and SIPV installation

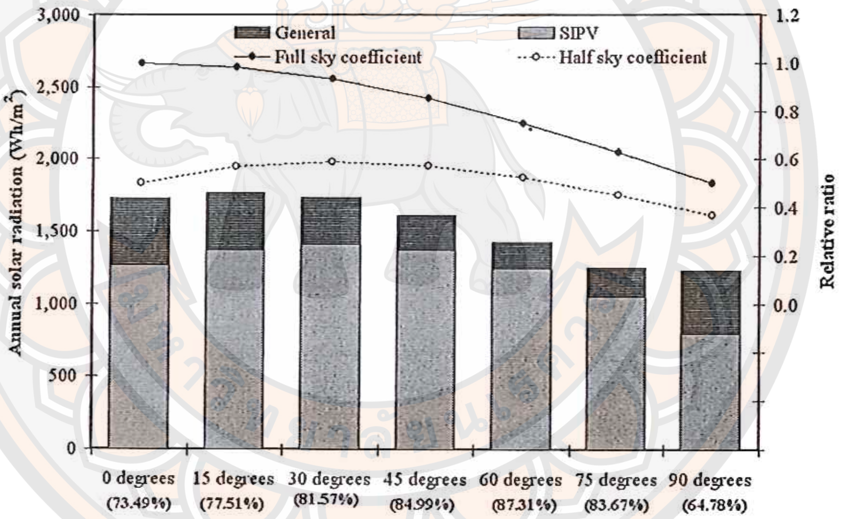

Figure 175 The annual solar radiation comparisons of South direction

Comparing between installation of SIPV and regular installation at the same tilt angle shows ratio as in Figure 174. It is also found that the ratio of North East, North and North West is decreasing more than 40%. Ratio of the South is decreasing the least which contains tilt angle of 30 degrees to 75 degrees.

Building is parameter causing SIPV to receive lower solar irradiance when compared to regular installation. As Figure 175 shows the ratios for installation turning towards south, it is found that the decrease ratio is corresponding to relative coefficient of diffuse solar radiation in the case of half sky condition.

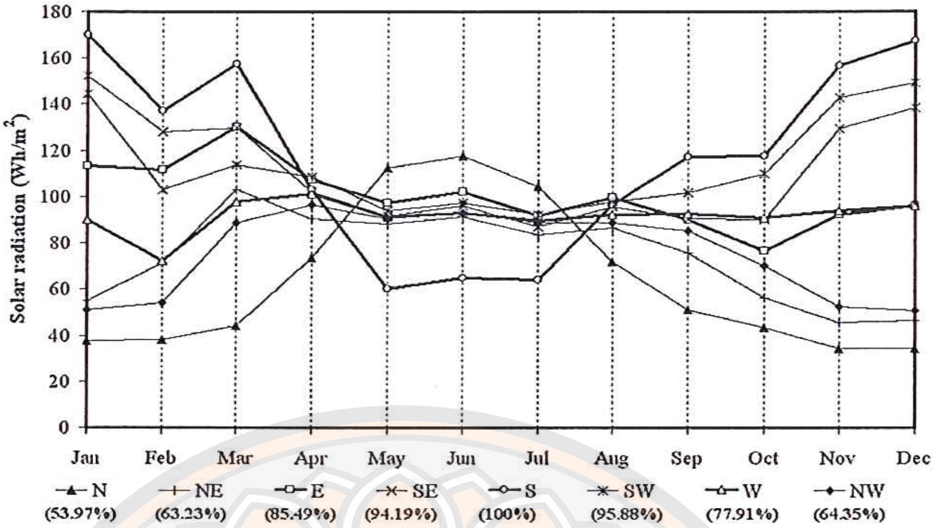

Figure 176 The solar radiation comparisons every month on SIPV surface

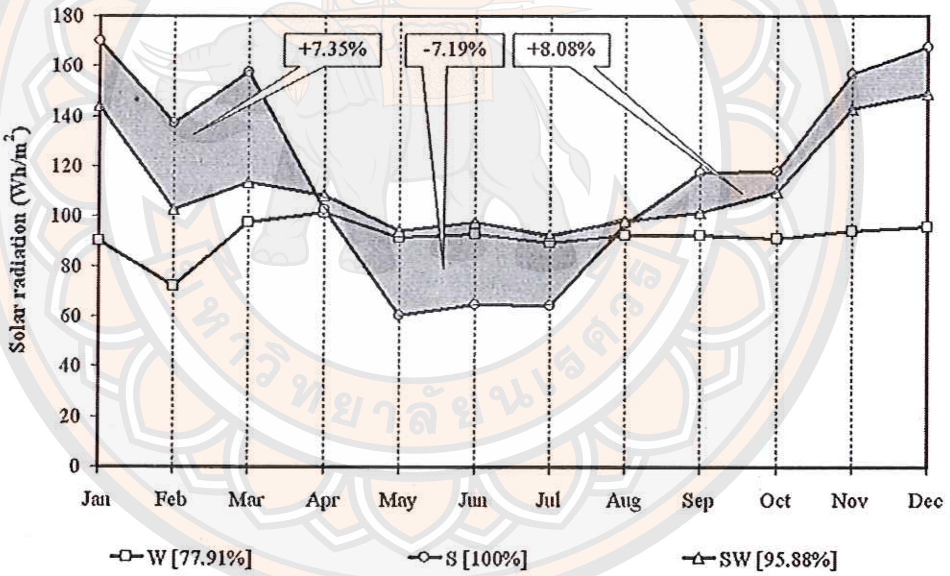

Figure 177 The solar radiation comparisons of East, South and West direction

Although installation in the South receives the highest level of energy, sun encircling towards North in summer time of a year can cause the decrease of solar irradiance and the increase in the winter as shown in Figure 176. Installation in the south in summer provides total solar irradiance less than installation in the South West at about 7.19% and only 4.12% higher for the whole year while installation in the South West is more stable for the whole year as shown in Figure 177.

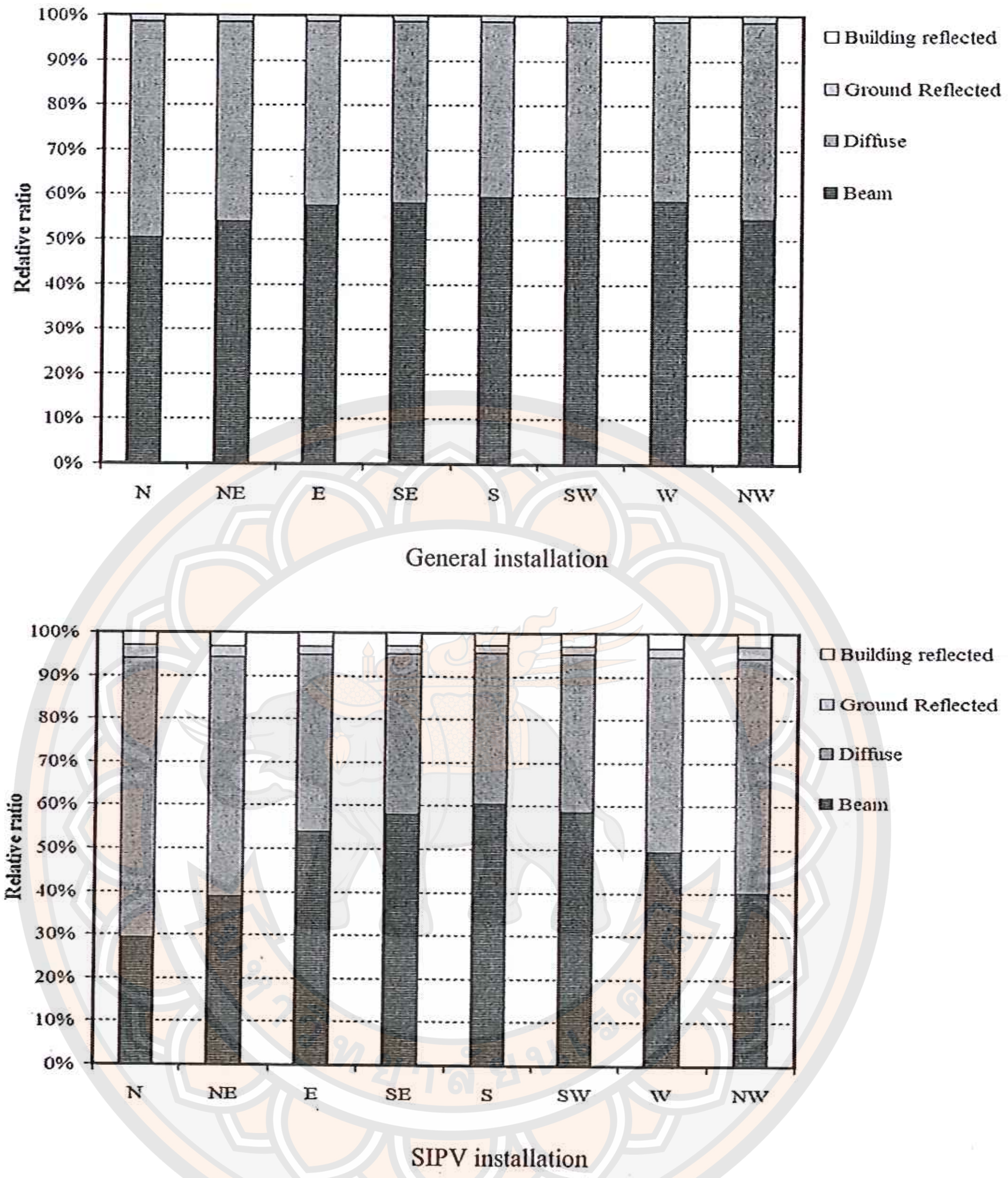

Figure 178 The comparisons of annual solar radiation on SIPV every direction

Figure 178 shows ratio of solar irradiance falling down on module. It is found that in the case of general installation, most effects cause from solar direct irradiance. In contrast to the case of SIPV installation only in the East, South East, South, South West and South, most effects cause from solar direct irradiance and a little bit of effects from building reflected solar irradiance at about 2.5%.

2. Energy production from SIPV

To convert energy gain from solar irradiance, the following equations are used: Eq. 104, Eq. 105, Eq. 106 and Eq. 107. This is to predict electric power by SIPV as shown in Figure 179.

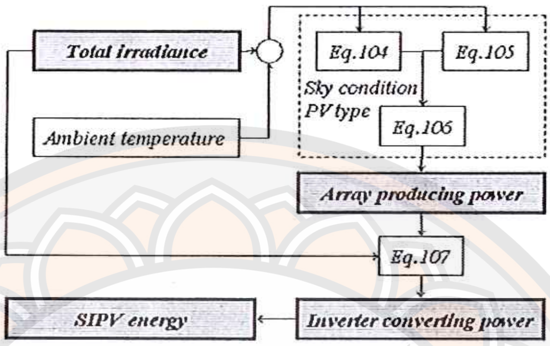

Figure 179 The process of SIPV energy calculation

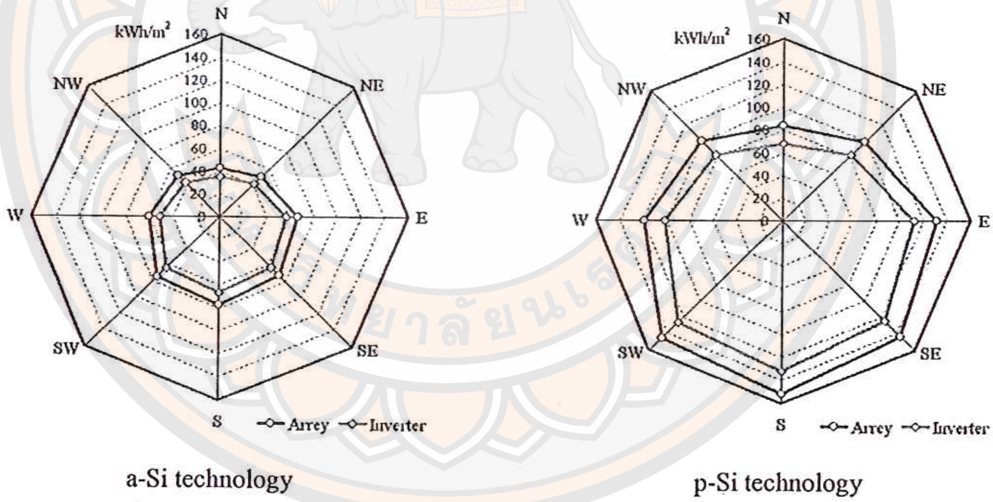

Figure 180 The annual producing comparisons between array and inverter yield

The estimation is for both technologies such as amorphous silicon technology, a-Si and polycrystalline silicon technology, p-Si, technologies in order to compare benefits gained. Figure 180 shows that installation turning towards South with tilt angle of 30 degrees is still the best option. When comparing energy generation per area, polycrystalline silicon technology can generate more energy due to a clear higher efficiency. When considering the need to use the area for shading devices installation, solar cells technology with high efficiency can be chosen as suitable option throughout the year for the best installation. Amorphous silicon technology, a-Si and polycrystalline silicon technology can generate energy 77 and 152 kWh/m^2 respectively and the energy generation can be decreased due to electricity conversion of inverter.

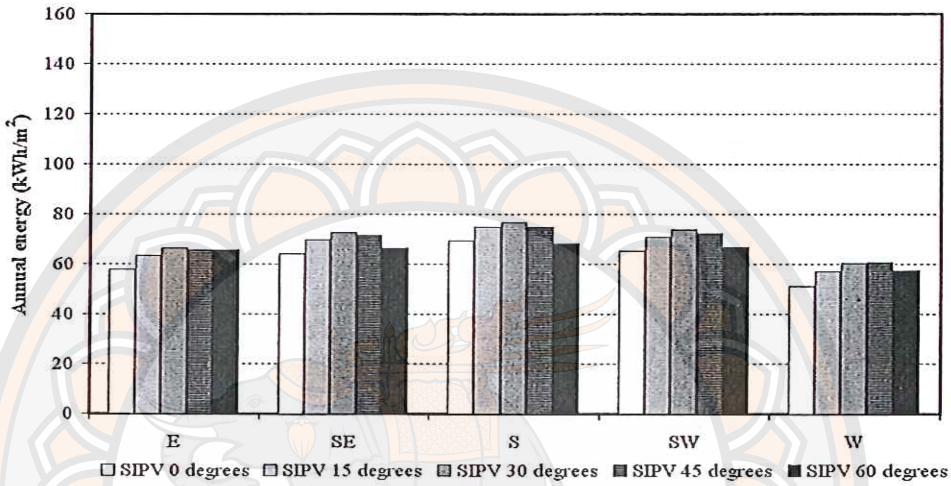

a-Si technology

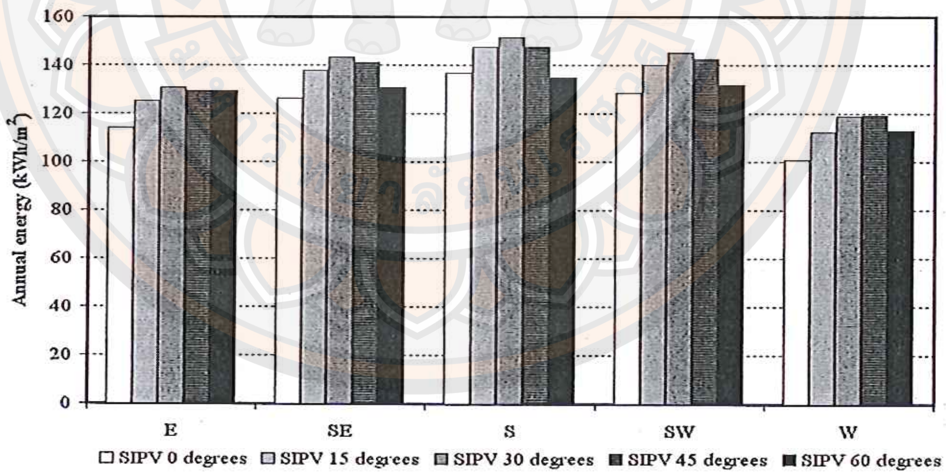

p-Si technology

Figure 181 The annual energy from SIPV array

Figure 181 shows the amount of energy generated from SIPV of amorphous silicon technology, a-Si and polycrystalline silicon technology in each direction and tilt angle of module.

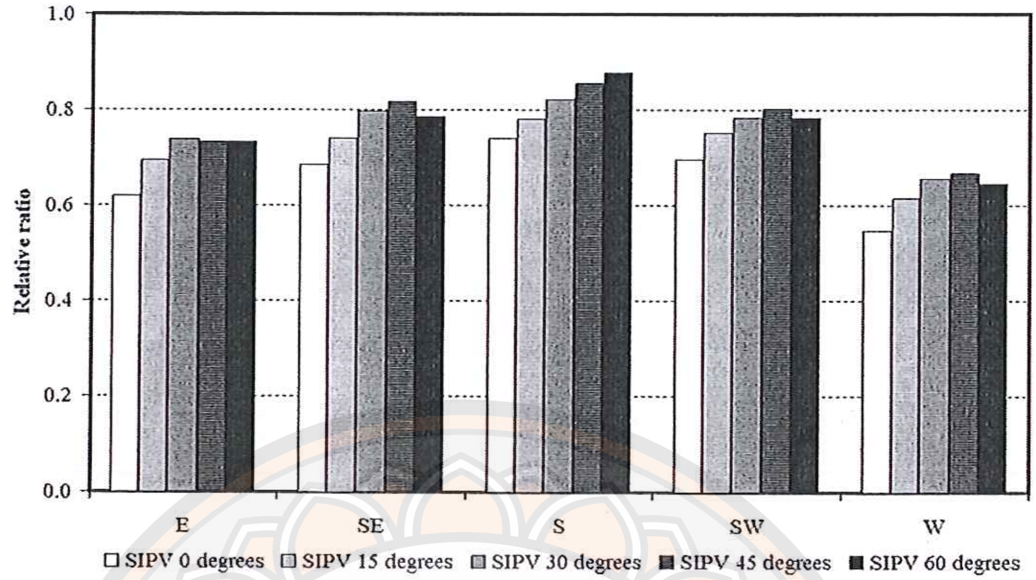

a-Si technology

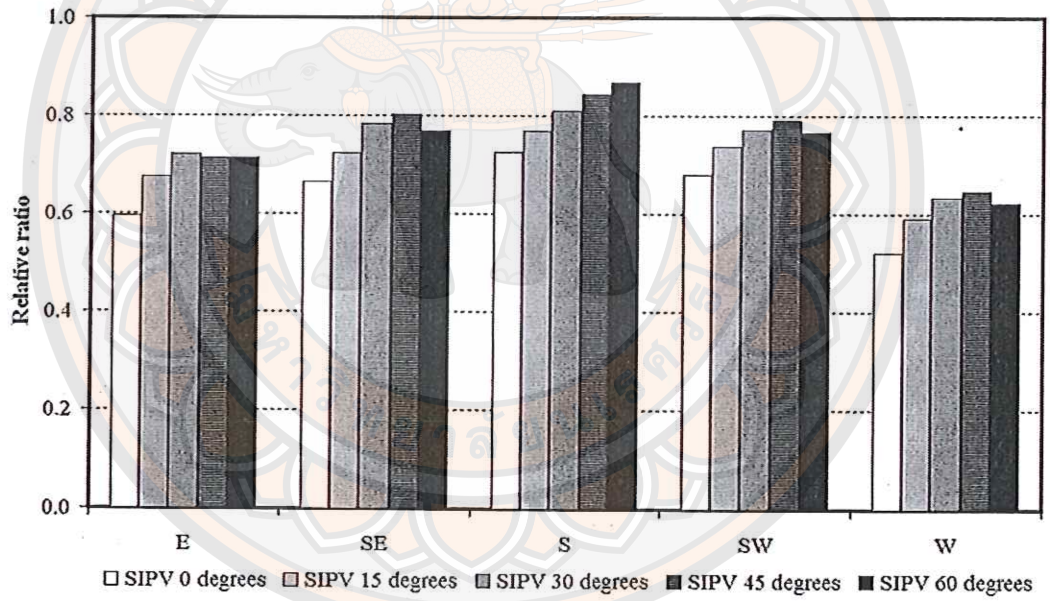

p-Si technology

Figure 182 The annual array yields ratio of SIPV to general installation

Figure 182 shows ratio of comparing the amount of energy produced by SIPV of amorphous silicon technology, a-Si and polycrystalline silicon technology and general installation in each direction and tilt angle of module.

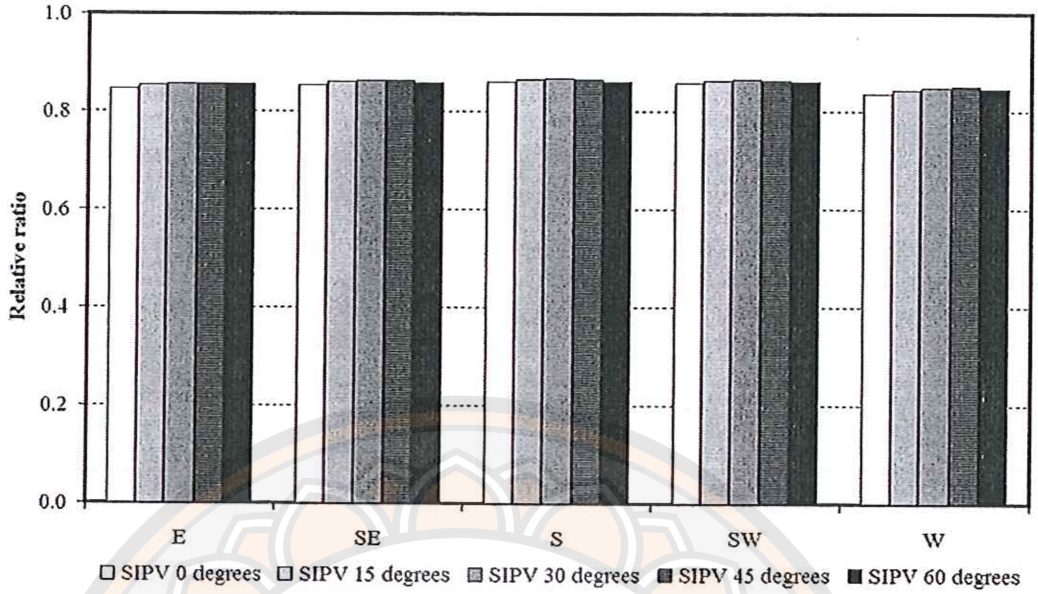

a-Si technology

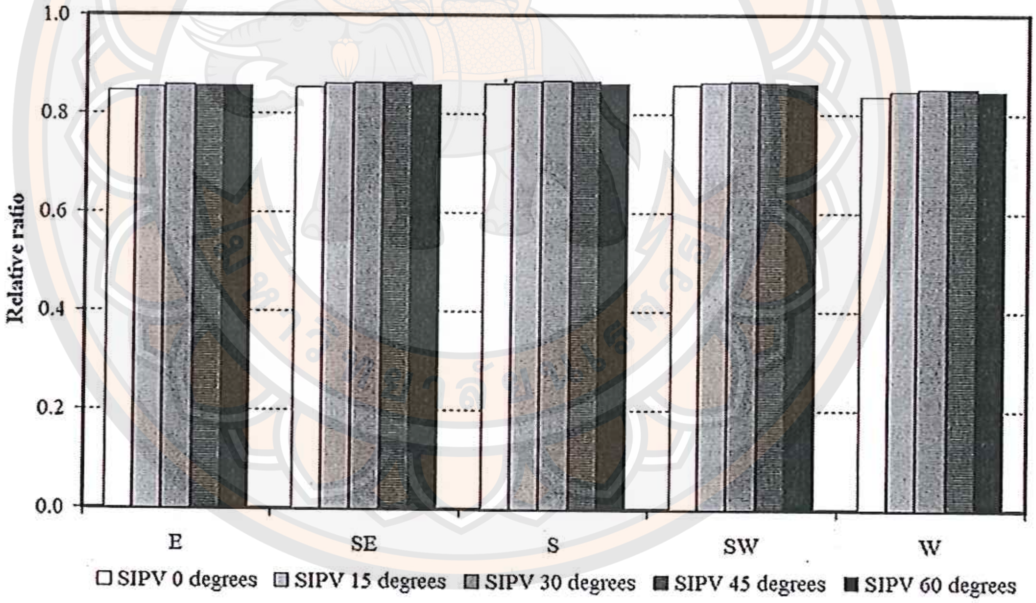

p-Si technology

Figure 183 The annual yields ratio of inverter to array conversion

Figure 183 shows ratio of the decrease because of converting electric current from inverter of amorphous silicon technology, a-Si and polycrystalline silicon technology in each direction and tilt angle of module. It is found that the ratio of both technologies is similar.

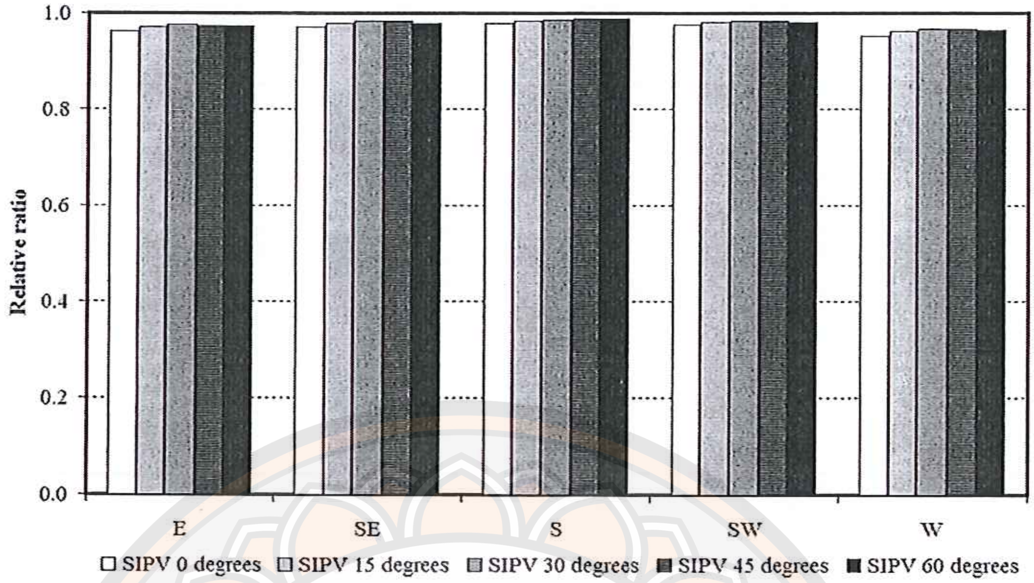

a-Si technology

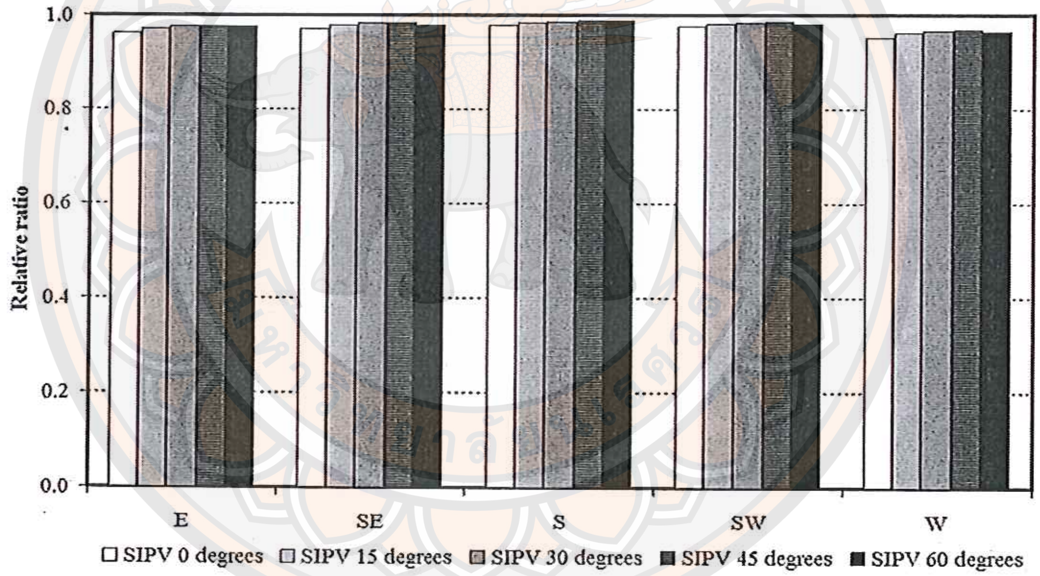

p-Si technology

Figure 184 The annual inverter yields ratio of SIPV to general installation

Figure 184 is to compare ratio of the decrease because of electric current conversion from inverter between SIPV installation and general installation of amorphous silicon technology, a-Si and polycrystalline silicon technology in each direction and tilt angle of module.

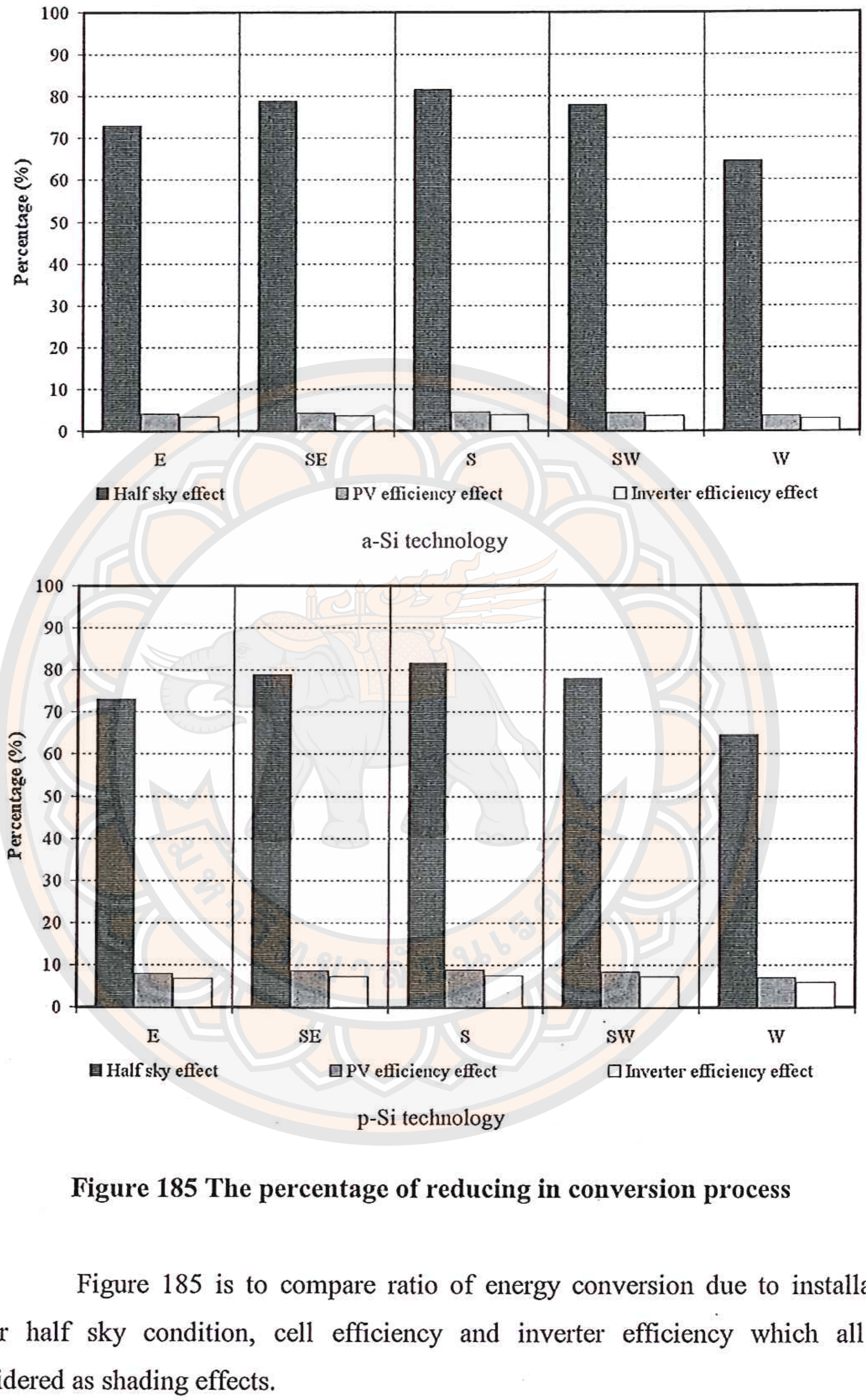

Figure 185 The percentage of reducing in conversion process

Figure 185 is to compare ratio of energy conversion due to installation under half sky condition, cell efficiency and inverter efficiency which all are considered as shading effects.

Table 27 The percentage of energy conversion

Direction	Percentage of energy conversion				
	Half sky	Technology		Inverter	
		a-Si	p-Si	a-Si	p-Si
E	27.05	94.52	89.17	14.36	14.33
SE	20.99	94.55	89.22	13.75	13.74
S	18.43	94.56	89.26	13.34	13.32
SW	22.07	94.56	89.27	13.59	13.55
W	35.27	94.52	89.21	15.08	15.02

3. Energy saving in lighting system

One of benefits gained from shading function by using daylight within buildings to replace light from light bulbs. To estimate electric energy, Eq. 112 is used to estimate illuminance level on working plane with the minimum of 300 Lux as shown in Figure 186.

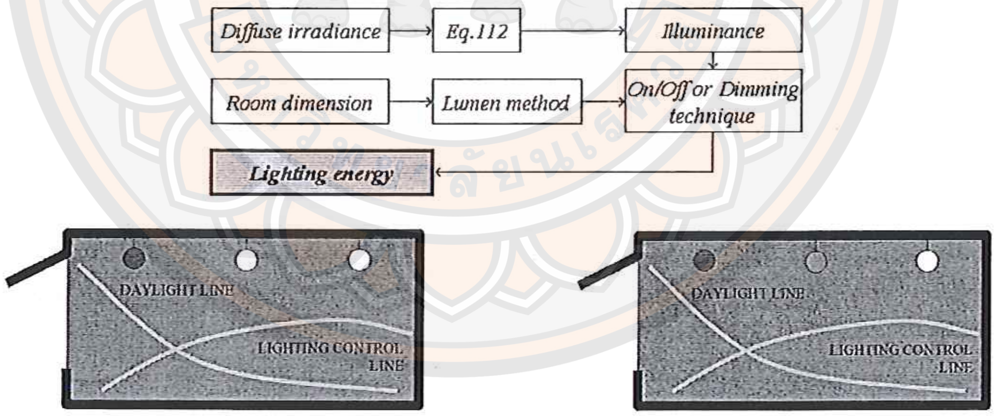

On/Off technique　　　　Dimming technique

Figure 186 The process of lighting system energy calculation

When there is not enough daylight in any position of room, energy from light bulbs is considered as options with the use of control techniques as follows:

1. On/off technique
2. Dimming technique

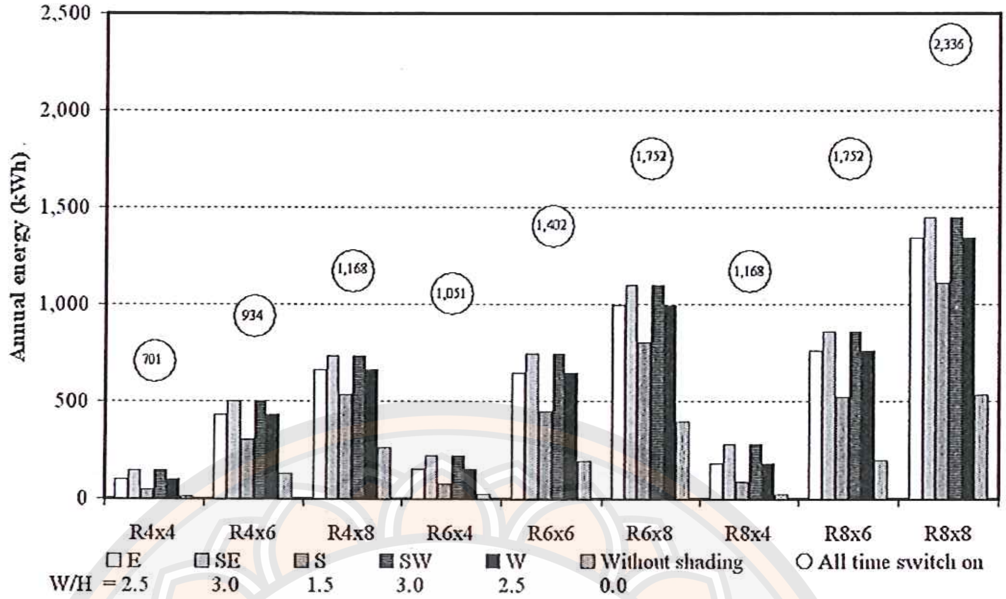

On/Off technique

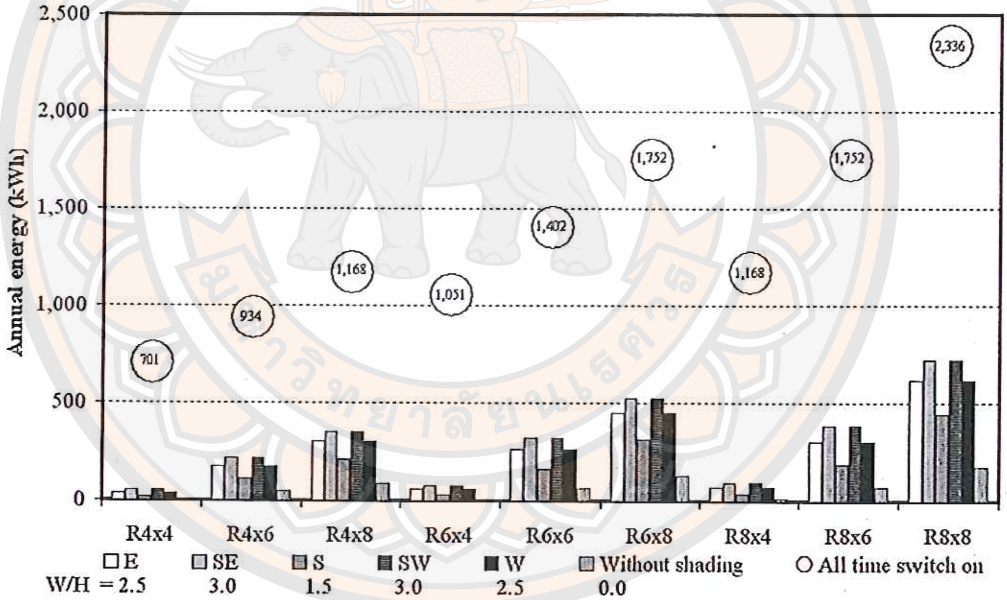

Dimming technique

Figure 187 The using energies of lighting system with lighting controls

Figure 187 shows the comparison of energy saving by using on/off technique and dimming technique in electric energy control. It is found that dimming technique can save more energy; especially without shading devices will save the most and shading devices being installed in the south will save the second most.

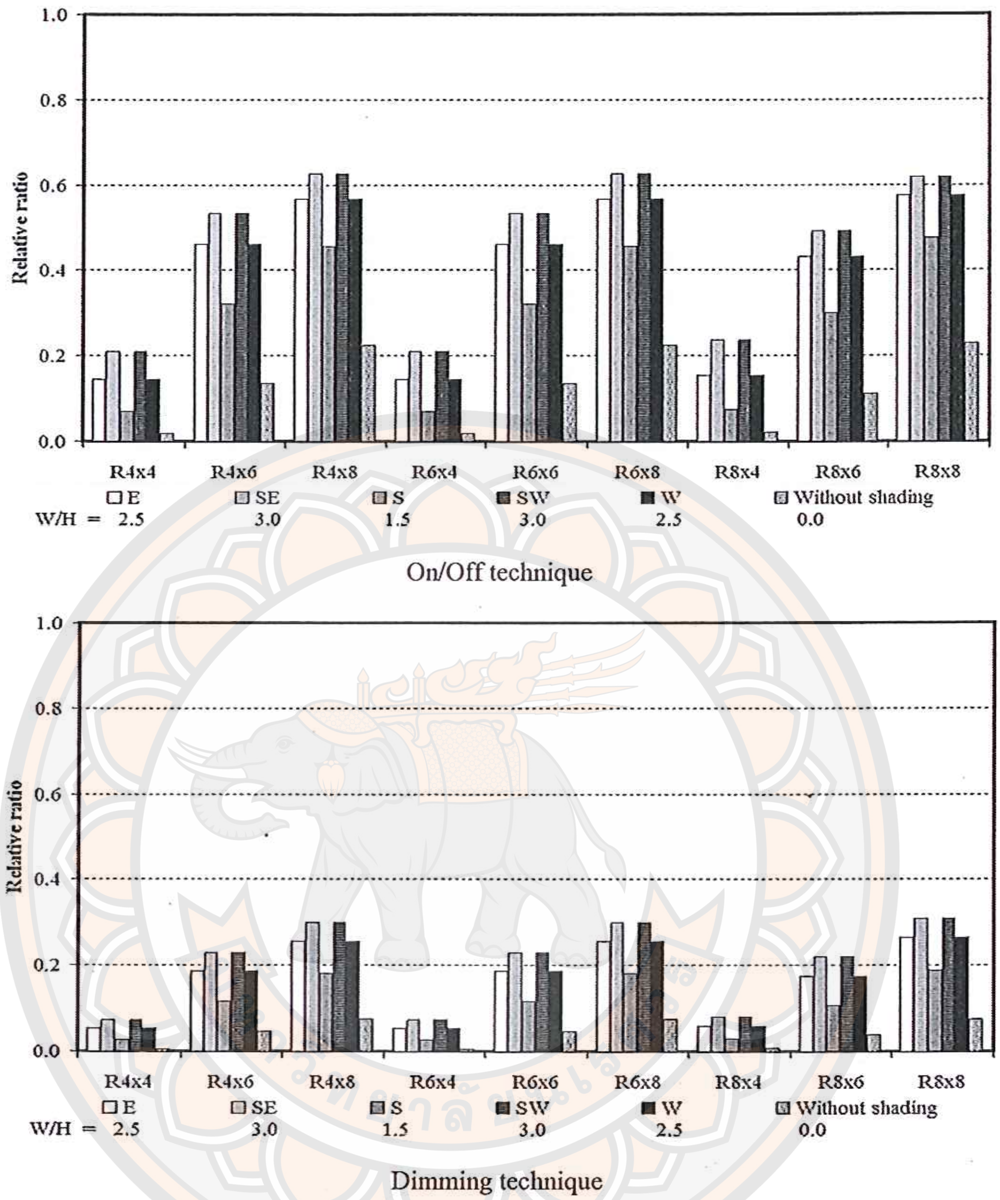

Figure 188 The using energies ratio of control technique to switch on all time

Figure 188 shows ratio of the use of electricity in lighting system. It is found that room with depth of 4.0 m. 6.0 m. and 8.0 m. can save electricity respectively from most to least using both control techniques due to receiving more daylight from position near window.

4. Cooling load reduction of air conditioning system

Air conditioning system is another system with the use of energy depending on cooling load. In the process of calculating cooling load gained from solar irradiance, outside temperature coming through glass of window and heat from light bulbs, Eq. 109 is used with ASHRAE's equation under the condition of COP at 3.22 in electric energy use to make a cooling as shown in Figure 189.

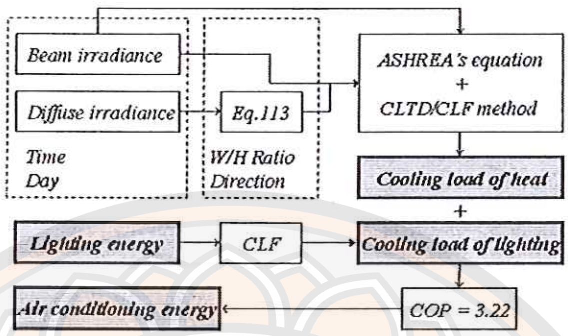

Figure 189 The process of air conditioning system energy calculation

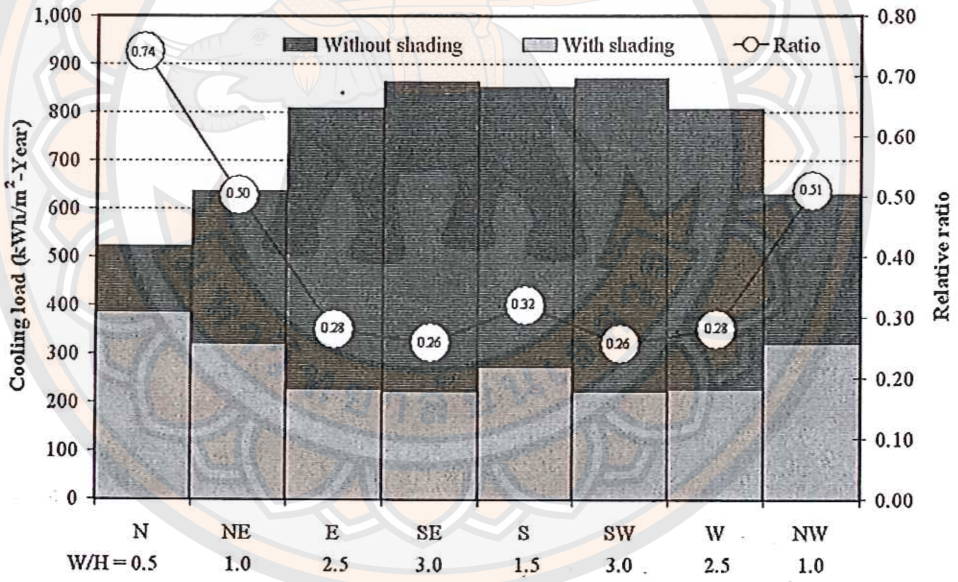

Figure 190 The cooling load ratio of the design with shading to without shading

Figure 190 shows the decrease of cooling load due to the sizes of shading devices determined by W/H ratio. As for direction calculated to prevent direct solar irradiance for the whole considered period of time, it is found that in the South East, South West, East, West, South, North East, North West and North provide the values from the least to the most respectively. The case of being installed in the South provides the value different from the best case only 0.06.

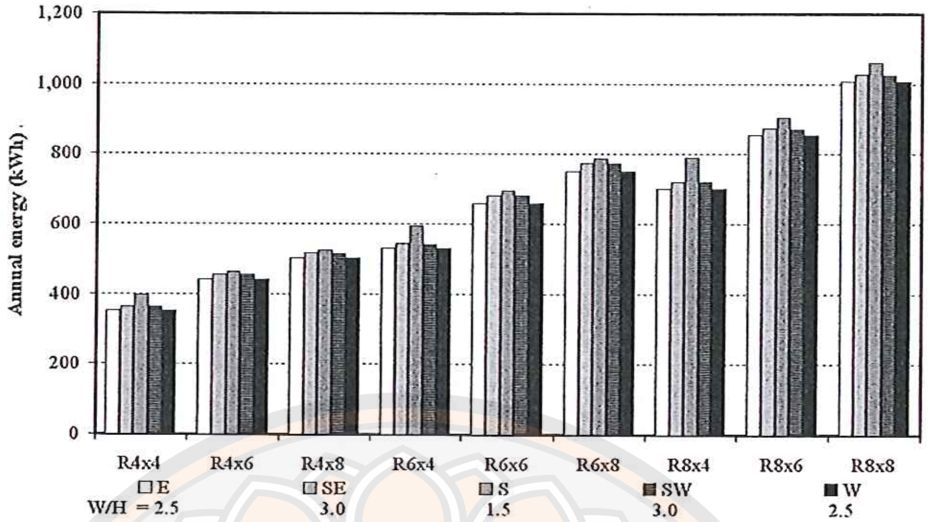

On/Off technique

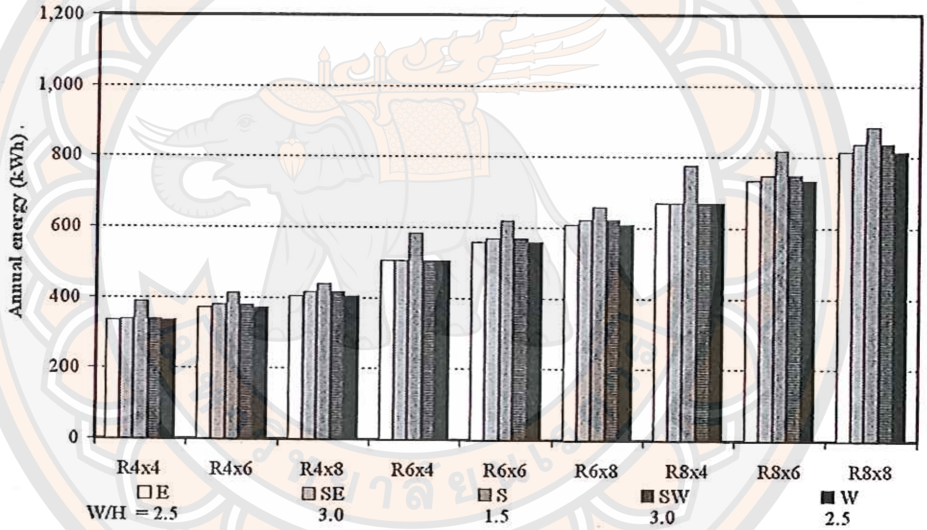

Dimming technique

Figure 191 The using energies of air conditioning system with lighting controls

Figure 191 shows annual total energy use of air conditioning system separated by room size and direction. It is found that the use is changed according to room sizes due to the glass sizes and the number of light bulbs.

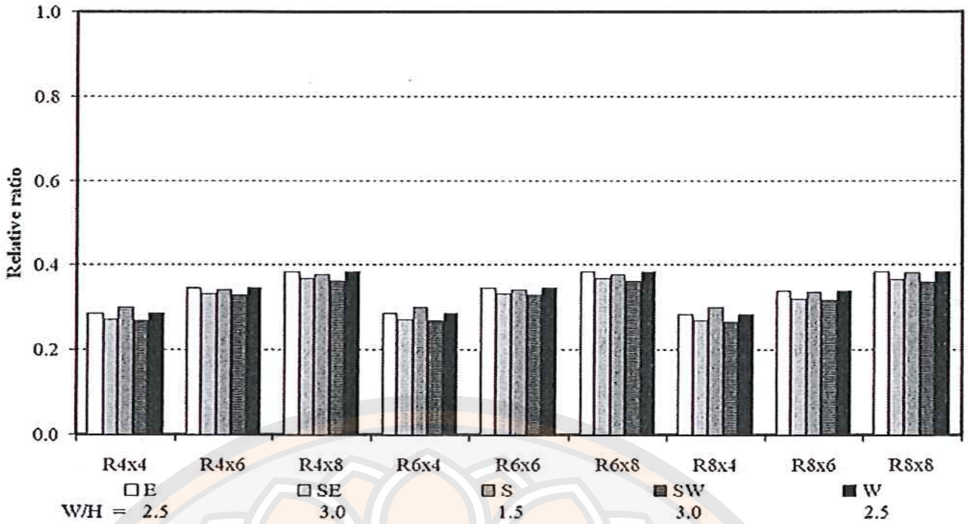

On/Off technique

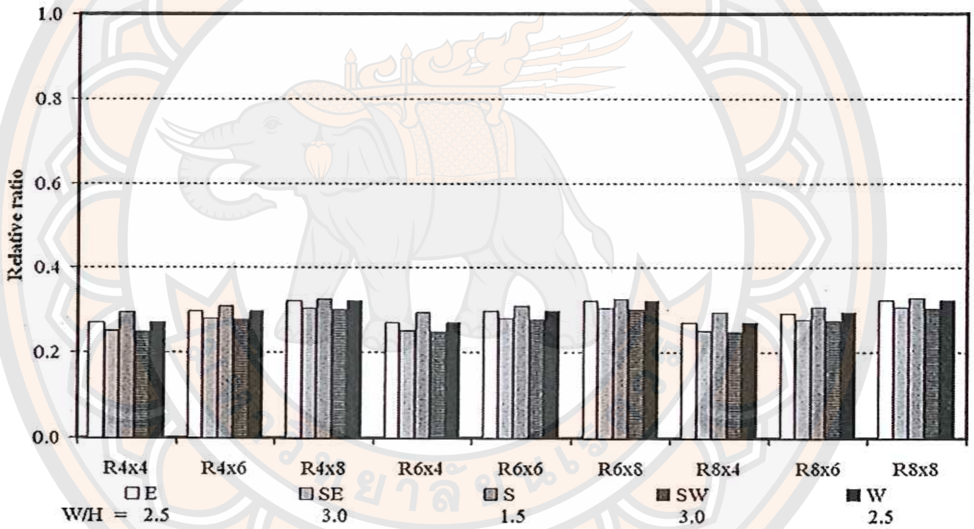

Dimming technique

Figure 192 The reducing ratio of the design with shading to without shading

Figure 192 shows decreasing ratio of energy use when compared to the case of without shading devices and with light control system. It is found that room with depth of 4.0 m. 6.0 m. and 8.0 m. can save electricity respectively from most to least using both control techniques like the case of lighting system.

5. Tracking technique

In the case of system being installed in the East and West with the widest space of solar altitude as shown in Figure 193 of more than 50 degrees throughout the year and quite stable degree throughout the day as shown in Figure 193, energy generation of SIPV tracking system is estimated when being installed in the mentioned directions.

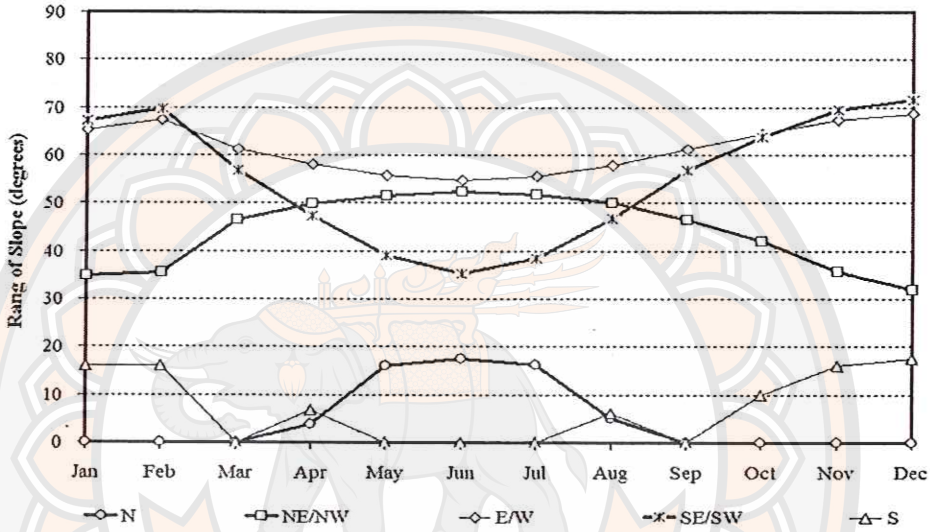

The comparison of the angle every direction

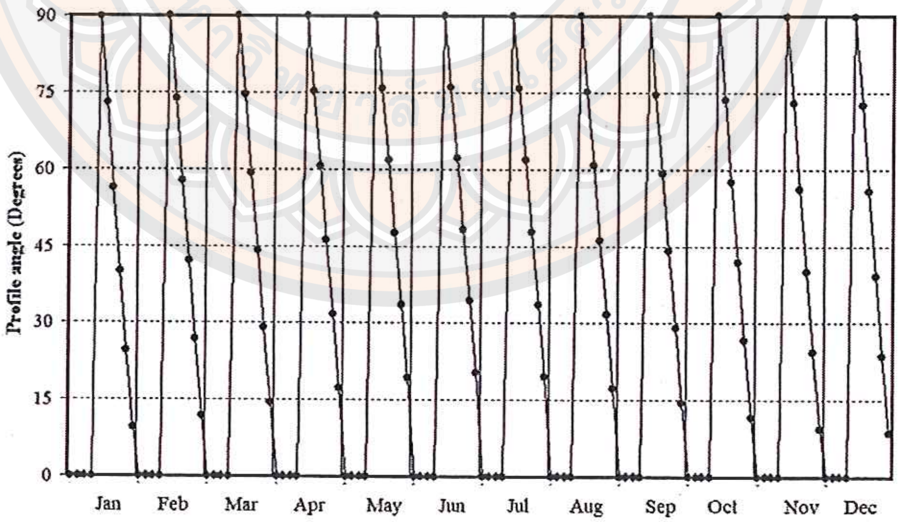

The profile angle of West direction

Figure 193 The moveable effect of the sun angle every month

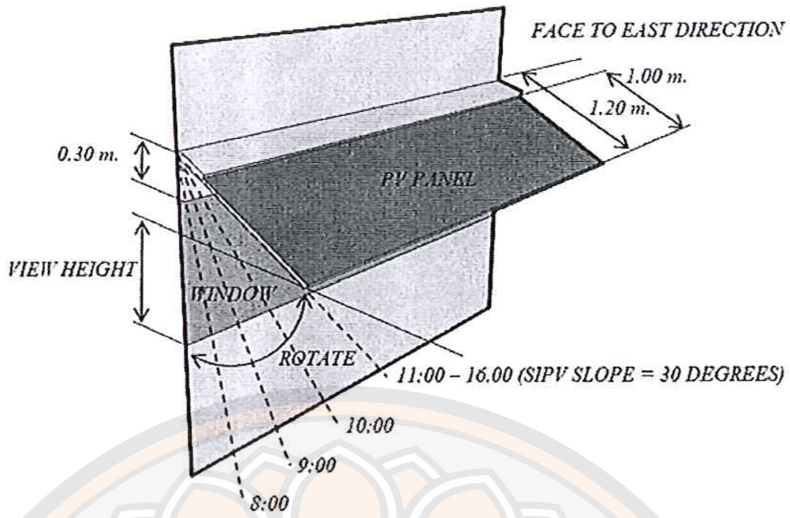

Figure 194 The shading design guideline

Table 28 The estimation of SIPV tracking design

Solar Time	8.00	9.00	10.00	11.00	12.00	13.00	14.00	15.00	16.00	
SIPV Slope	75	60	45	30	30	30	30	30	30	
W/H ratio	2.2	2.3	1.89	1.49	1.49	1.49	1.49	1.49	1.49	
View area						(%)				
Tracking	14	26	45	70	70	70	70	70	70	
Fixed	40	40	40	40	40	40	40	40	40	
Room dimension		R4x4	R4x6	R4x8	R6x4	R6x6	R6x8	R8x4	R8x6	R8x8
SIPV energy						kW-hr/m^2-Year				
Fixed		448	448	448	672	672	672	896	896	896
tracking		447	447	447	670	670	670	894	894	894
Lighting energy	All time	701	934	1168	1051	1402	1752	1168	1752	2336
	On/Off	58	325	559	88	487	838	112	583	1167
	Dimming	20	119	224	29	179	337	37	206	470
A/C energy	All time	557	619	680	835	928	1020	1052	1206	1360
	On/Off	387	458	519	581	687	779	773	898	1052
	Dimming	377	403	431	566	605	647	754	798	868

From the calculation result in Table 28 and installation example as shown in Figure 194 shows that the result of total energy generation throughout the year is not different when compared to fixed installation. However, there is an opportunity of more view opening. Therefore, it is not considered for design due to the need of maintenance and more complicated design with indifferent result.

6. Summary of the estimation part

From estimation, the points concluded are as follows:

6.1 p-Si technology is suitable for usability because it has a smaller area than a-Si technology for installation. It is designed to use the area of building envelope efficiently

6.2 The tilt angle of module should be between 0-45 degrees for beauty design. At 30 degrees is considered the best angle in energy generation

6.3 The suitable installing directions of SIPV include E, SE, S. SW. W. The best direction is in the South for energy generation

6.4 Suitable size of the room for energy saving should not be deep. The depth of the room at 4.00 m. can save energy the most

6.5 The best lighting system control technique is dimming technique

6.6 Fixed installation should be considered for SIPV installation because the maintenance is easier when compared to similar benefits gained

Optimization part

1. Optimization of shading design

The first objective of the study is to optimize shading in order to decrease heat gain and increase daylight of shading devices integrated photovoltaic system

1.1 Benefits gained from the comparison of energy usability

1.1.1 Reducing cooling load of air conditioning system

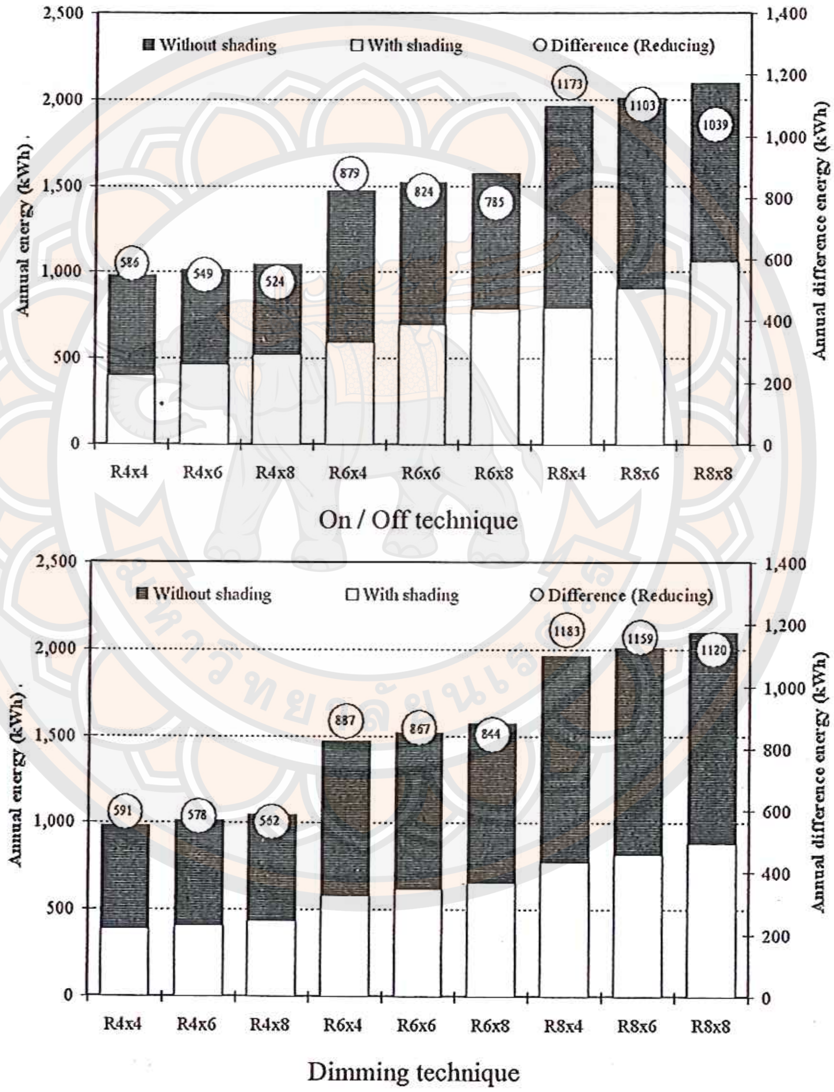

Figure 195 The annual of air condition system energy comparisons between the design with shading and without shading

Figure 195 shows the comparison of decreasing energy usability due to SIPV installed in the South. It is found that room with small depth can reduce the use of energy more when compared with the equal width of the room. It is because of the decrease in heat caused from light bulbs as a result from daylight used in both cases of light control techniques and with the same appearances when being installed in other directions

1.1.2 Saving energy of lighting system

Figure 196 shows the comparison of lighting energy saving results due to SIPV installed in the South. It is found that in the case of light control using on/off technique from room with wide format of 4.0 m. and 6.0 m. Room with small depth can save more energy. In the case of room with large width but with more depth can save even more energy which shows the same appearances as the case of light control technique using dimming technique

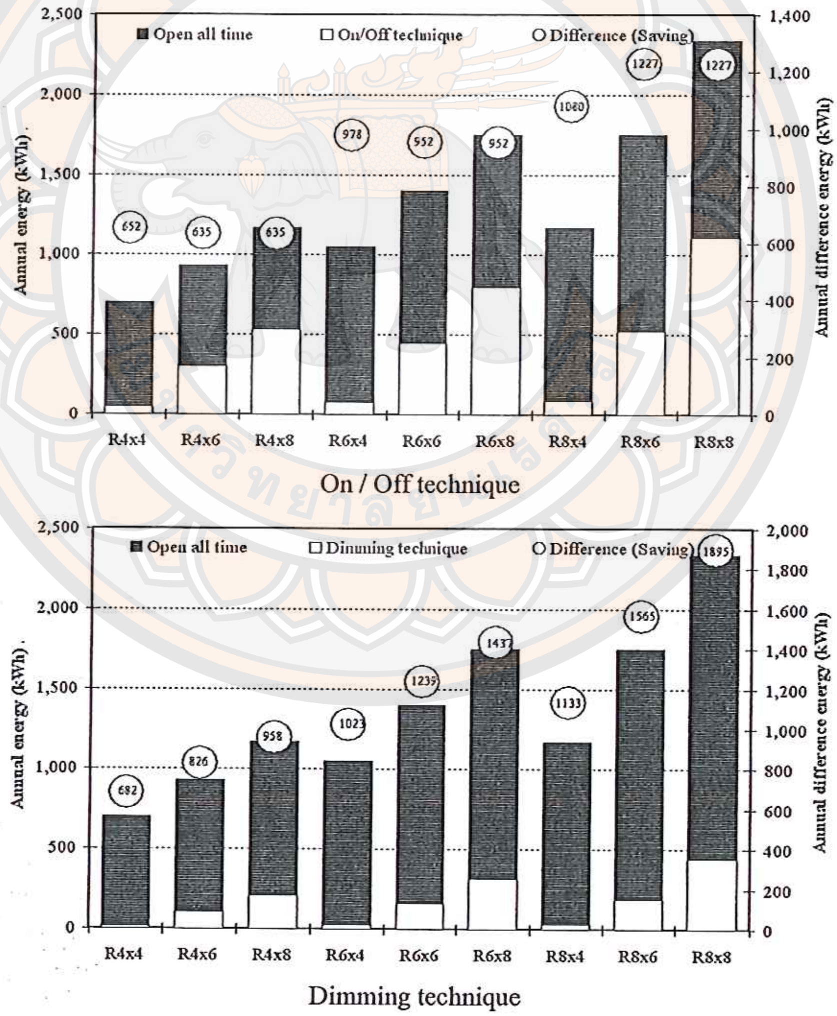

Figure 196 The annual of lighting system energy comparisons of the lighting control techniques

1.1.3 Producing energy using photovoltaic system

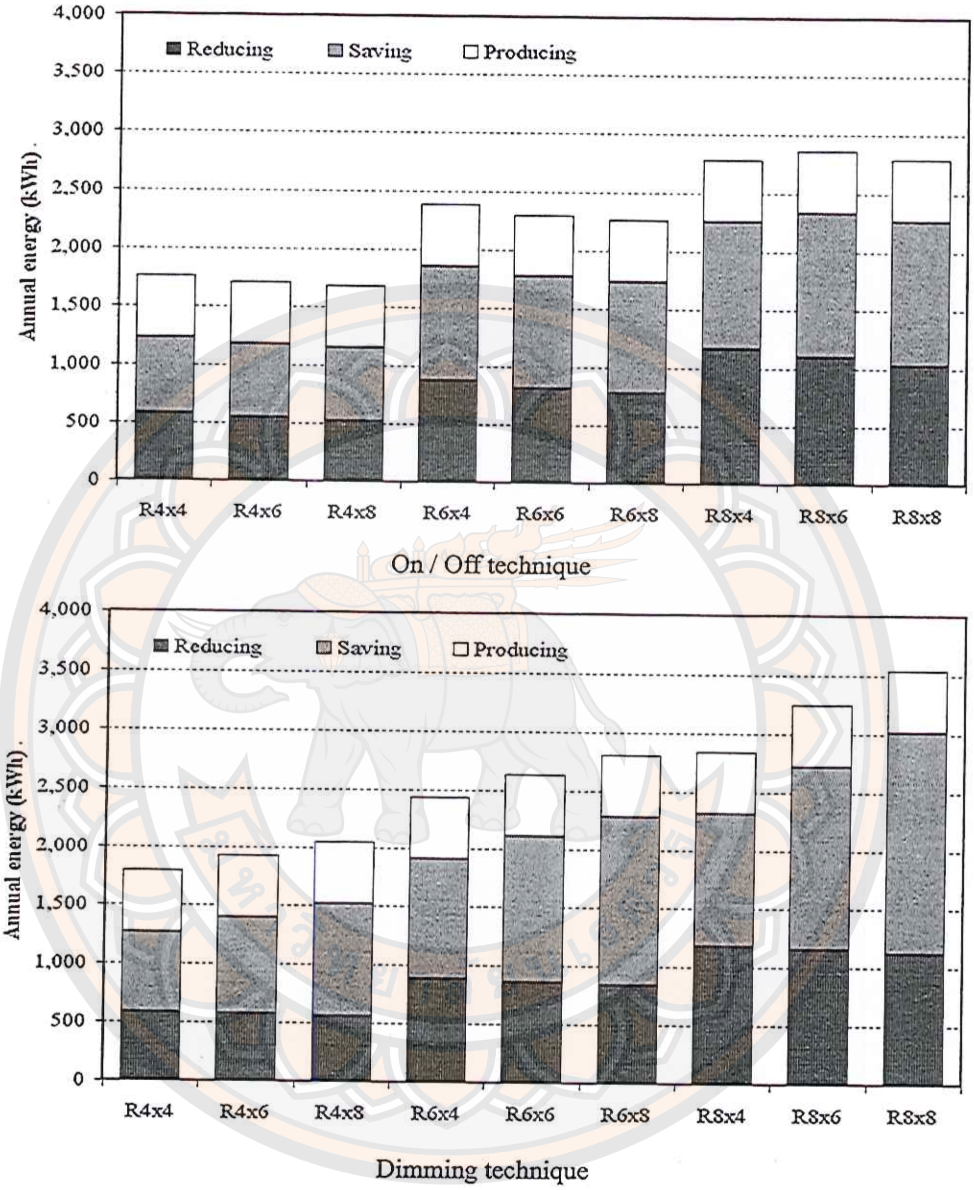

Figure 197 The annual of SIPV system of slope 30 degrees comparisons with the reducing and saving energies

Figure 197 shows the comparison of electrical energy production results due to the use of SIPV installed in the south with tilt angle of 30 degrees. It is found that the use of on/off technique provides less total benefit ratio gained from energy production than the use of dimming technique.

1.2 Comparison of installing directions

Figure 198 show the best case of installation with tilt angle of 30 degree. It is found that the highest benefit per using area is the case of room with small depth using both cases of light control techniques. However, installation using on/off technique turning towards the South receives the highest benefit. As for dimming technique in room with small depth of 4.0 m., the best option of installation must be in the South East and South West. The installation must be in the South for room with more depth for the best result

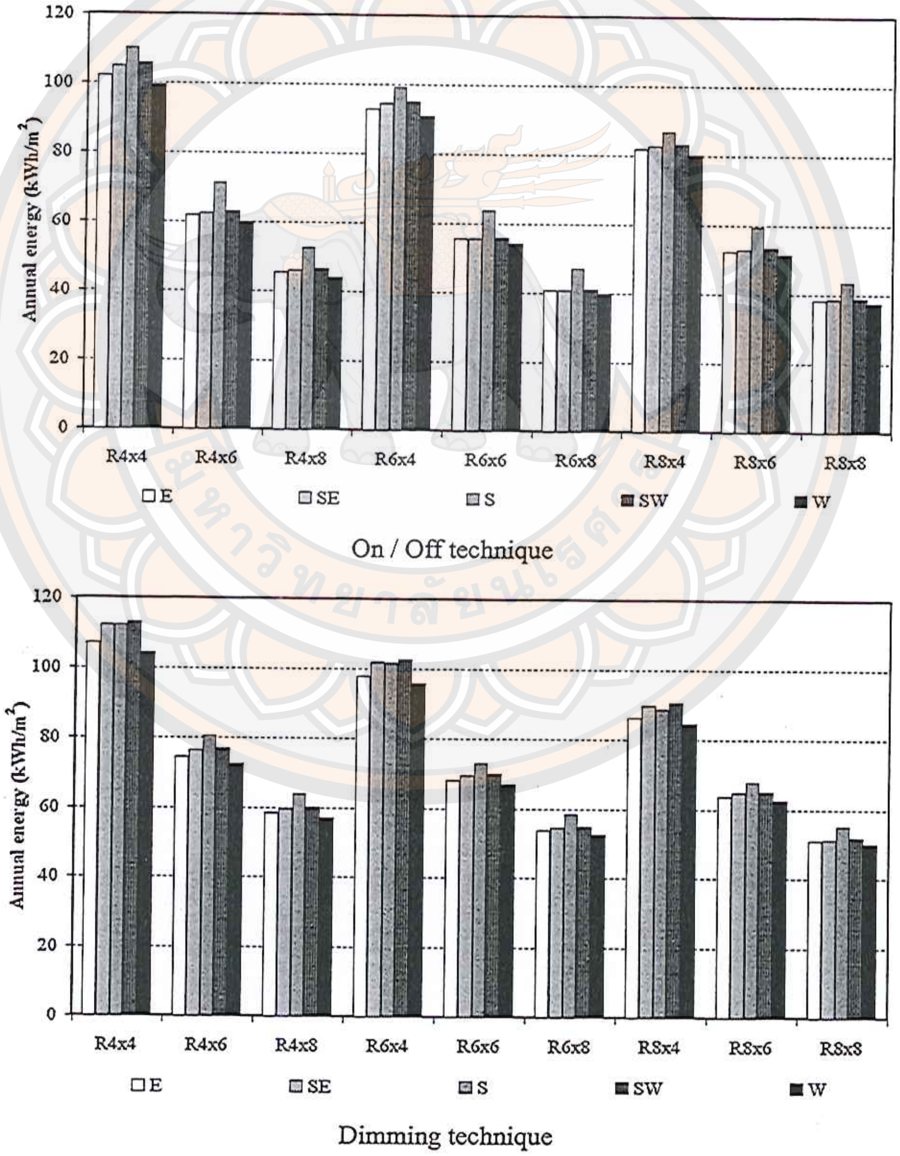

Figure 198 The annual energy saving of comparisons SIPV slope 30 degrees

1.3 The comparison to replace the use of energy

Figure 199 shows the comparison of the factors of SIPV design providing benefits in each part of the use of energy from air conditioning system and lighting system and part of energy production to replace the use of energy causing the decrease in total energy. It is found that for the on/off technique, the best ways to use the benefit from renewable energy production are the system being installed in the South and system being used in room with small depth (4.0 m.)

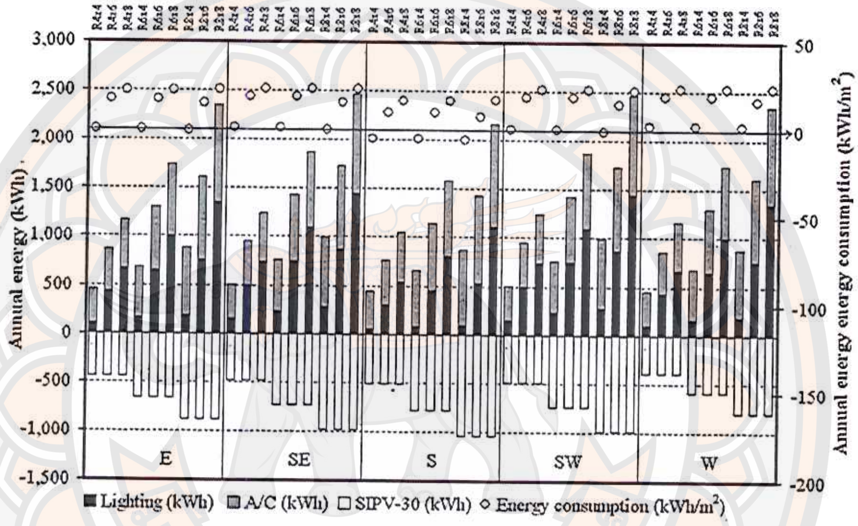

On/Off technique

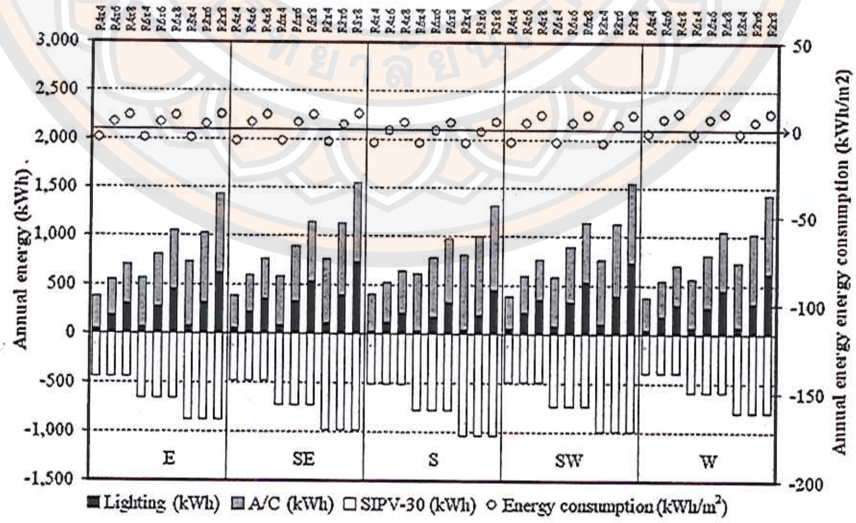

Dimming technique

Figure 199 The energy consumption comparisons of air conditioning system, lighting system and SIPV system

In contrast to dimming technique, the installation can be in any direction because ratio of benefit occurred in the part of air conditioning and lighting systems is more than benefits gained from energy production system. However, in order to make the best case, room with small depth (4.0 m.) is considered. As for the case of being energy producing tools, the suitable installing direction is in the South for the most of energy production

1.4 Visual comfort

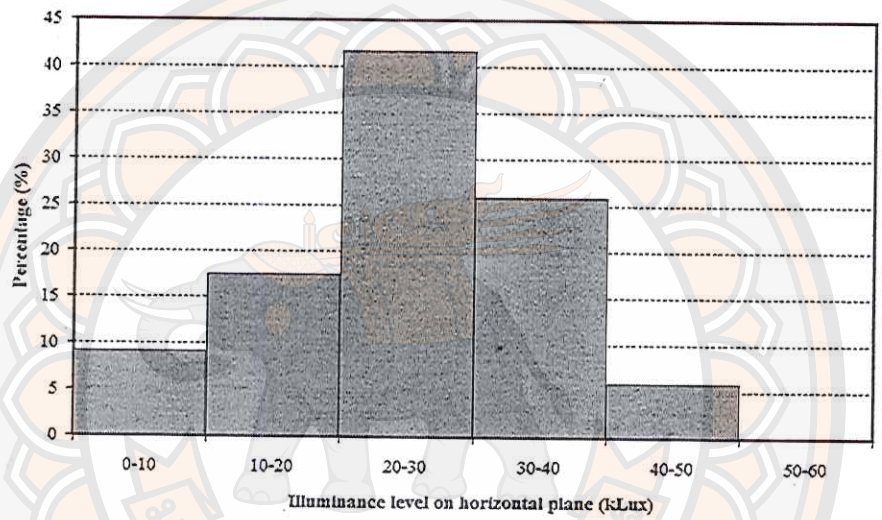

Figure 200 The percentage of illumminance level on horizontal plane

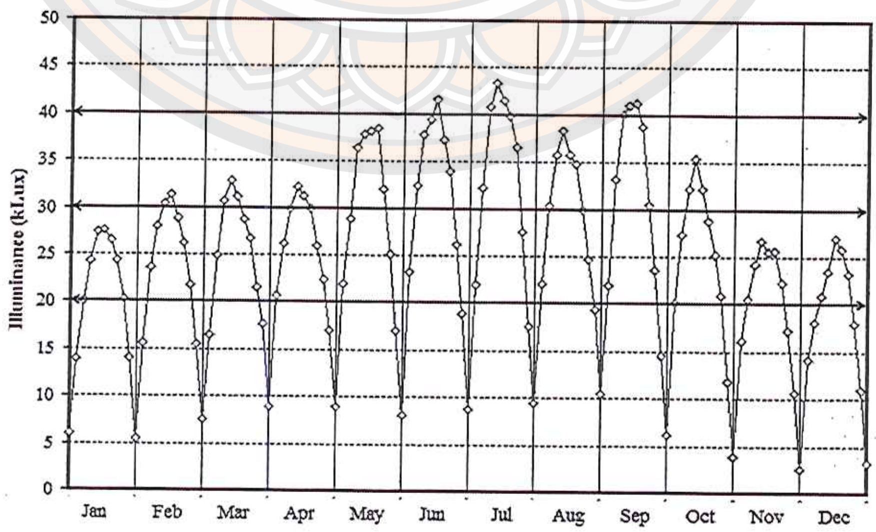

Figure 201 The monthly average of illumminance level on horizontal plane

In order to create proper usability corresponding to window function, there must be a consideration of glare conditions which is a qualitative measurement. In Figure 200, it is found that mostly illuminance level on horizontal plane of sky at 20-30 klux is about 40% and at 20-40 klux is about 65% as shown in Figure 200. Illuminance level at 30 klux is the highest average found almost throughout a year as shown in Figure 201. Besides, illuminance level at 50 klux is the highest value for this consideration.

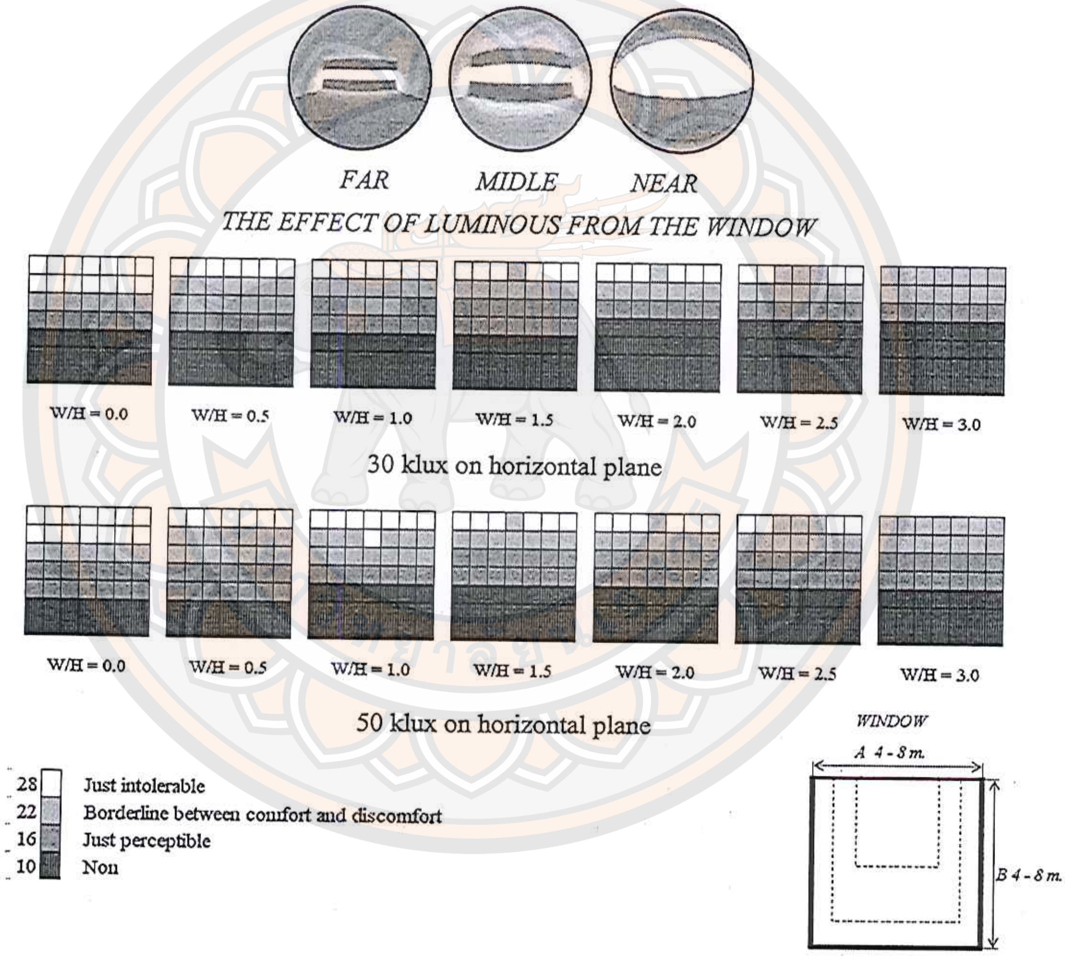

Figure 202 The DGI planning every W/H ratio

Figure 197 shows DGI in each area of room turning towards window. It is found that area nearby the window is not proper in every case except the case of shading devices with W/H ratio equivalent to 2.5 in room with width of 4.0 m. and the case of shading devices with W/H ratio equivalent to 3.0.

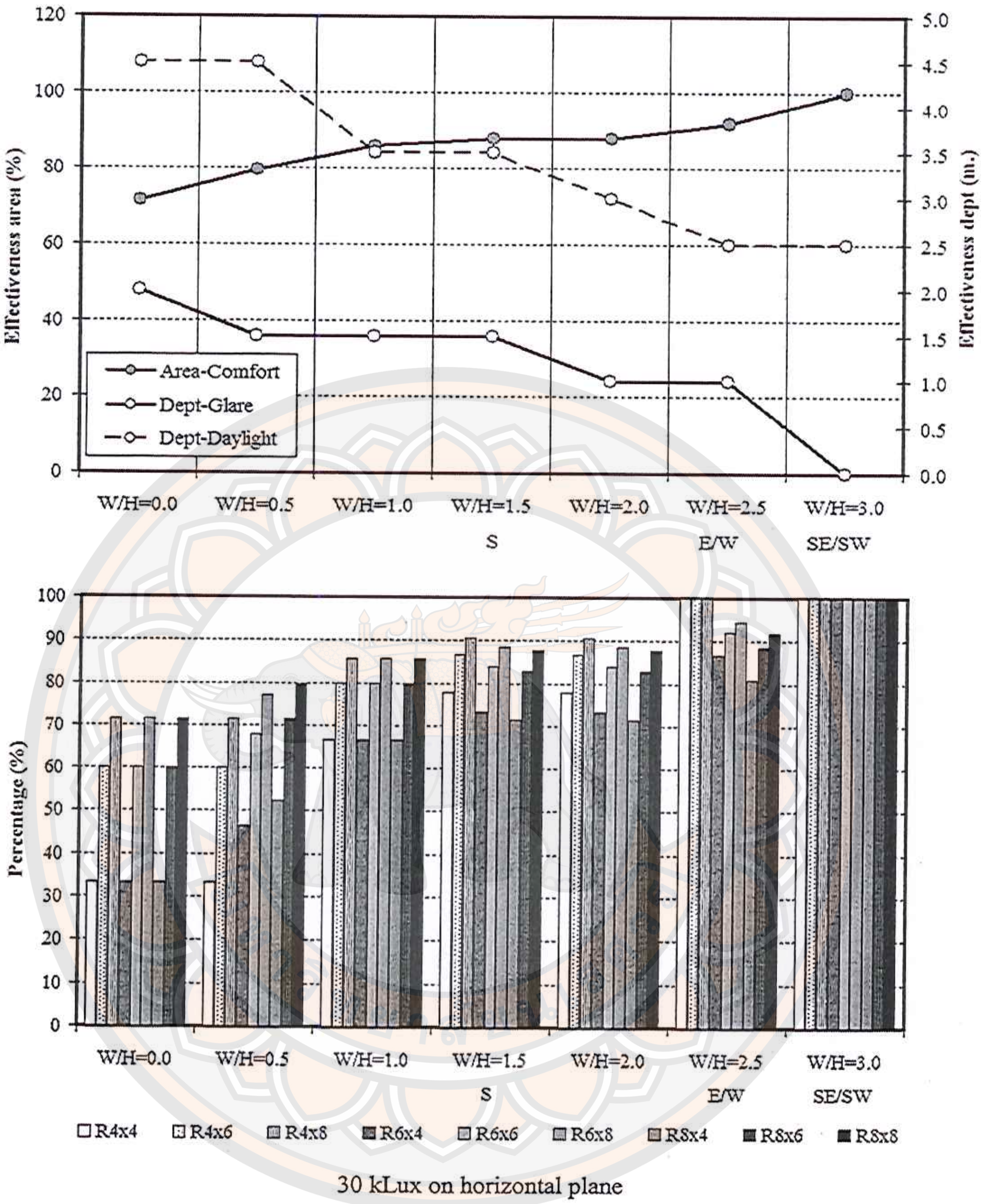

Figure 203 The performance of visual comfortable every W/H ratio from 30 klux

Figure 203 shows the comparison of benefits of daylight and the area usability in the case of illuminance level outside is at 30 klux. It is found that the more the shading devices has W/H ratio, the less of the area usability because of glare is. In the same way, the benefit from daylight is also less. However, shading devices with W/H ratio = 1.5 is installed in the south is considered the most suitable

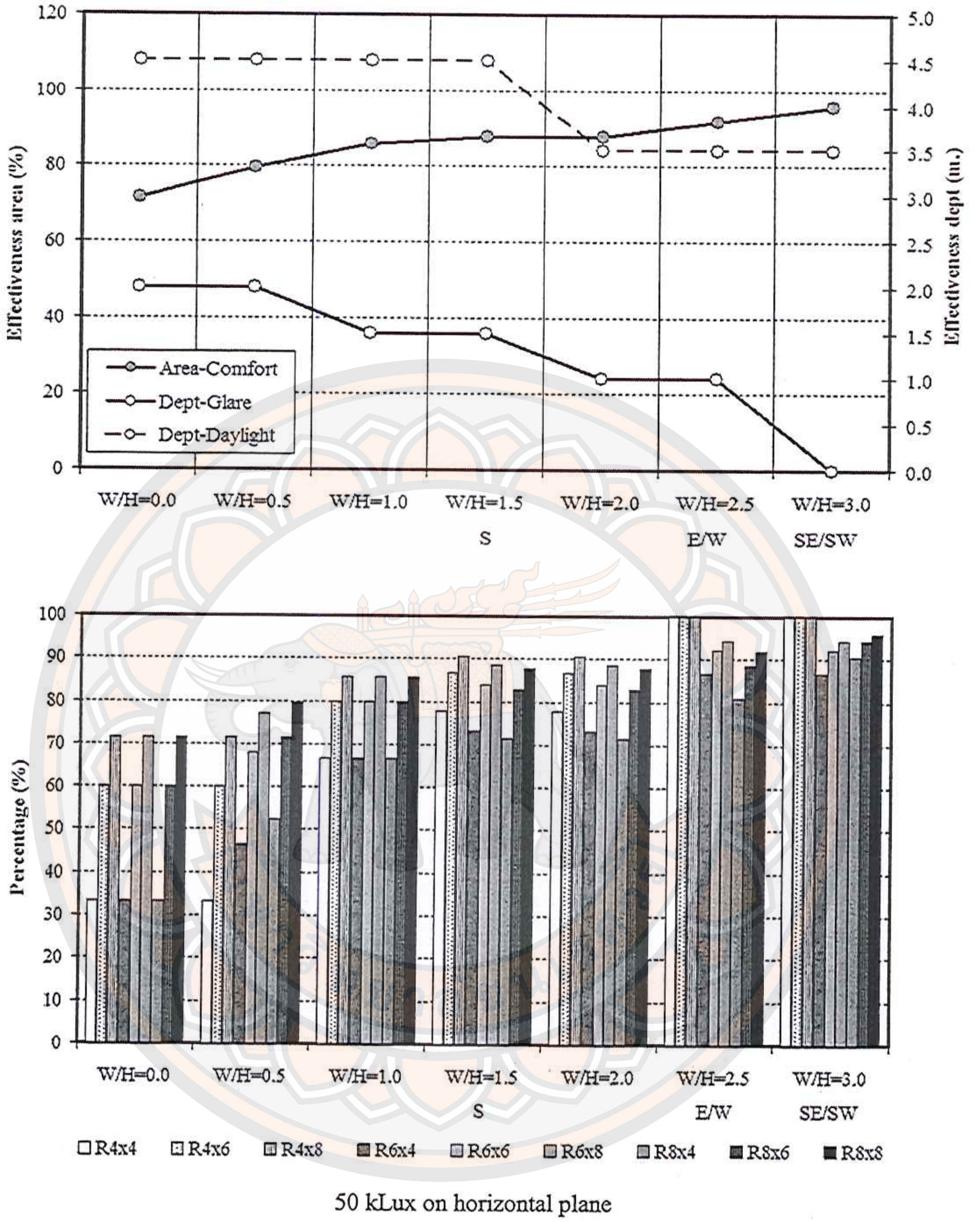

Figure 204 The performance of visual comfortable every W/H ratio from 50 klux

Figure 204 shows the comparison of benefits of daylight and the area usability in the case of illuminance level outside is at 50 klux. It is found that the more the shading devices has W/H ratio, the less of the area usability because of glare is. In the same way, the benefit from daylight is also less. However, shading devices with W/H ratio = 1.5 is installed in the south is considered the most suitable as well

2. Optimization of economical impact

Another objective is to optimize cost and benefits of shading devices integrated photovoltaic system.

2.1 SIPV (Cost of SIPV system)

2.1.1 Price of solar module

In present, world market has explored that the price of p-Si technology is determined at 23 THB/W_p – 40 THB/W_p. As for Thailand market, the price of p-Si technology is determined at 45 THB/W_p as shown in Figure 205 showing that devices with defect is not considered in searching for cost because of its low price

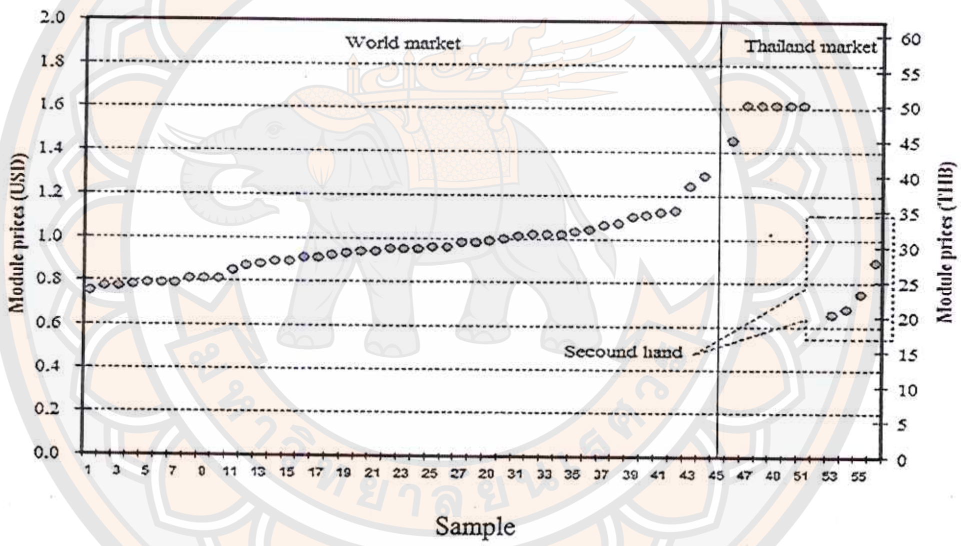

Figure 205 The price of PV modules

Source: Amornsolar [57]; Benefit media Co.ltd [60]; Blogger [61]; Chawna [64]; Ecobusinesslinks [66]; Kamsopha, Sarawut [71]; Mechashop [76]; MJ Shiao [79]; Solartech center limited partnership [84]; tarad.com [85]; Vera [92]

2.1.2 Total cost of SIPV

Cost of SIPV is different from PV with general installation. There are several reasons as follows:

1) The support of structure is different. The cost of land price is not included

2) Some parts of expenses are included with budget for building construction

To calculate cost of system, it is to consider from cost proportion of normal system by deducting some parts off and adding some parts in as shown in Figure 206 causing the decrease in cost of system. The price is separated into 2 levels according to market trend as shown in Table 29 for world market and Table 30 for domestic market

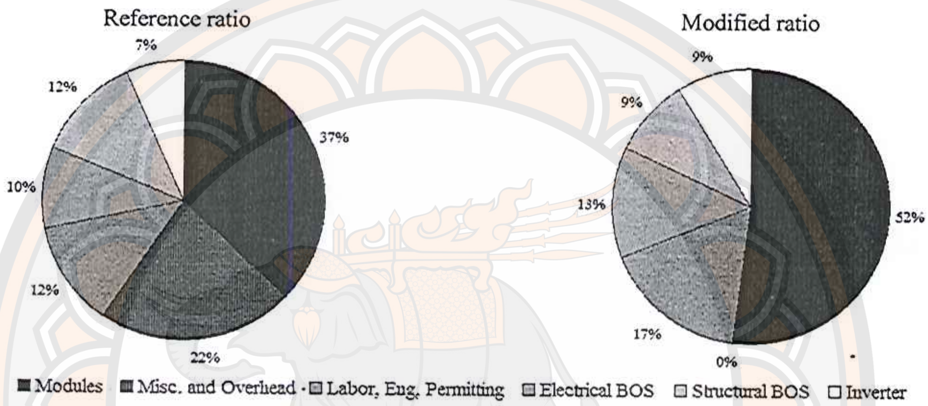

Figure 206 The ratio of system costs

Source: Martin LaMonica [75]; Michael S. Davies [77]; MJ Shiao [79]

Table 29 The SIPV system costs of the world market prices

	Bath	**%**	**Remark**
Modules	3,750	49	30 THB/ Wp and 125 W/m^2
Misc. and Overhead	-	-	Include with building investment
Labor, Eng, Permitting	1,731	16	Reference ratio
Electrical BOS	1,406	13	Reference ratio
Structural BOS	1,000	13	Aluminum cladding
Inverter	948	9	Reference ratio
Total	8,835	100	
Total adjustable prices	8,800		For minimum estimation
SIPV system prices	**70 THB/W$_p$**		

Table 30 The SIPV system costs of Thailand market prices

	Bath	%	Remark
Modules	5,625	52	45 THB/ Wp and 125 W/m^2
Misc. and Overhead	-	-	Include with building investment
Labor, Eng, Permitting	1,839	17	Reference ratio
Electrical BOS	1,406	13	Reference ratio
Structural BOS	1,000	9	Aluminum cladding
Inverter	948	9	Reference ratio
Total	10,818	100	
Total adjustable prices	10,800		For maximum estimation
SIPV system prices	**86 THB/W$_p$**		

2.2 Interest

From statistic 5 years back of the Bank of Thailand as shown in Figure 207 found that interest in the case of minimum retail rate: MRR was at about 8.0 to 8.5. For this study, constant at 8.0 was chosen because of its suitability in investment choice.

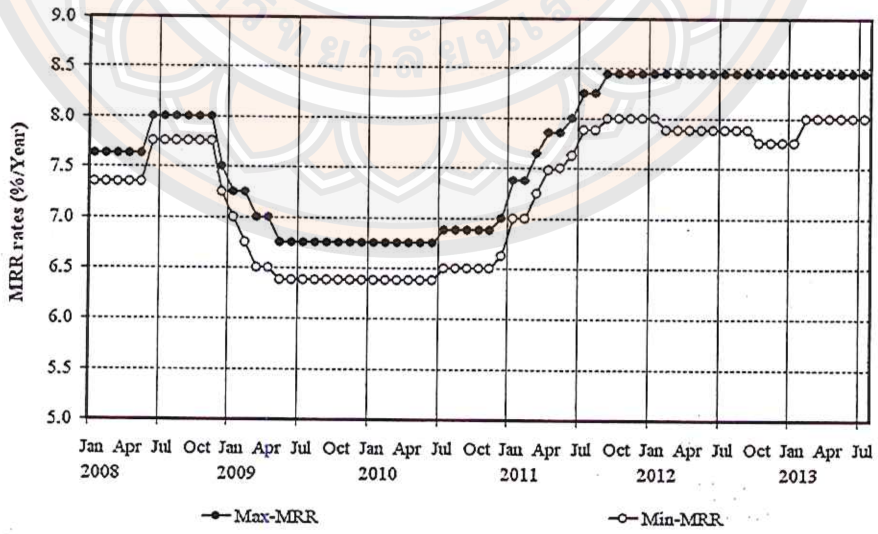

Figure 207 The minimum Retail Rates of Thailand banking

Source: Nitidow [80]

2.3 Price of electricity

Figure 207 shows price of electricity tends to be stable at 4 Baht with condition of Ft at 0.9255. The use of electricity was more than 1,000 units

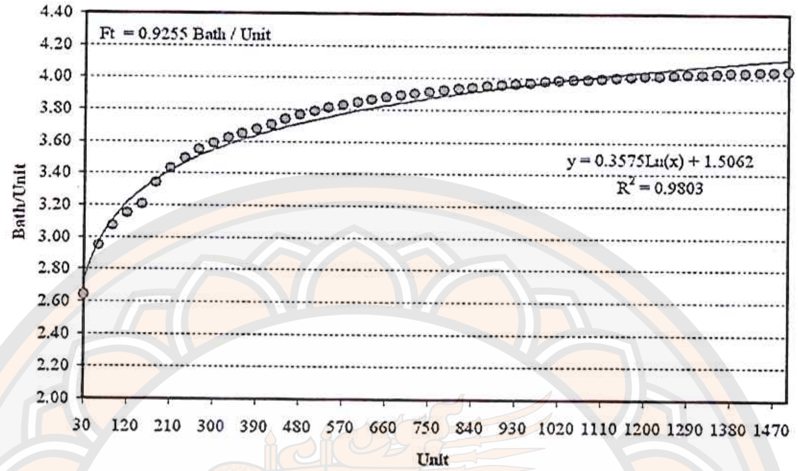

Figure 208 The electricity prices trend

2.4 SIPV degradation

Long term SIPV degradation is considered in Figure 209 as it is guaranteed by company in charge of module selling business mentioning SIPV degradation of not less than 80% in year 25th leading to the estimation of degradation of energy produced annually in a form of linear

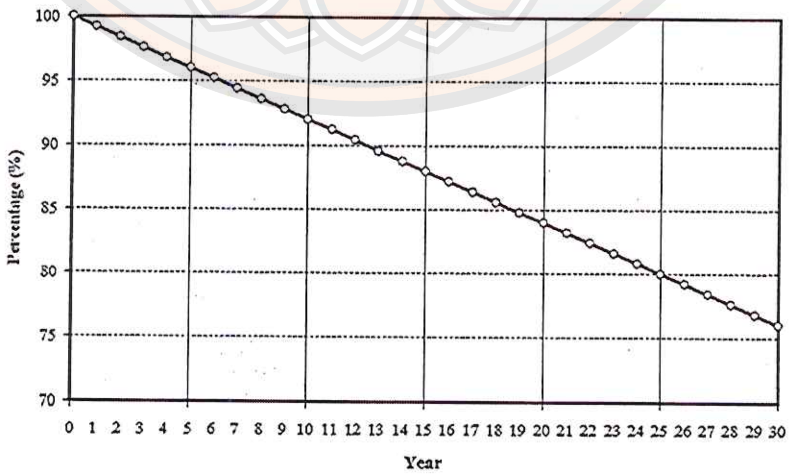

Figure 209 The degradation of PV efficiency

2.5 Benefits-Costs ratio (B/C)

The conditions of SIPV price at 70 THB/Wp and 86 THB/Wp are compared as 3 following options:

2.5.1 Only producing benefits

2.5.2 Producing and reducing benefits

2.5.3 Producing, reducing and saving benefits

From estimating B/C ratio, it is found that only producing benefit option is not suitable in the matter of investment due to the value of less than 1 in every case of design. Producing and reducing benefits option is suitable for investment in several cases of design. Besides, producing, reducing and saving benefits option is suitable for investment in all cases of design. However, the best case for investment of each option is shown in Table 31 which is SIPV system installation turning towards south with tilt angle of 30 degrees.

Table 31 the optimization of SIPV benefits

Direction	E	SE	S	SW	W
Shading form : W/H	2.50	3.00	1.50	3.00	2.50
Reducing heat ratio : HR	0.280	0.259	0.319	0.257	0.280
Saving lighting ratio : LR	0.26	0.30	0.18	0.30	0.26
Producing ratio	4 (0.85)	3 (0.94)	1 (1.00)	2 (0.96)	5 (0.77)
Reducing ratio	4 (0.92)	2 (0.99)	3 (0.94)	1 (1.00)	4 (0.92)
Saving ratio	2 (0.91)	3 (0.86)	1 (1.00)	3 (0.86)	2 (0.91)

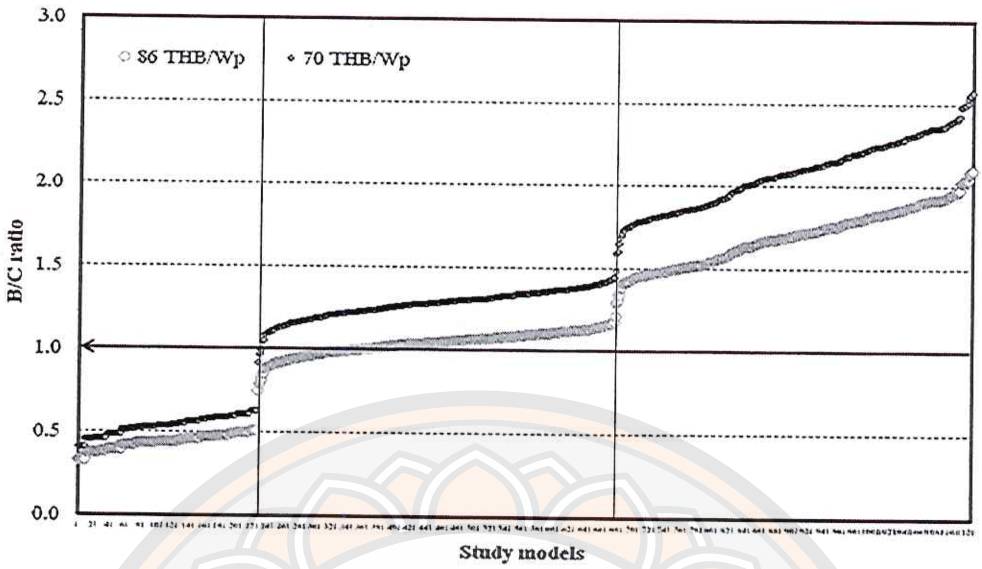

Figure 210 The B/C ratio comparison between 70 and 86 THB/Wp

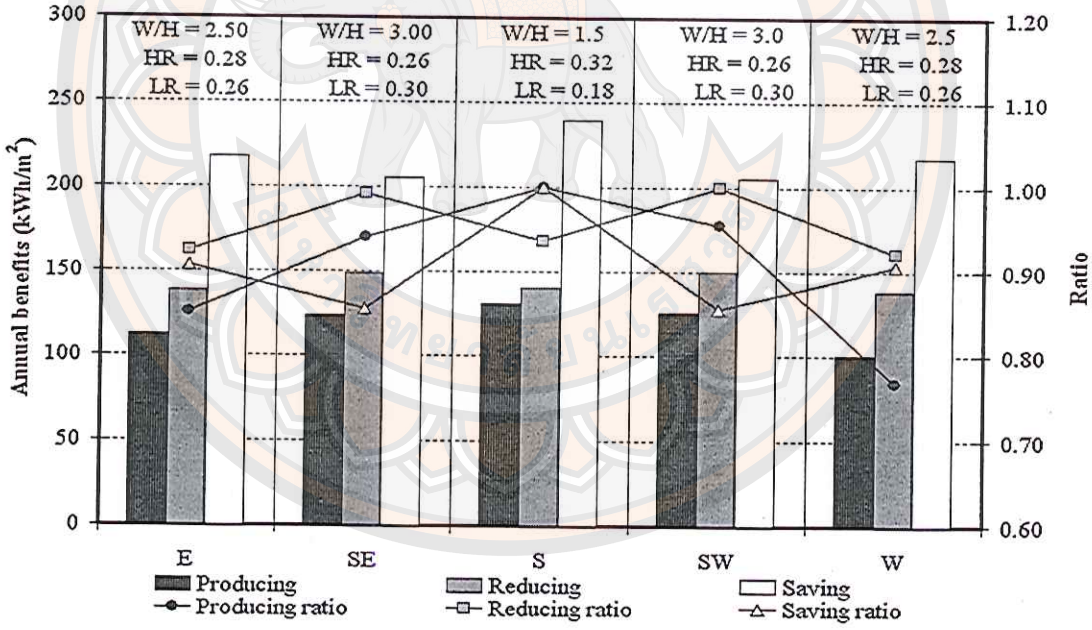

Figure 211 The impact of benefit options

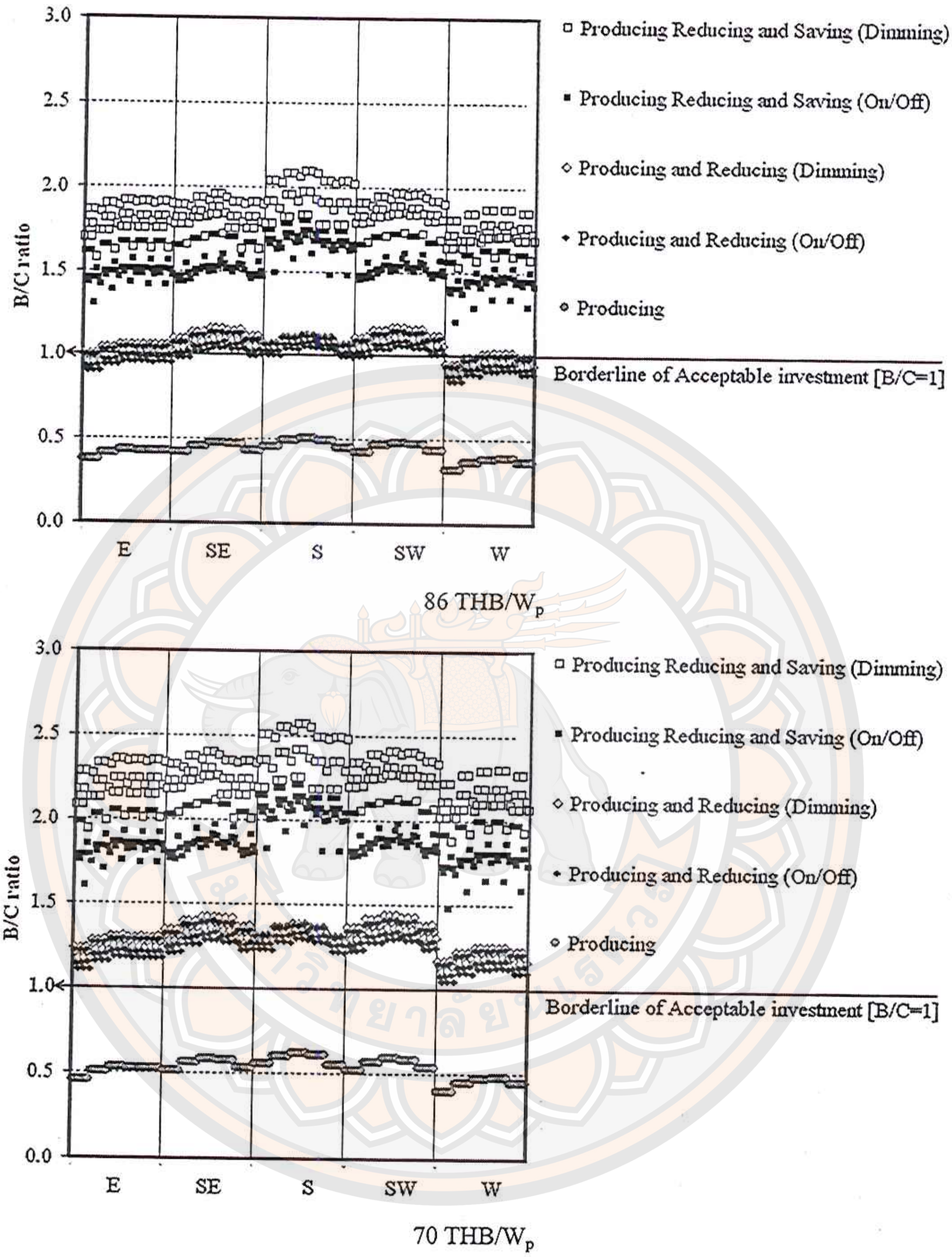

Figure 212 The B/C ratio comparison of the SIPV benefit options

Figure 212 shows trend of B/C ratio divided according to installation in all directions. It is found that only benefits from electricity production of SIPV are not suitable for investment. Considering producing and reducing benefits option of both cases of lighting control techniques, there is the similar B/C ratio. For producing, reducing and saving benefits option, dimming technique is the most suitable

2.6 Payback period

The optimization from considering payback period is divided into 3 following options:

2.6.1 The producing option

Payback period cannot be made in determined period of time for this option as shown in Figure 213 showing the comparison in a form of B/C ratio with value of less than 1.0 in all cases. It is found that the most suitable design is to install turning towards South with tilt angle of 30 degrees to create the highest level of energy generation

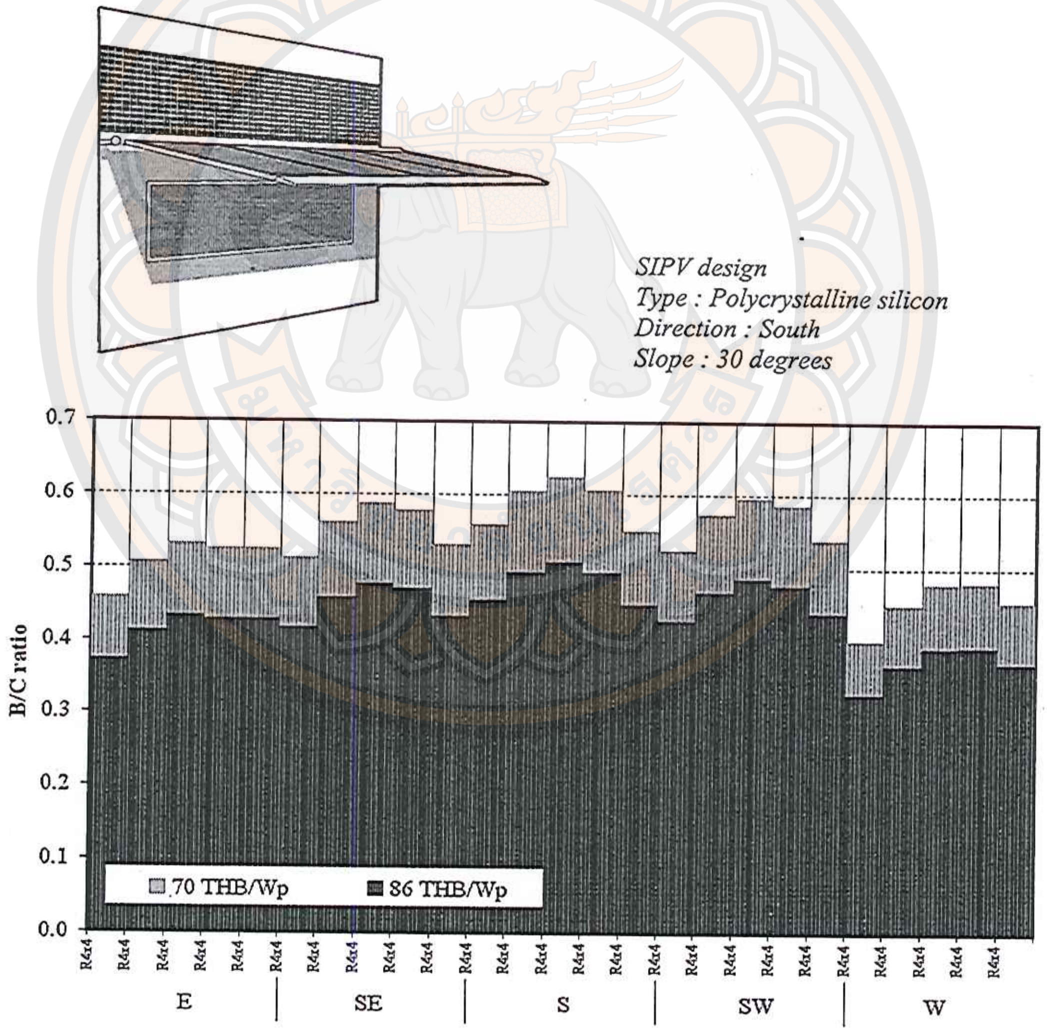

Figure 213 The B/C ratio of producing option

2.6.2 Producing and reducing option

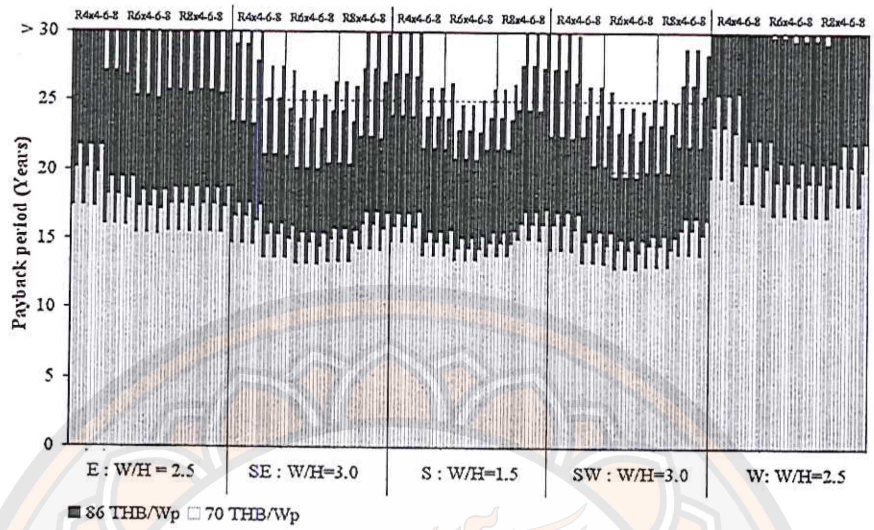

ON/Off technique

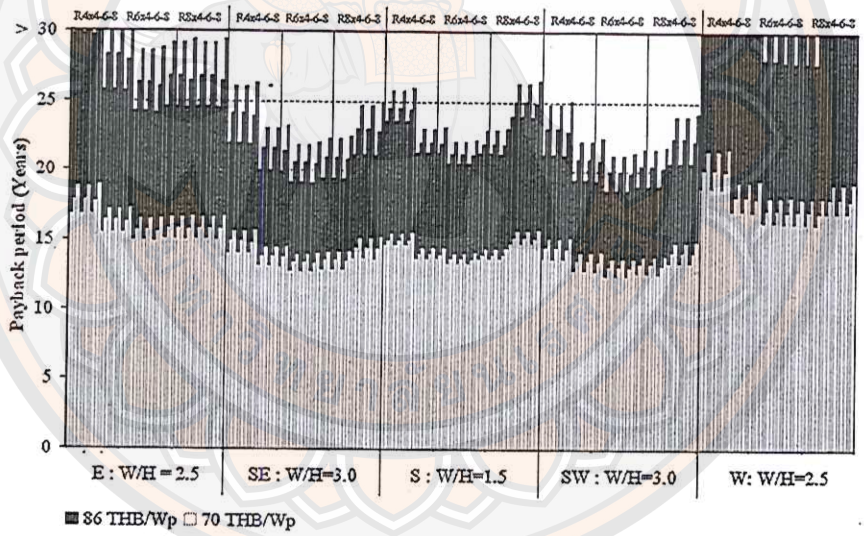

Dimming technique

Figure 214 The payback period of producing and reducing option

Figure 214 shows the payback of producing and reducing benefits option. It is found that the SIPV installed in the South West / East can make the fastest payback. However, it is the same to the installation in the south east and south arranged from the fastest to the slowest in both cases of lighting control techniques and in room with small depth. Figure 215 shows the resemble relation of both lighting control techniques

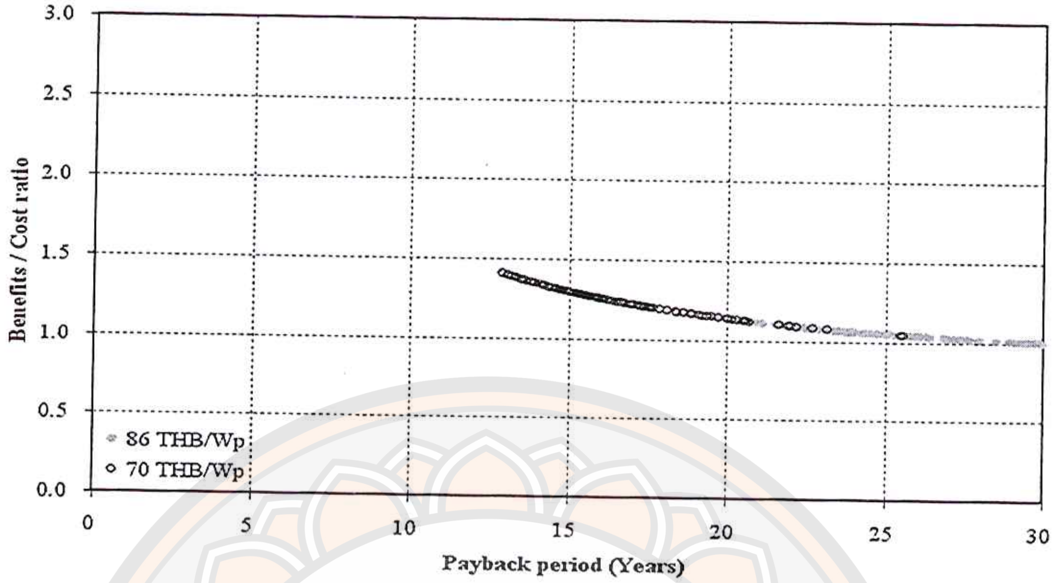

On/Off technique

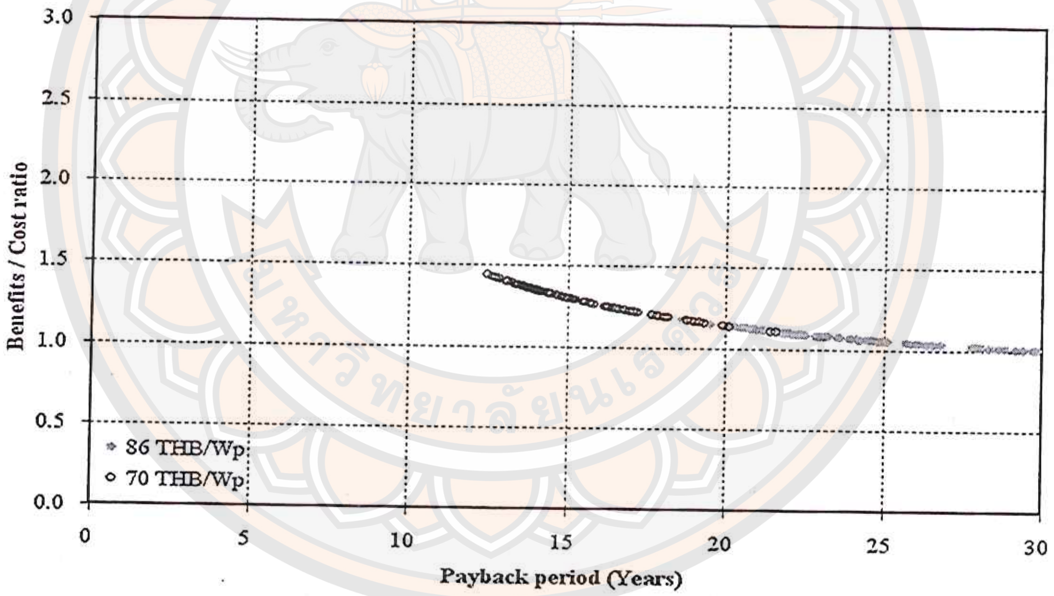

Dimming technique

Figure 215 The relations of B/C ratio and payback period of producing and reducing option

2.6.3 Producing reducing and saving option

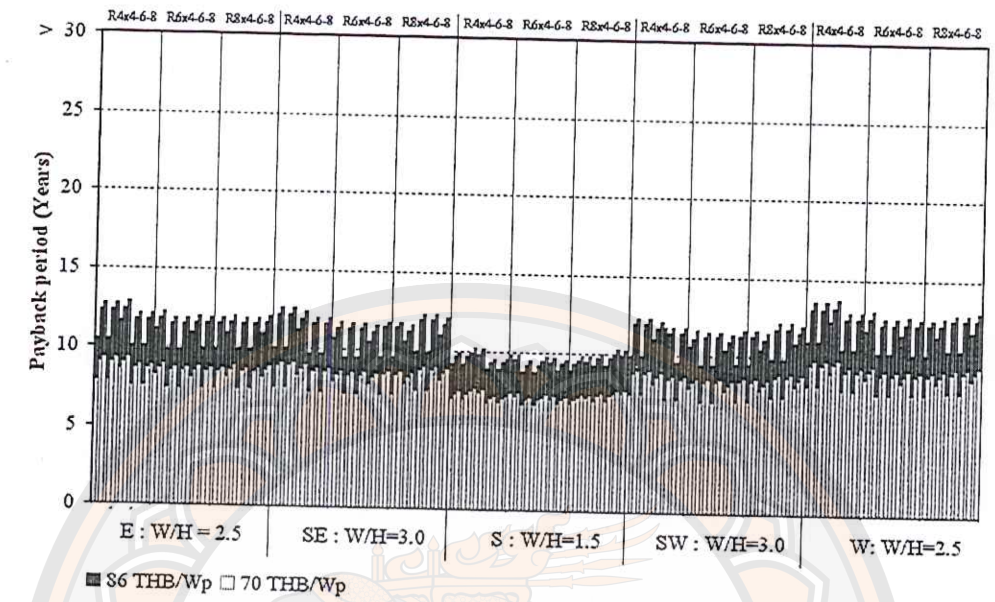

ON/Off technique

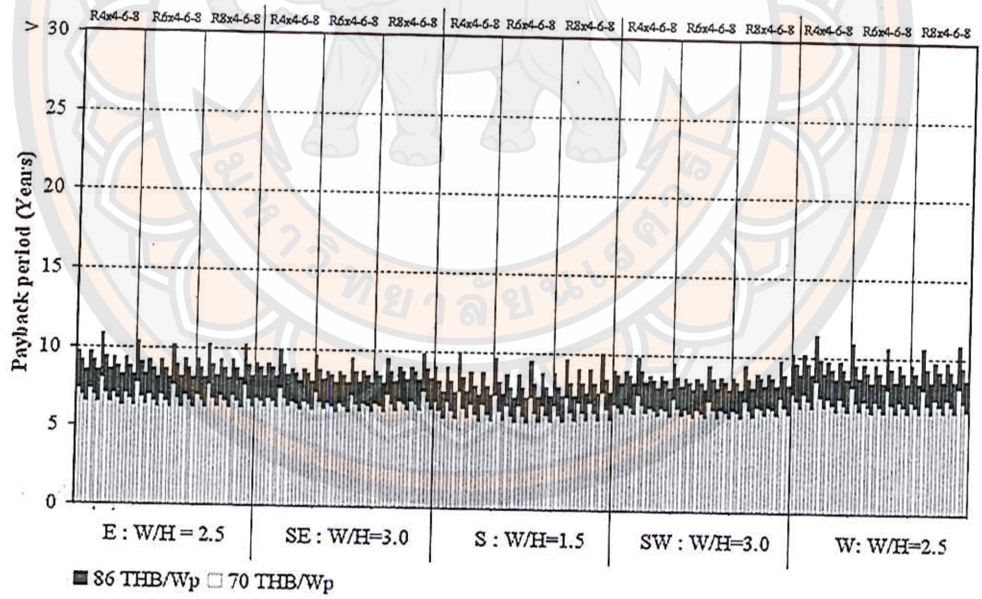

Dimming technique

Figure 216 The payback period of producing, reducing and saving option

Figure 216 shows payback of producing reducing and saving option. It is found that room with small depth of 4.0 m. using dimming technique can get payback sooner than room with big depth of 6.0 m. and 8.0 m. using on/off technique and being installed tuning towards South

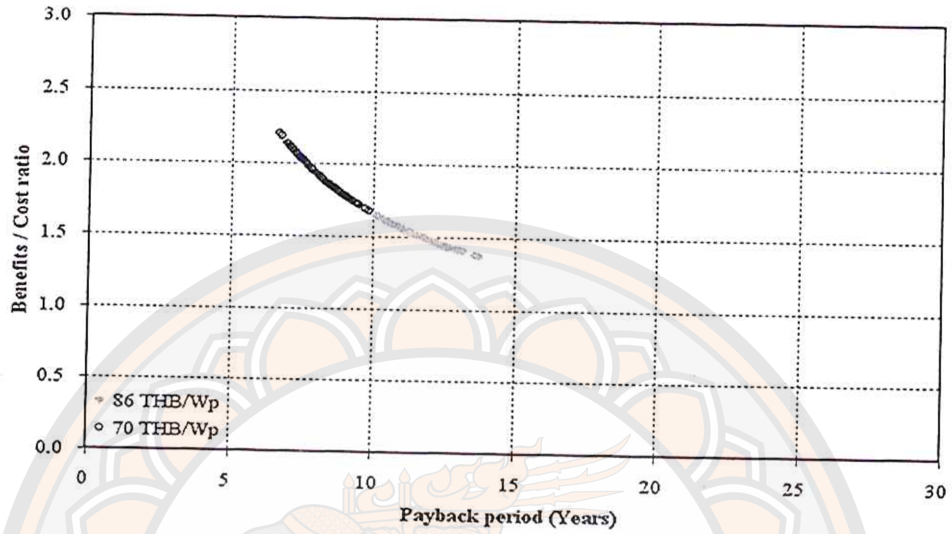

On/Off technique

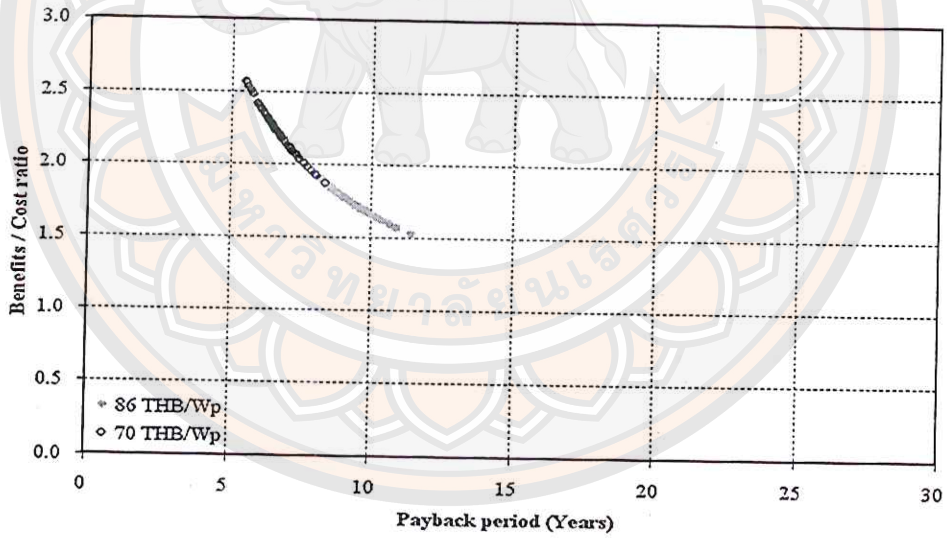

Dimming technique

Figure 217 The relations of B/C ratio and payback period of producing, reducing and saving option

Figure 217 shows the trend line which is clearly different. Dimming technique clearly shows the better trend

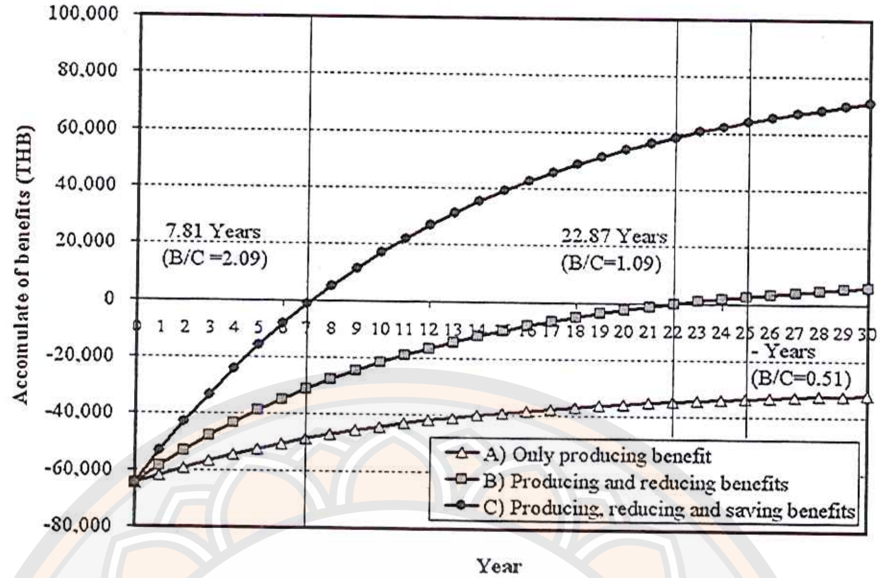

System cost = 86 THB/W_p

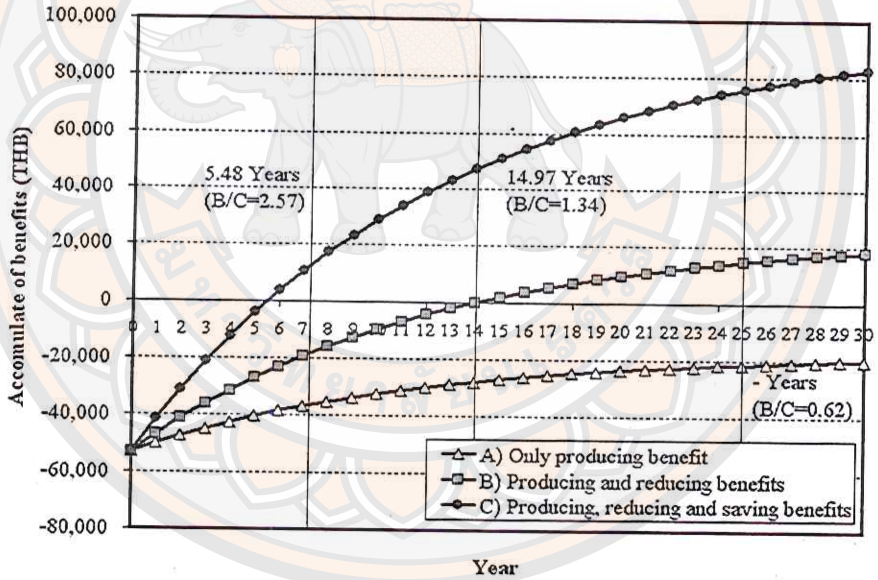

System cost = 70 THB/W_p

Figure 218 Trends of SIPV benefit options

Figure 218 indicates the best design conditions divided according to cost of system. It is found that the best case for option C is payback in 7.81 years for the cost of 86 THB/W_p and 5.48 years for cost of 70 THB/W_p

Table 32 The summary of design guild line

Option	control	B/C	Payback	Price	Slope	Direction	Room
			(Years)	(THB/Wp)	(Degrees)		Ranking (1-3)
producing	Both	0.51	-	86	30	S	All
	Both	0.62	-	70	30	S	All
Producing and reducing	On/Off	1.1	19.6	86	30	SW	8x4 6x4 4x4
	On/Off	1.4	12.9	70	30	SW	8x4 6x4 4x4
	Dimming	1.2	18.7	86	30	SW	8x4 6x4 4x4
	Dimming	1.4	12.5	70	30	SW	8x4 6x4 4x4
	On/Off	1.1	20.8	86	30	S	8x4 6x4 4x4
	On/Off	1.4	13.5	70	30	S	8x4 6x4 4x4
	Dimming	1.1	20.6	86	30	S	8x4 6x4 4x4
	Dimming	1.4	1.3.3	70	30	S	8x4 6x4 4x4
Producing reducing and saving	On/Off	1.8	8.9	86	30	S	6x4 4x4
	On/Off	2.2	6.7	70	30	S	6x4 4x4
	Dimming	2.1	7.2	86	30	S	6x8 4x8 8x8
	Dimming	2.6	5.5	70	30	S	6x8 4x8 8x8

The determination of 2 rates of system price has the same trend in design. Benefits of SIPV system gained from shading function and PV function is considered attractive for investment despite the drawback of receiving lower solar irradiance on solar module. However, there are still the benefits from shading function

Therefore, SIPV system can reduce cooling load of air conditioning system and use daylight to save energy from lighting load. There are also clear angles for buildings in Thailand

The suitability of design is to install turning towards south with tilt angle of 30 degrees in order to reduce heat gain and increase daylight usability of shading device integrated photovoltaic system as much as possible. It is also to create the suitability of price and benefits of shading device integrated photovoltaic system due to benefits gained from air conditioning system, lighting system and energy generation system by using dimming technique to control light within the

CHAPTER V

CONCLUSION

When considering the general energy usage of buildings in Thailand, it is found that between 75-80% of total energy usage originates from air conditioning system and lighting systems. From the idea of Green Building design of trying to solve energy and environment crisis, Shading Device Integrated Photovoltaic system: SIPV is considered one of design strategies providing more benefit than electricity generation alone. This system includes the reduction of heat gain from sunlight affecting cooling load reduction of an air conditioning system and natural lighting control affecting energy saving of lighting system. It is still considered beneficial despite the fact that its installation causes less solar radiation receiving than other installations on rooftop.

The purposes of the study to create suitable design ideas in order to gain the most advantages out of utilization of installations affected by shading on solar modules are as follows: first is optimization of solar heat reduction and increase of daylight utilization of Shading Device Integrated Photovoltaic system including price and economic benefits optimization of Shading Device Integrated Photovoltaic system.

However, estimation of solar radiation appeared on inclined plane of sun shading and reflectance of solar radiation from buildings envelope down on sun shading cannot be calculated by applying normal equations presented by ASHRAE. It is because there is a condition of shading and patterns of buildings causing half of diffuse sky radiation. Therefore, adjustment of some variables in equations is a must through data collection using models. Besides, there is the study of illuminance level on working plane in a form of Daylight Factor (DF) and the study of heat reduction due to diffuse solar radiation in a form of Shading Coefficient (SC_d) in term of entire prevention of direct solar radiation. Features of shading device design are decided by proportion of extension distance of sun shading to the height of window (W/H ratio) and clear obstruction in front of the window.

The result of analyzing the weather and solar radiation from database of Thai Meteorological Department in Bangkok where it was considered as an example of the areas with potential in installing the mentioned system and as it is located in the middle of the country or at latitude 14 degrees North, it was found that the energy calculated averagely per day was at 18 MJ/m^2, the ratio of diffuse solar radiation was at 40%, the air temperature was higher than comfort zone from 8.00 AM., total solar irradiance was decreased lower than the maximum value of diffuse solar radiation providing less heat at 16.00 PM; and quite small amount of light. Calculation of energy value of 3 systems such as photovoltaic energy generating system, air conditioning system and lighting system were determined to be at the period of time mentioned above.

The condition of calculation determined by the reference from the National Energy Conservation Promotion Act (Revised Edition) B.E.2550 was to calculate lighting level in the working area at 300 lux and use air conditioning system containing Coefficient of Performance: COP of 3.22. The indicator in suitability evaluation determined for this calculation was the benefits from energy use for the whole year. In addition, the determined variables used in the study for the design were as follows: window direction specified in the pattern of shading device suitable for sun protection in each direction in W/H ratio, variable of incline angle of solar module, variable of room size affecting number of light bulb being used and variable of lighting level control technique. When considering the system working all year long for 30 years, cost of electricity is at 4 Baht per unit and MRR loan rate is at 8%. There are 2 levels of stages of cost price: 70 and 86 THB/W_p. For 25 years of usability, efficiency of energy generation has been reduced 20% and amorphous silicon and polycrystalline silicon modules have been used as case study.

From calculating values, there are many points found as follows:

1. The installation directions appropriate to electric power generation are such as South, South West, South West, East and West arranged from the most to the least. Other directions only provided less energy due to sun orbit encircling more to the south all this period of time

2. Cooling load value as a result of diffuse solar radiation causing heat transfer, heat conduction of air temperature outside and heat from light bulbs located in South West, South East, West, East and South directions arranged from the least to the most. It is because the stretched out parts of shading device in descending order from the most to the least and the difference between south west and south is only 5%

3. Incline angle of solar module should do an angle of 30 degrees to the horizontal plane to be able to produce most energy although incline angle at 0 degrees is receiving solar radiation reflecting from building envelope the most

4. The stretched out parts of shading device in the South, East, West, South East and South West directions will allow daylight in arranged in order from the most to the least

5. Stacking vertically of shading device integrated photovoltaic system causes the decrease in energy generation due to the devices covering one another

6. Rooms with more distance from windows will receive averagely less light according to order of distance

7. Glare in case of any usability facing the windows will happen less as it is manageable through working area arrangement and change in eyesight direction

8. Dimming technique creates most efficient daylight use and helps room located long distance from the light save energy in total per square metre

9. Proportion of energy generation as a result of shading device integrated photovoltaic system was less than the rooftop installation, in case of comparing to the maximum case, about 20%

10. The influence of shading of the buildings slightly affected efficiency of inverter

When considering the optimization in design from the determined purposes, it can be concluded as each purpose as follows:

The optimization of solar heat gain reduction and increase in daylight usability of shading device integrated photovoltaic system by considering an amount of energy being saved for the whole year, it is found that shading device integrated photovoltaic system should be installed in the south side which allows solar radiation in the most. Besides, there should be the stretched out parts of shading device gaining heat from diffuse solar radiation moderately most suitable for structure and angles of windows. In addition, there should be solar module making an angle of 30 degrees to the horizontal plane and rooms with less distance from light to allow daylight in the most.

The optimization of economic price and benefit of shading device integrated photovoltaic system by considering from benefit, investment and payback in suitability evaluation when determining energy saving strategy, it is found that

1. As solar module only being used to generate energy, there was no cases of design worth for investment (B/C<1) and no payback during life cycle operation

2. As for the utilization of energy generation and heat reduction, the benefit of shading was more than benefit in electric power production creating the fact that the installation of shading device integrated photovoltaic system should be in the South West or South East direction. However, if the utilization is mainly for energy generation, installation in the south side should still be considered which provides similar benefit of total energy, solar module making an angle of 30 degrees to the horizontal plane and rooms with less distance from windows. This is to say that there was only a slight difference between lighting control system and light dimming at about 5%

3. The utilization of energy generation, heat reduction and electricity saving causes one-third of total energy benefit of producing electricity from solar cell and lesser when using dimming technique. Therefore, besides the installation of shading device integrated photovoltaic system in the south side which receive more benefit from daylight, there is solar module making an angle of 30 degrees to the horizontal plane, rooms with less distance from windows in case of controlling light by using lighting control technique and rooms with long distance from the windows in case of controlling light by using dimming technique

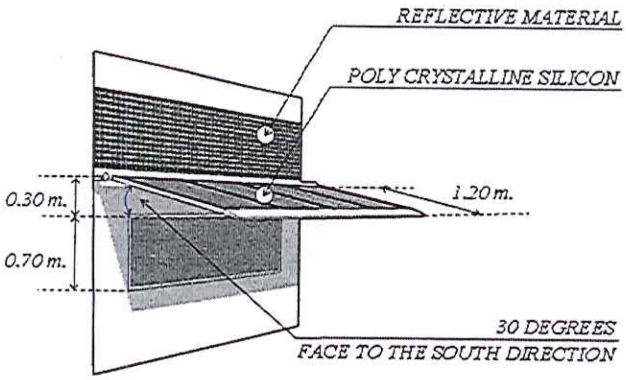

Figure 219 The design guild line of SIPV

In conclusion, it showed that the utilization with shading device results in the decrease of electricity production comparing to rooftop installation. However, more benefit has been shown in more proportion and it is enough for gaining payback which is faster than rooftop installation design. The example of installation presented in Figure 219.

REFERENCES

REFERENCES

[1] American Society of Heating Refrigerating and Air-Conditioning Engineers. (1989). **ASHRAE handbook: fundamentals**. Atlanta, GA: American Society of Heating Retrigererting and Air Coudition in Engineers.

[2] American Society of Heating Refrigerating and Air-Conditioning Engineers. (2001). **ASHRAE handbook: fundamentals**. Atlanta, GA: American Society of Heating Retrigererting and Air Coudition in Engineers.

[3] B. Sulee. (2001). **Lighting engineering**. Bangkok: SE-education.

[4] Benjamin Stein and John S. Reynolds. (1992). **Mechanical and electrical equipment for buildings**. New York: J. Wiley & Sons.

[5] Bernhard Weller, Claudia Hemmerle, Sven Jakubetz and Stefan Unnewehr. (2010). **Photovoltaics: technology architecture installation**. Basel: Edition Detail.

[6] Boubekri Mohamed Daylighting. (2008). **Architecture and health: building design strategies**. Great Britain: Elsevier Ltd.

[7] Chao-Yu Chan. (2010). **Evaluation of photovoltaic applied in building design**. Lexington, KY: n.p.

[8] Claude L. Robbins. (1986). **Daylighting design and Analysis**. New York: Van Nostrand Reinhold.

[9] Cowan, Henry J. (1983). **Environmental systems**. New York: n.p.

[10] Deo Prasad and Mark Snow. (2005). **Designing with solar power: a source book for building integrated photovoltaics (BIPV)**. Mulgrave, Vic.: Images Publishing.

[11] Egan, M. David. (1983). **Concepts in architectural lighting**. New York: McGraw-Hill.

[12] Energy Market Authority and Building and Construction Authority. (n.d.). **Handbook for Solar Photovoltaic (PV) Systems**. N.P.: n.p.

[13] Flynn, John E., Kremers, Jack A., Segil, Arthur W. and Staffy Gary R. (1992). **Architectural interior systems: lighting, acoustics, air conditioning** (3rd ed.). New York: Van Nostrand Reinhold.

[14] Frank, H. Mahnke. (1996). **Color environment and human response: an interdisciplinary understanding of color and its use as a beneficial element in the design of the architectural environment**. New York: Wiley.

[15] I, Kasadit. (2008). **Interior environment quality**. N.P.: King Mongkut's Institute of Technology Ladkrabang.

[16] Janjai, S. (2004). **Handbook of solar radiation and climatic data for renewable energy applications**. Bangkok: n.p.

[17] Jesse Henson. (2010). **Hybrid photovoltaic shade elements: passive and active benefits**. Lexington, KY: LAMBERT Academic Publiching.

[18] John, A. Duffie and William, A. Beckman. (1991). **Solar engineering of thermal processes**. New York: Wiley.

[19] Kreider, F. Jan and Curtiss, S. peter. (2002). **Heating and cooling of building design for efficiency**. Ari Rabl: McGraw-Hill.

[20] Lechner, Norbert. (2001). **Heating cooling, lighting: design methods for architects**. New York: John Wiley.

[21] M. David Egan and Victor W. Olgyay. (2002). **Architectural lighting**. Boston: McGraw-Hill.

[22] Magal, B.S. (1990). **Solar power engineering**. New Delhi: McGraw-Hill.

[23] Mann, Torbjoern. (1992). **Building economics for architects**. New York: Van Nostrand Reinhold.

[24] Marietta S. Millet. (1996). **Light revealing architecture**. New York: Van Nostrand Reinhold.

[25] Moor, Fuller. (1993). **Environmental control system heating cooling lighting**. Singapore: McGraw-Hill.

[26] R. G. Hopkinson, P. Petherbridge and J. Longmore. (1964). **Daylighting**. London: Heinemann.

[27] Simon Roberts and Nicolo Guariento. (2009). **Building integrated Photovoltaics a handbook**. Basel: Birkhauser.

[28] Sophia and Stefan Behling in collaboration with Bruno Schindler foreward by Norman Foster. (2000). **Solar power: the evolution of sustainable architecture**. Munich: Prestel.

[29] Srisutapan, A and T. Panjira. (2010). **Daylight in architecture**. Bangkok: Thammasat University.

[30] Sterling, VA. (2008). **Planning and installing photovoltaic systems: a guide for installers architects and engineers.** London: Earthscan.

[31] Szokolay, S. V. (2004). **Introduction to architectural science the basis of sustainable design**. Boston: Elsevier Architectural.

[32] T. Muneer. (2004). **Solar radiation and daylight models**. Amsterdam: Elsevier Butterworth Heinemann.

[33] The Association of Siamese Architects Under Royal Patronage. (2010). **Energy management & operation - maintenance service**. Bangkok: Plus press Ltd.

[34] Tregenza, Peter and Willson, Michael. (2011). **Daylighting architecture and lighting design**. New York: Routledge.

[35] V. Napatra. (2010). **Installing a solar electric system on their own**. Skybook: Pathumthani.

[36] Watson, Donald. (1993). **The energy design handbook**. Washington, D.C.: The American Institute of Architects.

[37] Williamson, S. J. and Cummins, H. Z. (1983). **Light and color in nature and art.** N.P.: Wiley.

[38] Danny, H.W., Li a, Tony, N.T., Lam, Wilco, W.H., Chan and Ada, H.L., Mak. (2008). Energy and cost analysis of semi-transparent photovoltaic in office buildings. **Applied Energy**, 86, 722-729.

[39] Danny, H.W., Li, Tony, N.T., Lam and K.L. Cheung. (2009). Energy and cost studies of semi-transparent photovoltaic skylight. **Energy Conversion and Management**, 50, 1981-1990.

[40] David Infield, Li Mei and Ursula Eicker. (2003). Thermal performance estimation for ventilated PV facades. **Solar Energy**, 76, 93-98.

[41] I. Spanos and L. Duckers. (2003). Expected cost benefits of building-integrated PVs in UK, through a quantitative economic analysis of PVs in connection with buildings, focused on UK and Greece. **Renewable Energy**, 29, 1289-1303.

[42] Ji Jie, He Weia and H.N. Lamb. (2001). The annual analysis of the power output and heat gain of a PV-wall with different integration mode in Hong Kong. **Solar Energy Materials & Solar Cells**, 71, 435-448.

[43] K.E. Park, G.H. Kang, H.I. Kim, G.J. Yu and J.T. Kim. (2009). Analysis of thermal and electrical performance of semi-transparent photovoltaic (PV) module. **Energy and Buildings**, 35(6), 2681–2687.

[44] L.L. Sun and H.X. Yang. (6-11; October 2009). Impacts of the shading-type building-integrated photovoltaic claddings on electricity generation and cooling load component through shaded windows. **Energy and Buildings**, 42(4), 455–460.

[45] Li Meia, David Infielda, Ursula Eickerb and Volker Fuxb. (2002). Thermal modelling of a building with an integrated ventilated PV fa?ade. **Energy and Buildings**, 35, 605-617.

[46] M. Oliver and T. Jackson. (1999). Energy and economic evaluation of building-integrated photovoltaics. **Energy and Buildings**, 26, 431-439.

[47] P.A.B. James, M.F. Jentsch and A.S. Bahaj. (2008). Quantifying the added value of BiPV as a shading solution in atria. **Solar Energy**, 83, 220-231.

[48] Seung-Ho Yooa and Eun-Tack Lee. (2002). Building integrated photovoltaics: a korean case study.**Building and Environment**, 37, 615-623.

[49] T. Miyazaki, A. Akisawa and T. Kashiwagi. (2004). Energy savings of office buildings by the use of semi-transparent solar cells for windows. **Renewable Energy**, 30, 281-304.

[50] Tapas K. Mallick, Philip C. Eames and Brian Norton. (2005). Non-concentrating and asymmetric compound parabolic concentrating building facade integrated photovoltaics: An experimental comparison. **Solar Energy**, 80, 834-849.

[51] Yiping Wang, Wei Tian, Jianbo Ren, Li Zhu and Qingzhao Wang. (2005). Influence of a building s integrated-photovoltaics on heating and cooling loads. **Applied Energy**, 83, 989-1003.

[52] Yu, G.J., So, J.H., Jung, Y.S., Kang, G.H. and Choi, J.Y. (2005). Performance results of 15 kW BIPV sunshade system. **IEEE**, 31, 1722 - 1725.

[53] Bunphan, Tharika. (2010). **Grid connected inverter efficiency in PV grid connected system.** Thesis M.S., Naresuan University, Phitsanulok.

[54] Chorchong, Titiporn. (2009). **Degradation of photovoltaic array efficiency after long term operation.** Thesis M.S., Naresuan University, Phitsanulok.

[55] Euvananont, Chanipat. (2006). **Feasibility study of building integrated photovoltaic systems for buildings in Bangkok.** Thesis M.S., King Mongkut's University of Technology Thonburi, Bangkok.

[56] Supheng, Wanchart. (1999). **Designing of a Multi-purpose PV-Window.** Thesis M.S., King Mongkut's University of Technology Thonburi, Bangkok.

[57] Amornsolar. (2010). **PV price.** Retrieved August 15, 2013, from http://www.amornsolar.com.

[58] Andersen, Marilyne. (June 9, 2001). **Comfort and technologies: from the individual's needs to cleantech.** Retrieved August 20, 2013, from http://infoscience.epfl.ch/record/166737

[59] Banmuang. (2011). **PEA shows the way to produce the electricity, Must be supported by alternative energy.** Retrieved November 5, 2011, from http://www.banmuang.co.th.

[60] Benefit media Co.ltd. (2009). **PV price.** Retrieved August 15, 2013, from http://freeenergy.tarad.com.

[61] Blogger. (n.d.). **PV price.** Retrieved August 15, 2013, from http://solartech-center.blogspot.com.

[62] British Standards Institution. (n.d.). **Photovoltaic system performance monitoring-Guidelines for measurement, data exchange and analysis.** Retrieved August 20, 2013, from ftp://158.132.178.85/wclo/61/IEC61724%20PV%20monit.

[63] Building and Construction Authority. (n.d.). **Handbook for Solar Photovoltaic (PV) Systems.** Retrieved August 20, 2013, from http://www.bca.gov.sg.

[64] Chawna. (n.d.). **PV price.** Retrieved August 15, 2013, from http://www.kasetporpeang.com.

[65] Department of Alternative Energy Development and Efficiency. (n.d.). **Solar map**. Retrieved November 4, 2011, from http://www.dede.go.th.

[66] Ecobusinesslinks. (2013). **Free Solar Panel Price Survey**. Retrieved August 15, 2013, from http://www.ecobusinesslinks.com.

[67] Energy market Authority. (n.d.). **Handbook for Photovoltaic (PV) Systems**. Retrieved August 20, 2013, from http://www.ema.gov.sg.

[68] Honsberg, Christiana and Bowden, Stuart. (n.d.). **Effect of Temperature**. Retrieved November 4, 2011, from http://pveducation.org.

[69] International Energy Agency. (2002). **Report IEA PVPS**. Retrieved August 20, 2013, from http://apache.solarch.ch.

[70] John Schmitz. (2008). **Solar Photovoltaic Electricity to hit the Power Grid?**. Retrieved October 30, 2011, from http://secondlawoflife.wordpress.com.

[71] Kamsopha, Sarawut. (n.d.). **PV price**. Retrieved August 15, 2013, from http://www.thaipowertech.com.

[72] LaMonica, Martin. **Economics of alternative energy improve**. Retrieved November 3, 2011, from http://news.cnet.com.

[73] Learner, Annenberg. (n.d.). **Earth-atmosphere energy balance**. Retrieved November 3, 2011, from http://learner.org.

[74] Leonics co., ltd. (n.d.). **Stand-alone solar** system. Retrieved August 20, 2013, from http://www.leonics.co.th.

[75] Martin LaMonica. (2008). **Economics of alternative energy improve**. Retrieved October 30, 2011, from http://news.cnet.com.

[76] Mechashop. (n.d.). **PV price**. Retrieved August 15, 2013, from http://xn--c3ca0b5bmba5hvfqa3a6b5c.com.

[77] Michael S. Davies. (2007). **Understanding the cost of solar energy**. Retrieved October 30, 2011, from http://greenecon.net.

[78] Ministry of Energy. (n.d.). **Annual report**. Retrieved July 20, 2013, from http://www.dede.go.th.

[79] M.J. Shiao. (n.d.). **Balance of system costs face PV pricing squeeze.** Retrieved August 15, 2013, from http://www.solarbusinessfocus.com

[80] Nitidow. (n.d.). **MRR.** Retrieved August 15, 2013, from http://www2.bot.or.th.

[81] Pearson, Chris. (2007). **Solar energy component costs.** Retrieved November 3, 2011, from http://greenecon.net.

[82] Rudolf C. John. (April 20, 2011). **Transparent photovoltaic cells turn windows into solar panels.** Retrieved November 7, 2011, from http://green.blogs.nytimes.com.

[83] Sapa build ing system ab offices. (2012). **Sapa solar BIPV.** Retrieved August 15, 2013, from http:// www.sapagroup.com.

[84] Solartech center limited partnership. (2012). **PV price.** Retrieved August 15, 2013, from http://www.solar-cell-system.com.

[85] tarad.com. (2009). **PV price.** Retrieved August 15, 2013, from http://freeenergy.tarad.com.

[86] Thai Meteorological Department. (2007). **The general weather conditions during the year 2006.** Retrieved November 3, 2011, from http://www.tmd.go.th.

[87] Thai Meteorological Department. (2011). **The general weather conditions during the year 2010.** Retrieved November 3, 2011, from http://www.tmd.go.th.

[88] Thai Meteorological Department. (2008). **The general weather conditions during the year 2007.** Retrieved November 3, 2011, from http://www.tmd.go.th.

[89] Thai Meteorological Department. (2009). **The general weather conditions during the year 2008.** Retrieved November 3, 2011, from http://www.tmd.go.th.

[90] Thai Meteorological Department. (2010). **The general weather conditions during the year 2009.** Retrieved November 3, 2011, from http://www.tmd.go.th.

[91] United Nations University. (n.d.). **PV mean module prices and PV market.** Retrieved October 30, 2011, from http://archive.unu.edu.

[92] Vera. (2009). **PV price.** Retrieved August 15, 2013, from http://www.mechashop.com.

[93] Volumatrix Group. (n.d.). **Green Architecture: 15 skyscrapers with integrated energy generators**. Retrieved July 9, 2013, from http://volumatrixgroup.com.

[94] William, L. Wolfe and George, J. Zissis. (n.d.). **Spectral distribution curve of incoming Solar Energy**. Retrieved November 3, 2011, from http://www.sunwindsolar.com.

[95] William Stine and Michael Geyer. (n.d.). **Standard time zones.** Retrieved November 3, 2011, from http://www.powerfromthesun.net.